NASA Conference Publication 2298

Digital Electronic Engine Control (DEEC) Flight Evaluation in an F-15 Airplane

(NASA-CP-2298) DIGITAL ELECTRONIC ENGINE CONTROL (DEEC) FLIGHT EVALUATION IN AN F-15 AIRPLANE (NASA) 243 p HC A11/MF A01 CSCL 21E H1/07

N86-25342 THRU N86-25356 Unclas 42942

Proceedings of a minisymposium held at
NASA Ames Research Center
Dryden Flight Research Facility
Edwards, California
May 25-26, 1983

NASA
National Aeronautics
and Space Administration

Scientific and Technical
Information Branch

1984

PREFACE

The control system of modern turbofan engines has an important impact on their performance. The control system must accurately and rapidly position the many variables on the engine in response to many sensor inputs. The logic involved in the system can be complex. Hydromechanical control systems are only marginally capable of controlling modern high-performance engines. Digital control systems can handle many inputs and outputs and perform complex computations, and are beginning to replace other types of control systems in many applications.

To investigate the application of digital control technology to a complex engine in a high-performance airplane, the National Aeronautics and Space Administration (NASA), the U.S. Air Force, and Pratt and Whitney Aircraft have recently completed a flight investigation of a digital electronic engine control (DEEC) system on an F100 engine in an F-15 airplane. Following extensive ground and altitude facility tests, a 30-flight program was conducted at NASA Ames Research Center's Dryden Flight Research Facility at Edwards, California. A minisymposium was held at Ames Dryden on May 24 and 25, 1983, to disseminate the results of the DEEC flight evaluation. This publication contains the papers that were presented.

As shown in the data presented, the DEEC system was found to be a powerful and flexible controller for the F100 engine. The F-15 aircraft was an excellent test bed for the flight evaluation. The value of flight test was conclusively demonstrated in exposing and solving problems and demonstrating performance improvements.

Frank W. Burcham, Jr.
Technical Chairman, DEEC Minisymposium

PRECEDING PAGE BLANK NOT FILMED

CONTENTS

Preface iii

Nomenclature vii

1. DIGITAL ELECTRONIC ENGINE CONTROL F-15 OVERVIEW 1
   Berwin Kock

2. DIGITAL ELECTRONIC ENGINE CONTROL HISTORY 15
   Terrill W. Putnam

3. F-15 DIGITAL ELECTRONIC ENGINE CONTROL SYSTEM DESCRIPTION 33
   Lawrence P. Myers

4. NASA LEWIS F100 ENGINE TESTING 55
   Roger A. Werner, Ross G. Willoh, Jr., and Mahmood Abdelwahab

5. EFFECTS OF INLET DISTORTION ON A STATIC PRESSURE PROBE MOUNTED ON THE ENGINE HUB IN AN F-15 AIRPLANE 73
   Donald L. Hughes and Karen G. Mackall

6. FLIGHT TESTING THE DIGITAL ELECTRONIC ENGINE CONTROL IN THE F-15 AIRPLANE 91
   Lawrence P. Myers

7. DIGITAL ELECTRONIC ENGINE CONTROL FAULT DETECTION AND ACCOMMODATION FLIGHT EVALUATION 107
   Jennifer L. Baer-Riedhart

8. AIRSTART PERFORMANCE OF A DIGITAL ELECTRONIC ENGINE CONTROL SYSTEM ON AN F100 ENGINE 127
   Frank W. Burcham, Jr.

9. FLIGHT EVALUATION OF A HYDROMECHANICAL BACKUP CONTROL FOR THE DIGITAL ELECTRONIC ENGINE CONTROL SYSTEM IN AN F100 ENGINE 141
   Kevin R. Walsh and Frank W. Burcham

10. BACKUP CONTROL AIRSTART PERFORMANCE ON A DIGITAL ELECTRONIC ENGINE CONTROL-EQUIPPED F100 ENGINE 157
    J. Blair Johnson

11. AUGMENTOR TRANSIENT CAPABILITY OF AN F100 ENGINE EQUIPPED WITH A DIGITAL ELECTRONIC ENGINE CONTROL 171
    Frank W. Burcham, Jr. and G. David Pai

12. INVESTIGATION OF A NOZZLE INSTABILITY ON AN F100 ENGINE EQUIPPED WITH A DIGITAL ELECTRONIC ENGINE CONTROL 201
    Frank W. Burcham, Jr. and John R. Zeller

PRECEDING PAGE BLANK NOT FILMED

13. REAL-TIME IN-FLIGHT THRUST CALCULATION ON A DIGITAL ELECTRONIC ENGINE CONTROL-EQUIPPED F100 ENGINE IN AN F-15 AIRPLANE 215
Ronald J. Ray and Lawrence P. Myers

14. CONTROL TECHNOLOGY FOR FUTURE AIRCRAFT PROPULSION SYSTEMS 231
John R. Zeller, John R. Szuch, Walter C. Merrill, Bruce Lehtinen, and James F. Soeder

NOMENCLATURE

AB	afterburner
ADIA	advanced detection-isolation-accommodation
AEDC	Arnold Engineering Development Center
AFAPL	Air Force Aeropropulsion Laboratory
AFM	advanced fuel management augmentor system
AFTI	advanced fighter technology integration
AJ	jet primary nozzle area
BIT	built-in tests
BOM	bill of materials
BUC	backup control
b factor	Pratt & Whitney radial distortion weighting factor
CENC	convergent exhaust nozzle control
CERT	combined environmental reliability test
CG	gross thrust coefficient
CIP	component improvement program
CIVV	compressor inlet variable vane
CMOS	complementary metal oxide semiconductor
COOP	cooperative
CRT	cathode ray tube
CV	coefficient of velocity
DEEC	digital electronic engine control
DIA	detection-isolation-accommodation
DMICS	design methods for integrated control systems
DTMM	distortion factor = (PT2MAX - PT2MIN)/PT2AVG
EMD	engine model derivative
EMDP	Engine Model Derivative Program

EPCS	electronic propulsion control system
EPR	engine pressure ratio, PT6M/PT2
EST	estimate
FA-AB	afterburner fuel-air ratio
FADEC	full-authority digital engine control
FAEC	full-authority electronic control
FAFTEEC	full-authority fault tolerant electronic engine control
FDA	fault detection and accommodation
FG	gross thrust
FN	net thrust
FPCC	flight-propulsion control coupling
FR	ram drag
FTIT	fan turbine inlet temperature
GAMA	ratio of specific heats
g	gravitational constant
HIDEC	highly integrated digital electronic control
HP	pressure altitude
IAPSA	integrated airplane propulsion system architecture
IFFC	integrated fire-fight control
IM	intermediate power
INTERACT	integrated research aircraft technology
INTERFACE	integrated reliable fault-tolerant control for engines
IPCS	integrated propulsion control system
IR	infrared
IR&D	independent research and development
JFET	junction field effect transistor
JFS	jet fuel starter
JTDE	joint technology demonstrator engine

KA2	fan distortion factor, KA2 = Kθ + b(KRA2)
KRA2	radial distortion factor
Kθ	circumferential distortion factor
LOD	light off detector
LQR	linear quadratic regulator
LRU	line-replaceable unit
M	Mach number
M.N.	Mach number
MNA	multivariable Nyquist array
MOA	memorandum of agreement
MTBF	mean time between failures
MVC	multivariable control
MVCS	multivariable control synthesis
N1	fan rotor speed
N1C2	corrected fan speed
N2	core rotor speed, rpm (100 percent N2 = 14,000 rpm)
N2C	corrected engine core speed
N2C25	corrected core rotor speed
O.D.	outer diameter
PAB	augmentor static pressure
PB	burner pressure
PBSYN	synthesized main burner pressure
PCM	pulse code modulation
PES	photoelectric scanning
PFMO	pressure of fuel for DEEC mode selection
PI	proportional plus integral
PLA	power lever angle
PLA-AB	afterburner power lever angle

PO	sea level static pressure
PROM	programmable read-only memory
PSL	propulsion system laboratory
PSNB	noseboom probe static pressure
PS2	fan inlet static pressure
PS2C	compensated fan inlet static pressure
PS2SYN	synthesized engine inlet static pressure
PT	total pressure
PTA	pressure-area thrust calculation method
PTINF	free-stream total pressure
PT2	fan inlet total pressure
$\overline{PT2}$	time-averaged fan inlet total pressure
PT2AVG	average value of total pressure at fan inlet
PT2C	calculated PT2
PT2MAX	maximum value of total pressure at fan inlet
PT2MIN	minimum value of total pressure at fan inlet
PT2UNDIST	undistorted (maximum) fan inlet total pressure
PT4	combustor exit total pressure
PT6	turbine discharge pres ure
PT6M	turbine discharge total pressure (mixed core and fan stream)
PT7	engine total exhaust pressure
P4	combustor exit static pressure
P6M01	turbine discharge total pressure production probe
Q	dynamic pressure
QCSEE	quiet, clean, short-takeoff-and-landing experimental engine
R	gas constant
RAEEC	reliability assessment for electronic engine control
RAM	random access memory

RAMP3L	left inlet third ramp angle
RCVV	rear compressor variable vane
REQ	request
ROM	read-only memory
RTES	real-time engine simulator
SA	swirl augmentor
SEC	secondary engine control
SFDV	single flow divider valve
S/L	sea level
S/R	spray ring
SVP	sequencing valve position
T	airstart time from pressurization to idle
TPB	PB transducer temperature
TPS2	PS2 transducer temperature
TPT6M	PT6M transducer temperature
TSFC	thrust specific fuel consumption
TTL	transistor-transistor logic
TTO	free-stream total temperature
TTW	temperature-weight flow method of thrust calculation
TT2	fan inlet total temperature
TT7	nozzle exit total temperature
T4	combustor exit temperature
t	time
U	uncertainty
UART	universal asynchronous receiver-transmitter
ULHC	upper left hand corner
UTRC	United Technology Research Center
V	velocity

VC	calibrated airspeed
WAC	corrected engine airflow, $W2\sqrt{\theta t2}/\delta t2$
WAC%	(WAC/98.43)100, where design corrected engine airflow = 98.43 kg/sec
WAC2	corrected engine airflow
WAT	total fan airflow
Wa1	fan inlet total airflow
WF	fuel flow
WFAC	core afterburner fuel flow
WFAD	duct afterburner fuel flow
WFC	augmentor fuel flow in core region
WFD	augmentor fuel flow in duct region
WFGG	gas generator fuel flow
WFT	total fuel flow
WG7	nozzle exit weight flow
W2	engine airflow
γ	ratio of specific heat
Δ	change in parameter
$\delta t2$	corrected average engine-face pressure ratio
$\delta 2$	ratio of fan inlet total pressure to standard sea level static pressure
$\theta t2$	corrected average engine-face total temperature ratio
$\theta 2$	ratio of fan inlet total temperature to standard sea level static temperature

N86
25343

UNCLAS

N86-25343

DIGITAL ELECTRONIC ENGINE CONTROL
F-15 OVERVIEW

Berwin Kock
NASA Ames Research Center
Dryden Flight Research Facility
Edwards, California

SUMMARY

NASA Ames Research Center's Dryden Flight Research Facility, in cooperation with the U.S. Air Force and Pratt and Whitney Aircraft, conducted a flight test evaluation of the digital electronic engine control (DEEC) system. This paper presents an overview of the flight program. The introduction describes the roles of the participating parties, the system, and the flight program objectives. The test program approach is discussed briefly, and the engine performance benefits are summarized. A brief description of follow-on programs is also included.

DRYDEN F-15 PROGRAMS

ORIGINAL PAGE IS
OF POOR QUALITY

NASA Ames Research Center, Dryden Flight Research Facility (DFRF) has operated two F-15 aircraft since 1976. One of these, the #2 F-15, was the propulsion test airplane in the full scale development program. The other, the #8 F-15, was the spin test airplane. NASA obtained these airplanes on loan to support a wide range of technology programs.

F-15 #2 supported a number of engine/inlet tests and engine component tests. Its major function was as the test aircraft for an extensive wind tunnel to flight correlation of pressure distributions and drag build-up data for the F-15 airplane. This program focused on the inlet and nozzle areas of the airplane. The airplane also supported a test of the shuttle tile system. A number of installations were made that simulated both the shuttle installation and induced the air loads the tile would experience while in flight. As a piggy-back experiment a probe that measured engine face static pressure (the PS2 probe) was tested. This probe later became one of the DEEC sensors. The airplane was retired following the shuttle tile/PS2 test program.

F-15 #8 was obtained to support a variety of handling qualities, buffet, tracking, and stability and control studies for this class of airplane. A major program, a test of a 10° included angle cone, is a standard wind tunnel calibration system for documenting turbulence. The flight program provided baseline data for tunnel to flight correlations. When the DEEC program began, the F-15 #2 was not available. The DEEC propulsion program was put on ship #8 as a matter of convenience.

DIGITAL ELECTRONIC ENGINE CONTROL PROGRAM

The DEEC program was a cooperative endeavor of the National Aeronautics and Space Administration (NASA), the U.S. Air Force (USAF), and Pratt and Whitney Aircraft (PWA). Each party had a desire to pursue the development of the DEEC through a technology development program that included flight test, but each party had limitations on its ability to support such a program. By combining forces in a cooperative program, the goals could be achieved.

NASA brought to the program a flight and ground test capability; Pratt and Whitney provided the engine control system and engine modification, along with engineering and technical support; and the USAF provided flight clearance support at Arnold Engineering Development Center (AEDC). From NASA's viewpoint, this was a nearly optimum way to conduct a program such as the DEEC flight test.

Because of the absence of written contracts outlining restrictions, a considerable amount of flexibility was allowed in the management of the program. This created an environment of mutual cooperation and support, and increased the productivity of individuals involved in the test program. In addition, this type of management allowed a quick response to technical concerns, a latitude in program adjustments when unforeseen circumstances occurred, and a lack of pressure, from a schedule viewpoint.

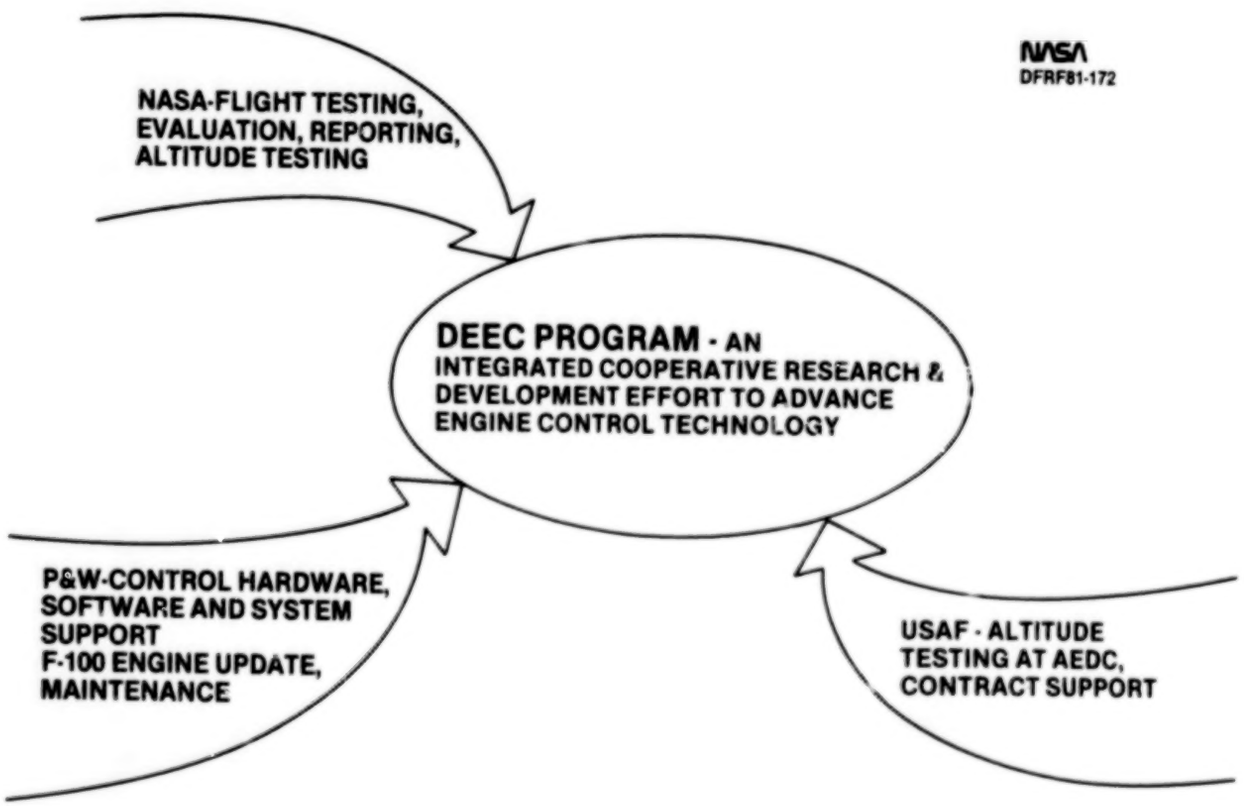
NASA
DFRF81-172
NASA-FLIGHT TESTING, EVALUATION, REPORTING, ALTITUDE TESTING
DEEC PROGRAM - AN INTEGRATED COOPERATIVE RESEARCH & DEVELOPMENT EFFORT TO ADVANCE ENGINE CONTROL TECHNOLOGY
P&W-CONTROL HARDWARE, SOFTWARE AND SYSTEM SUPPORT F-100 ENGINE UPDATE, MAINTENANCE
USAF - ALTITUDE TESTING AT AEDC, CONTRACT SUPPORT

DIGITAL CONTROL FOR THE F100

The DEEC is a full authority digital control system for the F100 Turbofan engine. It incorporates extensive fault detection and accommodation features that allow for safe and reliable operation on a single digital channel. The digital computer system also permits much simpler hardware to be used in the engine control system by the elimination of cams, valves, and other components that are necessary in a hydro-mechanical control system. The DEEC system does incorporate a backup control (BUC) that is used if the primary digital control should fail. The BUC is a simple hydro-mechanical system usable over the entire envelope; however, maximum thrust available is only about 80 percent of the DEEC intermediate thrust.

The benefits postulated for the DEEC system were numerous. Benefits assessed in the NASA program included increased thrust, faster response times, improved afterburner operation, improved airstart envelope, elimination of ground trimming, and the fail-operate capability. In addition, the DEEC system promised improved reliability over the basic F100 control system, and, because of a combination of factors, lower overall life cycle costs. The NASA program only addressed the performance aspects of the DEEC benefits.

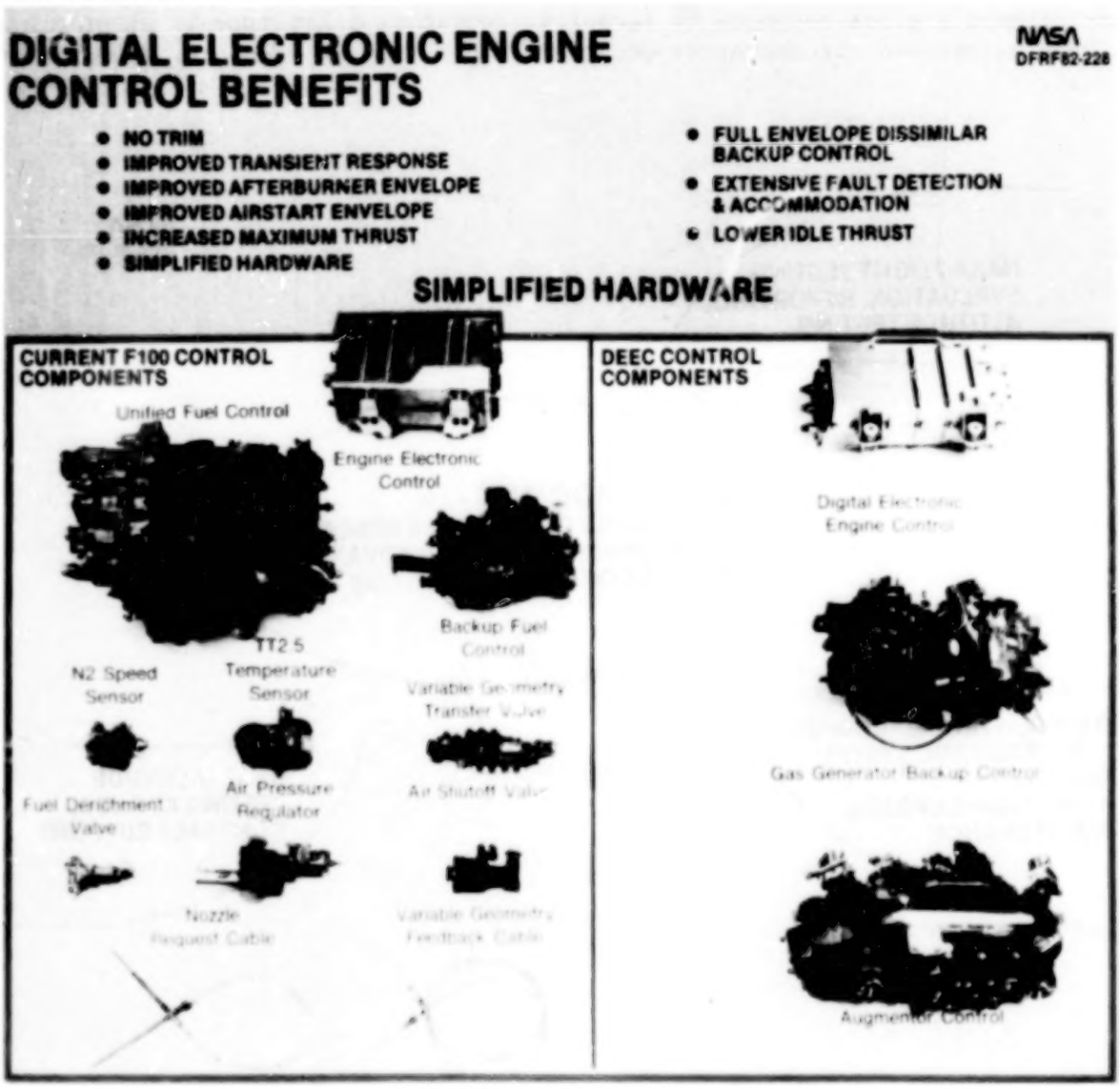

ORIGINAL PAGE IS
OF POOR QUALITY

The DEEC development started in the mid-1970's, largely through Pratt and Whitney independent research and development (IR&D). A series of sea level and altitude facility tests led to the USAF supporting the effort under the Engine Model Derivative Program (EMDP). At the same time the USAF was supporting the program, Pratt and Whitney and NASA were developing an approach that would permit a flight program to take place.

As illustrated, the flight program began in 1981. The program was broken into four phases, resulting in an orderly approach to maturing the system technology. The program was completed in early 1983.

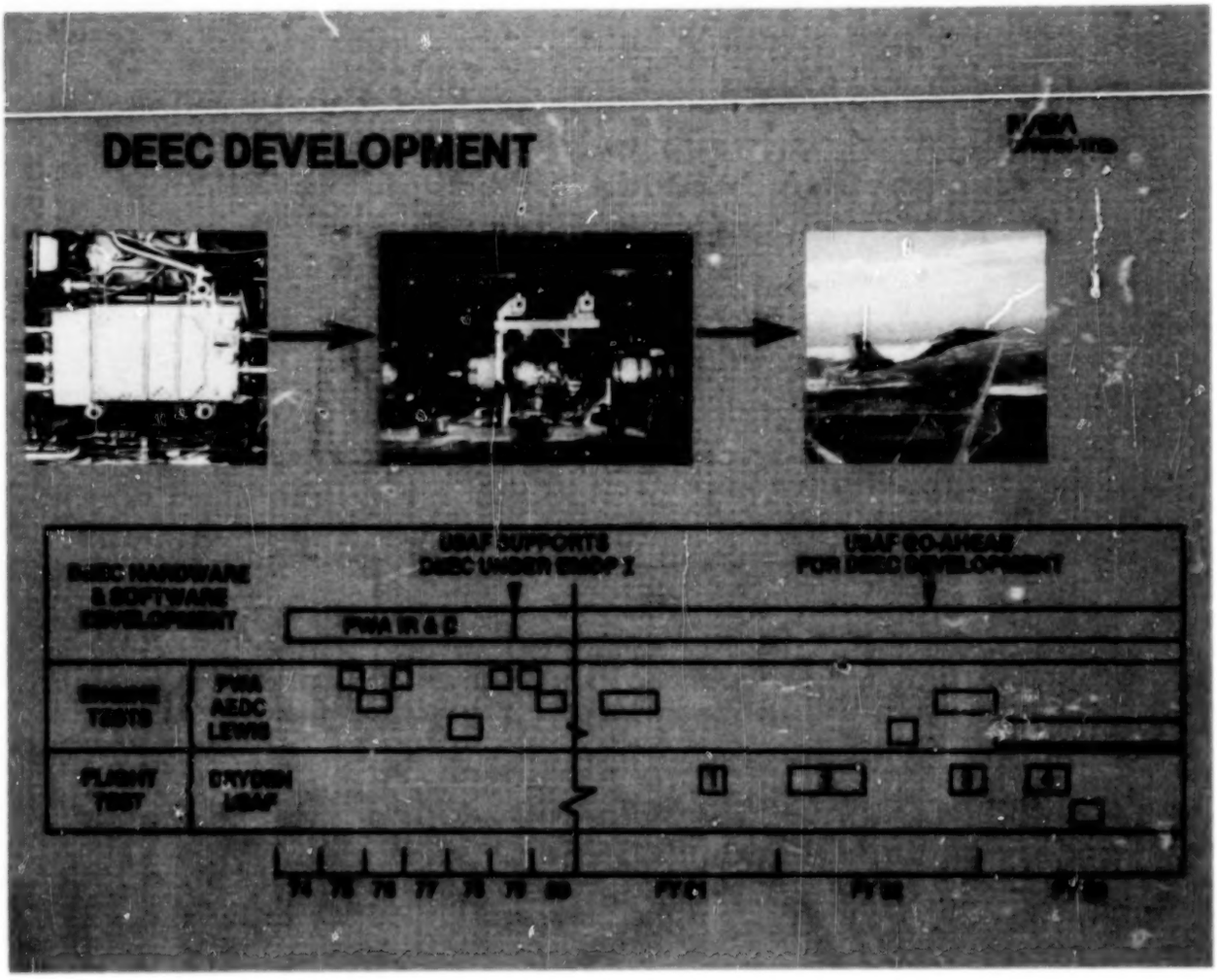

FLIGHT TEST OBJECTIVES

The objective of the program, from NASA's perspective, was to demonstrate and evaluate the DEEC system as applied to a modern turbofan engine and flown throughout the envelope of a high-performance fighter. Included within that overall objective were several subelements: to assess the fault detection and accommodation logic (which, as it turns out, was not a focus of the flight program); to evaluate the augmentor performance and durability improvements; and to validate the design and ground test procedures by comparison to flight tests. As shown later in the proceedings, the flight program surfaced some problem areas that were not predicted in ground facilities.

DEEC OBJECTIVES
NASA
DFRC81-173
• DEMONSTRATE AND EVALUATE A DIGITAL ELECTRONIC ENGINE CONTROL THROUGHOUT A MODERN FIGHTER ENVELOPE
NASA
10287
• ASSESS ENGINE CONTROL FAILURE DETECTION & ACCOMMODATION LOGIC
• EVALUATE ADVANCED AUGMENTOR PERFORMANCE AND DURABILITY IMPROVEMENTS
• VALIDATE DESIGN AND GROUND TEST PROCEDURES & RESULTS BY COMPARING WITH FLIGHT TEST RESULTS

INPUTS AND OUTPUTS

A modern turbofan engine has a large number of control variables and input parameters to the control laws. The DEEC system can control, over the entire range of authority, all the variables in the F100 engine. These include inlet guide vanes, compressor stators, bleeds, main burner fuel flow, the afterburner fuel flows, and the nozzle area. The inputs include static pressure at the compressor face (which is used to compute total pressure at that location), fan and core rpm, compressor face total temperature, burner pressure, turbine inlet temperature, turbine discharge pressure, an ultra violet detector in the afterburner to determine whether a flame is present, and the throttle position.

The extensive list of inputs and outputs graphically illustrates the difficulty of hydromechanical control system design and the need for digital controls.

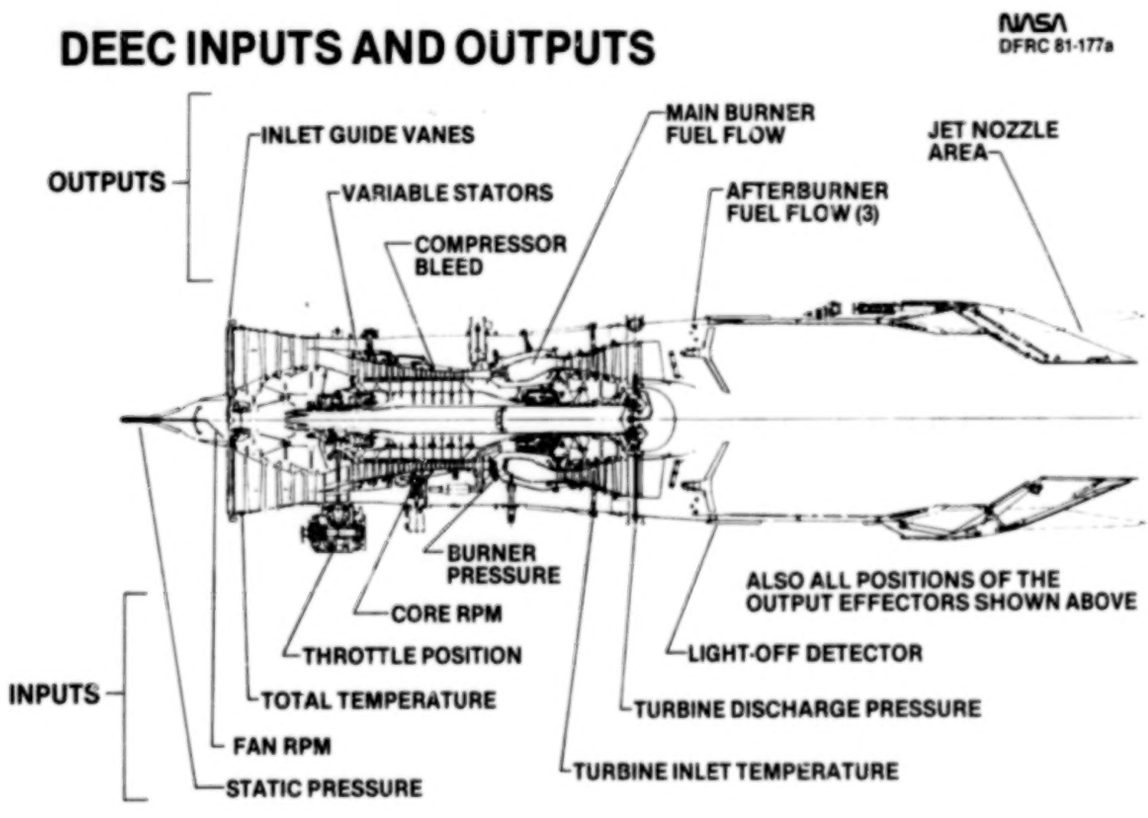

BASIC CONTROL MODES

The DEEC system has two basic control modes for the gas generator portion of the engine. The airflow control mode uses core fuel flow to control fan rotor speed (N1). The control mode transitions at military power to an engine pressure ratio (EPR) control, which uses the nozzle to maintain the proper turbine discharge total pressure/fan inlet total pressure (PT6M/PT2) relationship.

The logic involved in implementing these control modes is quite complex as is illustrated on the chart. Many inputs are required, which generate the engine state requests. These requests are compared to the actual conditions and then, through a series of schedules and closed-loop control algorithms, appropriate actions are implemented to bring the engine to the desired operating condition.

In addition to these functions the augmentor controls are resident in the DEEC system.

NASA
DFRF82-344

DEEC BASIC CONTROL MODES

CORE FUEL FLOW CONTROLS N1, NOZZLE AREA CONTROLS EPR

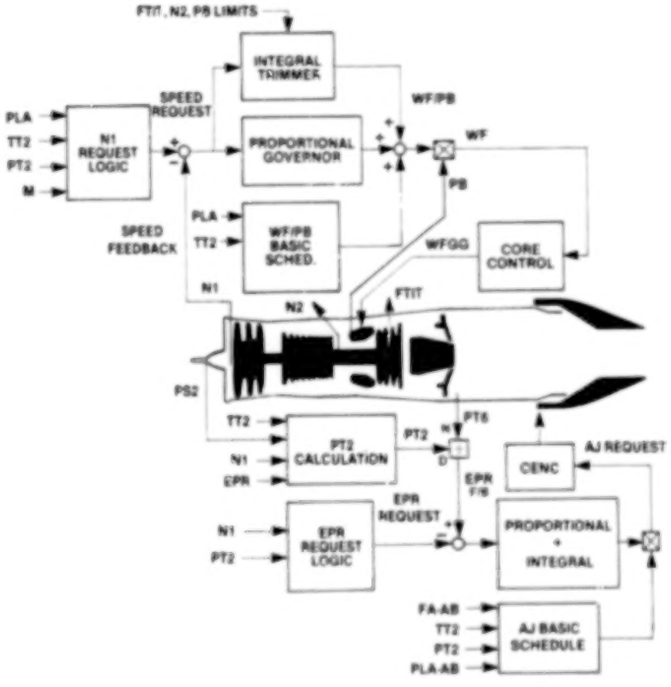

The test airplane was extensively instrumented, both for the engine and the basic airplane itself. The airplane data included airspeed, altitude, body-axis rates and attitude, accelerations, control-surface positions, and other parameters typical of a flight research program. The test engine was in the left side of the airplane and the right side engine had minimal data (that is, sufficient data to ascertain the health of the engine but not sufficient for any test work).

The parameters listed in the chart illustrate the extent of the engine instrumentation. As can be seen, the list is fairly extensive and includes all parameters necessary to monitor the health and performance of the engine. A major source of data was the DEEC digital words. This list grew with time, beginning with 50 words and increasing to 83 words by the end of the program. It has subsequently grown to 100 words. Included in this listing were 11 words (16 bits each) of diagnostic data — bits were turned on to indicate faults (malfunctions). In addition, the data stream output included the values used in the control calaculations.

All of these data were recorded on board and were also transmitted to the ground for use in NASA's real-time flight monitoring facility. The format was pulse code modulation (PCM), which permitted relatively quick and extensive post-flight processing.

DEEC FLIGHT INSTRUMENTATION

NASA
DFRF82-016b

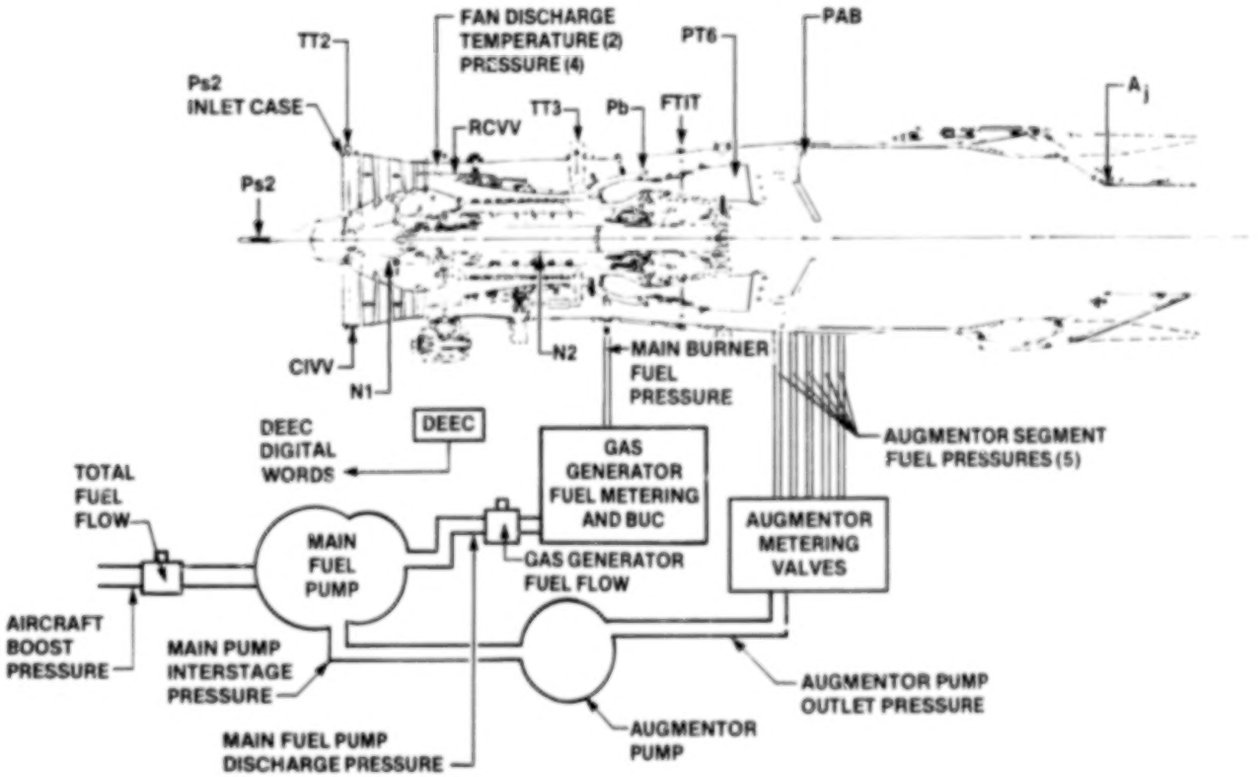

TEST POINTS FLOWN

This chart illustrates the flight envelope and types of tests conducted in the flight program. While the entire F-15 envelope was covered, the emphasis was on the ULHC of the envelope. Evaluation of the DEEC was accomplished through throttle transients, airstarts (spooldown and jet fuel starter (JFS)-assisted in both the primary and backup modes), back up control evaluations, augmentor transients of all varieties, and by maneuvering the airplane through climbs and accelerations. The number of flight conditions and types of evaluations conducted provide a sound basis for evaluating the performance and operability aspects of a DEEC-equipped F100 engine.

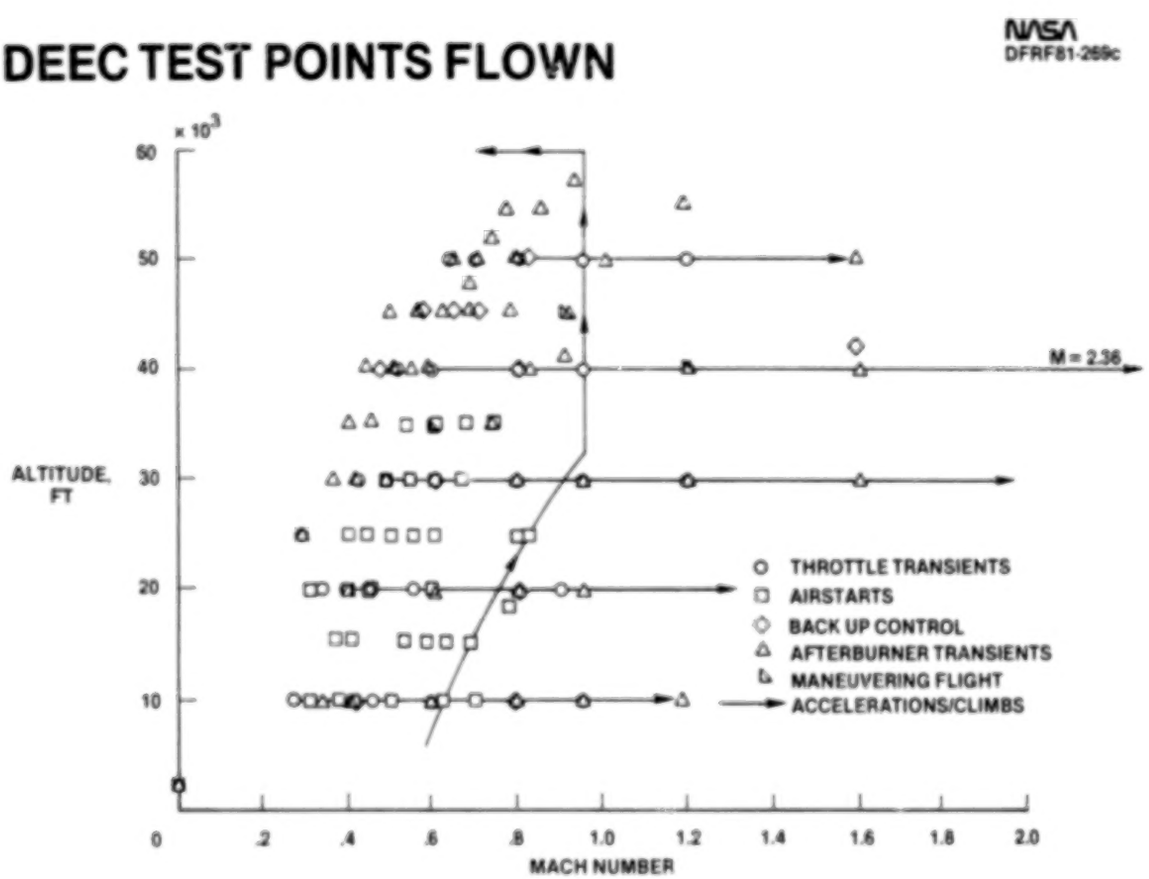

FLIGHT RESULTS

ORIGINAL PAGE IS
OF POOR QUALITY

The NASA flight program consisted of 30 flights with a total of 35.5 hours of flight time. This included seven aerial refuelings. The maximum Mach achieved was 2.36 and the maximum altitude was 60,000 feet. A large number of transients, airstarts, and other tests were accomplished during the relatively low number of flights. Almost 1300 total transients, in addition to more than 150 airstarts, were accomplished. BUC was also evaluated through throttle transients and other tests. Because there were no automatic transfers to BUC, the BUC was pilot-selected in each case.

TEST PROGRAM

As previously stated, the flight program was broken into four phases. The purpose of Phase I was to verify the airworthiness of the DEEC system. Phase II expanded the program to include the augmentor operability assessment, primarily in the upper left-hand corner (ULHC) of the envelope. While the augmentor worked reasonably well (slightly better than the production system), some problems did occur. These included an instability in the nozzle control loop, some instances of rumble, and some blow-outs. Phase III incorporated fixes to the nozzle instability and other hardware changes in the augmentor, in addition to the second-generation BUC. Phase IV added the light off detector (LOD) to the augmentor control logic, as well as software, to permit augmentor light off at less than military power. The software change in light-off logic (called the fast-acceleration) essentially halved the idle-to-maximum time at high-speed, low-altitude conditions. The time saving was eliminated as the speed dropped and altitude increased. The following papers will report on the results of the program through Phase IV.

Follow-on flight test programs include the F100 Engine Model Derivative (EMD), a DEEC-equipped growth version of the F100 and a program specifically intended to evaluate the fault detection/accommodation logic of the DEEC. In that program, faults will be intentionally induced to cause the DEEC to revert to a mode that will permit continued safe operation in the digital mode.

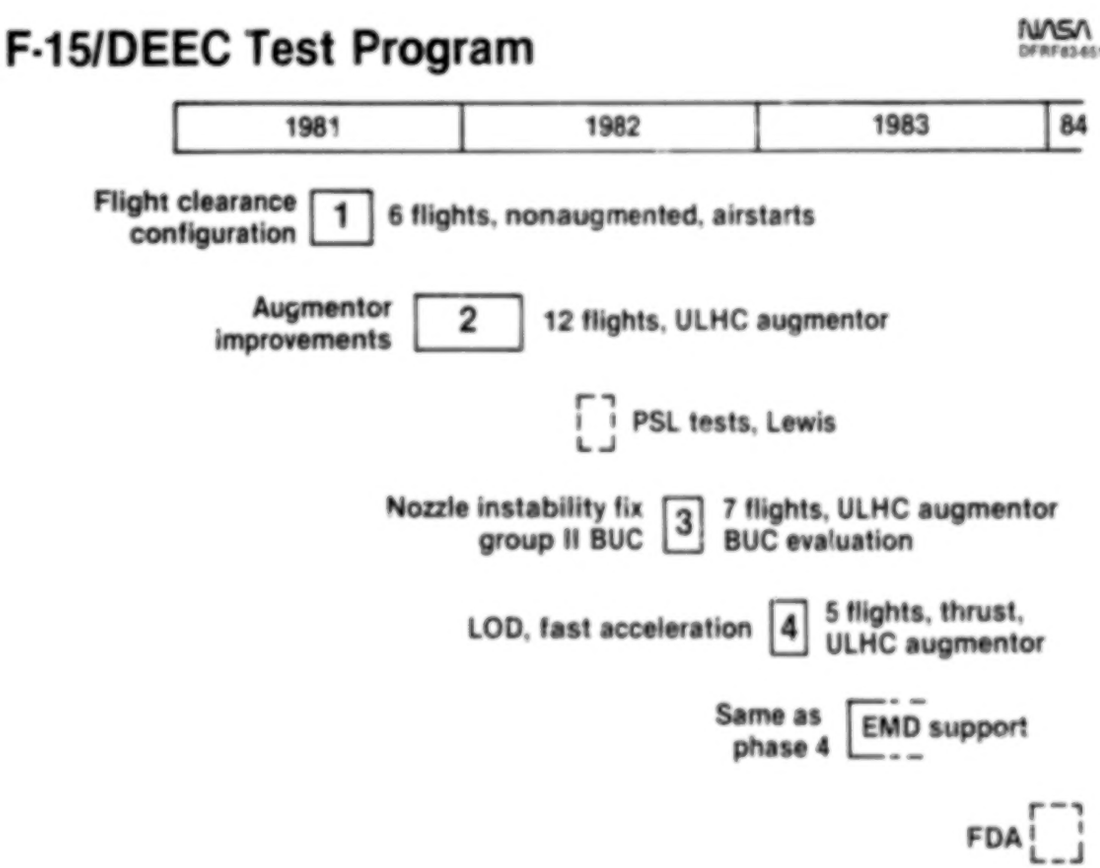

DESIGN OBJECTIVES MET

ORIGINAL PAGE IS
OF POOR QUALITY

The features of the DEEC were verified in the flight test program. For example, the no-trim feature, verified through methods such as computer hardware replacements and engine removals, effected a substantial savings. The operability of the augmentor was improved; for illustration, the idle to maximum altitude capability was increased nearly 15,000 feet. The spooldown airstart airspeeds were significantly reduced, thus allowing greater flexibility to the pilot in accomplishing an airstart. The fast-acceleration capability was also demonstrated. The DEEC system met its performance design objectives.

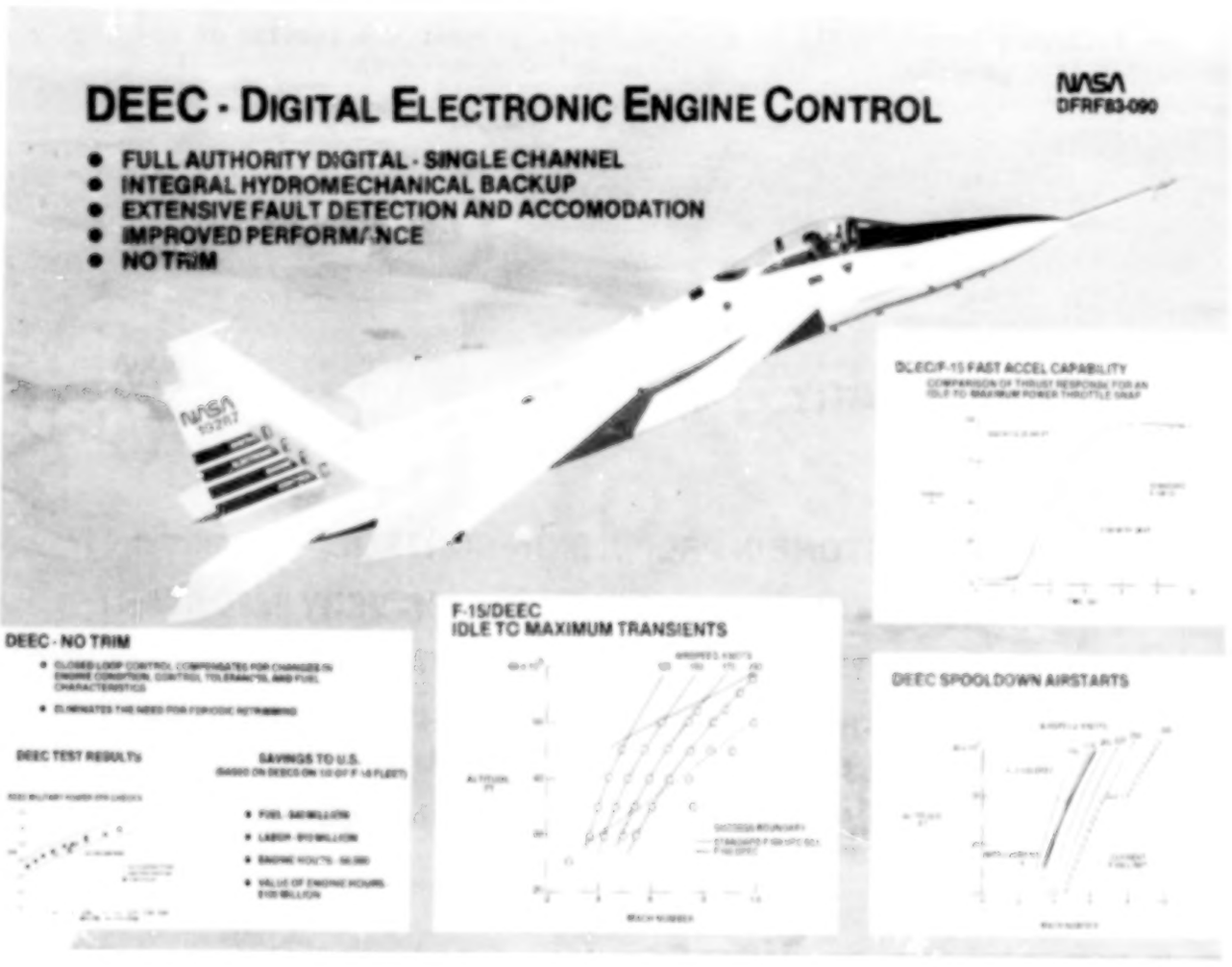

CONCLUDING REMARKS

The DEEC development is a milestone in propulsion control and marks the transition from hydromechanical control to the digital realm. NASA is proud of the technology contributions made to the program. As will be illustrated, the benefits to the F100 engine are substantial and include costs, performance, and operability considerations. The USAF has stated its decision to embark upon a full scale development program that is attributable, in part, to the success of the program reported herein.

From a technology viewpoint, the maturity of the DEEC system will permit follow-on research programs to take place. One of these is the fault detection and accommodation (FDA) program as well as an airframe/engine control integration program called highly integrated digital electronic control (HIDEC). A subsequent paper will address the HIDEC program.

The following papers will, in greater depth, present the results of the highly successful DEEC program.

DEEC SUMMARY

NASA
DFRF82 057

- A MILESTONE IN PROPULSION CONTROL
- NASA TECHNOLOGY CONTRIBUTION VERY IMPORTANT
- BENEFITS TO THE F100 ARE SUBSTANTIAL
- USAF FULL SCALE DEVELOPMENT PROGRAM – DIRECT RESULT OF F-15 FLIGHT PROGRAM
- FOLLOW-ON RESEARCH OPPORTUNITIES

N86
25344

UNCLAS

N86-25344

DIGITAL ELECTRONIC ENGINE CONTROL HISTORY

Terrill W. Putnam
NASA Ames Research Center
Dryden Flight Research Facility
Edwards, California

SUMMARY

Full authority digital electronic engine controls (DEECs) have been studied, developed, and ground tested for many years because of projected benefits in operability, improved performance, reduced maintenance, improved reliability, and lower life cycle costs. All of these benefits cannot be truly assessed until DEECs are produced in quantity and operated over a significant length of time. However, the issues of operability and improved performance can be assessed in a flight test program.

As part of NASA's ongoing commitment to extend and improve propulsion system technology, the NASA Dryden Flight Research Facility entered into an agreement with the U.S. Air Force (USAF) Deputy for Propulsion and the Government Products Division of Pratt and Whitney Aircraft to demonstrate and evaluate the DEEC on an F100 engine in an F-15 aircraft.

The events leading up to that flight test program are chronicled and important management and technical results are identified.

N86-27914

HISTORY

The DEEC program began in 1973 with configuration studies conducted by Pratt and Whitney. In 1978, NASA Lewis Research Center (LeRC) began its participation in the program by testing a breadboard version of a DEEC on engine P072 in an altitude facility. In 1979, the USAF requested that Dryden demonstrate and evaluate the DEEC by flying a DEEC-equipped F100 engine in one of the USAF F-15s loaned to NASA. The NASA flight test program began in 1981; this history covers the events up until that time.

It should also be observed that Pratt and Whitney developed the DEEC on independent research and development (IR&D) funds. During the mid-1970s, two other digital engine programs were also improving and adding to the digital engine control data base. They were the full authority digital engine control (FADEC) program sponsored by the U.S. Navy (USN) and the integrated propulsion control system (IPCS) program sponsored by the USAF and NASA.

NASA
DFRF83-617a

DEEC History

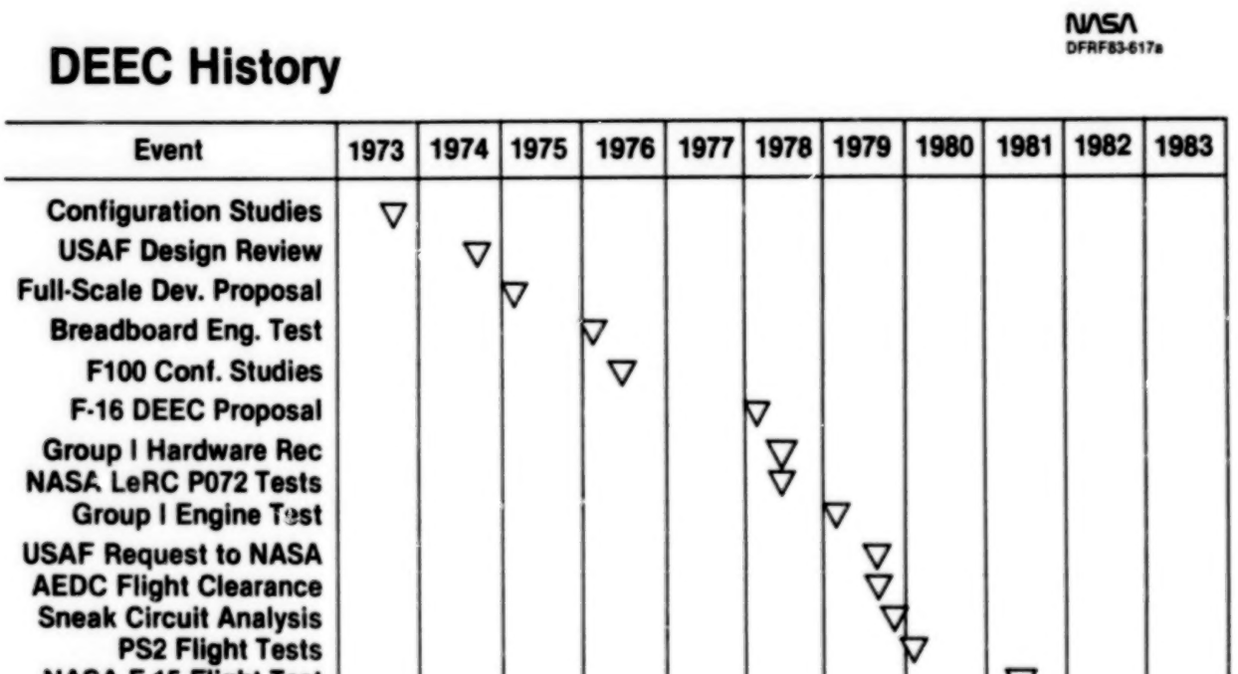

PROGRAM AGREEMENT

One of the keys to the succcess of the DEEC program was the agreement between NASA and the USAF. The existing USAF/NASA memorandum of agreement (MOA) for the F-15 program was used so that no new formal agreements had to be developed and approved. It was agreed among the program participants that the program would be cooperative and mutually beneficial to each participant.

NASA/USAF DEEC Program Agreement

NASA
DFRF83-618

1979 · USAF · ASD/YZ requests NASA to flight test the DEEC/SA in a mutually beneficial cooperative program

- **Related to NASA Interact Program**
- **USAF initiated Engine Model Derivative Program**
- **Utilized NASA/USAF F-15 MOA**
- **USAF & P&W propose cooperative DEEC/SA demonstration program**

Another key to the success of the DEEC program was the management structure. The program and technical decisions were usually made at the first level of management within the respective organizations. Also shown is the organizational level at which the loan agreement for engine P063 and the F-15 MOA were implemented.

NASA
DFRF83-1795

DEEC Program Management

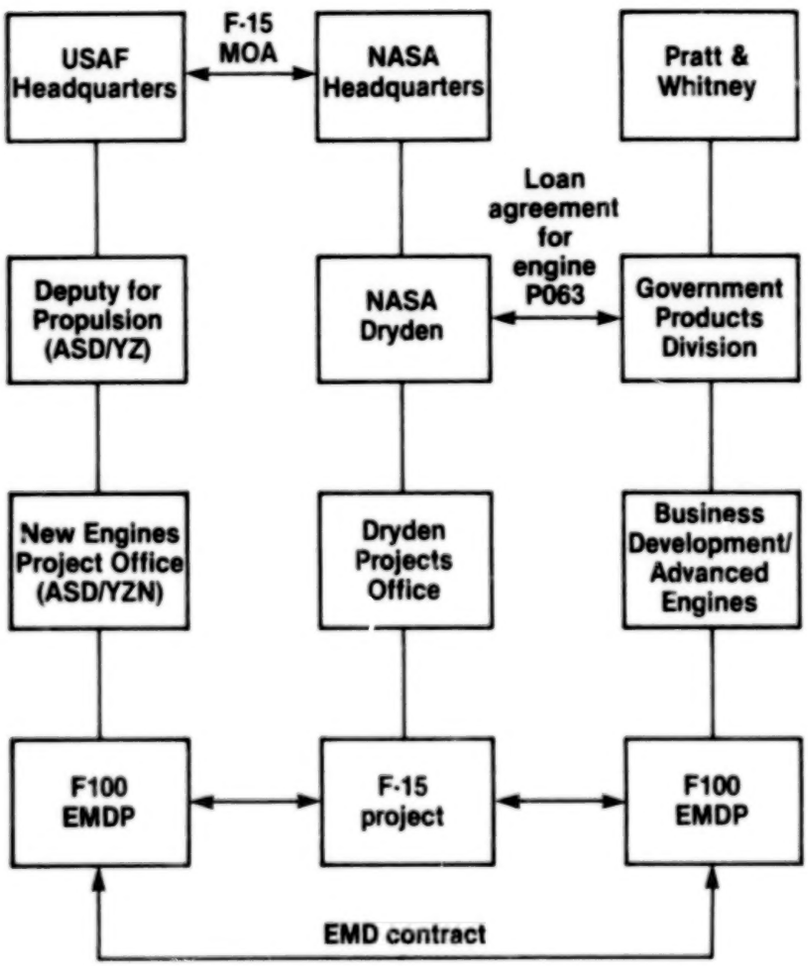

ORGANIZATIONAL RESPONSIBILITIES

The responsibilities for the DEEC program were divided between NASA, USAF, and Pratt and Whitney, as shown. There was practically no overlap and each organization possessed the knowledge, skills, and resources necessary to discharge respective responsibilities.

Organizational Responsibilities

NASA
DFRF83-620

NASA

- Conduct of the Flight Test Program & Reporting of Results
- Provide Altitude Facility Support as available
- Provide Funding for F-15 and Altitude Facility
- Responsible for Flight Safety

USAF

- Provide AEDC Test Support including funding
- Develop and implement USAF Flight Clearance Requirements
- Conduct Program Reviews

P & W

- Conduct S/L Tests and support Altitude & Flight Tests
- Provide DEEC control hardware and software
- Update F100 (2 7/8) engine to F100 (3) configuration
- Provide funding for hardware and software development and support

The program orginally agreed to by NASA, USAF, and Pratt and Whitney was for the demonstration and evaluation of both a DEEC and a swirl augmentor (SA). The objectives of that program are listed. The swirl augmentor was designed to primarily improve the steady state augmentor performance, increase the rumble altitude limit, reduce the idle thrust, and reduce the infrared (IR) signature of the engine.

DEEC/Swirl Augmentor

NASA
DFRF83-621

Objectives

- Improve Safety, Reliability and Maintainability
- Improve ULHC Transient Performance
- Improve Augmentor Steady State Performance
  - Raise Rumble Altitude limit
  - Reduce IR signature
- Reduce Ground Idle Thrust
- Reduce Required Air Start Airspeed
- Eliminate Ground Trim

(April 1979)

SYSTEM TEST EXPERIENCE

The DEEC software, control logic, and hardware were extensively tested on a variety of F100 engines, both at sea level and in altitude facilities. Prior to 1979, the software and logic were tested using breadboard hardware which had been developed in the full authority electronic control (FAEC) program. In 1979 and later, the flight prototype hardware was also tested. Because of various failures of ground test engines in 1979 and 1980, which were unrelated to the DEEC, the flight test engine P063 was ultimately tested at sea level and in the Arnold Engineering Development Center (AEDC) altitude facility to qualify the DEEC system for flight.

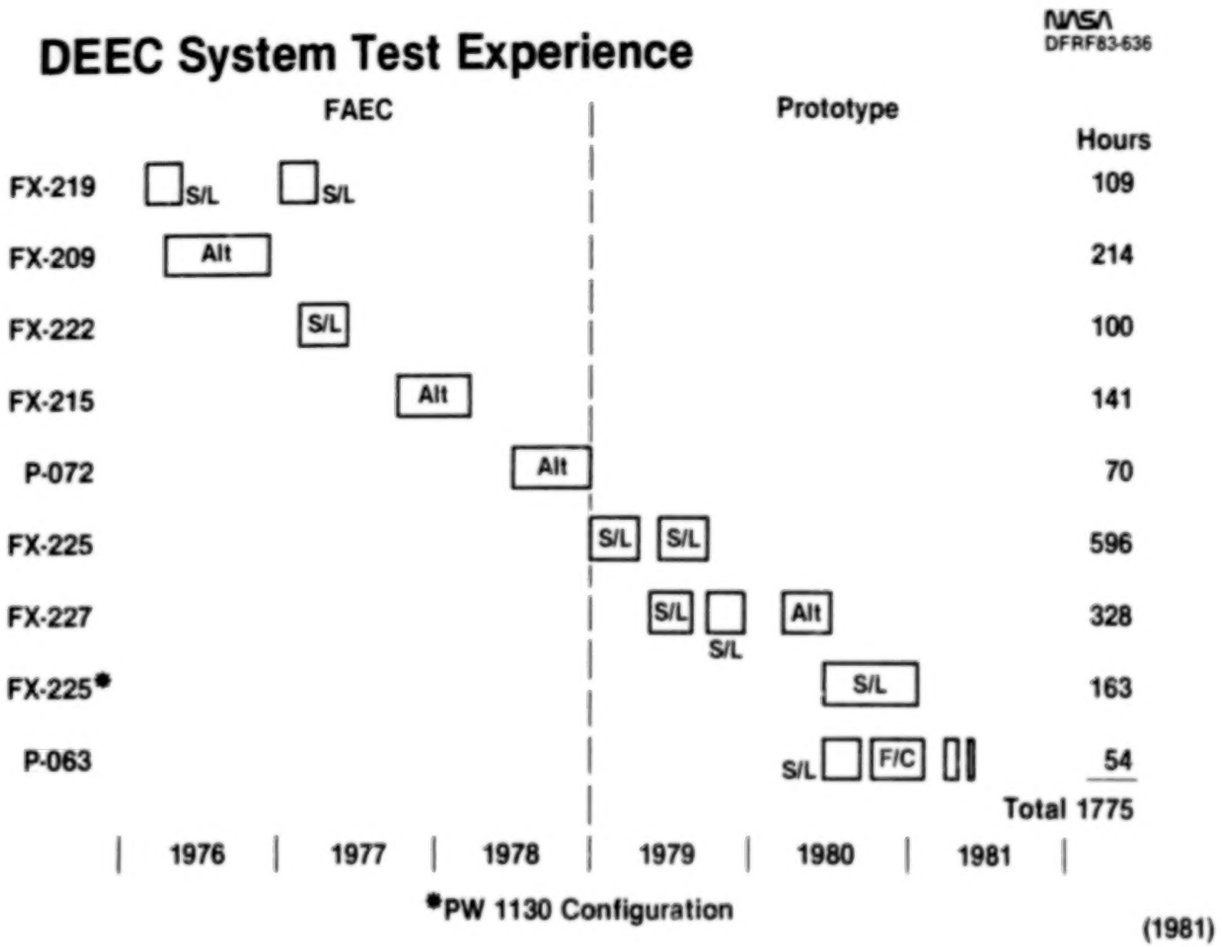

SUPPORT FOR PW 1128 PROGRAM

The LeRC altitude facilities and engineering expertise were extensively applied to the development of the DEEC/swirl augmentor system in 1978 and 1979. The basic calibration of the fan inlet static pressure (PS2), used by the DEEC for engine control, was established at LeRC. LeRC facilities and personnel were again used in 1980 to investigate a nozzle instability observed in flight and to assist in the development of a solution to the instability. Research and development on the light off detector (LOD) used by the DEEC was also conducted at LeRC.

NASA LEWIS SUPPORT FOR PW1128 PROGRAM

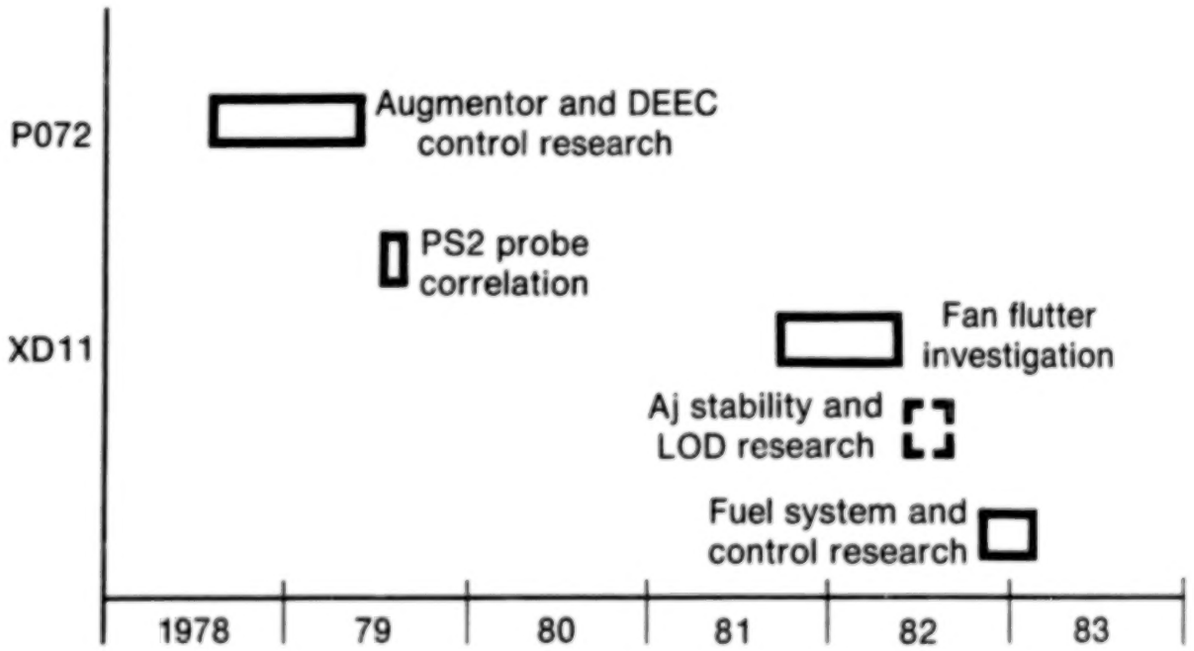

AV261031 831404 3631B

P072 ENGINE TESTING

Engine testing was completed at LeRC with DEEC and a swirl augmentor (SA). Preliminary results indicated the projected improvements in operability and performance were realized.

P072 at NASA Lewis with DEEC and SWIRL A/B

NASA
DFRF83-626a

- Successful demonstration in ULHC and supersonic with no trim or adjustments
- Improved rumble tolerance (+ 7000 ft)
- Successful idle-to-maximum transients at Mach 0.6 and 52,000 ft
- PT2/PS2 correlation test with distortion scheduled

(April 1979)

The early results of the AEDC altitude tests in late 1979 and early 1980 seemed to confirm the benefits of the DEEC swirl augmentor observed in the LeRC test. Throttle transients, performance, airstarts, and transfers to the backup control (BUC) were demonstrated and evaluated throughout the flight envelope.

F100 EMDP Accomplishments at AEDC

NASA
DFRF83-630a

FX-227 with DEEC/SA has demonstrated successful operation throughout flight envelope

- **ULHC idle-to-maximum transients at Mach 0.8 and 47,500 ft/0.040 F/A**
- **Spooldown restarts to 200 knots at 30,000 ft**
- **Steady-state performance and transients to Mach 2.3 and 50,000 ft**
- **BUC transfers throughout flight envelope to Mach 2.3 and 50,000 ft**
- **No trim demonstrated in 82 hours**

Additional analysis of the LeRC and AEDC altitude facility results indicated that the benefits observed were entirely due to the DEEC system, and not to the swirl augmentor. In fact, it was determined the swirl augmentor reduced the rumble-free altitude limits. This points out the danger of testing multiple system changes that interact with each other and where the benefits and losses due to each system are not easily separable.

P063 Augmentor Will be Non-Swirl

NASA
DFRF81-628a

Swirl Augmentor Has Less Rumble Margin

Facts

- P072 swirl augmentor test data show lower rumble-free altitude limits.
- FX-227 swirl augmentor shows low rumble capability.
- Analytical assessment predicts 1300 ft altitude loss. Test data shows 5000 ft loss.

Conclusion

- Non-swirl augmentation appears more stable.

(August 1980)

The augmentor features selected for incorporation into the flight test engine, P063, and DEEC system are shown below. Also shown are the benefits that were expected to be produced by each feature.

P063 Augmentor Features

NASA
DFRF83-629e

Augmentor Improvements Quantified and Added to P063 Flight Clearance Configuration

P063 Flight Clearance	
• Ducted flameholder	• Increase rumble-free altitude by 6000 ft
• Improved cooling zero aspiration liner	• Double liner life
• Dual ignition	• Reduce mislights by a factor of 3
• LOD	• Stall avoidance, faster accelerations
Additional Derivative II Features	
• Segment VI	• Increase supersonic thrust by 2 to 4%
• Cut-back nozzle cooling liners	• Increase non-augmented thrust by ½ %
• Retailored S/R's	• Increase combustion efficiency 5%
	• Reduce hot streaks by 200° F
	• Increase rumble-free altitude by 6000 ft
• CIP durability fixes	• Improved durability and reliability

(August 1980)

The major areas of test emphasis for the flight clearance of the flight test engine, P063, and DEEC system are shown below. Items VII and VIII were not accomplished because test time ran short and they were not critical for first flight. A new back up control (BUC) schedule was to have been implemented electronically to validate its operation. The mechanical schedules implemented in the prototype BUC hardware had already been identified as needing improvement.

P063 AEDC Test Plan

NASA
DFRF83-621

I. Instrumentation and installation checkout
II. Sea level performance and mini-checkout
III. ULHC A/B evaluation
IV/V. Failure detection and accommodation
VI. Stall recovery and avoidance
→ VII. Electronic BUC evaluation
→ VIII. Preliminary LOD evaluation
IX. ULHC A/B evaluation with improvements
X. Final flight checkout

ALTITUDE TEST RESULTS

The final flight clearance test of the flight test engine, P063, at AEDC are shown below. All major objectives were met successfully and the engine with the DEEC was declared ready for flight.

AEDC Altitude Test Results

NASA
DFRF83-053

- BUC transfers successful
- Steady state performance within bands
- Transients OK to Mach 0.8 and 45,000 ft
- Airstarts successful at 200 knots/30,000 ft
- Bode capacity demonstrated to Mach 0.8 and 45,000 ft
- Stall recovery demonstrated
- Failure detection and accomodation validated

SOFTWARE VERIFICATION TEST

The DEEC software verification and validation used by Pratt and Whitney is shown below. The original process did not include the real-time dynamic closed-loop simulation. During the DEEC system review process, Dryden assigned an engineer with substantial experience in qualifying digital flight control systems for flight. The real-time simulation was added to the verification test process at his request. The simulation subsequently proved its value by identifying a previously undetected fault in the software.

DEEC Software Verification Tests

NASA
DFRF83-635

- Verification achieved throught established/organized multi-level disciplines

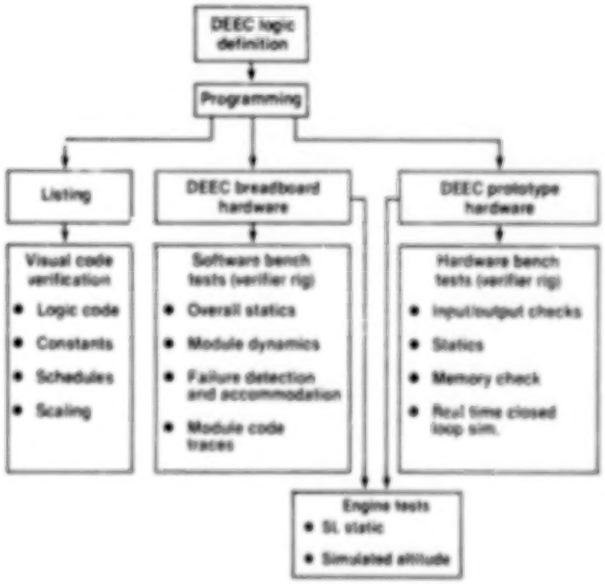

- Visual code verification, software and bench tests of 2.3.4 baseline logic completed 1980.
- Software verification review held for USAF and NASA 10/28-29/80.
- Updates incorporated in flight DEEC 2.3.6A logic.

COMBINED ENVIRONMENTAL RELIABILITY TEST

The DEEC computers underwent an extensive combined environmental and reliability test (CERT) in the laboratory as illustrated below. Six units were mounted in a chamber that was evacuated to simulate altitude. The chamber and computers were subjected to random vibrations and the air inside the chamber was conditioned to be similar to the engine bay environment. The computers were powered and running representative software programs, and were cooled with fuel. Fifty thousand hours of simulated field usage was completed on six units.

DEEC "COMBINED ENVIRONMENTAL RELIABILITY TEST" (CERT)

50,000 hours simulated field usage on 6 units, completed

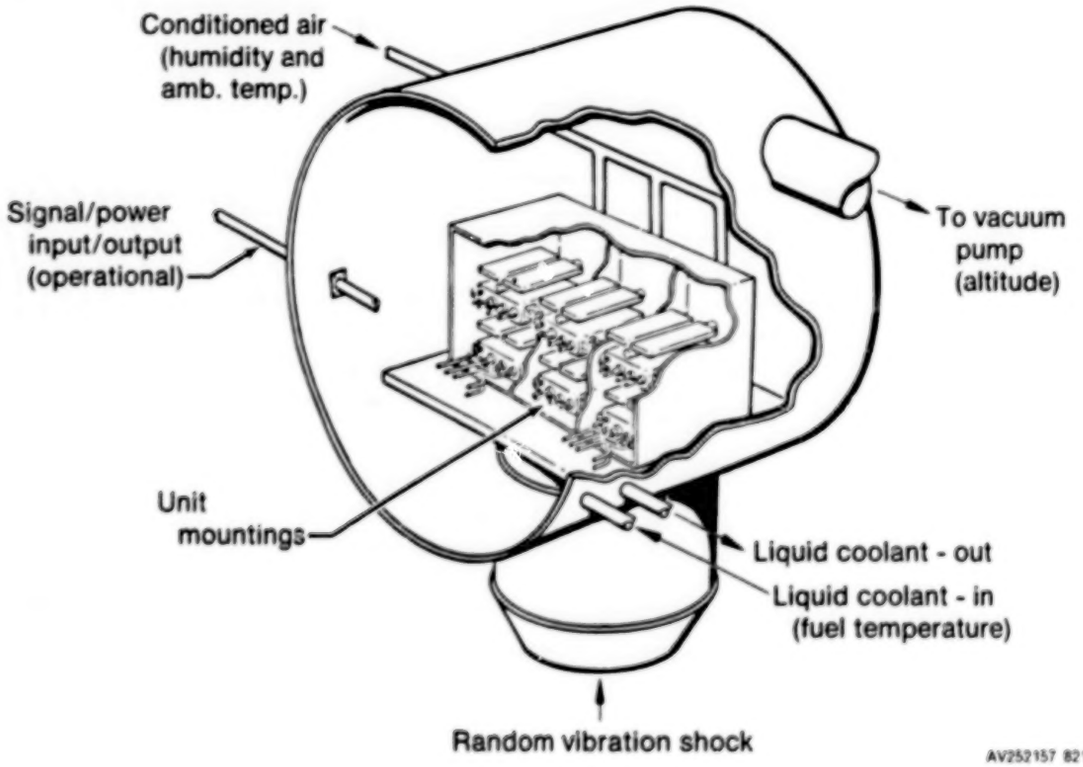
Conditioned air (humidity and amb. temp.)
Signal/power input/output (operational)
To vacuum pump (altitude)
Unit mountings
Liquid coolant - out
Liquid coolant - in (fuel temperature)
Random vibration shock

AV252157 821910 0576B

MEAN TIME BETWEEN FAILURE TRACKING

The mean time between failures (MTBF) for the DEEC computer, established during the CERT, is shown below. The cumulative MTBF exceeded 1390 hours after 50,000 hours of simulated field usage. Components that were found to have marginal or inadequate performance in the CERT were replaced in the flight DEEC units as they were identified.

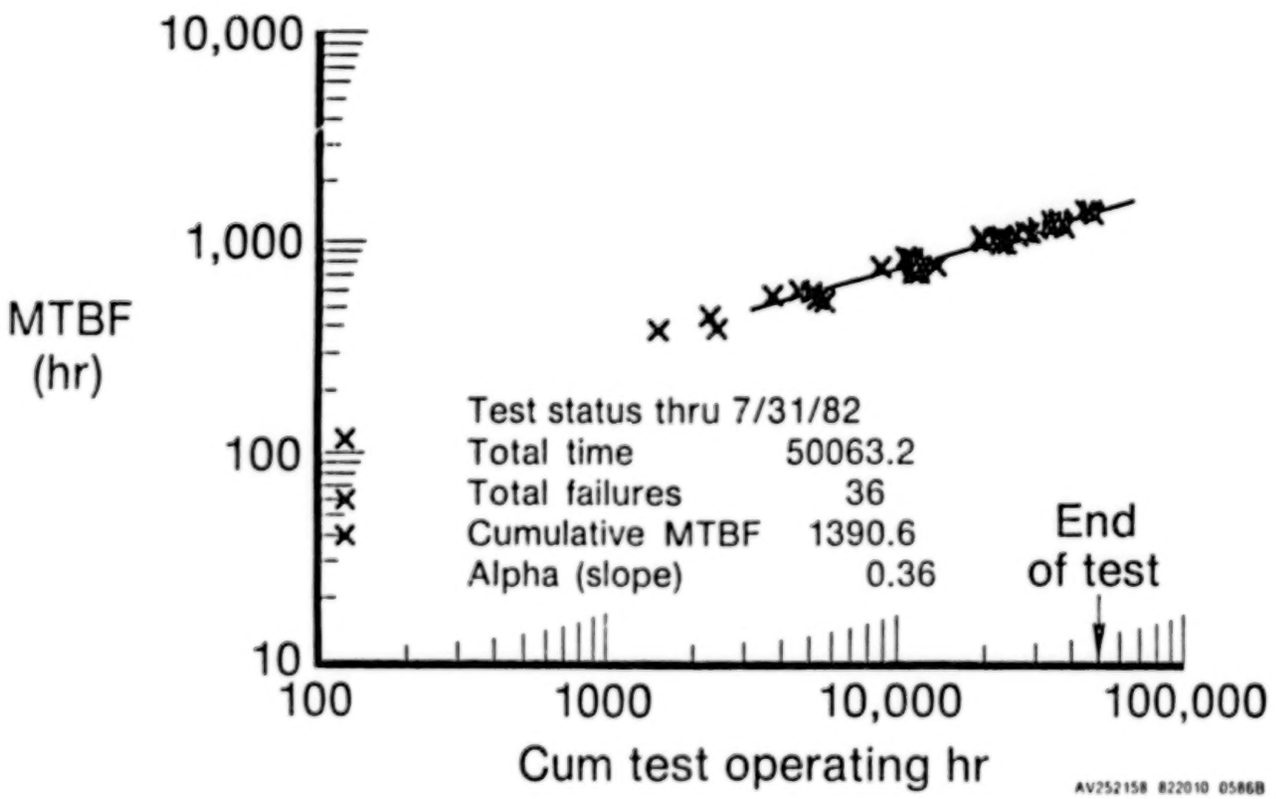

N86
25345

UNCLAS

N86-25345
Paper 3

F-15 DIGITAL ELECTRONIC ENGINE CONTROL SYSTEM DESCRIPTION

Lawrence P. Myers
NASA Ames Research Center
Dryden Flight Research Facility
Edwards, California

SUMMARY

A digital electronic engine control (DEEC) system has been developed by Pratt and Whitney Aircraft for use on the F100-PW-100 turbofan engine. This control system has full authority control, capable of moving all the controlled variables over their full ranges. The digital computational electronics and fault detection and accommodation logic maintains safe engine operation. A hydromechanical backup control (BUC) is an integral part of the fuel metering unit and provides gas generator control at a reduced performance level in the event of an electronics failure. This paper will describe the DEEC features, hardware, and major logic diagrams.

FEATURES

The DEEC control system has the following features:

- A full authority digital control system capable of moving all the controlled variables over a full range. The control is basically single channel with selective input/output redundancy to maintain gas generator control for any single failure.

- Improved afterburner operation in the upper left hand corner (ULHC) of the flight envelope by use of software logic to limit operation to segment 1 at about Mach 0.4 and 40,000 ft to Mach 1.0 and 50,000 ft; and at altitudes up to about Mach 0.9 and 20,000 ft allowing afterburner initiation to occur at idle on idle-to-maximum power throttle transients.

- Fault detection and accommodation by selective input and output redundancy and parameter synthesis to maintain gas generator control with any single failure.

- Dissimilar BUC, an integral part of the gas generator fuel metering valve unit. The BUC maintains hydromechanical control of the gas generator at a reduced performance level.

- Simplified hardware by reduction of the number of components and quick access to 15-line replaceable units (LRUs) which do not require calibration.

PRECEDING PAGE BLANK NOT FILMED

ORIGINAL PAGE IS
OF POOR QUALITY

- A fan inlet static pressure (PS2) probe extending about 18 inches in front of the engine inlet.
- A computer that is engine mounted on shock isolators and fuel cooled.

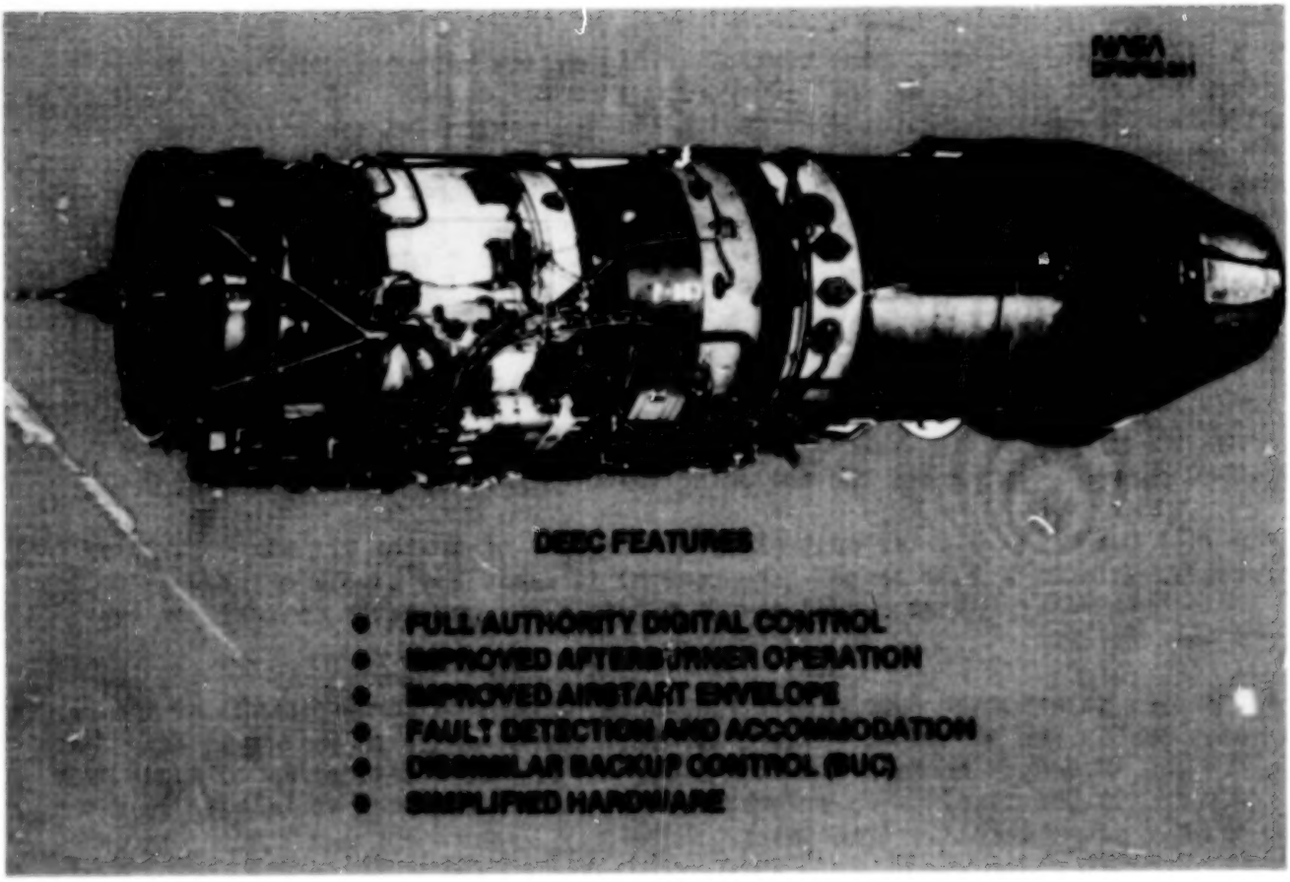
DEEC FEATURES
• FULL AUTHORITY DIGITAL CONTROL
• IMPROVED AFTERBURNER OPERATION
• IMPROVED AIRSTART ENVELOPE
• FAULT DETECTION AND ACCOMMODATION
• DISSIMILAR BACKUP CONTROL (BUC)
• SIMPLIFIED HARDWARE

F100 TEST ENGINE

The F100-PW-100 engine is a low-bypass ratio (0.8), twin-spool, afterburning turbofan. The three-stage fan is driven by a two-stage, low-pressure turbine. The 10-stage high pressure compressor is driven by a two-stage turbine. The engine incorporates compressor inlet variable vanes (CIVVs) and rear compressor variable vanes (RCVVs) to achieve high performance over a wide range of power settings; a compressor bleed is used only for starting. Continuously variable thrust augmentation is provided by a mixed-flow afterburner, which is exhausted through a variable-area convergent-divergent nozzle.

The augmentor incorporates five spray ring (S/R) segments which come on sequentially. Segments 1, 2, and 4 are located in the core stream, and segments 3 and 5 are located in the fan duct stream. The augmentor is equipped with dual-augmentor ignitors, whereas the standard F100 engine has only one. It also has a ducted core flameholder, which ducts a small amount of hot core flow to the flameholders located in the fan duct stream. The standard F100 engine flameholder does not duct any core air to the fan duct stream. The engine was also equipped with a static pressure probe on the engine hub which is not on the standard F100 engine.

The F100 engine used for the DEEC evaluation was Serial Number 680063. It had been rebuilt from an earlier F100(2) engine to a zero-time F100(3) configuration with the DEEC system before the DEEC flights. The engine had accumulated 9.8 hr of sea level testing and 45.4 hr at an altitude facility before the first DEEC flights.

F100 DEEC Test Engine

NASA
DFRF83-1802

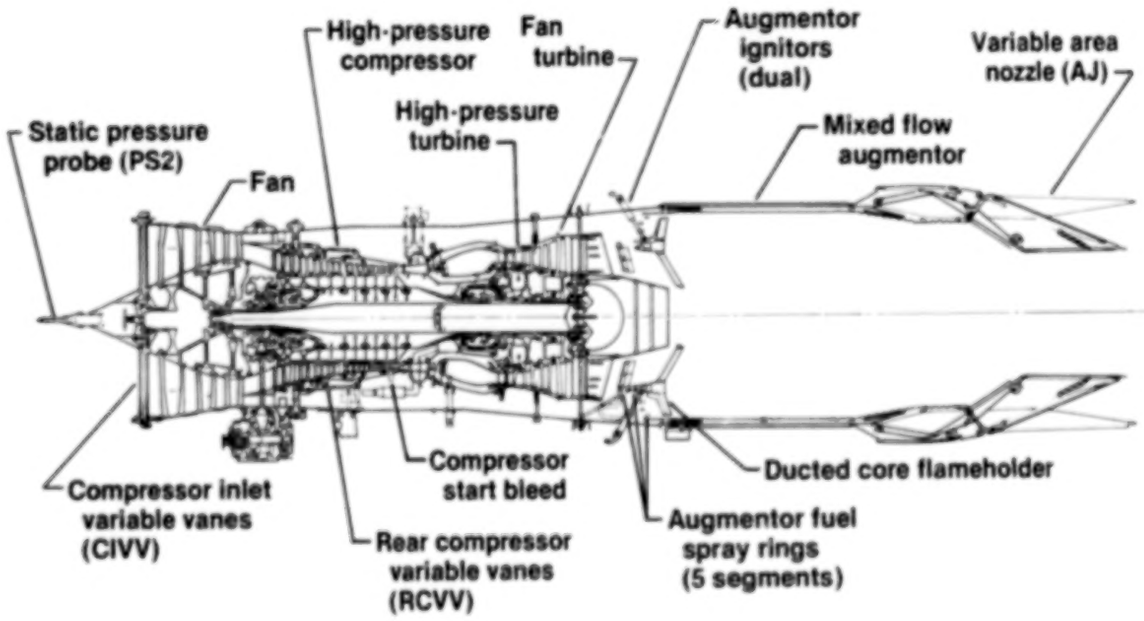

INPUTS AND OUTPUTS

Shown on the upper part of this figure are the controlled variables: compressor inlet variable guide vanes (CIVVs), rear compressor variable stators (RCVVs), start bleeds, main burner gas generator fuel flow (WFGG), afterburner fuel flow in the core (WFAC) and in the duct (WFAD), the sequencing valve position (SVP), and the jet nozzle (AJ).

The lower portion of the figure shows the input sensors to the DEEC: engine station 2 fan inlet static pressure (PS2), fan rotor speed (N1), core rotor speed (N2), power lever angle (PLA), engine station 2 fan inlet total temperature (TT2), main burner pressure (PB), fan turbine inlet temperature (FTIT), turbine discharge total pressure (PT6M), ultraviolet light off detector (LOD), and all resolver feedbacks. The DEEC schedules WFGG, RCVV, CIVV, start bleeds, WFAC, WFAD, SVP, and AJ as functions of PLA, PS2, PB, PT6M, N1, N2, TT2, and FTIT.

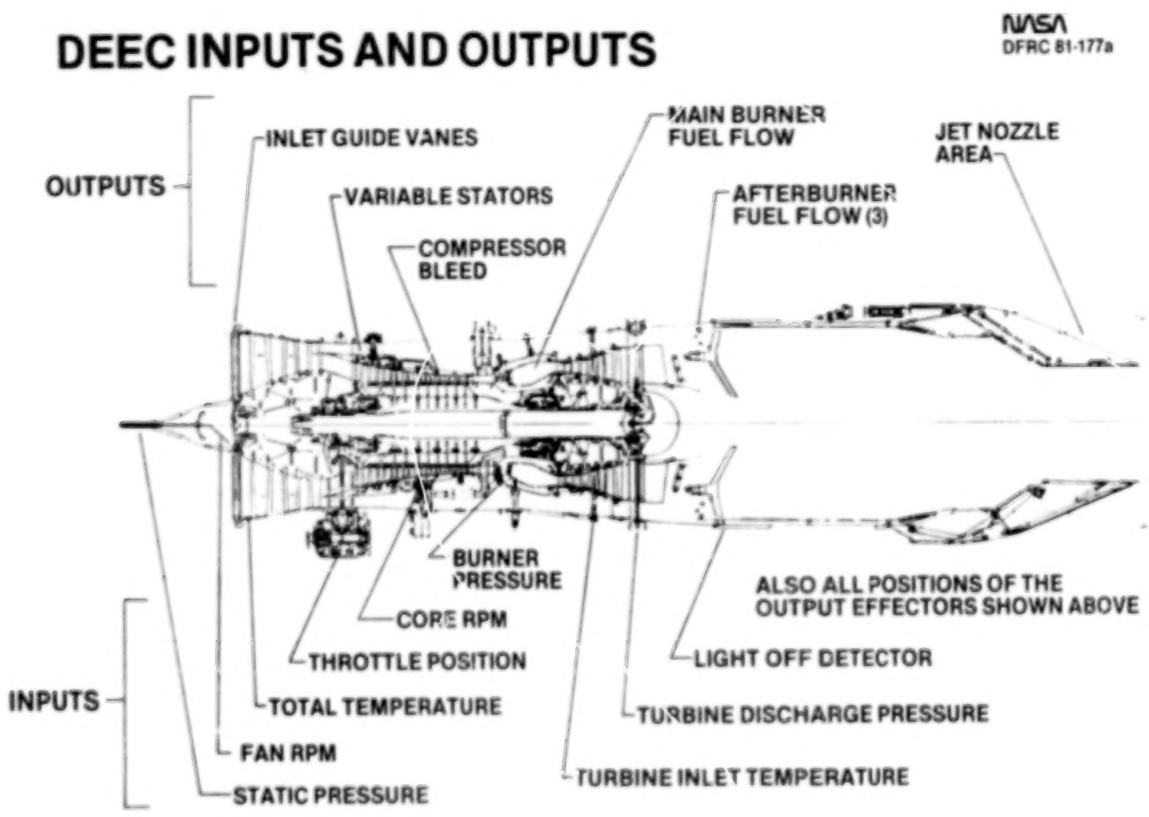

ORIGINAL PAGE IS
OF POOR QUALITY

SIMPLIFIED HARDWARE

Shown on the left side of this figure are the 11 control system components currently used on the production F100 engine in the F-16 airplane. Engine control is provided by the hydromechanical unified fuel control utilizing an engine electronic control to supervise or trim the hydromechanical control system. Also shown on the left side are various sensors, valves, and feedback cables of a current F100 control system. This control system represents the first operational use of a digital electronic computer on a high performance turbofan engine.

The DEEC control system components, shown on the right side of the figure, illustrate the reduced number, as well as the simplified DEEC hardware. The three major components of the DEEC control system are the DEEC computer, gas generator fuel metering valves and integral backup control, and the augmentor fuel metering valves unit.

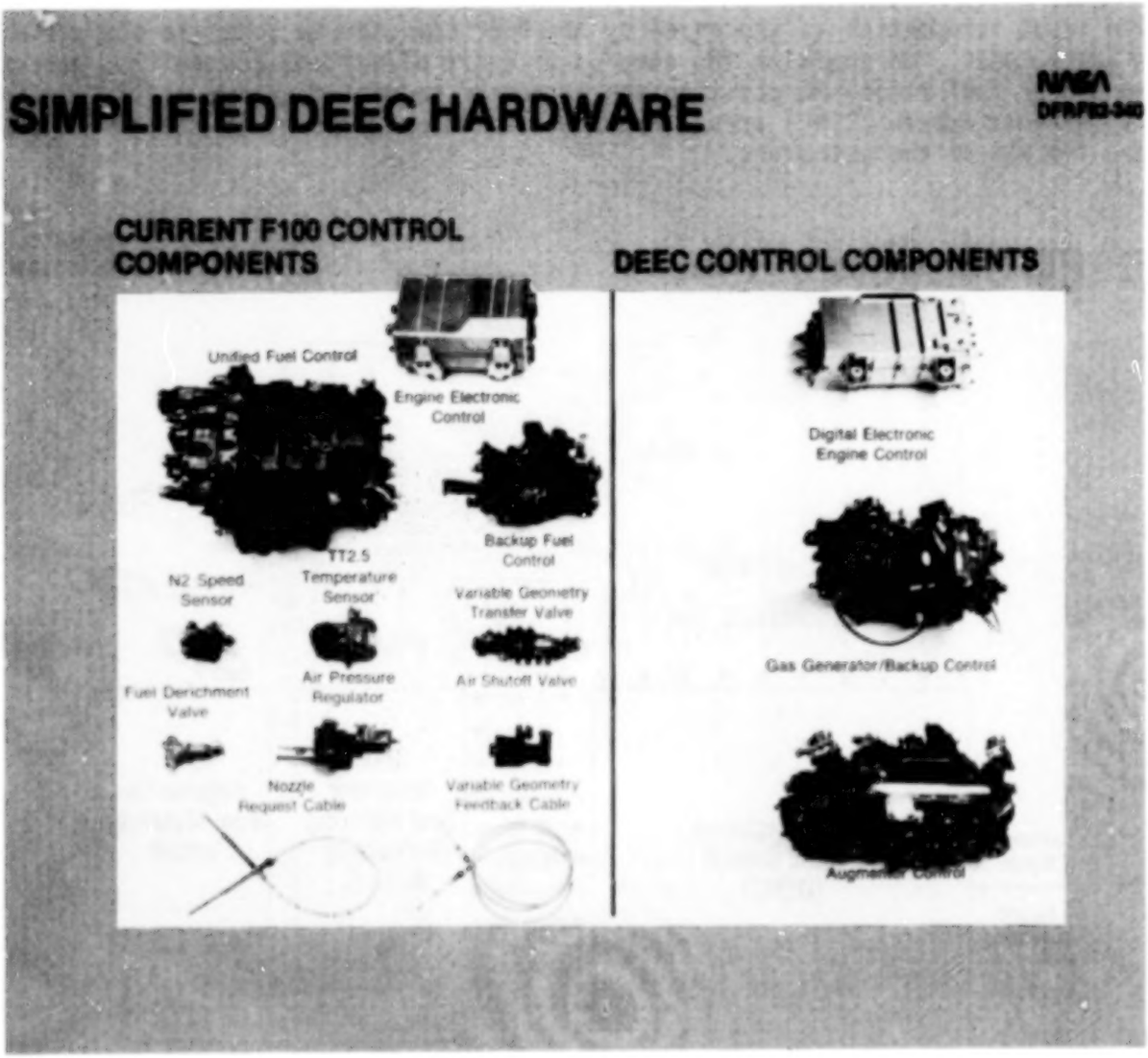

The DEEC system is functionally illustrated below. The three major components of the DEEC control system are the: DEEC computer, gas generator and integral BUC fuel metering valve unit, and the augmentor fuel metering valve unit. Note the shared information between the electronics and the metering valve units.

The DEEC computer receives inputs from the airframe through throttle position (PLA) and Mach number (M), and from the engine through pressure sensors (PS2, PB, PT6M), temperature sensors (TT2, FTIT), and rotor speed sensors (N1, N2). It also receives feedbacks from the controlled variables through position feedback transducers indicating variable vane (CIVV, RCVV) positions, metering valve positions for gas generator fuel flow (WFGG), augmentor core and duct fuel flow (WF), segment sequence valve position, and exhaust nozzle position (AJ). Dual sensors and position transducers are used as shown to achieve redundancy in key parameters as indicated by the (2).

The input information is processed by the DEEC computer to schedule the variable vanes (CIVV, RCVV), to position the compressor start bleeds, to control gas generator and augmentor fuel flows, to position the augmentor segment-sequence valve, and to control exhaust nozzle (CENC) area. Redundant coils are present in the torque motor drivers for all of the actuators.

DEEC Control System

NASA
DFRF83-426

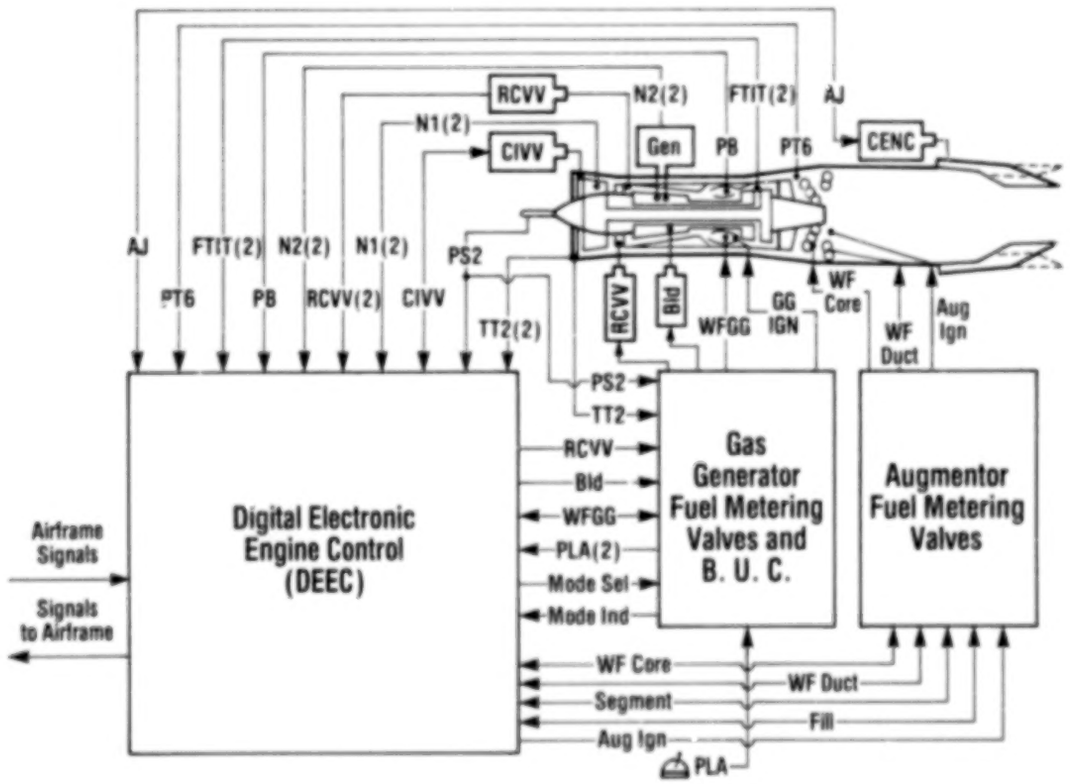

GAS GENERATOR AND BUC METERING VALVE UNIT

The next figure is a photograph of the gas generator fuel metering valve unit, including the integral backup control (BUC). The digital control uses torque motors to actuate the variables, such as the RCVV and gas generator fuel metering valve torque motors shown at the lower left. The torque motors have dual-wound coils; either coil can control the servovalve. At the lower right is the metering valve resolver feedback and the PLA resolver is illustrated at the upper right. All resolvers in the unit are dual for position feedback redundancy.

If the digital control system experiences a failure that requires a transfer to the backup control, a transfer valve translates to permit the hydromechanical control to schedule the gas generator metering valve and RCVV position. The BUC and electronic control components are functionally integrated to minimize the weight and volume. The BUC is described in Paper 9.

Gas Generator Fuel Metering Valve Unit

NASA
DFRF83-1808

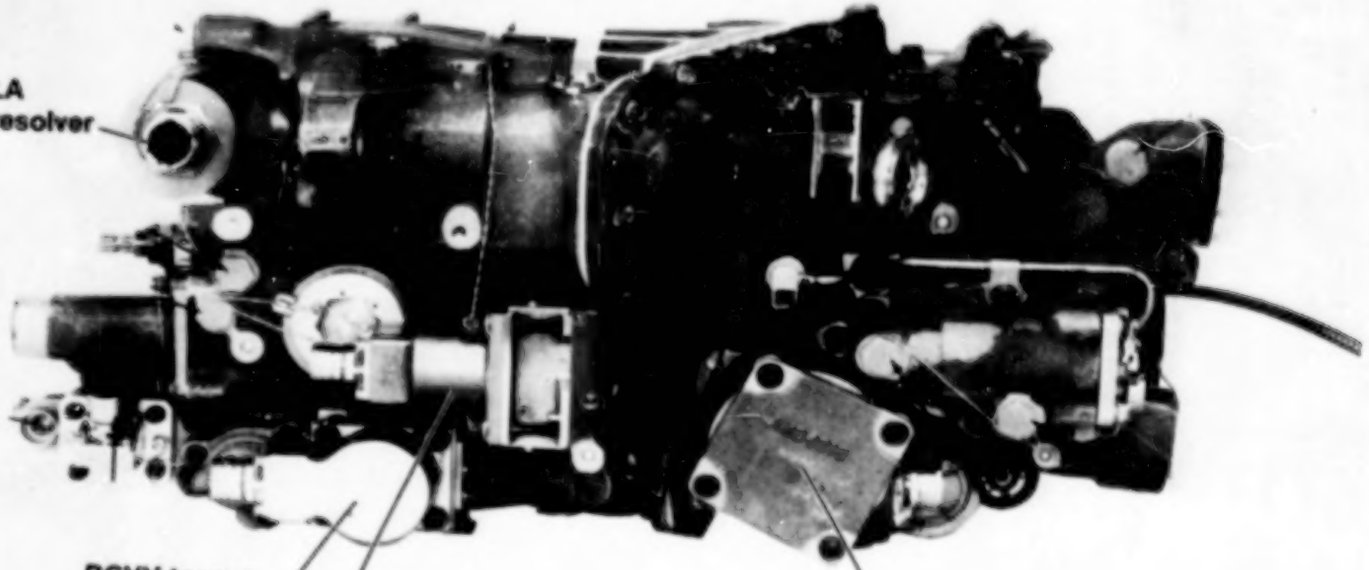

ORIGINAL PAGE IS
OF POOR QUALITY

AUGMENTOR FUEL METERING VALVE UNIT

The photograph below shows the augmentor metering valve unit. This unit combines fuel metering, manifold quickfill, and a fuel distribution system into a single unit controlled by signals from the DEEC. Again note the metering valve and segment sequencing valve torque motors and resolver locations.

Augmentor Fuel Metering Valve Unit

NASA

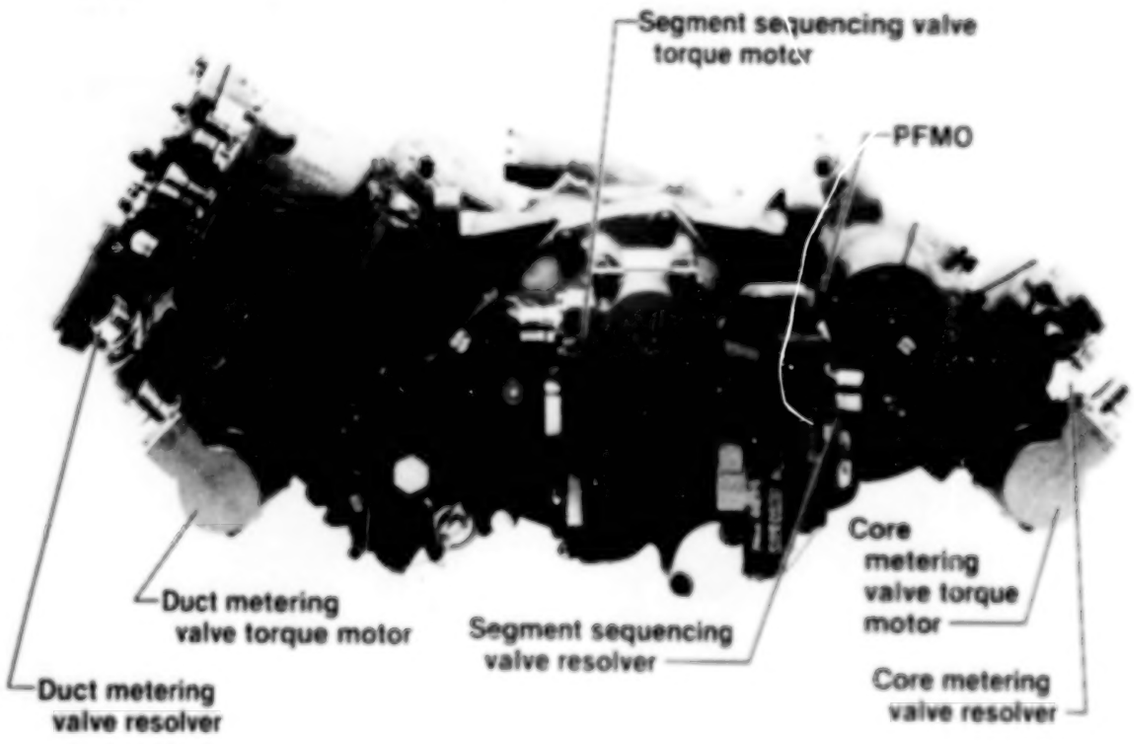
Segment sequencing valve torque motor
PFMO
Core metering valve torque motor
Duct metering valve torque motor
Segment sequencing valve resolver
Core metering valve resolver
Duct metering valve resolver

CONVERGENT EXHAUST NOZZLE CONTROL

The convergent exhaust nozzle control (CENC) positions the jet nozzle in response to commands from the DEEC. The CENC consists of a reversible air motor, a bidirectional control valve, a four-way torque motor, and a resolver. The air motor is driven by compressor bleed air. The torque motor is biased by a null voltage to provide for a fail-safe failure mode in the closed-nozzle direction.

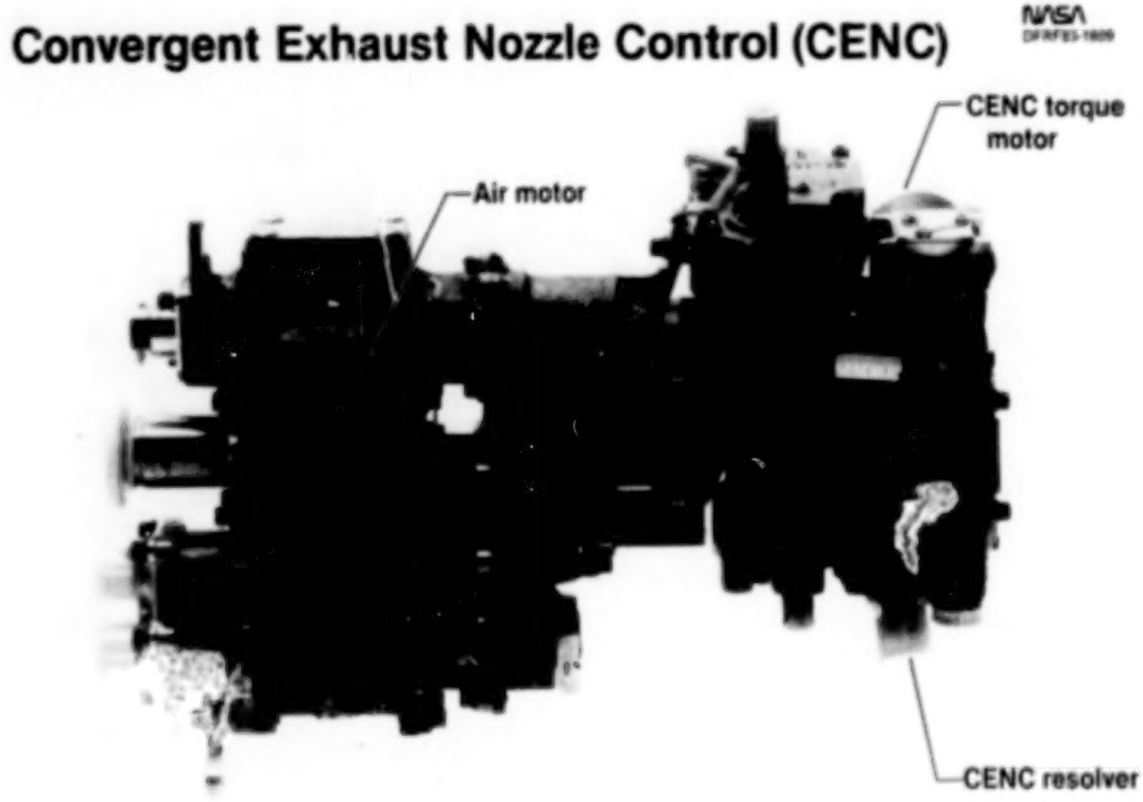

CIVV ACTUATOR

ORIGINAL PAGE IS
OF POOR QUALITY

The torque motor mounted on the actuator modulates the fuel pressure to position the compressor inlet variable vanes (CIVVs). The torque motor is controlled by a signal from the DEEC. The resolver provides position feedback. Both the torque motor and resolver are illustrated at the top of the actuator.

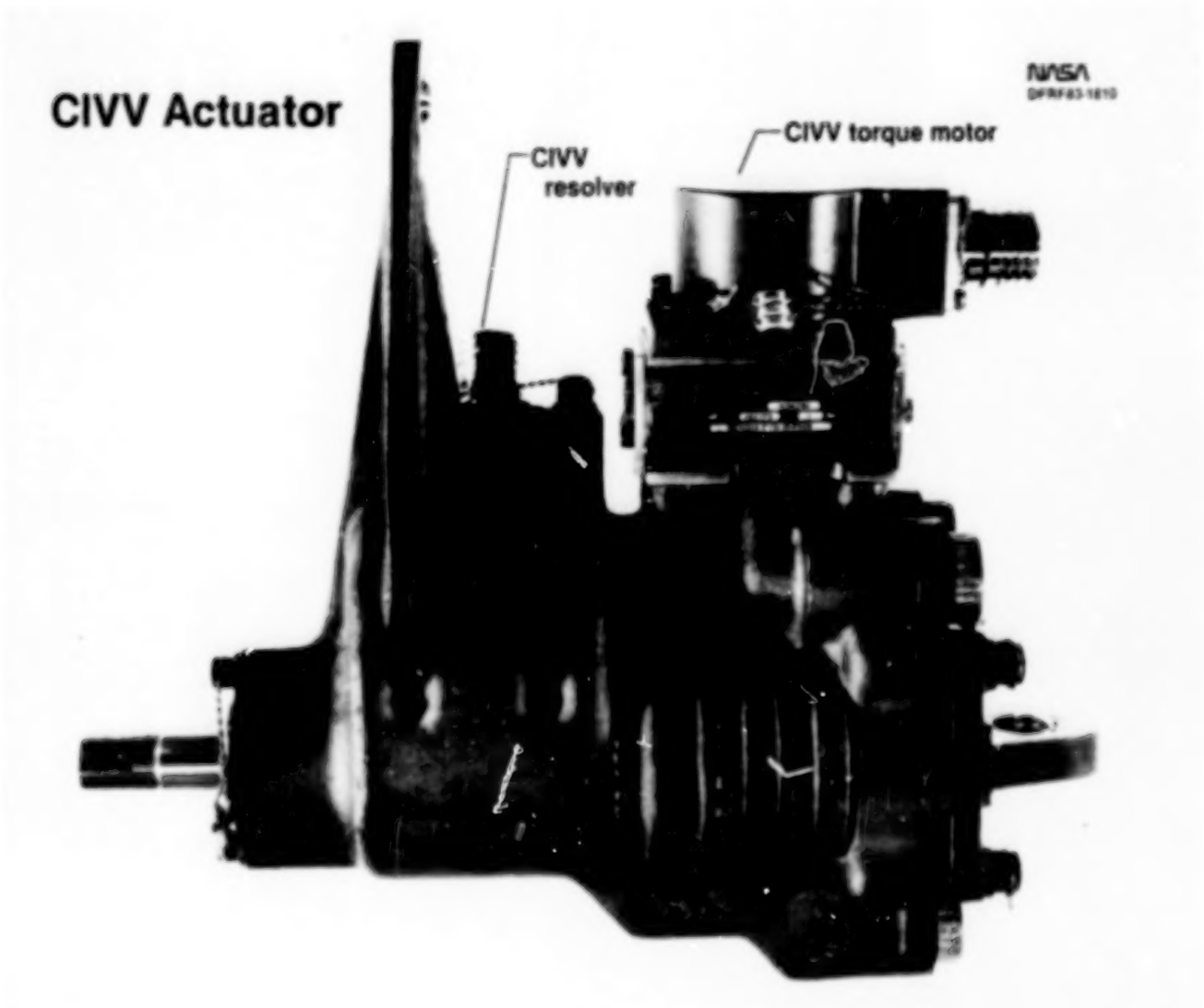

DEEC ON F100 ENGINE

The DEEC computer is engine mounted as shown in the next figure. The housing is split-cast aluminum and is mounted on shock isolators. Moving in a clockwise direction around the figure are the power supplies and aircraft interface, output interfaces, pressure sensors PS2, PB, and PT6M, vibrating cylinder transducers that are temperature compensated, input interface, and the computer processor and memory. The entire unit is fuel-cooled.

ORIGINAL PAGE IS
OF POOR QUALITY

DEEC COMPUTER

The DEEC computer is a fuel-cooled unit weighing 28 pounds. Inputs to the unit are:

4 temperature - TT2 a and b, FTIT a and b;

3 pressure - PS2, PB, PT6M;

4 speeds - N1 a and b, N2 a and b;

11 positions - PLA, RCVV, CIVV, WFGG, WFAC, WFAD, SVP, AJ;

1 LOD - ultraviolet flame detector with self-test bulb; and

1 digital word - Mach number from airframe inlet controller.

Outputs for the DEEC computer are:

7 servodrivers - CIVV, RCVV, WFGG, WFAD, WFAC, SVP, AJ;

3 solenoids - start bleed, mode select, augmentor fuel pump;

3 discretes - augmentor fault, DEEC fault, system fault; and

1 digital word - 9600 baud, universal asynchronous receiver transmitter (UART).

The DEEC unit processor includes:

11 chips - complementary metal oxide substrate (CMOS) construction;

3.4-MHz clock rate - quartz crystal;

1.2-microsecond cycle time;

14K memory - 16-bit words, 10K of programmable read-only memory transistor-transistor logic (PROM-TTL) and 512 random access memory transistor-transistor logic (RAM-TTL); and

110 watts of power used.

Logic of the DEEC is also illustrated on the figure on the next page.

DEEC Computer

NASA
DFRF83-420a

Input

• Temperature	4
• Pressures	3
• Speeds	4
• Positions	11
• LOD	1
• Digital	1

Processor

• Number chips	11
• Clock rate	3.4 MHz
• Cycle time	1.2 microseconds
• Memory	14K
• Power required	110 watts

Outputs

• Servo drivers	7
• Solenoids	3
• Discretes	3
• Digital	1

Logic

- 13 major paths
- 105 minor paths
- 79 schedules
- 500 constants

Physical

- 28 lb
- 801 cubic inches
- 200 lb/hr fuel cooled

LOGIC FEATURES

The figure on the next page shows the DEEC logic features. The basic nozzle area control modes include the idle nozzle area, set to a fixed value as a function of PLA, and the part power nozzle, set to a fixed value chosen to optimize thrust specific fuel consumption (TSFC).

At military power and above, at low Mach numbers, the nozzle controls engine pressure ratio (EPR) closed loop. At military power and above, at high Mach numbers (>1.4), the nozzle controls corrected fan rotor speed (N1C2) closed loop when fuel flow is controlling fan turbine inlet temperature (FTIT) and otherwise controls EPR closed loop. The basic EPR is a schedule of N1C2 biased by engine station 2 total pressure (PT2).

The gas generator fuel flow (WFGG) controls fan speed (N1) closed loop at all power settings, except when controlling to FTIT or running on FTIT limit.

Afterburner duct fuel flow (WFAD) is scheduled open loop to provide optimum fuel-air ratio for segments 3 and 5. The WFAD metering value position is controlled closed loop. Afterburner core fuel flow (WFAC) is scheduled open loop based on an optimum fuel-air ratio for segments 1, 2, and 4. The WFAC metering valve position is controlled closed loop. The sequencing valve position (SVP) regulates the fuel flow to the five segments of the augmentor.

Compressor inlet variable vanes (CIVVs) are scheduled open loop and are a function of corrected fan rotor speed (N1C2). Rear compressor variable vanes (RCVV) are scheduled open loop and are a function of corrected high compressor rotor speed (N2C25) and biased by engine station 2 total temperature (TT2). The start bleeds are controlled open loop and are a function of core rotor speed (N2) biased by TT2.

The DEEC performs the following functions:

(1) Detects engine stall by a certain rate of burner pressure (PB) decay and, as a function of PLA biased by PB, takes recovery action by cutting back fuel flow (WFGG) and opening the nozzle (AJ).

(2) Detects augmentor blowouts by one or more of the following indicators: a change in engine pressure ratio (EPR); a change in nozzle area; or loss of light off detector signal (LOD).

(3) Provides closed loop control of gas generator fuel flow (WFGG) during starts by trimming WFGG to obtain the desired high compressor rotor speed (see paper 8); and

(4) Provides fault detection and accommodation (FDA) by detecting 150 faults, some by use of range check and, if sensor is failed, will synthesize parameter (PB and FTIT) and detect open loop servovalve and actuator failures by voltage sum checks. Additional information on fault detection is in Paper 7.

DEEC Logic Features

NASA
DFRF83-422

- Nozzle controls EPR
- Gas generator fuel flow controls N1
- Schedule augmentor fuel flow
  WFAD, WFAC, SVP
- Schedule variable geometry
  CIVV = f (N1C2)
  RCVV = f (N2C25, TT2)
  SB = f (N2, TT2)
- Detects stalls - recovery action
  STLSIG = f (PLA, PB)
- Detects A/B blowout
  BLOSIG = f (ΔEPR, LOD, Δ AJ)
- Closed loop start
- Provide failure detection and accommodation
  - 150 Faults
  - Range check all inputs
  - Parameter synthesis
  - Open loop servovalve or actuator

CLOSED-LOOP CONTROL MODES

The upper part of the figure shows the total airflow logic in which gas generator fuel flow (WFGG) is controlled to maintain the scheduled fan speed and hence, airflow. Proportional-plus-integral control is used to match the N1 request to the sensed N1. Limits of N2, FTIT, and PB are maintained. The airflow loop is used for all throttle settings.

Shown in the lower part of the figure is the engine pressure ratio (EPR) loop. The requested EPR is compared with the EPR, based on PT2 and PT6M, and, using proportional-plus-integral control, the nozzle is modulated to achieve the requested EPR. The EPR control loop is only active for intermediate power operation and augmentation. At lower settings, a scheduled nozzle area is used.

With the closed-loop airflow and EPR logic, the DEEC control is capable of automatically compensating for engine degradation. EPR is directly related to thrust, so the DEEC can maintain an engine at a desired thrust level. As the engine degrades, the FTIT required to achieve the scheduled EPR will increase until it reaches its limit. The DEEC will then operate the engine on the FTIT limit.

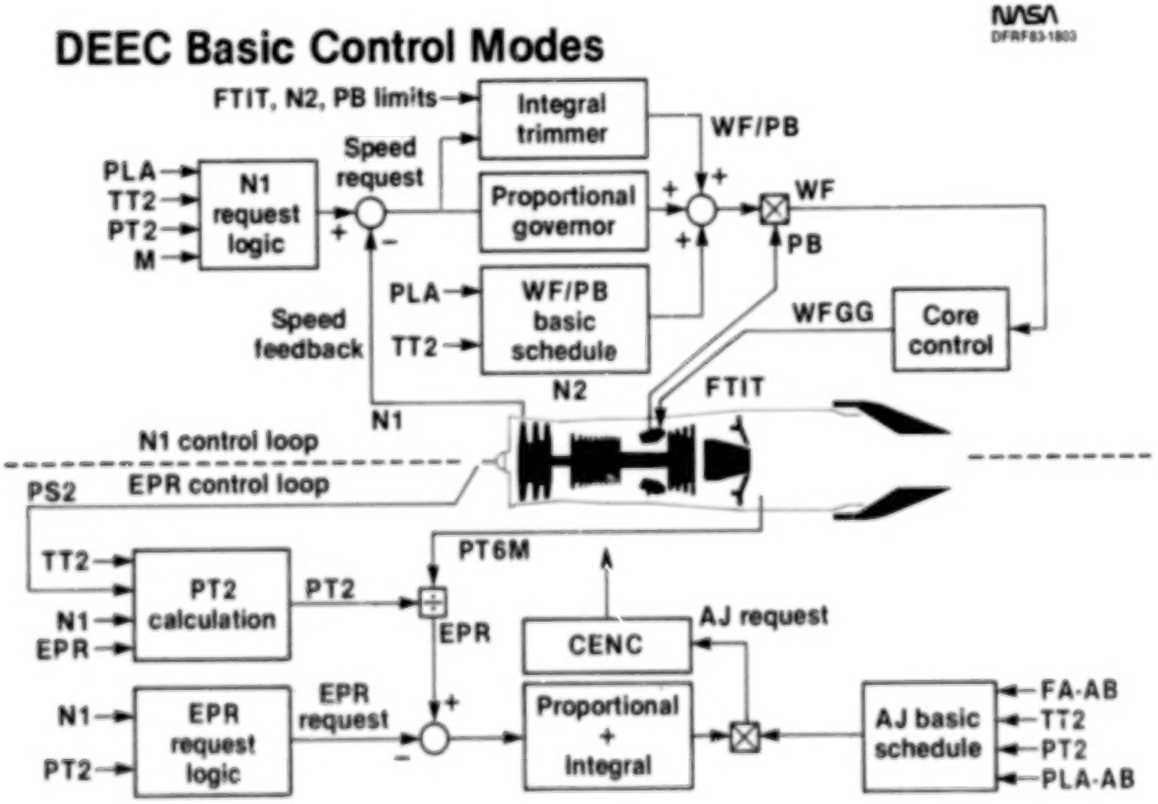

VARIABLE GEOMETRY LOGIC

RCVV and CIVV are scheduled open loop as shown below. The resolvers in the actuators are used to generate feedback to position the vanes.

The start bleeds are scheduled and controlled open loop. The start bleed solenoid controls compressor discharge bleed air to close the bleeds.

Variable Geometry Logic

NASA
DFRF83-424

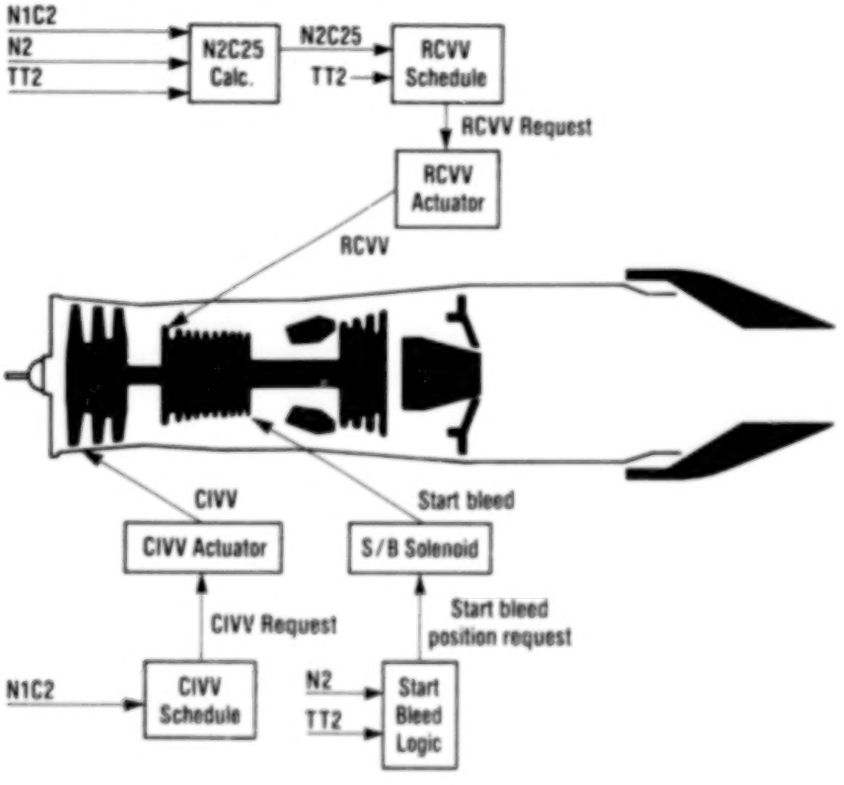

Power supply test - monitors internal power supply voltage and if a surge or drop is detected, will generate a power supply reset and transfer to BUC.

Cycle time test - monitors timely operation of program via software resets at specific intervals. Time out generates a reset signal for the processor and if repeated, transfers to BUC.

Clock loss test - monitors primary and secondary clocks for 1.7 MHz output. If output is not 1.7 MHz, it transfers to the secondary clock. If the secondary clock fails, it will transfer to BUC.

Amplifier drift test - monitors thermocouple amplifiers for voltage drift; failure of critical interface will transfer to BUC.

Feedback resolver test - monitors redundant resolver power supplies and tests resolver to digital converter.

Torque motor driver test - monitors "torque motor enable" and, "mode select" signals.

Open thermocouple test - monitors thermocouple amplifiers for off-scale voltage.

Torque motor "wrap around" test - monitors the two "sum" and four "difference" voltages of dual wound coils.

Processor test - checks for program "hangup" not detected in cycle test.

Scratch pad test - checks read and write integrity of each scratch pad location.

PROM check sum test - sum checks all read-only memories except vibrating cylinder sensor programmable read-only memories (PROMs).

Vibrating cylinder sensor checks - sum checks individual PROMs and range checks temperature input.

Parameter range check - checks for upper and lower limit.

Redundant parameter - checks for agreement within specified tolerances.

Open loop test - checks for nontracking actuator feedback versus command. Failure to correct "error" between request and feedback will generate a "loop shutdown".

More information on FDA is given in Paper 7.

Fault Detection & Accommodation

NASA
DFRF83-423

DEEC

HARDWARE

- Power supply
- Cycle time
- Clock loss
- Amplifier drift
- Feedback resolver
- Torque motor driver

SOFTWARE

- Processor
- Scratch pad
- Prom check sum
- Vibrating cylinder prom
  - Check sum
  - Range check temp.

DEEC SYSTEM

- Open thermocouple
- Torque motor "Wrap Around"
- Parameter range check
- Redundant parameter
- Open loop

N86
25346

UNCLAS

N86-25346

NASA LEWIS F100 ENGINE TESTING

Roger A. Werner, Ross G. Willoh, Jr., and
Mahmood Abdelwahab
NASA Lewis Research Center
Cleveland, Ohio

SUMMARY

Two builds of an F100 engine model derivative (EMD) engine, serial number XD11, were evaluated in the NASA Lewis Research Center (LeRC) propulsion system laboratory (PSL) altitude facility for improvements in engine components and digital electronic engine control (DEEC) logic. Two DEEC flight logics were verified throughout the flight envelope in support of flight clearance for the U.S. Air Force (USAF) F100 Engine Model Derivative Program (EMDP). A nozzle instability and a faster augmentor transient capability were sucessfully investigated in support of the F-15 DEEC flight program. Also included are identification of an off-schedule coupled-system mode fan flutter, DEEC noseboom pressure correlation, DEEC station 6 pressure comparison, and a new fan inlet variable vane (CIVV) schedule.

INTRODUCTION

An F100 EMD engine, serial number XD11, was tested in the LeRC PSL facility for altitude evaluations of advanced engine components and DEEC control logics. Two engine builds have been investigated at this time. Build 11 supported part of the flight clearance portion of the Air Force F100 EMDP. Two DEEC flight logics for this program were verified for use in F-15 flight testing that began in March of 1983. Build 10 underwent fan flutter and fan performance evaluations. Build 10 was also used in support of a F-15 DEEC flight program, specifically in the areas of nozzle stability (ref. 1) and augmentor performance upgrade.

The test conditions for these flight support tests are summarized on the engine flight envelope. In addition, results of the fan flutter investigation, noseboom and station 6 pressure probe correlations for DEEC control inputs, and some engine performance at axially off-schedule CIVV positions, and presented.

NOMENCLATURE

AJ	jet primary nozzle area
BOM	bill of material
CIVV	compressor inlet variable vane

PRECEDING PAGE BLANK NOT FILMED

DEEC	digital electronic engine control
EMD	engine model derivative
EMDP	Engine Model Derivative Program
EPR	engine pressure ratio, PT_{6M}/PT_2
FDA	failure detection and accommodation
FTIT	fan turbine inlet temperature
IM	intermediate power
LOD	light off detector
N1	fan rotor speed
O.D.	outer diameter
PES	photo electric scanning
PLA	power lever angle
PLA-AB	afterburner power lever angle
PS_{NB}	noseboom probe static pressure
PT_2	fan inlet total pressure
PT_2 UNDIST	undistorted (maximum) fan inlet total pressure
PT_{6M}	turbine discharge total pressure (mixed core and fan stream)
P6M01	turbine discharge total pressure production probe
SFDV	single flow divider valve
seg	augmentor spray ring segment
TT_2	fan inlet total temperature
Wa_1	fan inlet total airflow
δ_2	ratio of fan inlet total pressure to standard sea level static pressure
θ_2	ratio of fan inlet total temperature to standard sea level static temperature

APPARATUS

Engine

Tests were conducted with a F100 EMD (Pratt and Whitney Aircraft designation PW1128) engine, serial number, XD11. This engine is a low-bypass, high-compression ratio, twin spool turbofan with a mixed-flow augmentor. The EMD engine is similar to the production F100 but has a new advanced fan design, improved high-pressure compressor, a recontoured combustor, a higher-temperature capability turbine system, an advanced fuel management (AFM) augmentor system, and a DEEC control system.

Evaluations were made with two engine builds (10 and 11). XD11-10 had a six-segment augmentor instead of the AFM. For the F-15 DEEC flight support tests, the ducted-core augmentor flameholder of XD11-10 was replaced with an F100 bill of material flameholder. XD11-11 had a redesigned third-stage fan, high-pressure compressor modifications, and the low-pressure AFM augmentor system. During tests with XD11-11, the single flow divider valve (SFDV) main fuel system was replaced with the F100 bill of material fuel system, and the AFM augmentor was updated with the high delta-pressure spray rings.

Fuel Control

A breadboard version of the DEEC was used. This unit provided the capability of modifying control loops, logic, and schedules, both on and off line. A further description of the DEEC is given in reference 1.

Facility

Engine tests were conducted in an altitude test chamber of the LeRC PSL. The altitude facility includes a forward bulkhead which separates the inlet plenum from the test chamber. Conditioned air at the desired inlet pressure and temperature flowed from the inlet plenum through a bellmouth and inlet duct to the engine. The test chamber was evacuated to the desired altitude pressure. Exhaust from the engine was captured by a collector which extended through the rear bulkhead of the test chamber.

TESTS AND RESULTS

F100 EMD Flight Support Tests

Logic Verification and Fault Detection and Accommodation. Figure 1 shows the flight envelope test conditions for the DEEC logic verifications and the DEEC fault detection and accommodation (FDA) tests using XD11-11. The logic verifications were a final check of the logic operability throughout the flight envelope before manufacture of the flight DEEC units (burning the programmable read-only memories (PROMs)). The PD 4.2.0 designation corresponds to the AFM augmentor system and incorporates all of the logic improvements made since an earlier version (PD 4.1.1) was defined.

PD 4.2.1 logic has some additional stall recovery improvements. PD 4.2.0 logic verifications included augmentor transients, bodies, closed-loop starts, and a zoom climb. Of the supersonic points, augmentor transients were evaluated only at Mach 1.6 and 35,000 ft altitude condition.

The PD 4.2.1 tests included gas generator transients, augmentor transients, and bodies for the stall recovery logic verifications. In addition, PD 4.2.1 included a post-stagnation spooldown airstart, part power jet primary nozzle area (AJ) scheduling to lower sea level fan turbine inlet temperature (FTIT), and AJ oscillation with power lever angle (PLA) noise investigations. The DEEC FDA tests included steady-state and transient engine running for verification of DEEC parameters, demonstration of operation with failed inputs, and transfer to secondary control mode with high-sensed burner pressure.

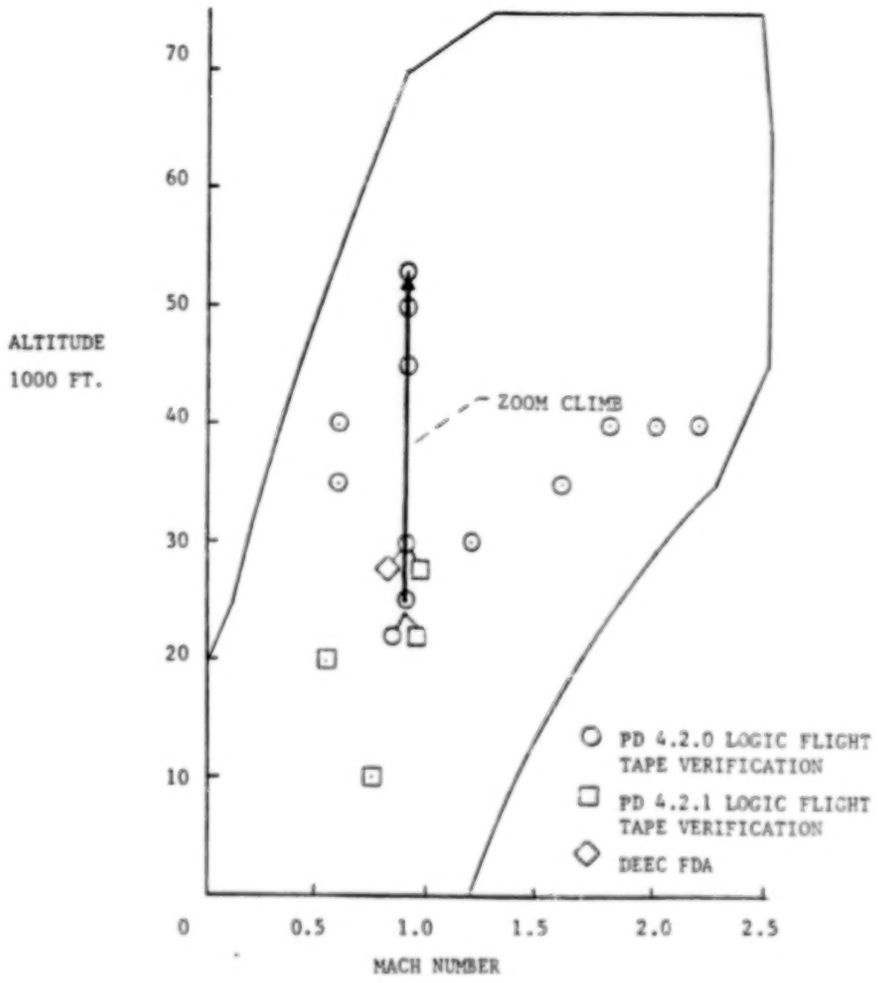

Fig.1 - XD11-11 EMD FLIGHT SUPPORT

- DEEC LOGIC VERIFICATION AND FDA

Stall Recovery and Bodie Test Points. The test conditions for stall recovery and bodie evaluations are shown in figure 2. The stall recovery of both PD 4.2.0 and PD 4.2.1 logics was demonstrated with high-power stalls which utilize a delayed augmentor ignition to create an engine stalling pressure pulse. The recovery demonstration was well within the success criteria as only one nonrecoverable stall occurred out of more than 60 attempts. This stagnation was at Mach 0.6 and 40,000 ft altitude with the PD 4.2.1 logic.

Individual removal of bodie stall protection logics were evaluated at two conditions. With all the protection logic removed, a bodie stall occurred at Mach 0.8 and 45,000 ft altitude condition. Bodie stall margin was demonstrated at three flight conditions with idle dwells varying from 3 to 60 sec. Stall margin was verified by increasing the fuel flow during the acceleration portion of the bodie; this fuel flow addition moved engine operation closer to the stall line. No engine stalls were found. At 40,000 ft altitudes, successful bodie stall margin was demonstrated with both the single flow divider valve and F100 BOM fuel systems. Only the SFVD system was tested at 30,000 ft.

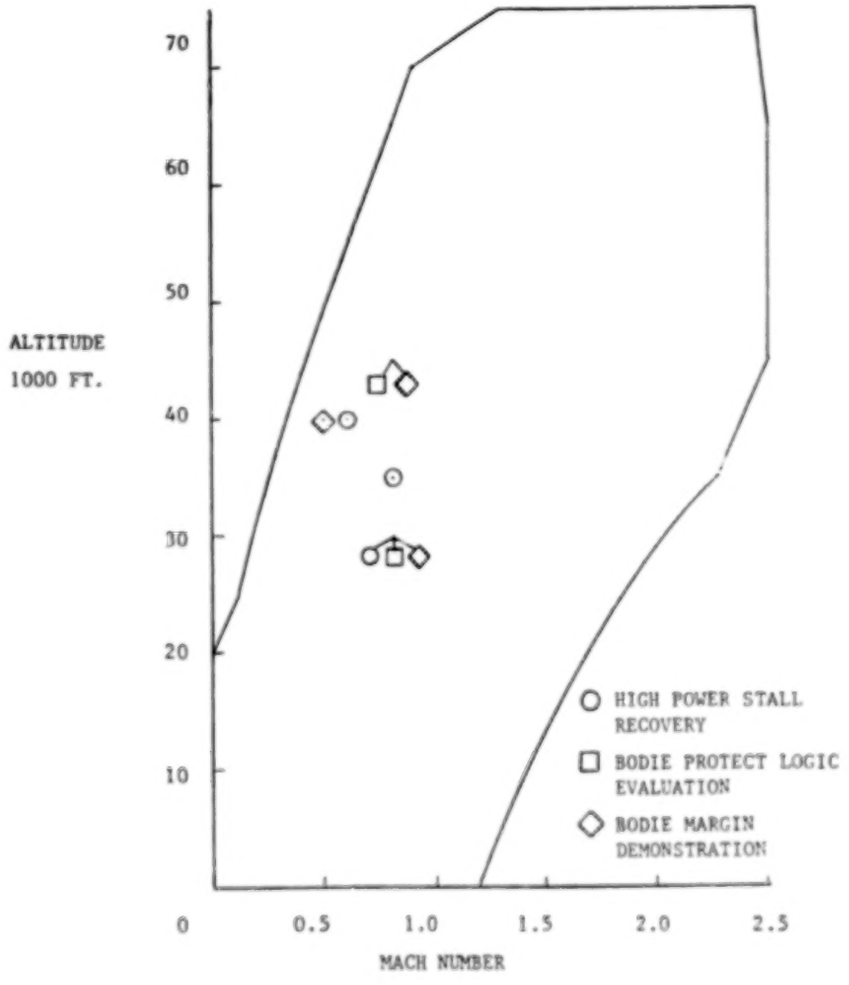

Fig.2 - XD11-11 EMD FLIGHT SUPPORT

- STALL RECOVERY AND BODIE TEST POINTS

Spooldown Airstart Test Points. Figure 3 shows the spooldown airstart test conditions. With the SFDV fuel system and ambient fuel, four unsuccessful starts occurred with 40-percent spooldown attempts. Because of suspected fuel vaporization problems, the SFDV system was replaced by the F100 BOM fuel system. Using hot fuel and the BOM fuel system, successful airstarts were recorded at 200 knots for 40-percent and 25-percent spooldown for primary control mode and 40-percent spooldown for secondary mode. At 300 and 350 knots, successful 40-percent spooldown airstarts were recorded for both primary and secondary modes with the BOM system and hot fuel. Also, at 350 knots and 10,000 ft altitude, a 25-percent spooldown airstart for primary mode was recorded.

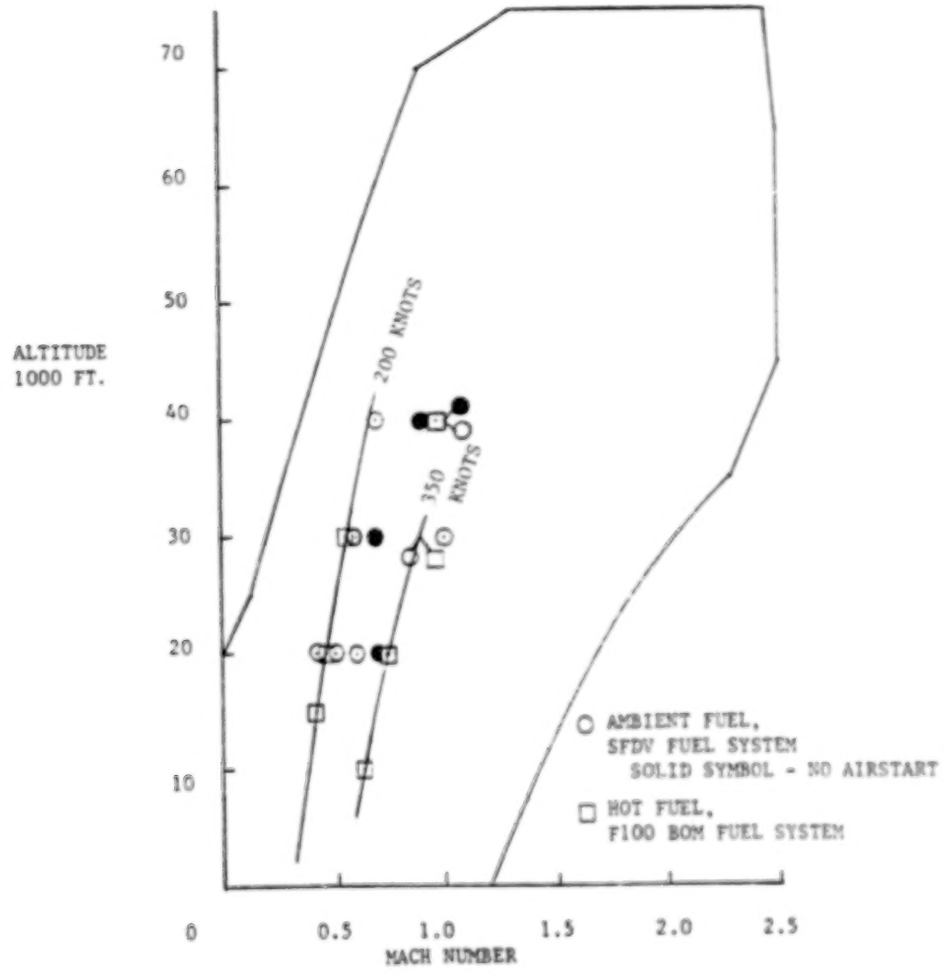

Fig.3 - XD11-11 EMD FLIGHT SUPPORT

- SPOOLDOWN AIRSTART TEST POINTS

F-15 Flight Support Tests

Figure 4 shows the exhaust nozzle stability and light off detector (LOD) fast acceleration optimization investigations conducted with XD11-10. With the F100 BOM augmentor flameholder and XD11-10's six-segment spray rings, representative tests for the F100 flight engine (P063) could be made at altitude conditions in the ground-level facility.

The F-15 DEEC flight program encountered AJ nozzle oscillations during augmentation, which had not been predicted from previous tests and could not be reproduced with engine/control simulations. The engine pressure ratio (EPR) control loop nozzle instability was investigated at the four conditions shown. Using the DEEC breadboard to vary control constants, nozzle stability could be controlled with a reduction in the EPR/AJ loop gain. This evaluation with XD11-10 has been reported in reference 1.

XD11-10 was also used to verify DEEC control and augmentor upgrades for the DEEC flight program. An augmentor LOD and DEEC fast-acceleration logic was successfully demonstrated and optimized at the test conditions shown here. For this engine, augmentor transients to segments 4 and 5 are shown above the F100 segment 1 transient limiting boundary. To acheive these transients, DEEC breadboard logic included modifications of segment 1 limit, segment 5 redistribution, segment 1 hold, afterburner power level angle (PLA-AB) rate, AJ schedule, and fuel schedule. This again demonstrates the flexibility of the breadboard unit.

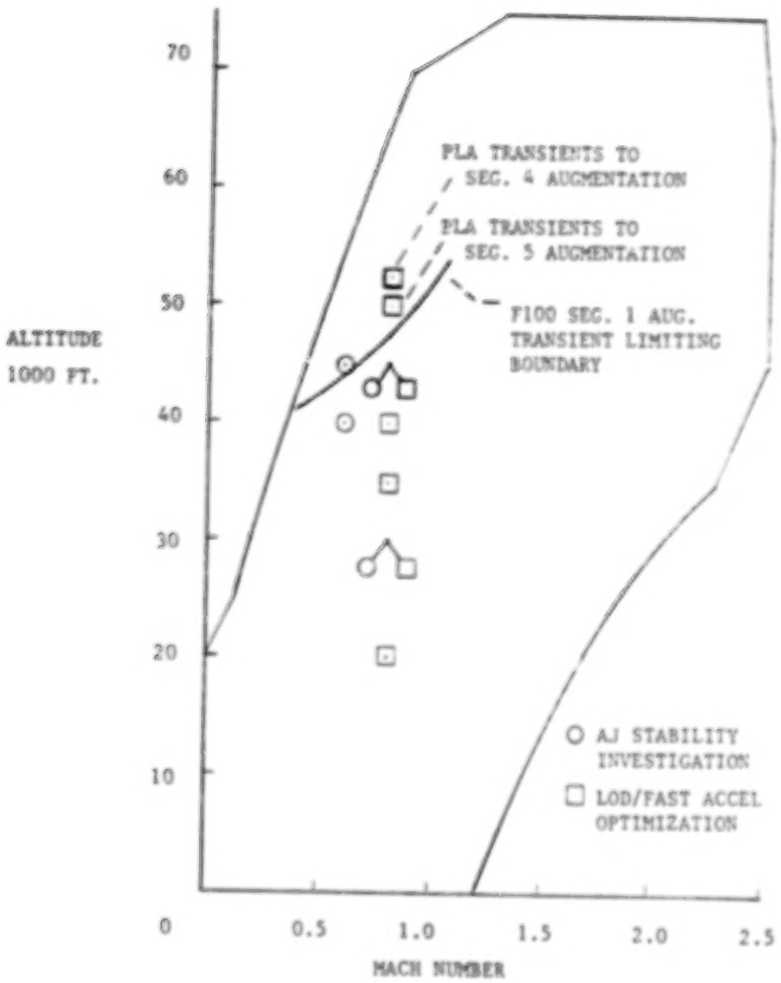

Fig.4 - XD11-10 DEEC FLIGHT SUPPORT - TEST POINTS

XD11-10 Results

Compressor Inlet Variable Vane Excursions. An extensive fan flutter investigation was conducted with XD11-10 throughout the flight envelope. Blade flutter was monitored by a photo electric scanning (PES) system and by strain gages which required the use of a slip ring assembly. Seven flutter points were found by taking the fan inlet variable vanes (CIVVs) off schedule with the breadboard control. This flutter is a fan-coupled-system mode of rotor 1. The corresponding fan inlet total pressure (PT_2), fan inlet total temperature (TT_2) and screen is indicated on figure 5.

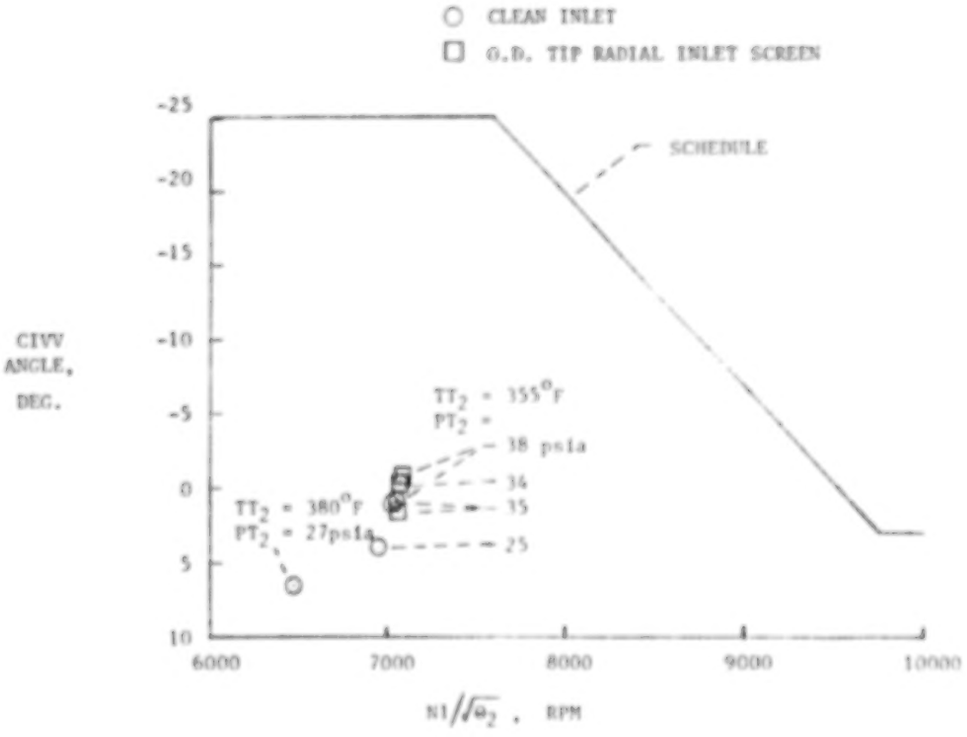

Fig.5 - XD11-10 FLUTTER POINTS - CIVV EXCURSIONS

Pressure-Airflow Correlation. Upon completion of the flutter program, the slip ring was removed, and the DEEC noseboom probe was installed. Figure 6 shows the noseboom pressure-airflow correlation at two pressure levels for the XD11-10 engine. Also included is an F100 engine (P072) correlation from reference 2. The P072 airflow is the unadjusted, originally measured airflow. The 1-percent difference could be a result of the nonlinear transducer corrections, which were not used with the P072 data, and of possible improvements in pressure averaging and airflow calculation.

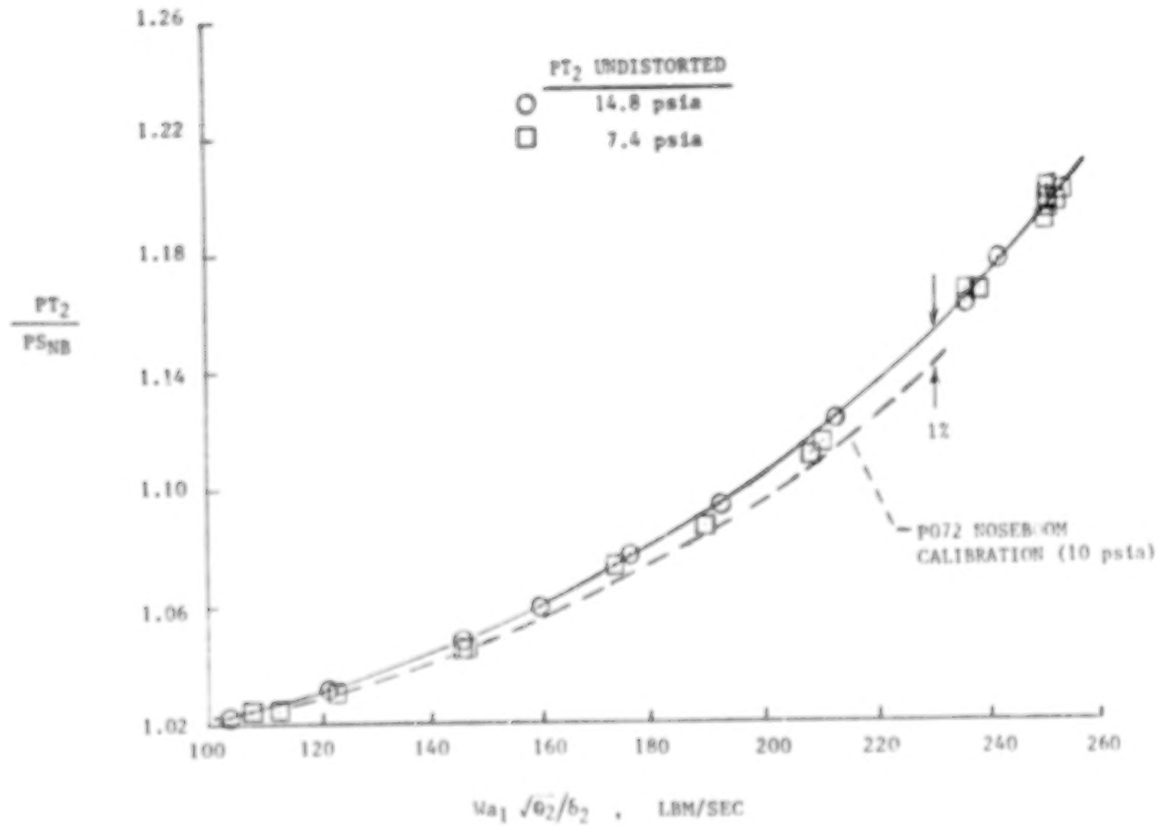

Fig.6 - XD11-10 PT/PS NOSEBOOM CORRELATION - CLEAN INLET

Noseboom Correlation. Figure 7 shows the noseboom correlation for two inlet screens – a radial and a circumferential. Data for both of these screens are nearly the same and lie about 4.5 percent above the clean inlet correlation.

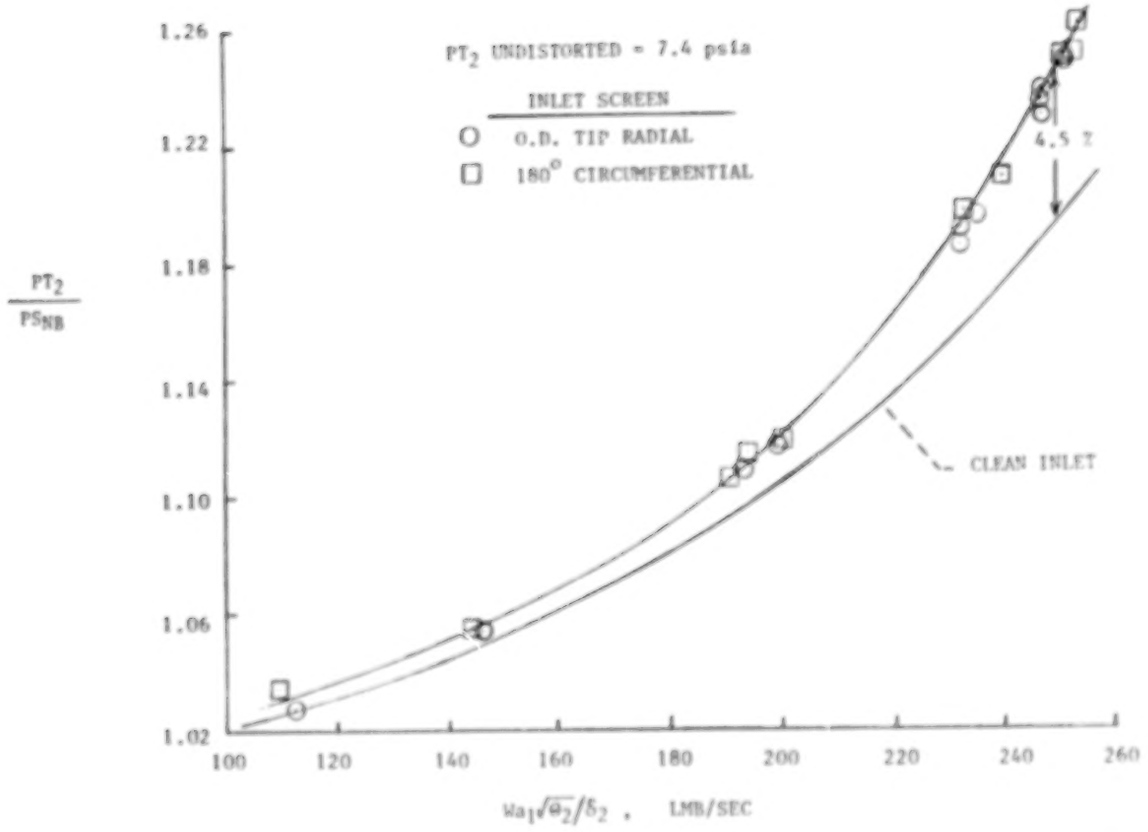

Fig.7 – XD11-10 PT/PS NOSEBOOM CORRELATION – INLET SCREENS

Inlet Total Pressure Recovery. The engine inlet pressure recovery for the clean inlet and inlet screen conditions is illustrated in figure 8. The recovery here is the ratio of the average to the undistorted or maximum average pressure at the engine inlet. Recovery levels at intermediate power (IM) are about 99 percent for clean inlet, 95 percent for the radial screen, and 90 percent for the circumferential screen.

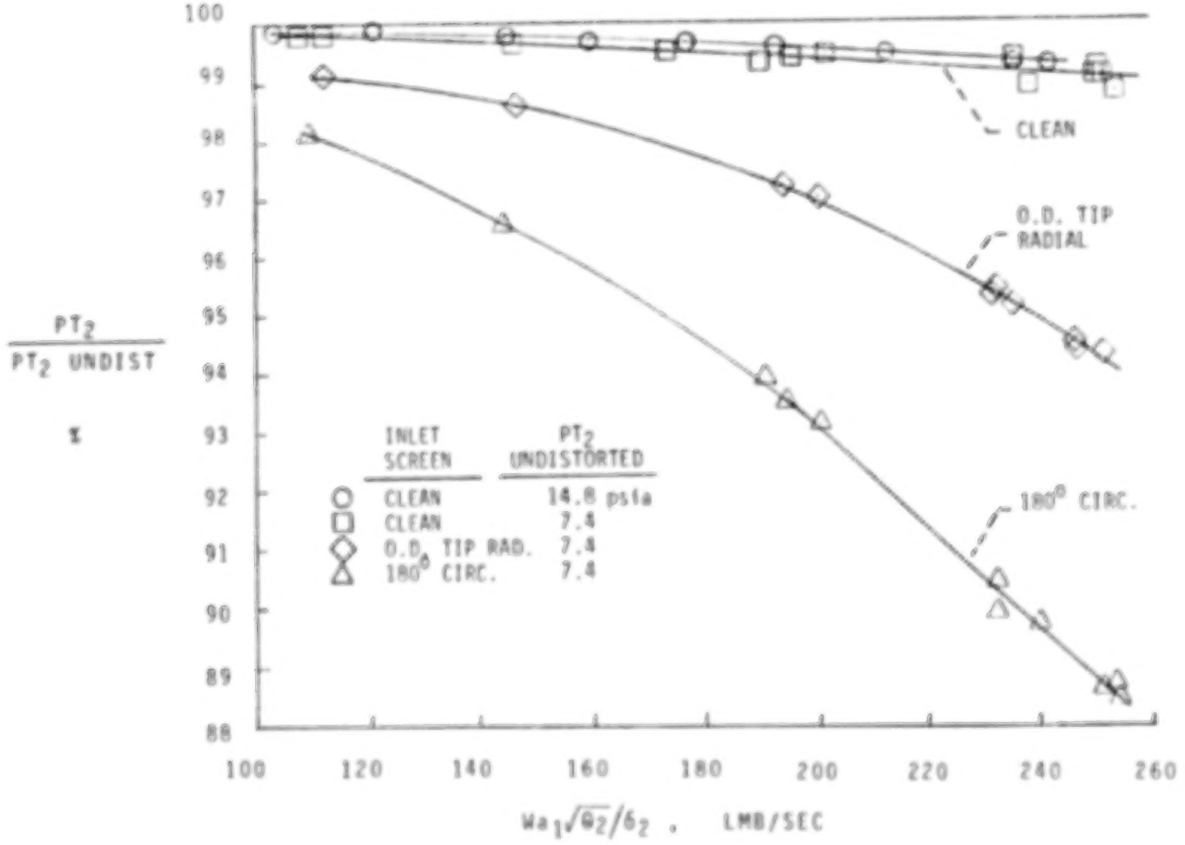

Fig.8 – XD11-10 INLET TOTAL PRESSURE RECOVERY

Comparisons. Figure 9 compares the engine station 6 DEEC turbine discharge total pressure production probe (P6M01) to the mass-weighted average. The data is for engine speeds at IM and above when the DEEC is on EPR control for both clean inlet and inlet screens. The 0.6 percent variation is nearly the same as reported in reference 2 (0.5 percent).

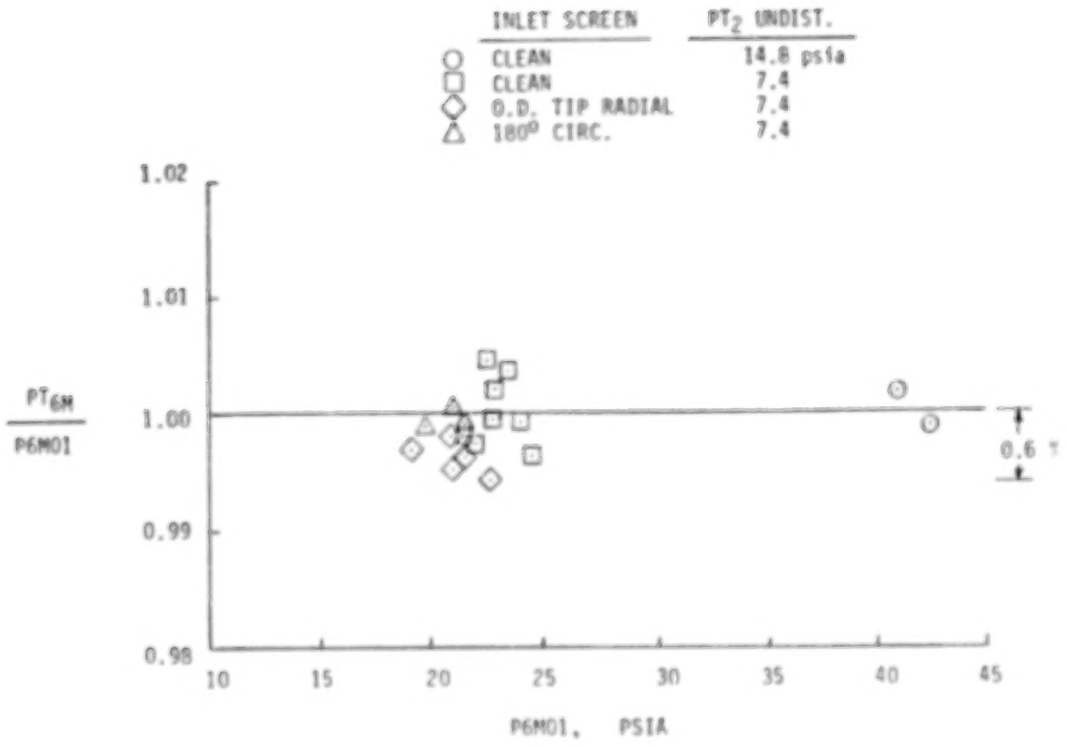

Fig.9 - XD11-10 COMPARISON OF DEEC P6M PROBE TO PT6M - ENGINE SPEEDS AT I/M POWER AND ABOVE

Variations With Speed, Airflow, and Pressure. At the end of the XD11-10 test program, the CIVV schedule was found to be set open (axial) by 10°. The following three figures show CIVV variations with corrected fan speed, corrected total airflow, and engine pressure ratio (EPR). Based on XD11-10 testing and a CIVV variation investigation with an F100 EMD engine (FX227-12) at Arnold Engineering Development Center (AEDC), a new CIVV schedule resulted and is shown in figure 10. An increase in airflow with open CIVV is shown in figure 11 with maximum airflow occurring between CIVV angles of 10° and 15° open. Figure 12 shows the increase in EPR as CIVVs are opened.

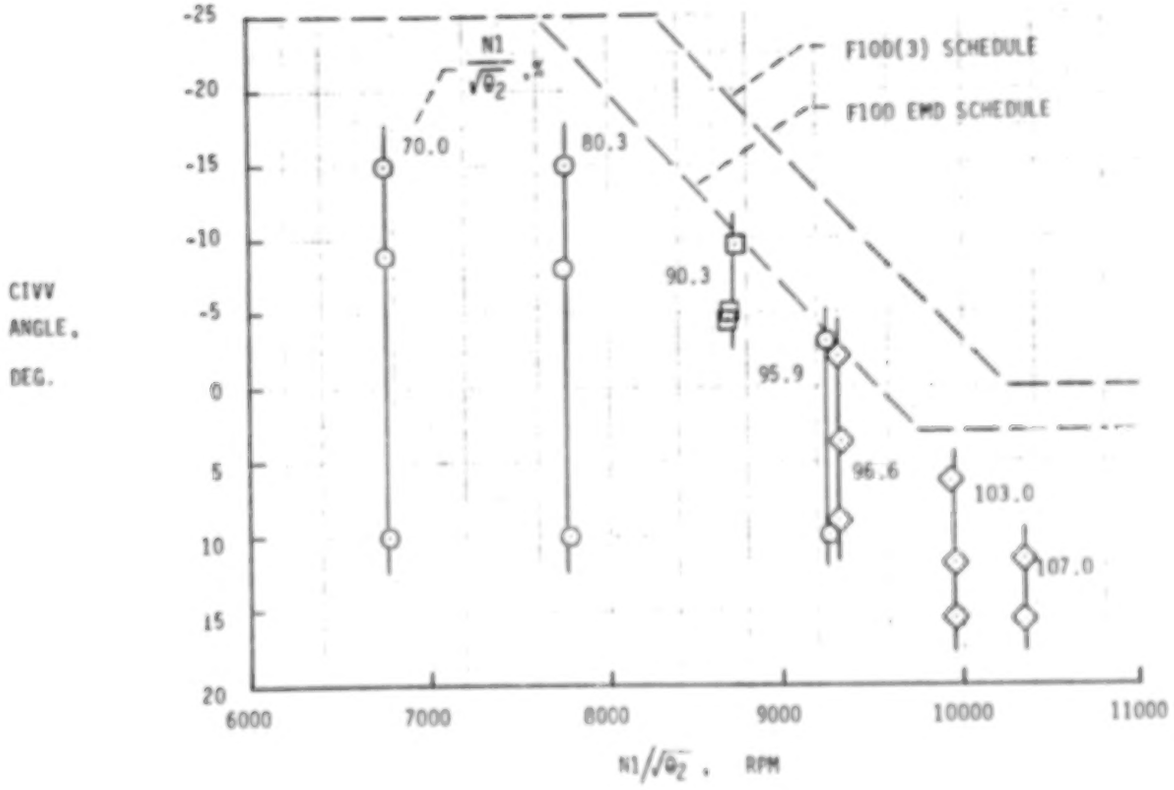

Fig.10 - XD11-10 CIVV VARIATION VS CORRECTED FAN SPEED

ORIGINAL PAGE IS
OF POOR QUALITY

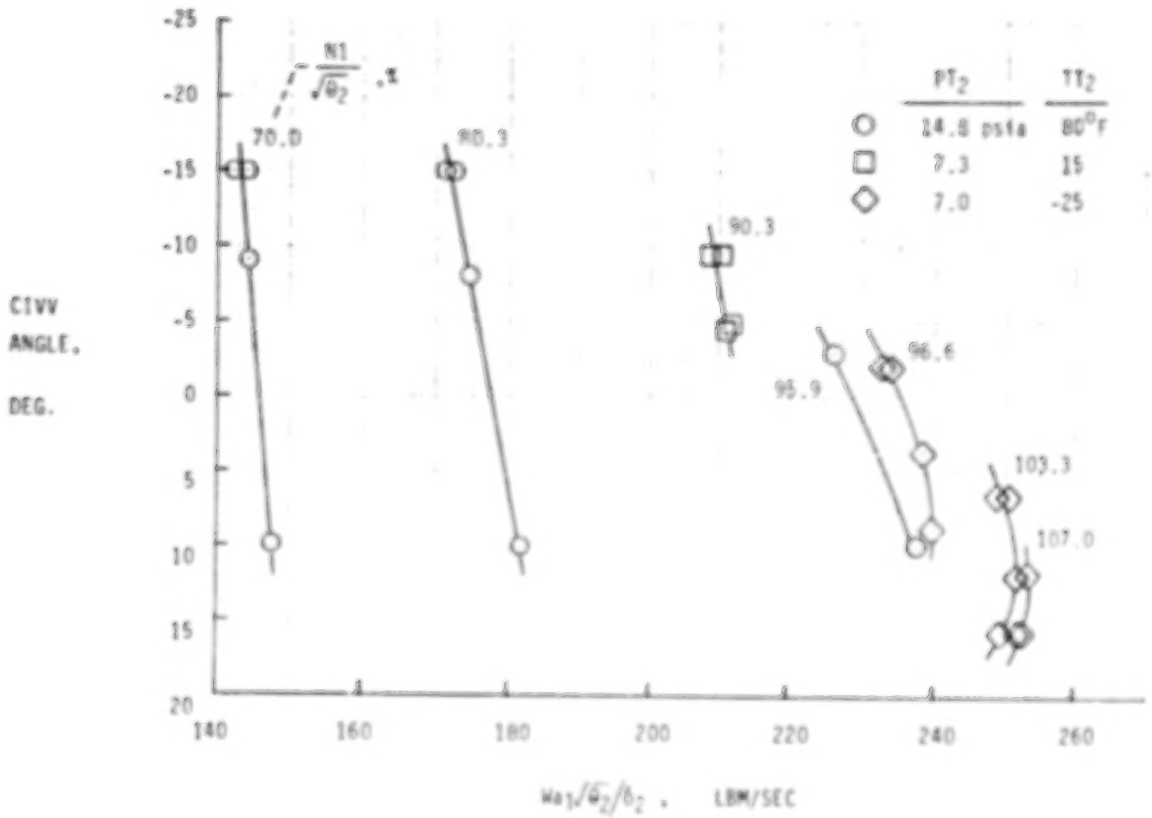

Fig.11 - XD11-10 CIVV VARIATION VS CORRECTED TOTAL AIRFLOW

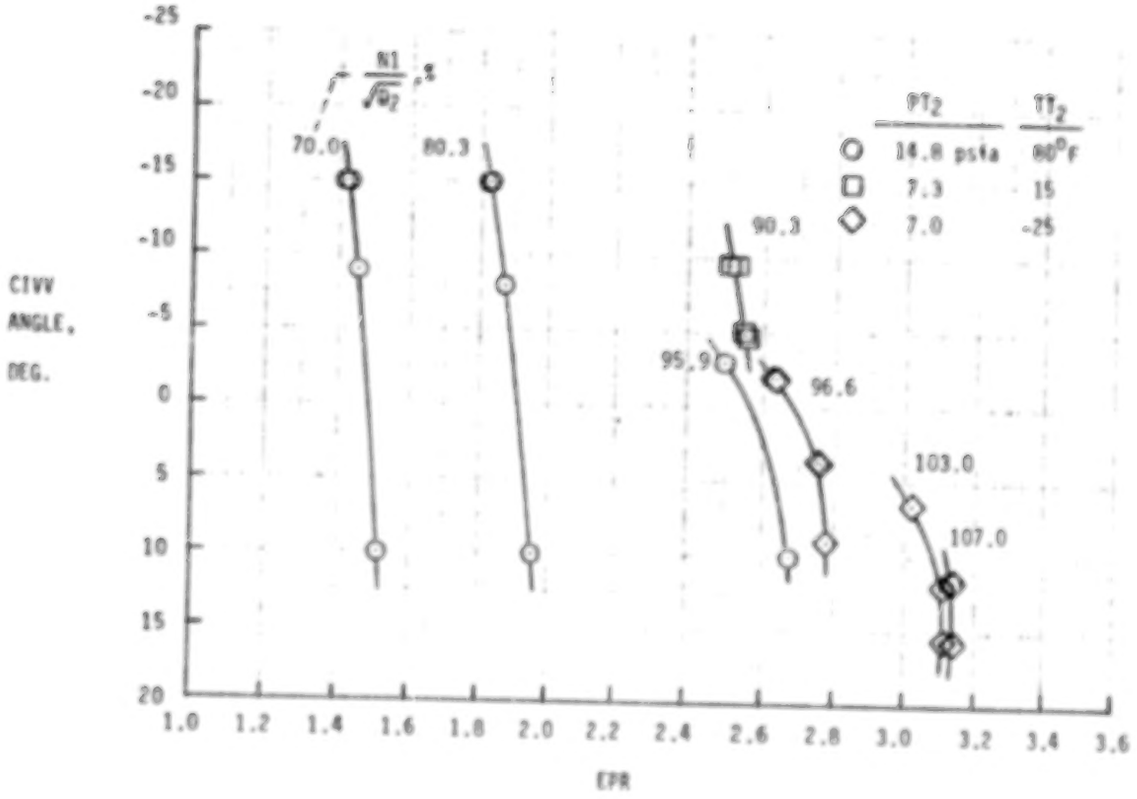

Fig.12 – XD11-10 CIVV VARIATION VS ENGINE PRESSURE RATIO, EPR

CONCLUDING REMARKS

Some of the results of evaluations with the XD11-11 and XD11-10 engine are summarized as follows:

(1) Two DEEC control flight logics were verified for F100 EMD flight tests.

(2) An EPR control loop nozzle instability was successfully investigated.

(3) The LOD/fast acceleration was optimized, resulting in five-segment augmentor system transient operation above the previous F100 limits.

(4) An earlier version of the F100 EMD fan was cleared of flutter throughout the flight envelope. An off-schedule CIVV fan-coupled system mode flutter for rotor 1 was identified.

(5) DEEC noseboom and P6M01 measurements performed satisfactorily.

(6) A new CIVV schedule for increased airflow was formulated.

REFERENCES

1. Burcham, F.W., Jr.; Myers, L.P.; and Zeller, J.R.: Flight Evaluation of Modifications to a Digital Electronic Engine Control System in an F-15 Airplane. AIAA Paper 83-0537 (NASA TM-83088), Jan. 1983.

2. Foote, C. H.: Data Analysis of PT/PS Noseboom Probe Testing on F100 Engine P680072 at NASA Lewis Research Center. NASA CR-158816, 1980.

N86
25347

UNCLAS

N86-25347

Paper 5

EFFECTS OF INLET DISTORTION ON A STATIC PRESSURE PROBE MOUNTED ON THE ENGINE HUB IN AN F-15 AIRPLANE

Donald L. Hughes and Karen G. Mackall
NASA Ames Research Center
Dryden Flight Research Facility
Edwards, California

SUMMARY

Knowledge of the pressure conditions at the engine face is important for the efficient control of an air-breathing engine. However, there are many problems encountered in obtaining good engine face pressure data. In a special study, a single static measurement located upstream of the engine hub in the stream flow was found to provide a pressure signal suitable for engine control.

A probe for measuring fan inlet static pressure (PS2) was designed for and mounted on the hub of the left F100-PW-100 turbofan engine installed in the F-15 test aircraft for flight evaluation at the NASA Ames Research Center Dryden Flight Research Facility (ARC-DFRF) (ref. 1). This same probe was also evaluated on the hub of another F100 engine in the NASA Lewis Research Center (LeRC) altitude facility (ref. 2). The probe is currently being used as a static pressure sensor for a digital engine control system (ref. 3).

PRECEDING PAGE BLANK NOT FILMED

WHY IS PS2 NEEDED?

Fan inlet total pressure (PT2) is a critical control parameter, so how is it measured? Using a single PT2 probe would be acceptable for uniform flow conditions but when the flow is distorted the PT2 measurement varies significantly across the engine face. An alternative is to use a multiple probe rake array; however, this array is complex and expensive to install. One alternative is a static pressure measurement mounted on the engine hub to provide a total-to-static pressure ratio, which is a function of airflow. Digital controls can calculate airflow, and hence PT2, but what are the effects of distortion on PS2? And are they correlatable? This paper attempts to answer these questions.

Why PS2?

NASA
DFRF83-644

- PT2 (Engine Face Total Pressure) is a critical engine control parameter
- Measure PT2 with a single probe ?
  - OK for uniform flow
  - For distorted flow, PT2 = ?

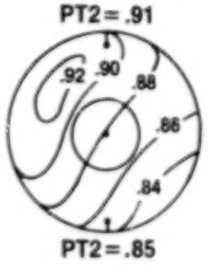

- Measure PT2 with a multiprobe rake ?
  - Great PT2 data
  - Complex
  - Expensive

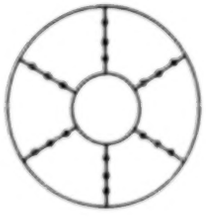

- Use an indirect measurement ?
  - Static pressure measured on hub mounted probe provides a total-to-static pressure ratio which is only a function of airflow
  - Digital controls can calculate airflow, and hence, PT2
  - Distortion effects ?

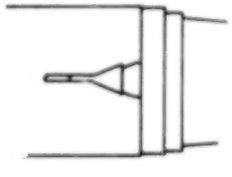

ORIGINAL PAGE IS
OF POOR QUALITY

PS2 PROBE AND PT2 RAKE ON F100 ENGINE

A closeup photo of the F100-PW-100 engine face shows the PS2 static probe mounted on the hub center. The PT2 probes, of which there are 35, can be seen mounted in seven of the inlet guide vanes. The 35-probe seven-rake array of total pressure probes at the engine face provides the data needed to determine total pressure recovery and to calculate various distortion factors. The distortion factors are:

DTMM = (PT2MAX - PT2MIN)/PT2AVG

$K\theta$ = engine manufacturers' cicumferential distortion factor

KRA2 = engine manufacturers' radial distortion factor

KA2 = $K\theta$ + b(KRA2)
where b is a weighting factor (function of airflow)

The equations for these distortion factors are given in reference 4.

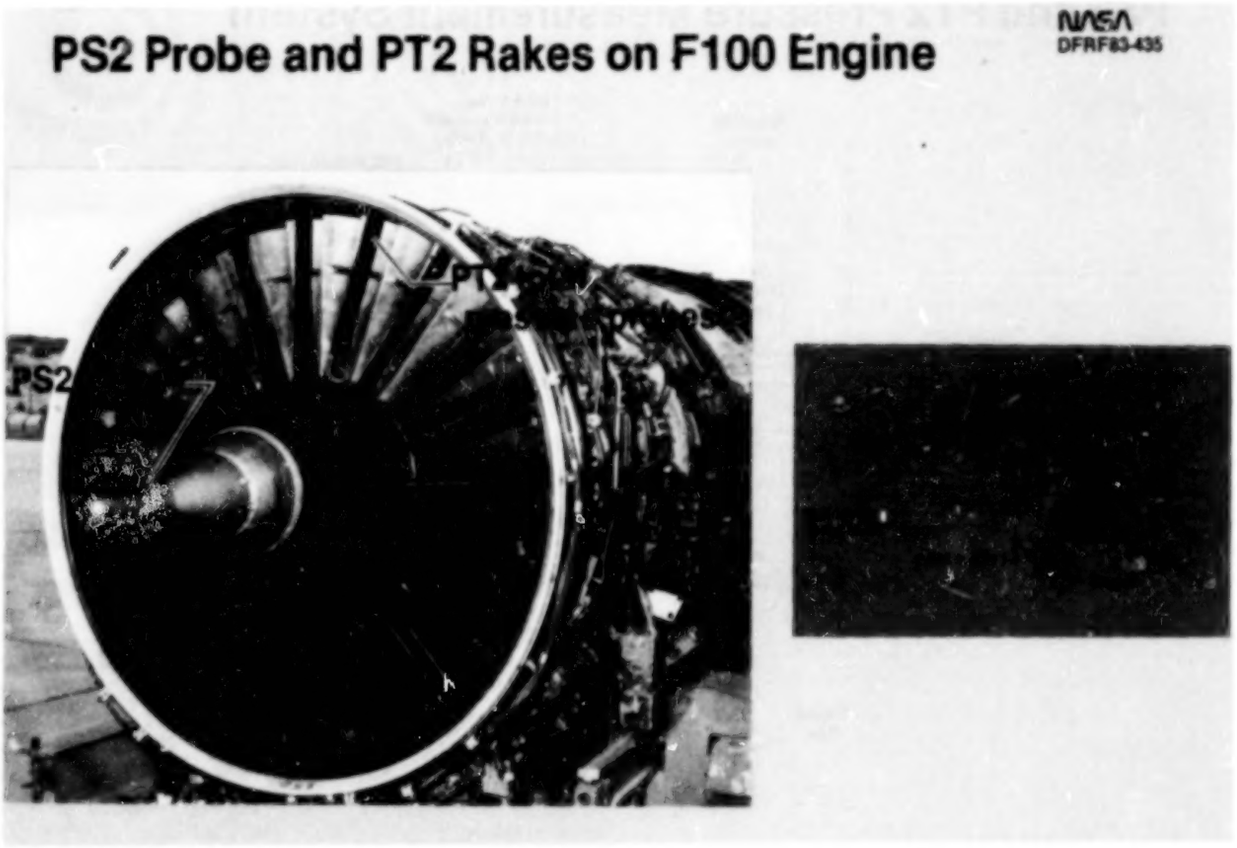

PRESSURE INSTRUMENTATION

The schematic of the pressure instrumentation is shown below. In order to increase the accuracy of all of the results, the engine face pressures were measured with differential pressure transducers. Pressure accuracy was approximately 1 percent. Reference pressure was obtained from an inlet wall static pressure tap and was stabilized by the use of a pressure reservoir. The reference pressure was measured with a highly accurate digital quartz pressure transducer. All transducers were located in an environment that was temperature controlled. The resulting accuracy was estimated to be ±1 percent. The PS2 pressure was measured with three differential transducers, and the measurements were averaged for improved accuracy. With a pressure accuracy of 1 percent, calculated distortion factor accuracy was 3 percent (ref. 5). The long lines between pressure probes and transducers resulted in the data being usable for steady-state information only.

PS2 and PT2 Pressure Measurement System

NASA
DFRF83-436

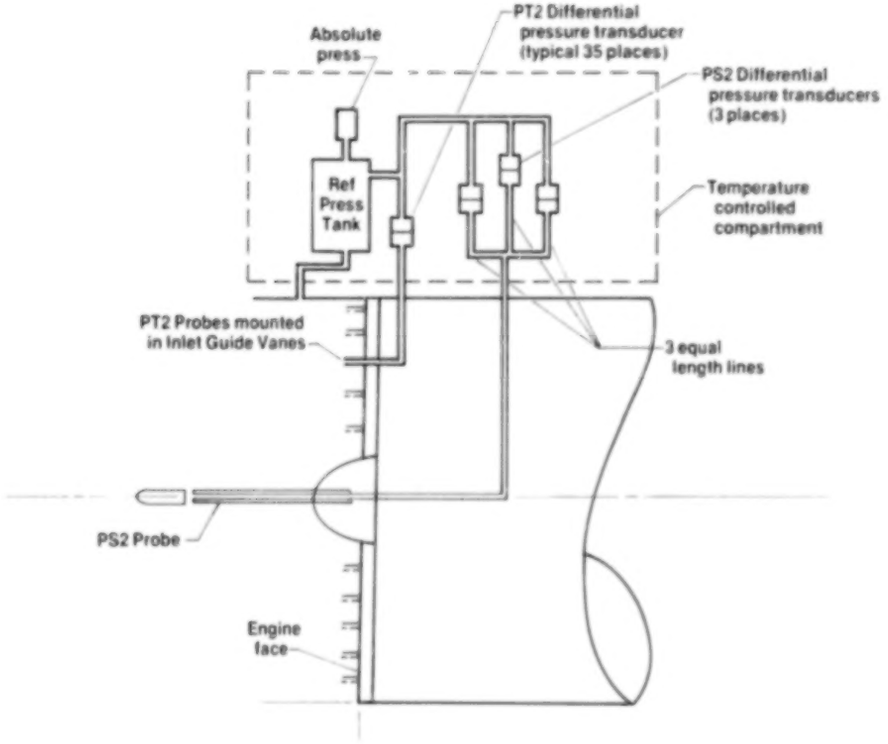
PT2 Differential pressure transducer (typical 35 places)
Absolute press
PS2 Differential pressure transducers (3 places)
Ref Press Tank
Temperature controlled compartment
PT2 Probes mounted in Inlet Guide Vanes
3 equal length lines
PS2 Probe
Engine face

F-15 INLET

The F-15 aircraft has two side-mounted inlets of a two-dimensional horizontal ramp design. The inlets provide external compression with three ramps and feature variable capture area by rotating the inlet about a transverse hinge point at the lower cowl lip. The ramps and bypass doors are automatically scheduled by the air inlet controllers. For the distortion data presented in this paper, the third inlet ramp was controlled manually in flight to vary the third ramp angle in increments. The third ramp is shown in the "down" position. As the third ramp angle is increased, the inlet throat area is decreased, the inlet Mach number is increased, and the distortion at the engine face is increased until the engine stalls.

F-15 Inlet

NASA
DFRF83-437

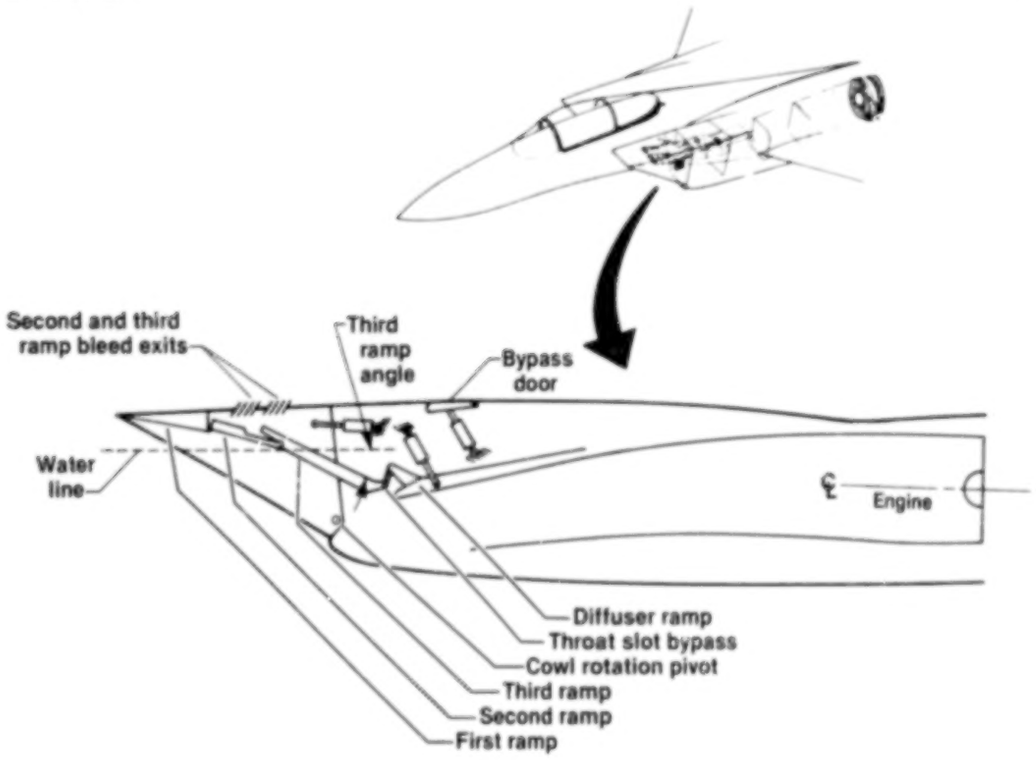

PT2 CALCULATION

On those systems that do not have engine face PT2 measurements, the PT2 can be calculated as schematically shown below. Engine corrected airflow (WAC2) is obtained from the engine pumping curve by the input of fan-corrected rotor speed and engine pressure ratio. The DEEC logic contains a table of PT2/PS2 as a function of airflow, so entering the table with airflow and PS2, PT2 can be obtained. Since engine pressure ratio (EPR) requires the PT2 measurements, an iterative procedure is required.

PT2 Calculation

NASA
DFRF83-438

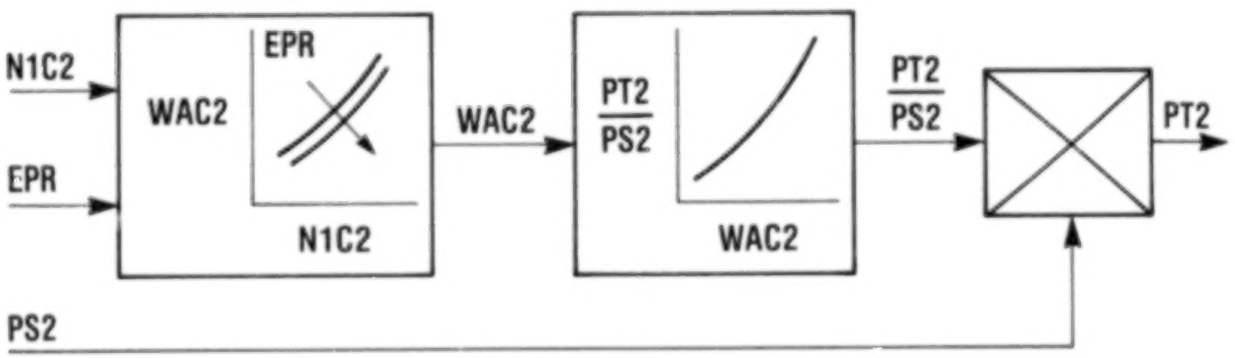

$\overline{PT2}/PS2$ AT LOW DISTORTION

The PS2 static pressure probe was tested in an altitude facility on an F100 engine and in the inlet of an F-15 airplane while in flight. Steady-state low distortion data, obtained over a range of engine throtle settings at Mach 0.9 and 40,000 ft, was compared with low distortion data obtained on a different engine in an altitude facility (ref. 6). The data from flight and the altitude facility compared $\overline{PT2}/PS2$ pressure ratio with corrected engine airflow (WAC2) and showed no measurable shift in $\overline{PT2}/PS2$. Other flight test conditions, including Mach number excursions and maximum load factor turns, also correlated with previous altitude facility test results.

Low Distortion Flight Conditions

NASA
DFRF83-439a

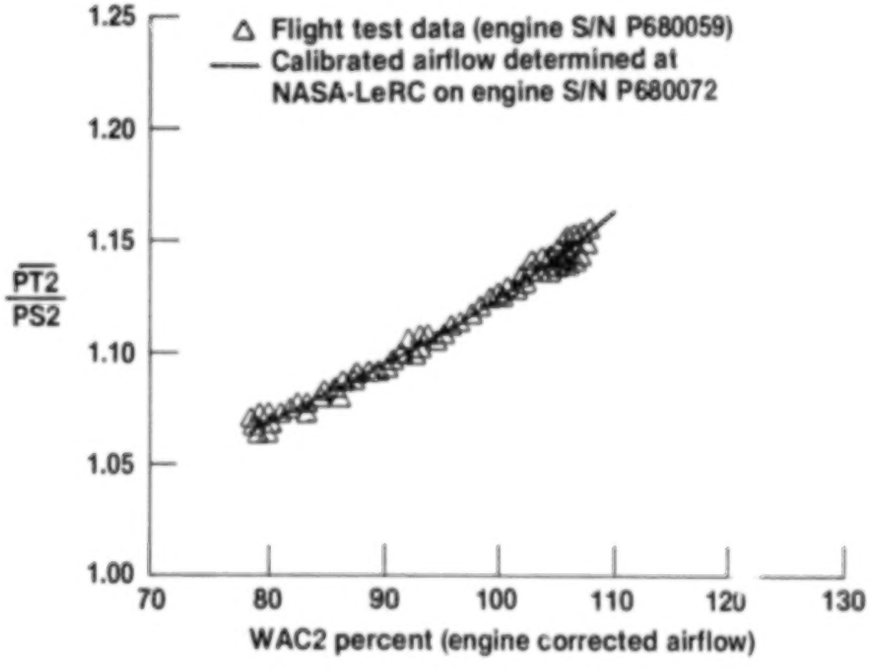

INDUCED DISTORTION

Increased levels of distortion were desired to evaluate effects on the PT2/PS2 relationship. Increased levels of distortion in the inlet were induced during flight test by lowering the inlet third ramp in a series of steps, with each step being held for about 10 sec. With increasing third ramp angle, the inlet throat area was reduced, causing the inlet throat Mach number to increase. The $\overline{PT2}/PS2$ pressure ratio also gradually increased until engine stall occurred. Four of these tests were conducted at Mach 0.8 and 0.9 at altitudes of 30,000 and 40,000 ft.

$\overline{PT2}/PS2$ Variation with Ramp Step Inputs

NASA
DFRF83-440

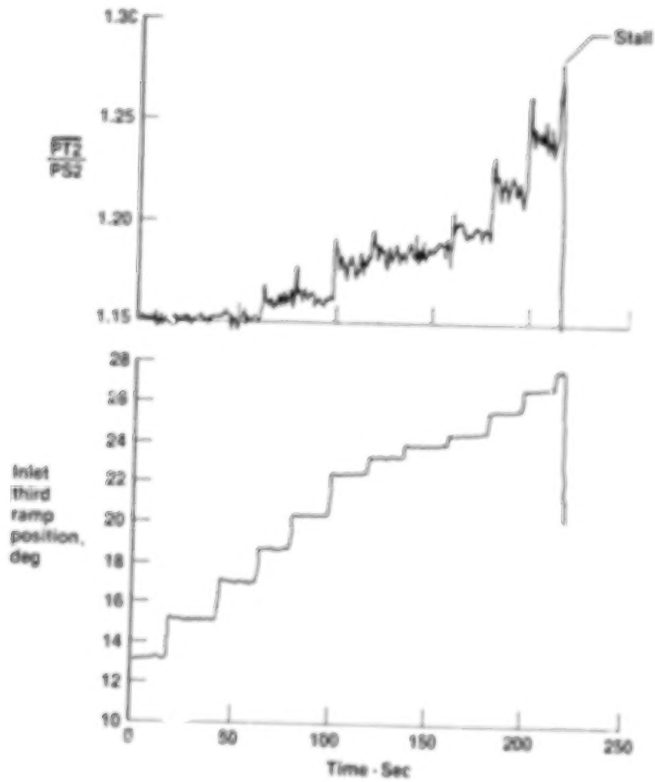

INCREASING INLET THIRD RAMP ANGLE

A typical data run showing a plot of all of the distortion factors and the pressure ratios versus inlet third ramp angle is given below. The distortion factor (DTMM), circumferential distortion factor (KΘ), and overall distortion factor (KA2) increase with increasing third ramp angle, while the radial distortion factor (KRA2) changes very little. The engine face pressure ratio PT2/PS2 gradually increases with increasing third ramp angle while the fan inlet total pressure recovery (PT2)/free stream total pressure (PTINF) decreases.

Typical Ramp Excursion

NASA
DFRF83-441

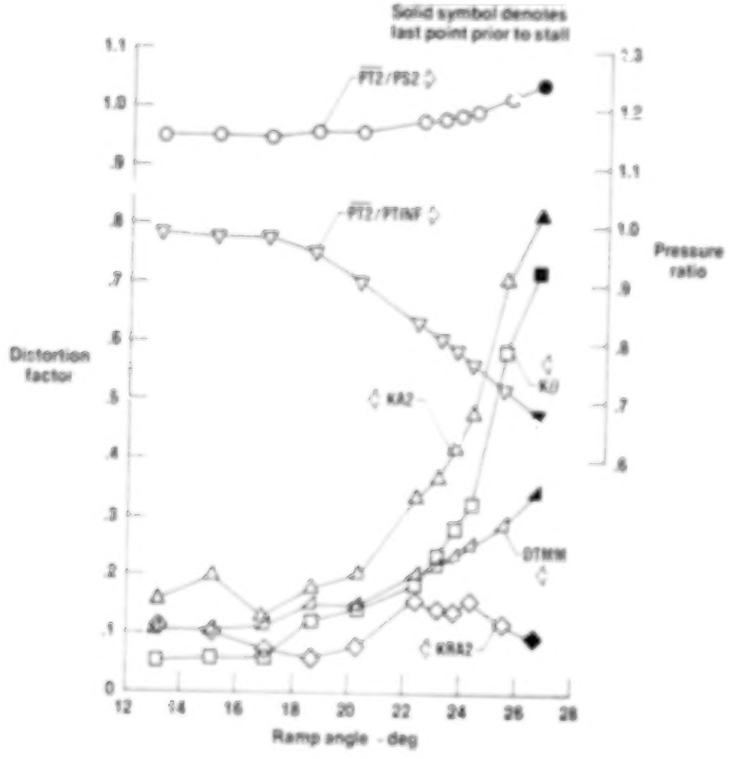

COMPRESSOR FACE DISTORTION MAPS

The compressor face distortion maps, illustrated below, show increasing pressure distortion as the inlet third ramp angle is increased. The pressure patterns change from the relatively symmetrical shapes of low distortion to a classical 180° distortion pattern seen just before engine stall and depicted in figure (d). These 180° distortion patterns have relatively large pressure gradients across the engine face with high pressure on the inboard side and low pressure on the outboard side. These distortion maps are a graphical presentation of the pressure distributions at the engine face. The calculated distortion factors KΘ, KA2, and DTMM, however, provide numerical values that can be better evaluated and compared.

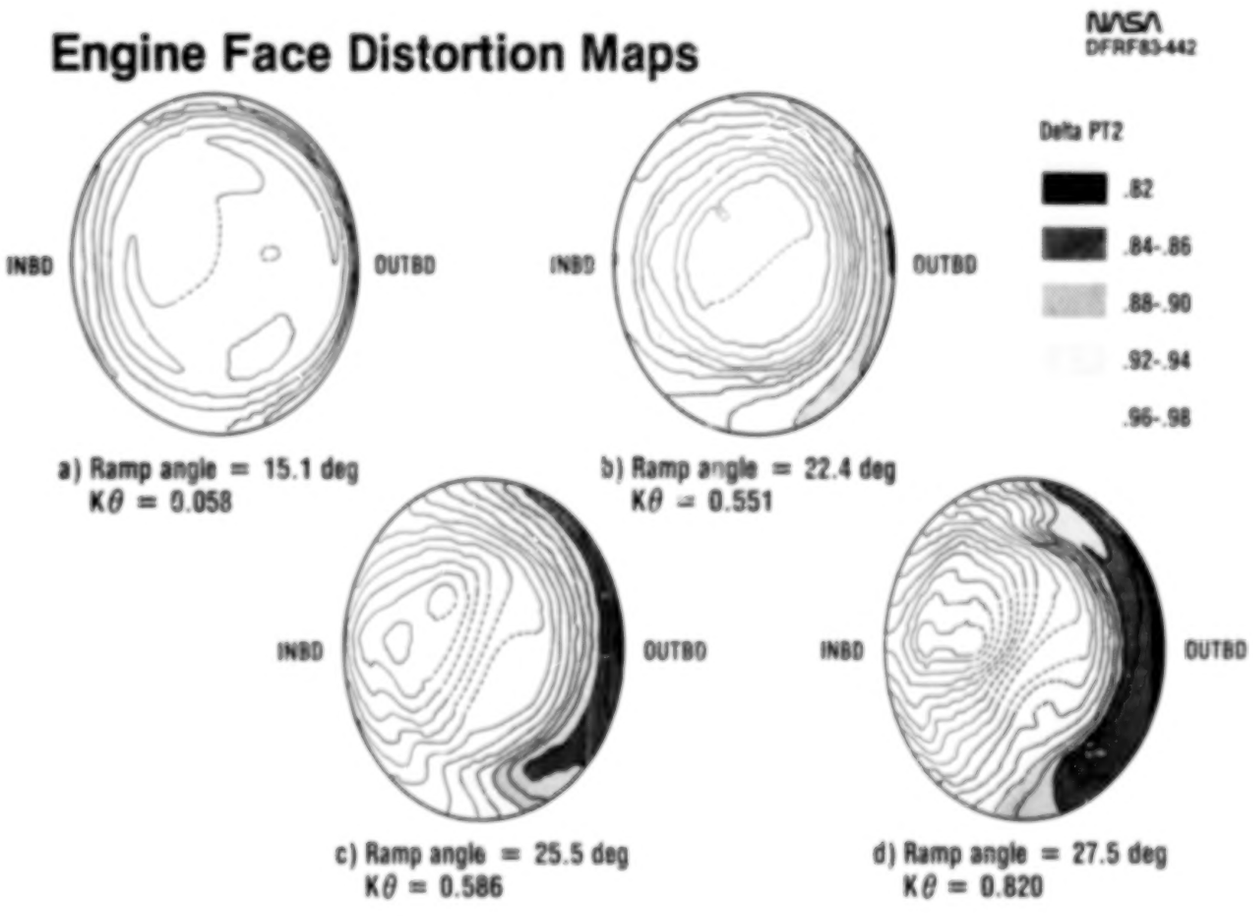

KA2 VERSUS RAMP ANGLE

When the distortion factor data from each of the four ramp excursions are combined on one plot, the repeatable nature of each of the distortion factors is shown. The KA2 distortion factor increases very rapidly and goes to large values with increasing inlet third-ramp angle. The three tests (I, III, and IV), run at maximum airflow, show excellent agreement. Run II was conducted at a slightly lower airflow, and deviates from the other three runs.

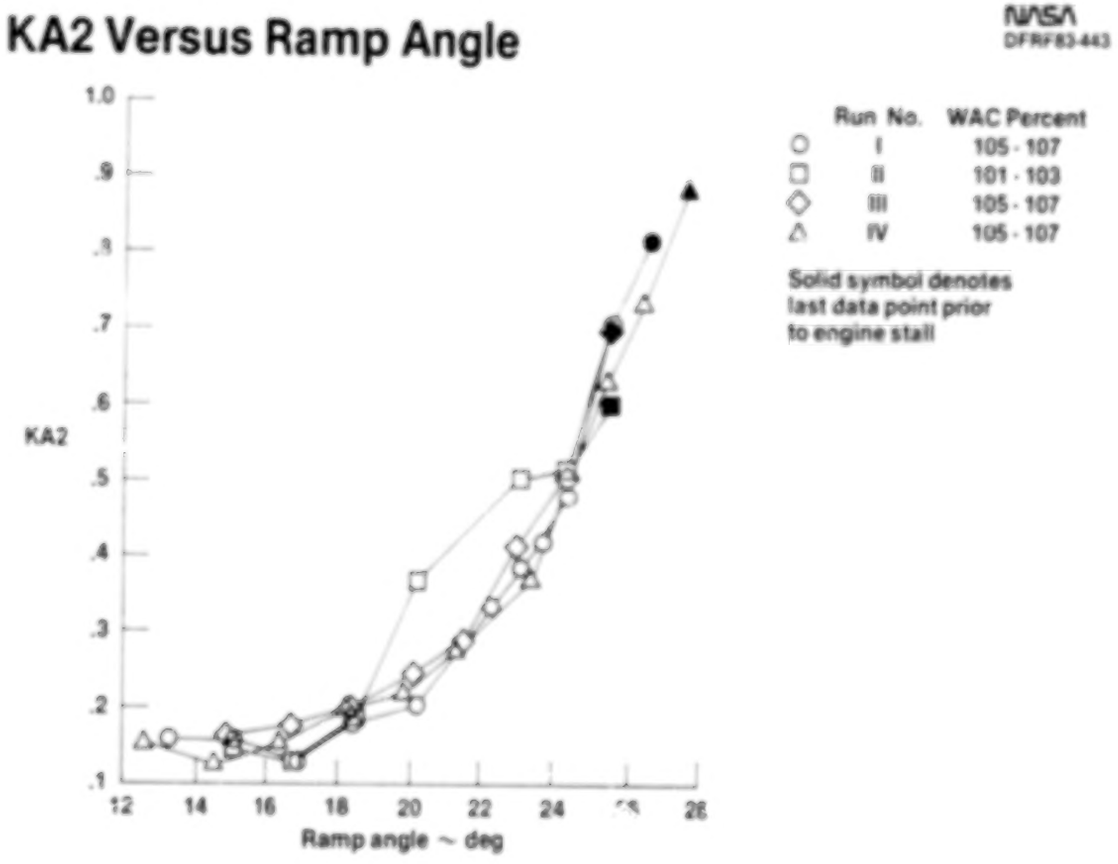

Kθ VERSUS RAMP ANGLE

The circumferential distortion factor Kθ also increases rapidly at the higher third ramp angles, and minor differences between the four runs are seen. DTMM increases less than Kθ and is not shown.

Kθ Versus Ramp Angle

NASA
DFRF83-444

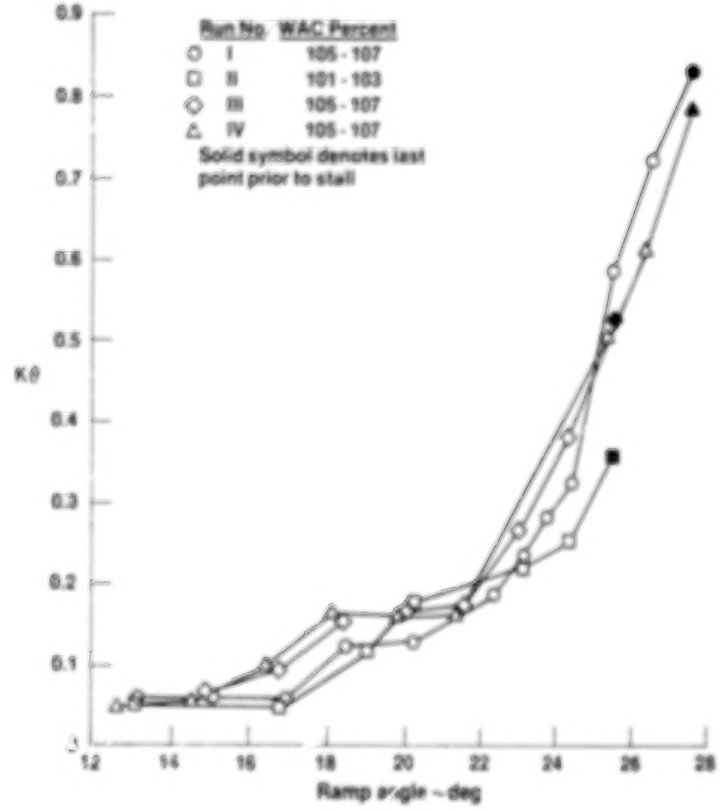

KΘ VERSUS $\overline{PT2/PS2}$

When the pressure ratio $\overline{PT2/PS2}$ is compared against the distortion factors, a definite correlation exists for all except the radial distortion factor KRA2. The circumferential distortion factor KΘ, shown below, exhibits a good linear correlation with $\overline{PT2/PS2}$ for all four tests. The effects of free-stream Mach number, altitude, or airflow differences are not evident in the data.

$\overline{PT2/PS2}$ Versus Kθ

NASA
DFRF83-445

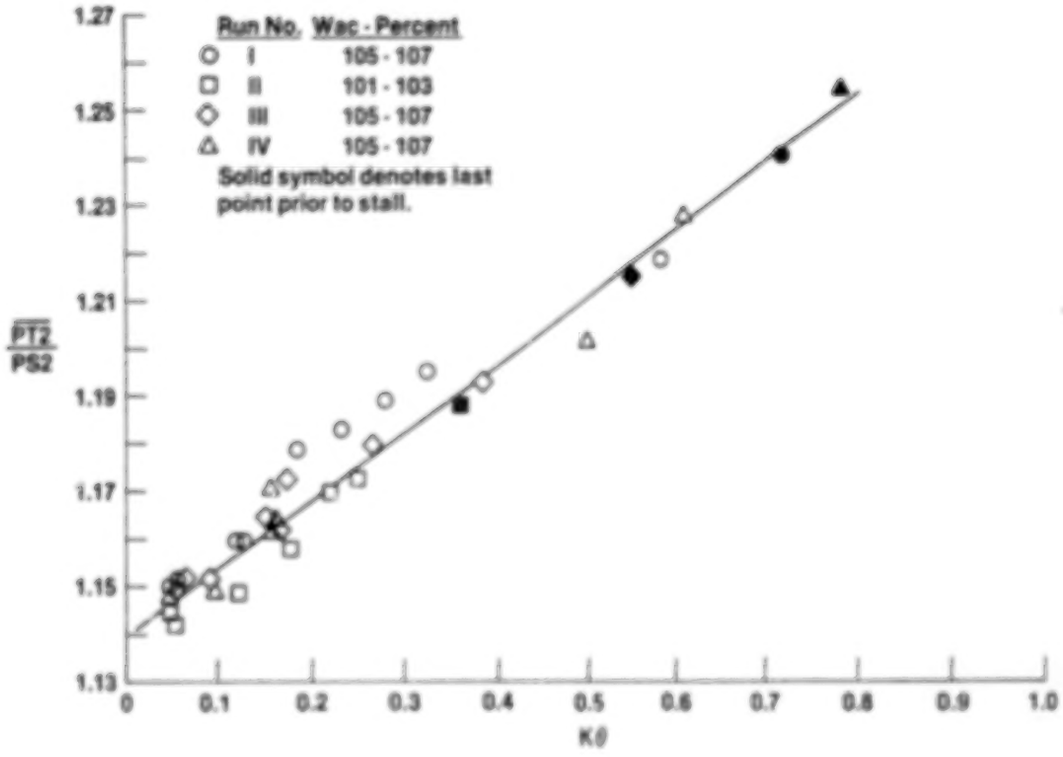

DTMM VERSUS $\overline{PT2}/PS2$

The distortion factor DTMM also shows good correlation, with no apparent effect of free-stream Mach number, altitude, or airflow differences for the four tests conducted.

$\overline{PT2}/PS2$ Versus DTMM

NASA
DFRF83-446

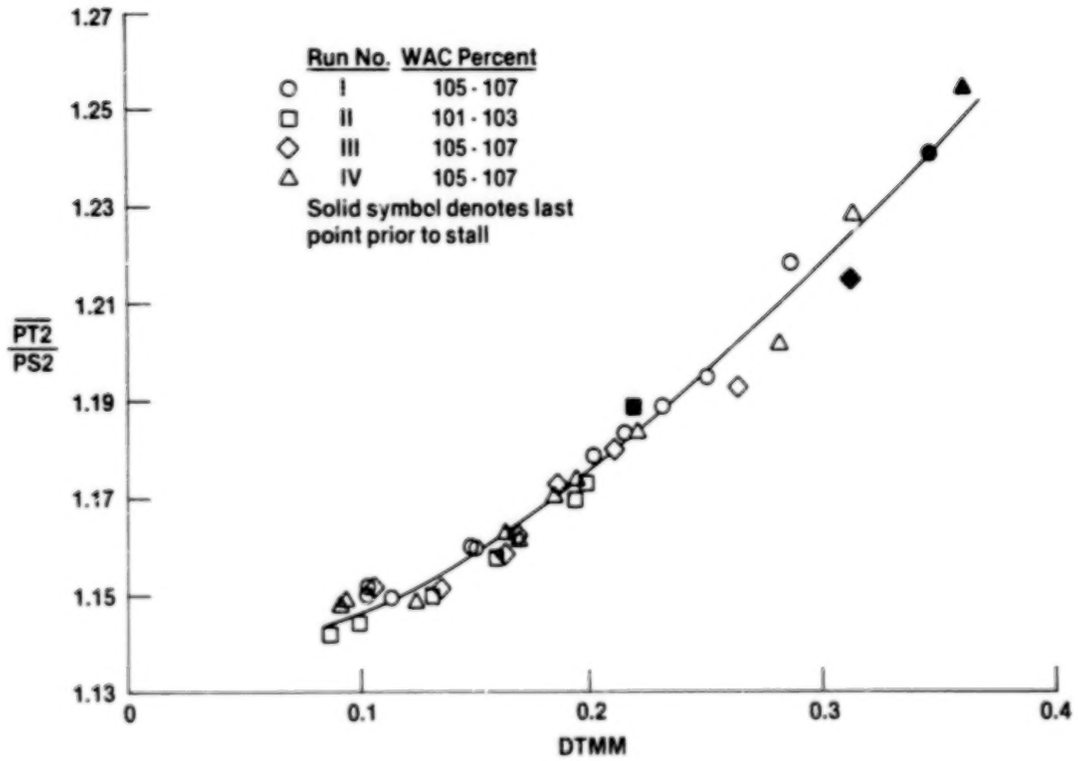

C-2

EFFECT OF DISTORTION ON EPR

As distortion increases, the engine without the DEEC control logic remains at about a constant EPR, whereas the engine operating with PS2 input to DEEC will compensate by downtrimming the engine. When the Kθ distortion increases to about 0.8, EPR is reduced by about 10 percent, thus effectively downtrimming the engine by about 10 percent and automatically helping the engine avoid stall.

Effect of $K\theta$ on EPR

NASA
DFRF83-447

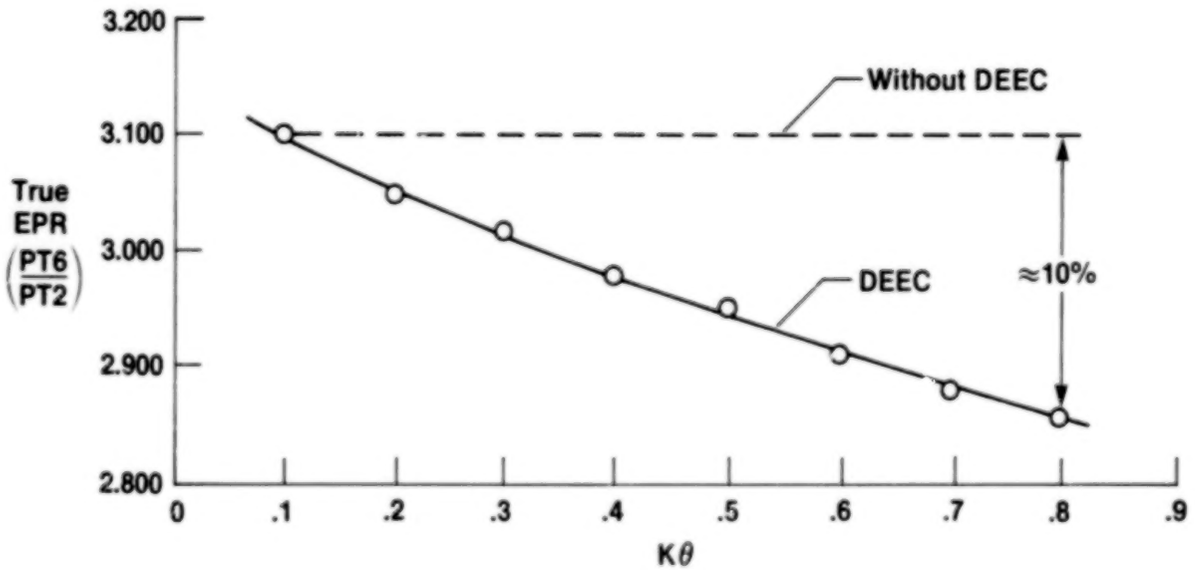

CONCLUSIONS

1. For low distortion conditions, the ratio of engine face total pressure to static pressure agreed well with previous altitude facility data.

2. During tests in which the inlet throat area was reduced, large amounts of circumferential distortion occurred, but only small amounts of radial distortion occurred.

3. The ratio of engine face total pressure to static pressure correlated well with the distortion factors $K\theta$, KA2, and DTMM.

4. The PS2 probe can be useful as an engine control parameter as part of an algorithm to provide automatic compensation for distortion.

REFERENCES

1. Foote, C. H.; and Jaekel, R. J.: Flight Evaluation of an Engine Static Pressure Noseprobe in an F-15 Airplane. NASA CR-163109, 1981.

2. Foote, C. H.: Final Report Analysis of PT/PS Noseboom Probe Testing on F100 Engine at NASA Lewis Research Center. NASA CR-159816, 1980.

3. Barrett, W. J.; Rembold, J. P.; Burcham, F. W.; and Myers, L.: Flight Test of a Full Authority Digital Electronic Engine Control System in an F-15 Aircraft. AIAA Paper 81-1501, AIAA/SAE/ASME 17th Joint Propulsion Conference, Colorado Springs, Colo., July 27-28, 1981.

4. Stevens, C. H.; Spong, E. D.; and Hancock, M. S.: F-15 Inlet/Engine Test Techniques and Distortion Methodologies Studies, Vol. 1 Technical Discussion. NASA CR-144866, 1978.

5. Farr, A. P.; and Schumacher, G. A.: System For Evaluation of F-15 Inlet Dynamic Distortion. McAir 72-043, Sept. 1972.

6. Biesiandny, Thomas J.; Lee, Douglas; and Rodriguez, Jose R.: Airflow and Thrust Calibration of an F100 Engine, S/N P680059, at Selected Flight Conditions. NASA TP-1069, 1978.

N86
25348

UNCLAS

N86-25348

Paper 6

FLIGHT TESTING THE DIGITAL ELECTRONIC ENGINE CONTROL IN THE F-15 AIRPLANE

Lawrence P. Myers
NASA Ames Research Center
Dryden Flight Research Facility
Edwards, California

SUMMARY

The digital electronic engine control (DEEC) is a full-authority digital engine control developed for the F100-PW-100 turbofan engine; it has been flight tested on an F-15 airplane at the NASA Ames Research Center's Dryden Flight Research Facility (DFRF). The objectives of the flight test were to evaluate the DEEC hardware and software throughout the F-15 flight envelope. New real-time data reduction and data display systems were implemented. New test techniques and stronger coordination between the propulsion test engineer and pilot were developed which produced efficient use of test time, reduced pilot work load, and greatly improved quality data. The engine pressure ratio (EPR) control mode was demonstrated. Nonaugmented throttle transients and engine performance were satisfactory.

PRECEDING PAGE BLANK NOT FILMED

F-15 INSTRUMENTATION SYSTEM

The figure below shows the instrumentation system for the F-15. Starting at the top, airframe parameters, such as altitude, airspeed, and Mach number were recorded directly. Several engine parameters were recorded and are shown in detail on the next figure. The DEEC computer outputs a serial digital data stream that is processed through an interface box to make the signal compatible with the pulse code modulation (PCM) system. A breadboard diagnostic unit was used on the ground for interrogating and powering the DEEC without starting the engine. Finally, the data was recorded onboard the aircraft and also telemetered to the ground for recording and real-time analysis and display.

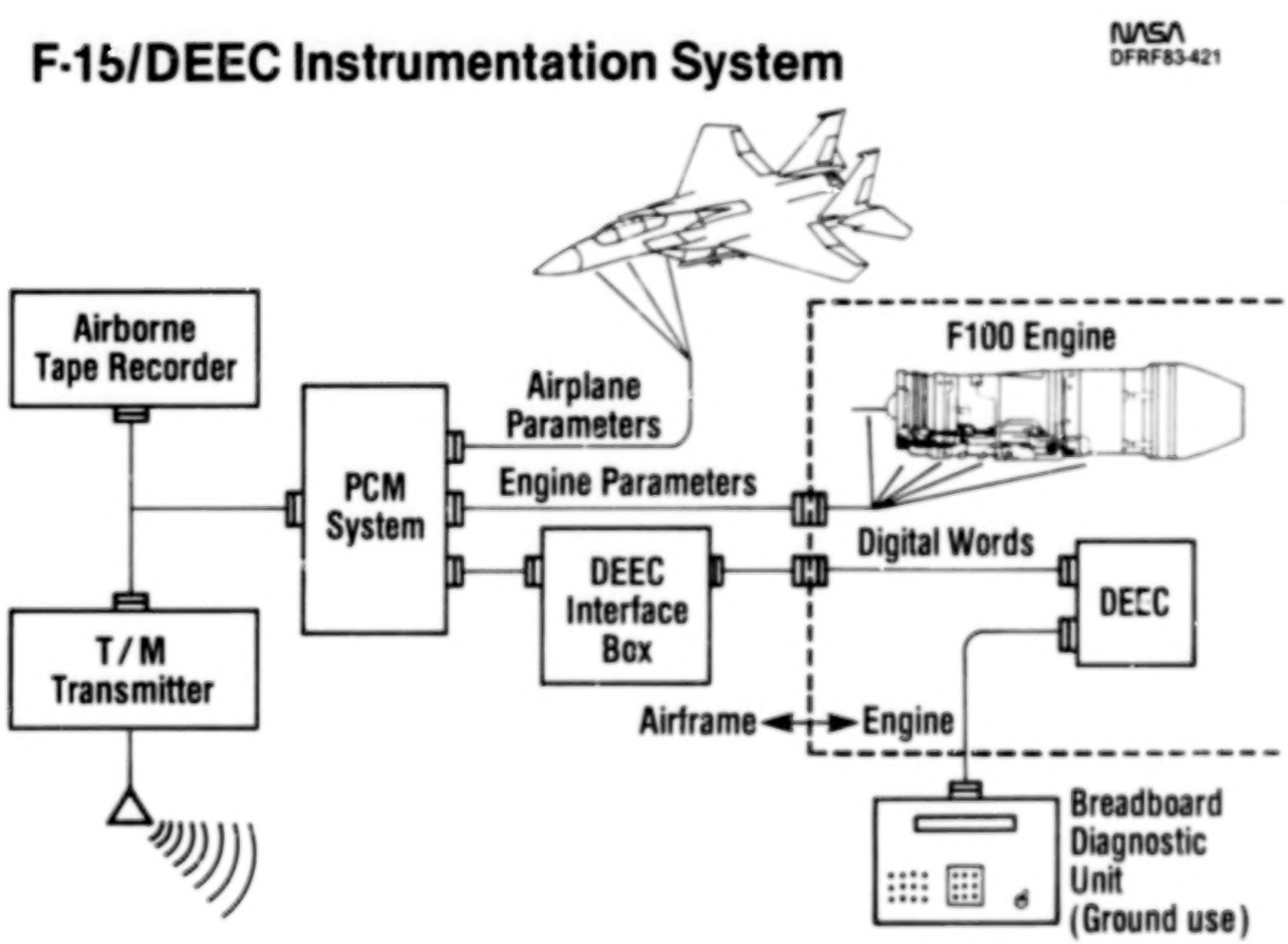

Shown on this figure are engine parameters recorded on the data system. A continuous serial digital word from the DEEC computer was also recorded. High frequency response parameters such as burner pressure (PB), augmentor static pressure (PAB), turbine discharge pressure (PT6), and the augmentor segment fuel pressures were recorded at 200 samples per sec. The other engine and aircraft parameters were recorded at 20 samples per sec. The various parameters were filtered before digitization by the PCM system to prevent aliasing error.

The 50 DEEC digital words were updated at eight samples per second. The DEEC digital data included pressures and temperature throughout the engine, position requests and feedback, internal calculations, and eleven 16-bit diagnostic words.

DEEC FLIGHT INSTRUMENTATION

NASA
DFRF82-0156

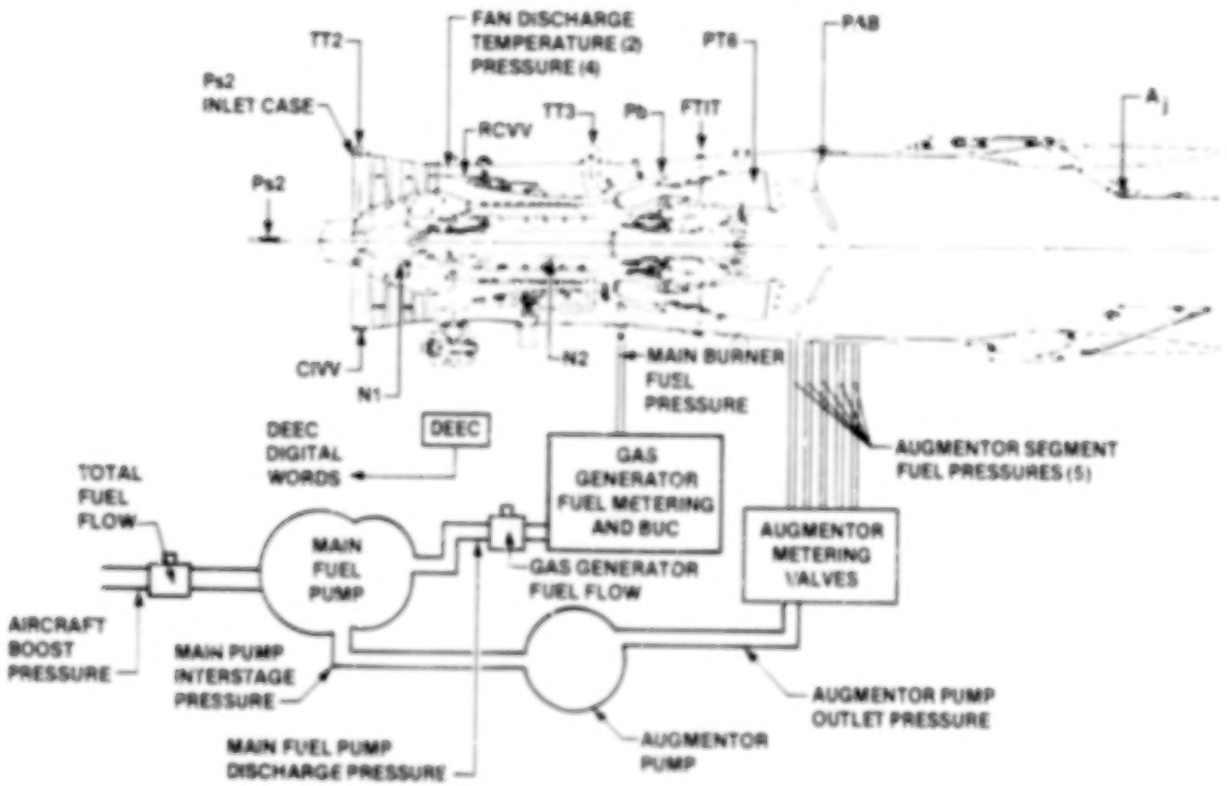

F-15 REAL-TIME DATA SYSTEM

Data from the test airplane and engine were taken from the telemetry signal and processed in real time by using a series of digital computer programs. The raw data was converted to engineering units and various computations were performed. The 11 DEEC diagnostic words were displayed on a color cathode ray tub (CRT). In-flight thrust was also calculated and displayed. The four methods of displaying the processed data were: CRT, eight-channel strip charts, X-Y plotters, and tabulated hard-copy listings.

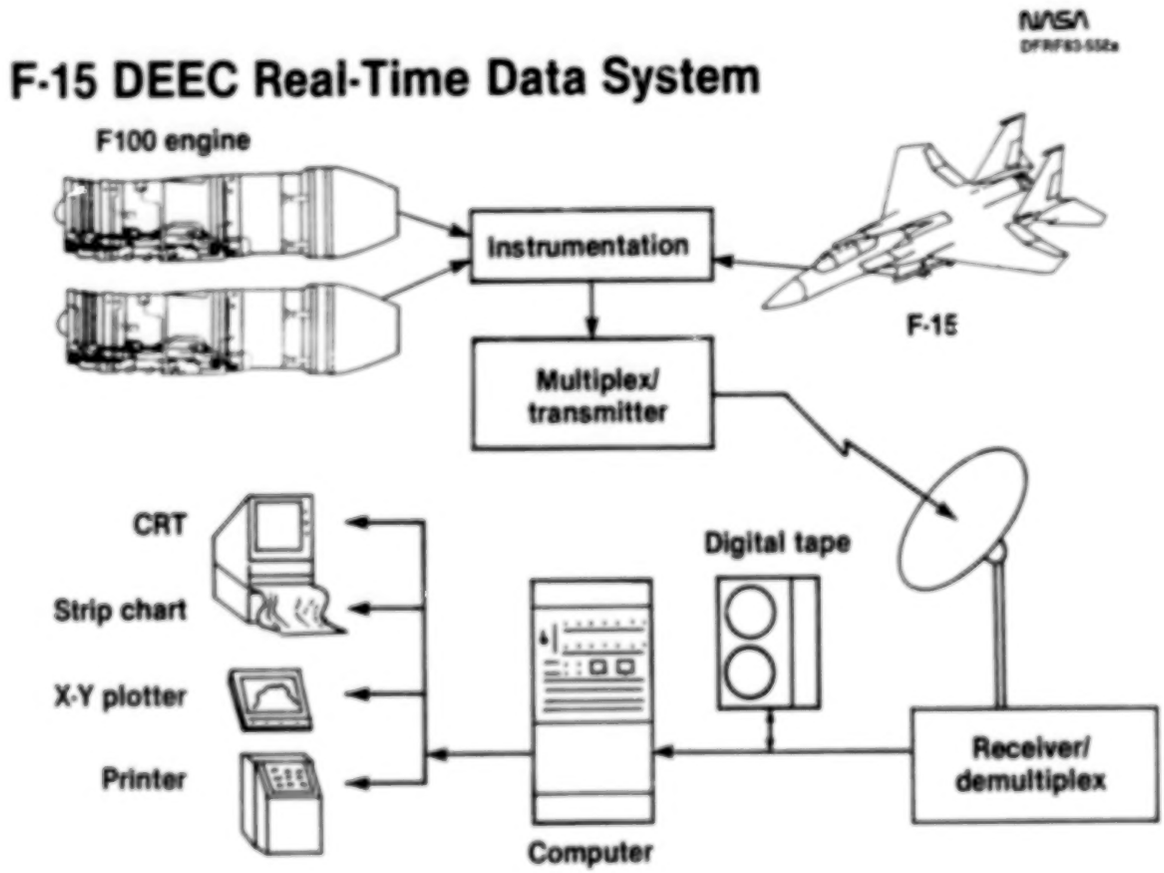

MISSION CONTROL ROOM

ORIGINAL PAGE IS
OF POOR QUALITY

The NASA mission control room, shown below, is equipped for real-time monitoring and control of research flights. For the F-15 DEEC flights, the 12 eight-channel strip charts, seven CRT displays, two X-Y plotters, and seven status light displays were used to display DEEC test data. Test engineers and technicians monitored the data and fed appropriate information to the flight controller and the research test engineer. A series of television cameras with long range optics, displayed overhead, was used for visual tracking of the airplane. Radar data on space position of the aircraft was plotted on the large consoles at the far right of the room.

STRIP CHARTS

The 12 eight-channel strip charts were the primary source of the data in monitoring the DEEC system performance. The research test engineer sat in front of the strip charts which displayed the critical engine parameters necessary to conduct an efficient and safe flight evaluation. The test engineer assisted the pilot during test maneuvers by monitoring engine conditions and requesting throttle transients at the correct revolutions per minute (RPM) values or time. The engineer assessed the results and requested that test points be repeated or deleted as appropriate. He also monitored data on the CRT and diagnostic displays. With all of the data displays, the test engineer had access to virtually all the DEEC information in real time.

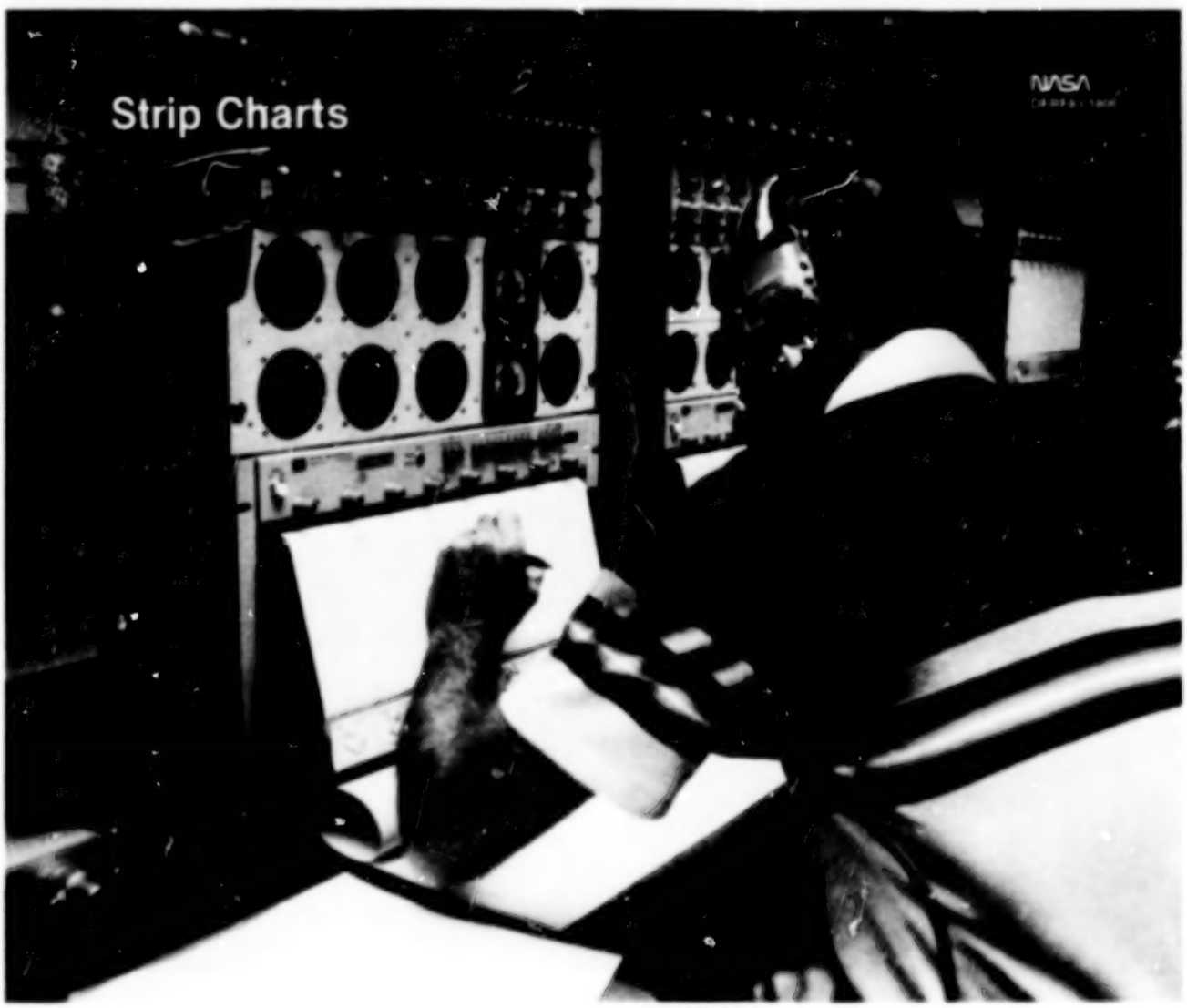

THROTTLE TRANSIENT SERIES

Two basic types of throttle transients were used: the throttle snap, a rapid single-direction movement from one stabilized power setting to another, and the bodie, which begins with a snap in one direction, followed closely by a snap in the other direction before stabilization.

For augmented transients, a series consisted of an intermediate-to-maximum-to-intermediate throttle sequence, followed by idle-to-maximum-to-idle snaps. No attempt was made to allow the augmentor manifolds to drain completely between transients. When stalls or blowouts occurred at a given test point, the transient was repeated until the same result was achieved in two out of three trials. Augmentor transients were performed in the upper left-hand corner with maximum segment limiting and, with the override switch, with full augmentation.

The throttle transient series shown below illustrates a typical transient sequence. The propulsion engineer monitoring this strip chart called the throttle sequence to the pilot. The engineer analyzed the data to determine when the engine stabilized and called for the next step in the series. This technique reduced the pilot workload and greatly improved the quality of data. The pilot concentrated on holding speed and altitude, using the right engine to compensate for the changing thrust of the test engine.

DEEC Throttle Transient Series

NASA
DFRF81-268a

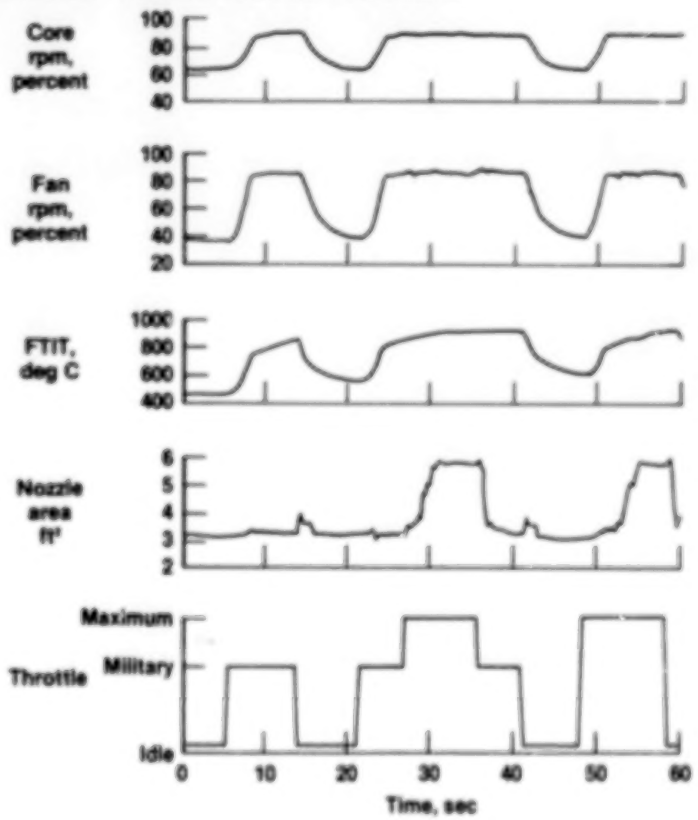

CRT DISPLAY

This figure shows a sample of the data available on the CRT. Each CRT has two data formats and a color graphics panel that can be individually selected by the engineers at the console. The long-range optics television pictures are displayed below the CRT.

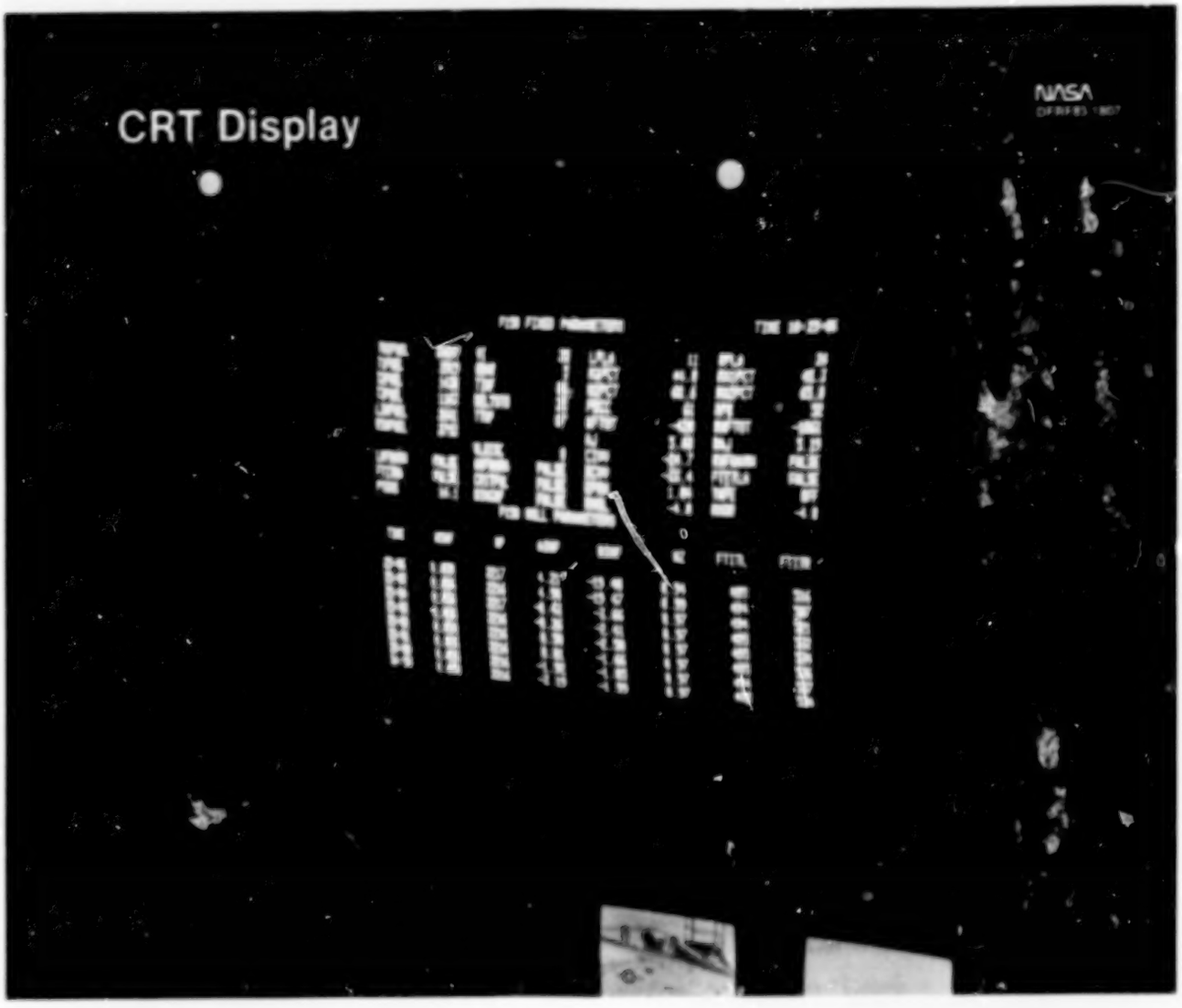

COLOR GRAPHICS PANEL

ORIGINAL PAGE IS OF POOR QUALITY

The color graphics panel is the third format on the CRT and is an 11 by 16 array. Eleven of the DEEC serial digital words were used for diagnostic words, each having 16 discrete bits. Each bit represented a discrete fault or failure in not only the DEEC computer, but the entire DEEC control system. The colors used to display the discrete bits were: gray, if the bit was not set; yellow, if the bit was set, but advisory in nature; and red, if the bit was set and the fault or failure should have caused an automatic transfer to the backup control (BUC).

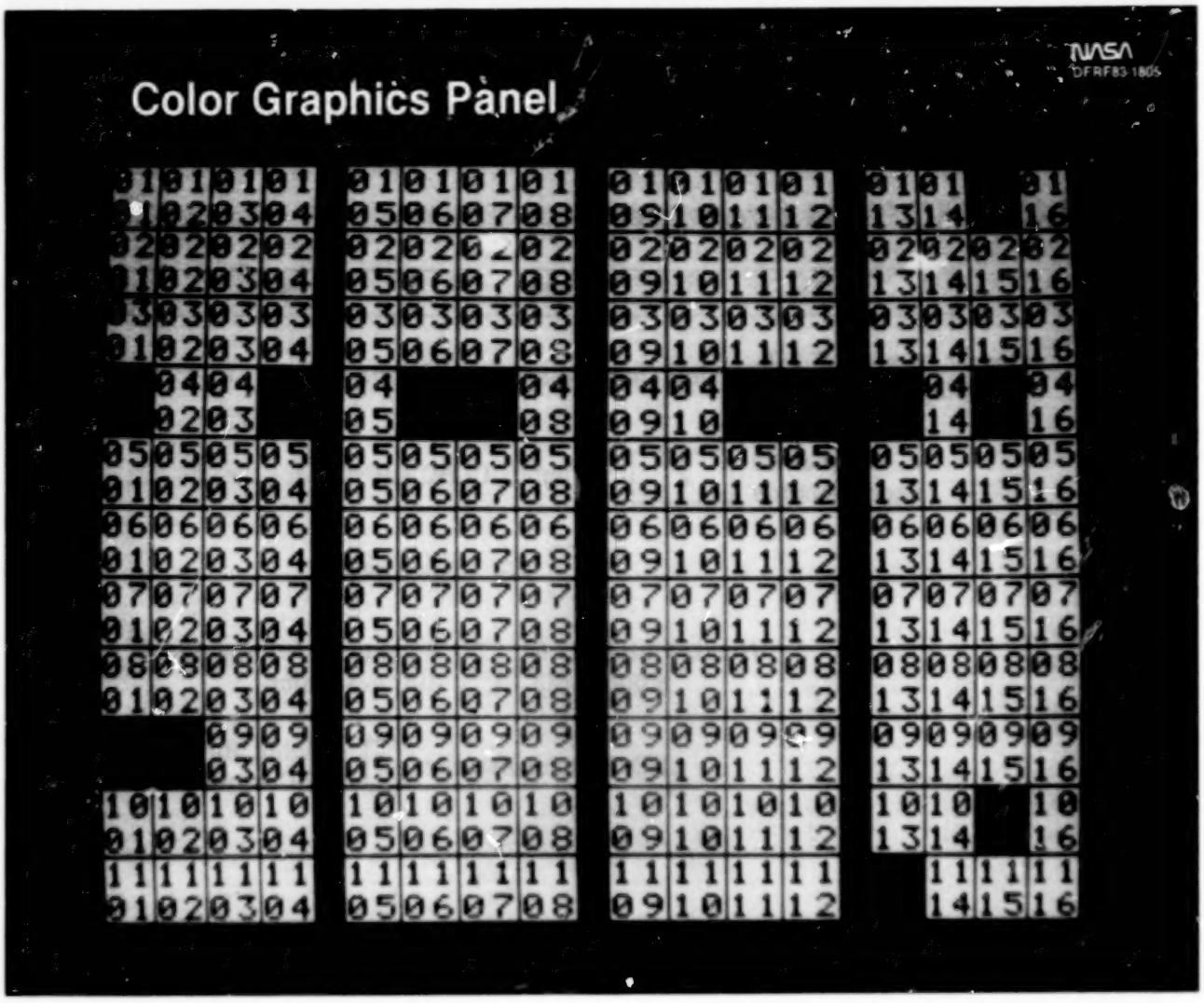

TEST PROGRAM

The DEEC test program consisted of four phases. On the chart below, each phase is illustrated with a number in a block. To the left of the block is the configuration or change from the previous phase, and to the right is the number of flights and major evaluation of the phase. The four DEEC test phases were completed in one and one-half years.

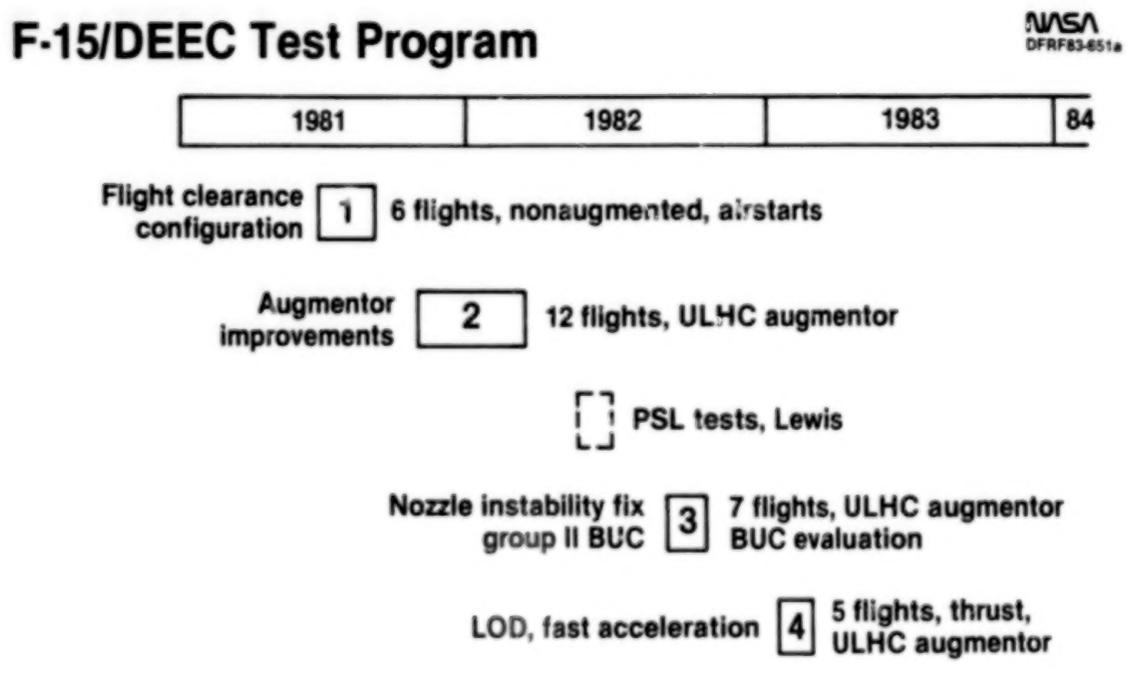

FLIGHT RESULTS

ORIGINAL PAGE IS
OF POOR QUALITY

The DEEC was evaluated in a series of 30 flights totaling 35.5 hours. On three flights, aerial refuelings were used to extend test time. A maximum Mach of 2.36 was reached at 40,000 ft. Climbs to 60,000 ft were made to determine upper limits of augmentor operation. More than 200 nonaugmented and almost 1000 augmented throttle transients were accomplished as well as 155 airstarts and 125 manual transfers to the backup control.

TEST POINTS FLOWN

The DEEC flight test points are shown in the figure below. The test program concentrated on the upper left hand side of the F-15 envelope to determine the operability limits. For points in which stabilized speed and altitude were required, the pilot used the right engine to control speed while the left engine was evaluated.

In maneuvering flight, large angles of attack and sideslip (up to about 25^{o} and 15^{o}, respectively) were flown and throttle transients were performed. Airplane accelerations in intermediate and maximum power were flown at several altitudes. Transfers to backup control were made at the conditions indicated.

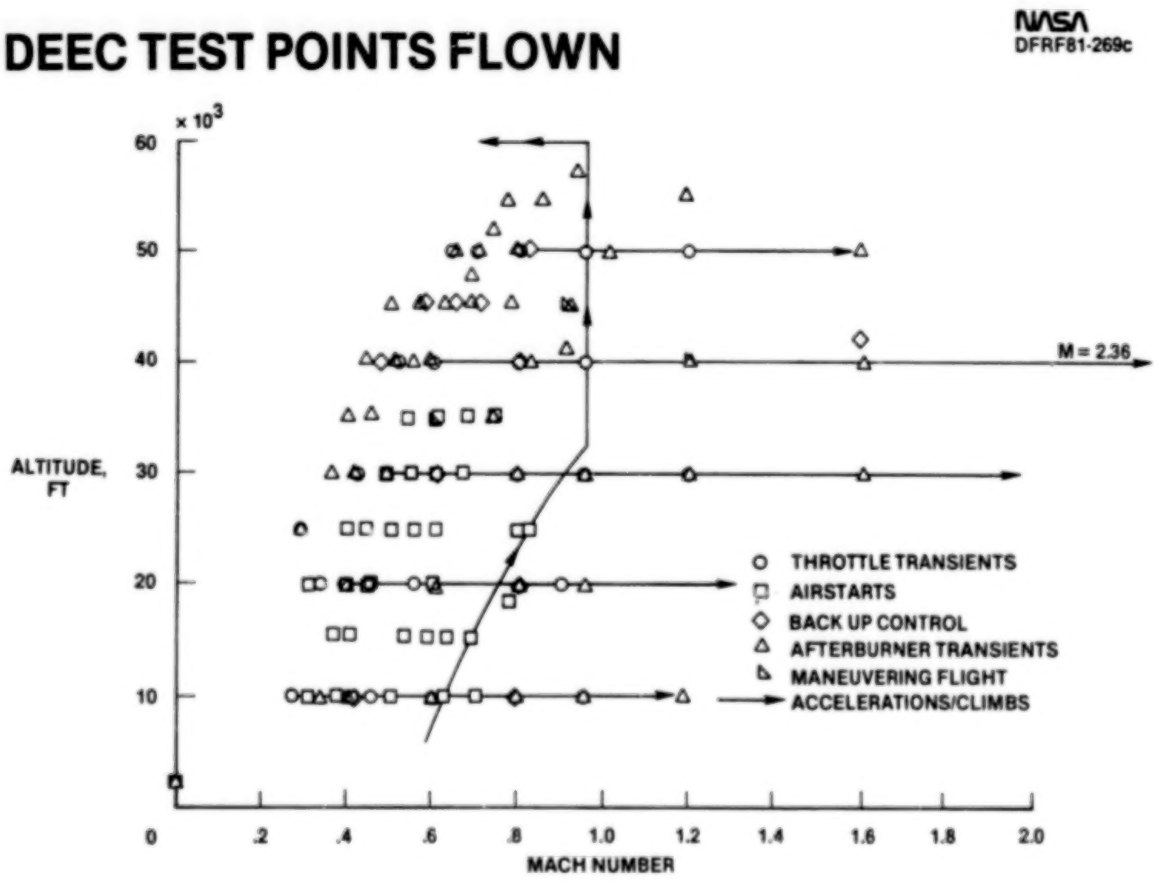

NONAUGMENTED THROTTLE TRANSIENTS

Nonaugmented throttle transients in the DEEC primary mode consisted of snaps and bodies. Throttle transients were idle-intermediate and were performed from a Mach 0.6 at 50,000 ft to Mach 1.2 at 30,000 ft. During the transients no anomalies or engine limitations were encountered. The part-power small-transient response of the DEEC was evaluated in formation flying and aerial refueling, and was satisfactory.

Overall nonaugmented transient performance was excellent, particularly since this was the first flight evaluation of the DEEC system.

NON AUGMENTED THROTTLE TRANSIENTS

NASA DFRF82-343

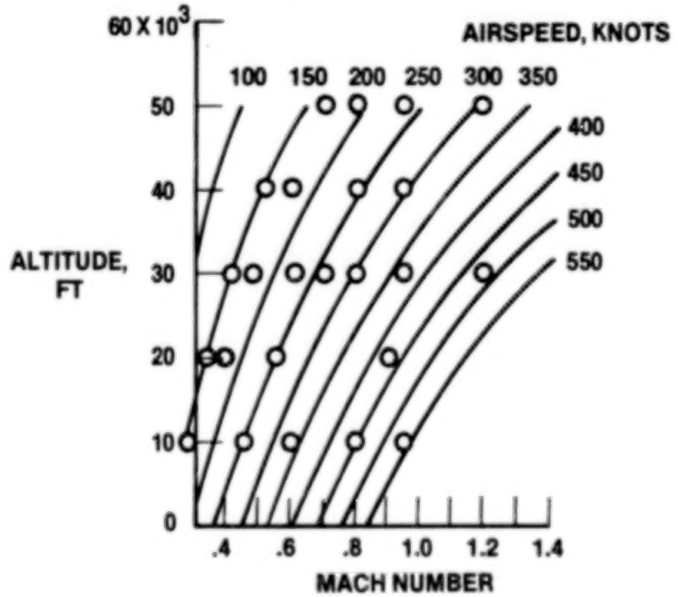

- SNAP ACCELERATIONS
- SNAP DECELERATIONS
- BODIES

} 100 PERCENT SUCCESSFUL

- NO AUTOMATIC TRANSFERS TO BACKUP CONTROL
- NO STALLS
- NO ENGINE LIMITS EXCEEDED
- PILOTS LIKED RESPONSE

One of the most important features of the DEEC system is the capability to maintain a desired engine performance level without adjusting or trimming the engine. The DEEC maintains a desired performance by use of an EPR control mode as previously described. Approximately 100 hours of altitude-cell, sea level, and flight tests have been accomplished on the P063 with the DEEC system, without the need to retrim the engine. EPR plotted against corrected fan rotor-speed data from altitude-cell, sea level, and flight tests are shown in the lower left hand figure. This figure indicates that the engine maintained a desired performance level throughout the ground and flight tests.

During the flight-test phase, new software logic packages were provided. The DEEC computer was removed from the engine and replaced by another computer with different software without the need to adjust or trim the engine or remove the engine from the airplane.

The lower right hand figure indicates the possible savings of the U.S. Air Force if DEEC control systems were installed on one-half of the F-16 fleet, with a total savings of $150 million.

DEEC - NO TRIM

NASA
DFRF82-952

- CLOSED LOOP CONTROL COMPENSATES FOR CHANGES IN ENGINE CONDITION, CONTROL TOLERANCES, AND FUEL CHARACTERISTICS
- ELIMINATES THE NEED FOR PERIODIC RETRIMMING

DEEC TEST RESULTS

DEEC MILITARY POWER EPR CHECKS

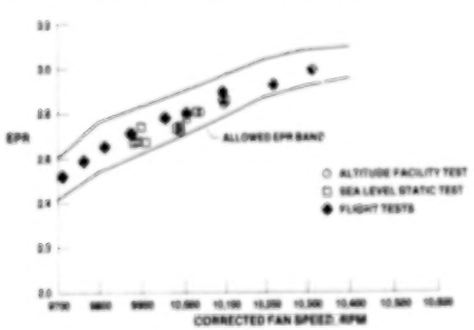

SAVINGS TO U.S.
(BASED ON DEECS ON 1/2 OF F-16 FLEET)

- FUEL - $40 MILLION
- LABOR - $10 MILLION
- ENGINE HOURS - 50,000
- VALUE OF ENGINE HOURS - $100 MILLION

CONCLUDING REMARKS

With the real-time data and displays available, the test engineers in the control room had access to virtually all the DEEC information in real time. The test program involved large numbers of throttle transients to determine the operability of the DEEC. A propulsion engineer, watching a strip chart, called the throttle sequence to the pilot. The engineer analyzed the data to determine when the engine had stabilized and called for the next step in a throttle transient series. This technique reduced the pilot workload and greatly improved the quality of data.

The EPR control mode feature was demonstrated; engine performance remained at an acceptable level without trimming or adjusting the engine throughout the ground and flight program.

Nonaugmented throttle transients and engine performance were satisfactory; the DEEC maintained control without exceeding any engine limits.

Summary

NASA
DFRF83-647a

- **Real-time data and displays extremely valuable**
- **Propulsion engineer assistance to pilot made more productive and efficient test time**
- **No trim verified—substantial savings shown**
- **All nonaugmented throttle transients successful**

N86
25349

UNCLAS

N86-25349

Paper 7

DIGITAL ELECTRONIC ENGINE CONTROL FAULT DETECTION AND ACCOMMODATION FLIGHT EVALUATION

Jennifer L. Baer-Riedhart
NASA Ames Research Center
Dryden Flight Research Facility
Edwards, California

SUMMARY

The National Aeronautics and Space Administration (NASA), the U.S. Air Force (USAF), and the U.S. Navy (USN), along with other government agencies, are conducting various studies of existing and projected engine control systems to investigate the capabilities and performance of various fault detection and accommodation (FDA) schemes. These studies have made extensive use of analytical methods and simulations. Limited altitude testing has also been accomplished in support of these studies. With the advancement of the full-authority digital engine control systems, there has been an increasing desire to perform in-flight evaluations of FDA methodology for substantiating the predictions and facility results of the studies. Recent flight tests of the digital electronic engine control (DEEC) in an F-15 airplane have shown discrepancies between flight results and predictions based on simulation and altitude testing, and thus reinforce the need for flight evaluations. However, the difficulty of inducing realistic faults in flight has so far minimized flight testing of the FDA logic.

The DEEC is a full-authority, engine-mounted, fuel-cooled digital electronic control system that performs the functions of the standard F100 engine hydromechanical unified fuel control and the supervisory digital engine electronic control. The DEEC consists of a single-channel digital controller with selective input-output redundancy, and a simple hydromechanical backup control. The FDA features of the system are a significant portion of the control program. During the course of the recent flight program, the DEEC detected and accommodated two sensor faults, with no false failure indications.

An opportunity exists to conduct further flight evaluations of the DEEC FDA in the near future. The objectives of the program will be to induce selected faults and evaluate the resulting actions of the controller. Comparisons will be made between the flight results and predictions, as part of the evaluation. It is anticipated that the FDA data base will be expanded and techniques developed for safely evaluating FDA methodology in flight that may be useful on future programs.

This paper will describe the FDA methodology and logic currently in the DEEC system, and discuss the results of the flight failures that have occurred to date. The proposed flight program and anticipated results will be presented at this time.

PRECEDING PAGE BLANK NOT FILMED

N86-23340

ENGINE FAULT PROTECTION

The objective of the fault protection for the DEEC engine is to provide additional aircraft safety and operation in the event of an engine control system anomaly. This is accomplished through the FDA logic and the engine protection logic. The FDA provides three basic levels of engine operability in the event of an engine control system anomaly. The first level maintains normal operation of the engine with notification that a failure of a redundant parameter has occurred. The second fault accommodation level also maintains normal operation of the gas generator, but inhibits augmentor operation. This level is "instituted" for inputs which are critical to augmentor operation but not to the gas generator. Failure of parameters which are critical to the safe operation of the engine cause the system to automatically revert to the hydromechanical backup engine control. At each of these levels, the failures are annunciated through a caution light in the cockpit and specifically identified on one of the DEEC diagnostic words.

The engine protection logic provides an ultimate level of protection in addition to the FDA logic and the normal engine control scheduling. The logic is used to detect impending overspeeds and overtemperatures as a result of unpredicted multiple failures and automatically transfers the engine control to the hydromechanical backup system.

NASA
DFRF83-613

DEEC Engine Fault Protection

Objective:

To provide for *additional* aircraft safety and operation in the event of an engine control system anomaly

- **Failure Detection and Accommodation "Levels"**
  1. **Maintain normal engine operation**
  2. **Loss of augmentation maintaining primary mode**
  3. **Automatic transfer to hydromechanical backup**

- **Engine Protect Logic:**
  Ultimate engine protection beyond FDA.

CONTROL SYSTEM

The DEEC system shown on the next page incorporates significant fault detection and accommodation logic. Part of the FDA methodology which is used in the DEEC system is reflected in the amount of redundancy of the system. Dual sensors and position transducers are used to achieve redundancy in key parameters such as engine speeds, temperatures, throttle position, gas generator fuel flow (WFGG), and rear compressor variable vane (RCVV). Redundant coils are present in the torque motor drivers for all actuators. Nonredundancy is retained in the less critical parameters of pressures, augmentor fuel flow, nozzle area, compressor inlet variable vane (CIVV), and aircraft Mach number.

The DEEC performs internal self-test and memory checks, processor instruction tests, interface tests, clock tests, and computational cycle-time tests. The built-in test (BIT) during normal engine operation includes: (a) read-only memory (ROM) check sum test as time permits during the execution of the control algorithm; (b) processor instruction checks as time permits; (c) input range checks: (d) torque motor coil testing to determine if the predescribed amount of current is flowing to each coil; (e) actuator loop test for torque motor integrity (as in (d)); (f) range checks to identify failed resolvers or actuators; and (g) loop dynamic checks for degradation of actuator response. These diagnostic test programs are provided for the DEEC controller to identify incipient anomalies before they can seriously affect the aircraft mission.

The selective input-output redundancy allows the system to maintain gas generator control with any single input-output failure. The control detects hard and soft failures of the dual sensors. Hard failures are declared when a sensor exceeds its maximum or minimum expected values. Soft failures are declared when the two signals disagree by more than a predetermined tolerance; the more conservative (safer) sensor value is then used. The pressure sensors (fan inlet static pressure (PS2), burner pressure (PB), turbine discharge total pressure (PT6M)) are not redundant, but the approximate value of one can be determined from the other two pressures. Failure of any nonredundant sensor will result in a loss of augmentation capability. Second failures of the dual sensors will result in an automatic transfer to the BUC, as will failures in the computer internal checks.

DEEC Control System Block Diagram

NASA
DFRF83-319

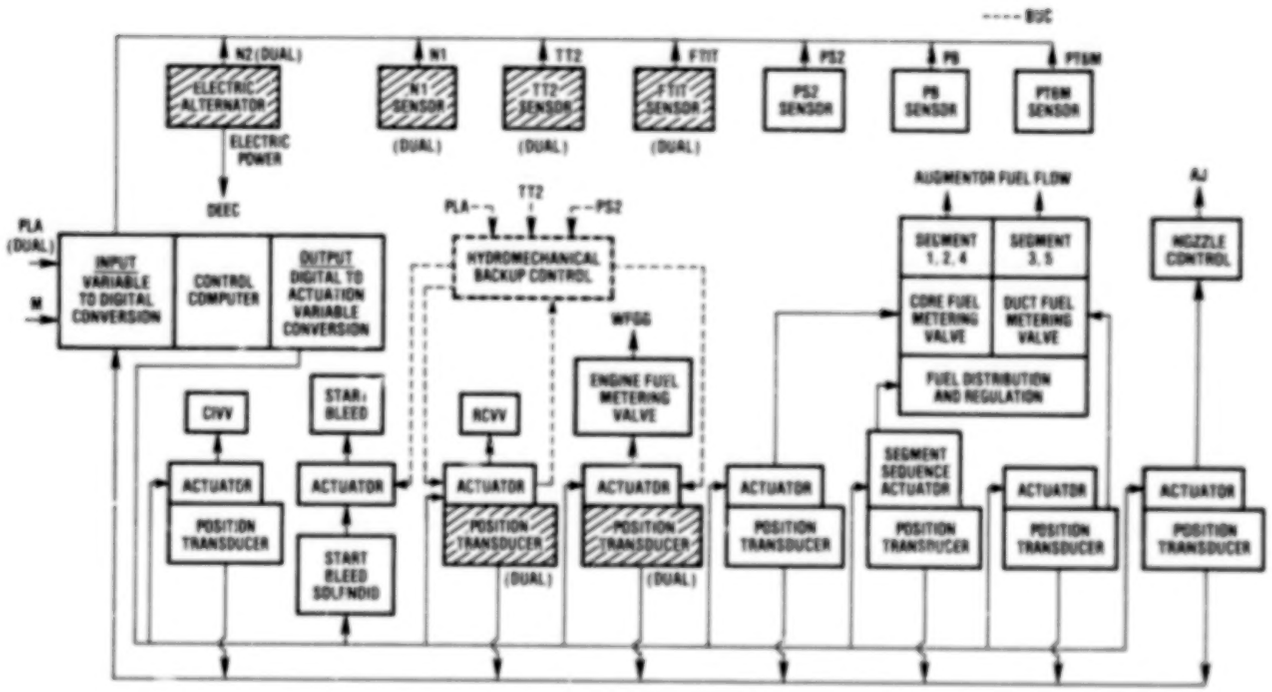

FAULT DETECTION AND ACCOMMODATION LEVELS

The fault detection and accommodation (FDA) shows that when the DEEC system is operating without faults, the level of activity of FDA is normal, as illustrated at the top of the figure. The next level occurs when the first system fault is detected and one of two possible fault accommodations can take place. One possibility is to accommodate the fault internally in the DEEC controller and the second is to transfer to the backup control system (BUC).

The decision to transfer to BUC is based on one of three possible detected conditions: (a) the DEEC controller has detected a fault which will not allow the controller to be in charge of the main core fuel flow or RCVV position; (b) the engine protection logic has detected a variable (fan rotor speed (N1), core rotor speed (N2), turbine inlet temperature (FTIT)) is either over the limit condition or its rate is such that the variable will reach an over-limit condition; or (c) a hardware independent fan speed (N1) circuit built into the DEEC controller detects an overspeed condition.

Other faults at this detection level drop down to the accommodation level (third level) where one of four operational conditions is selected, depending upon the fault condition. The operational accommodation, which has one-for-one hardware redundant fault replacement, yields a normal operating system. If the fault lies within the augmentor control of segment 3 or 5 (for example, duct metering valve fault), these elements are inhibited and the control system has an operational degradation. If the fault is more inclusive in the augmentor control, the engine augmentation function is inhibited with further reduction in operational capability. Should the synthesis of a control variable be required, then additional operational restriction is imposed, because the synthesized variable will be a conservative estimate of the replaced control variable. When operating in this level of accommodation (three levels down) and a second "like" fault occurs, the DEEC control automatically transfers operational control to BUC. The sensor failures which are detected by the DEEC FDA logic and the resulting actions are summarized in table 1.

DEEC Fault Detection/Accommodation

NASA
DFRF83-487

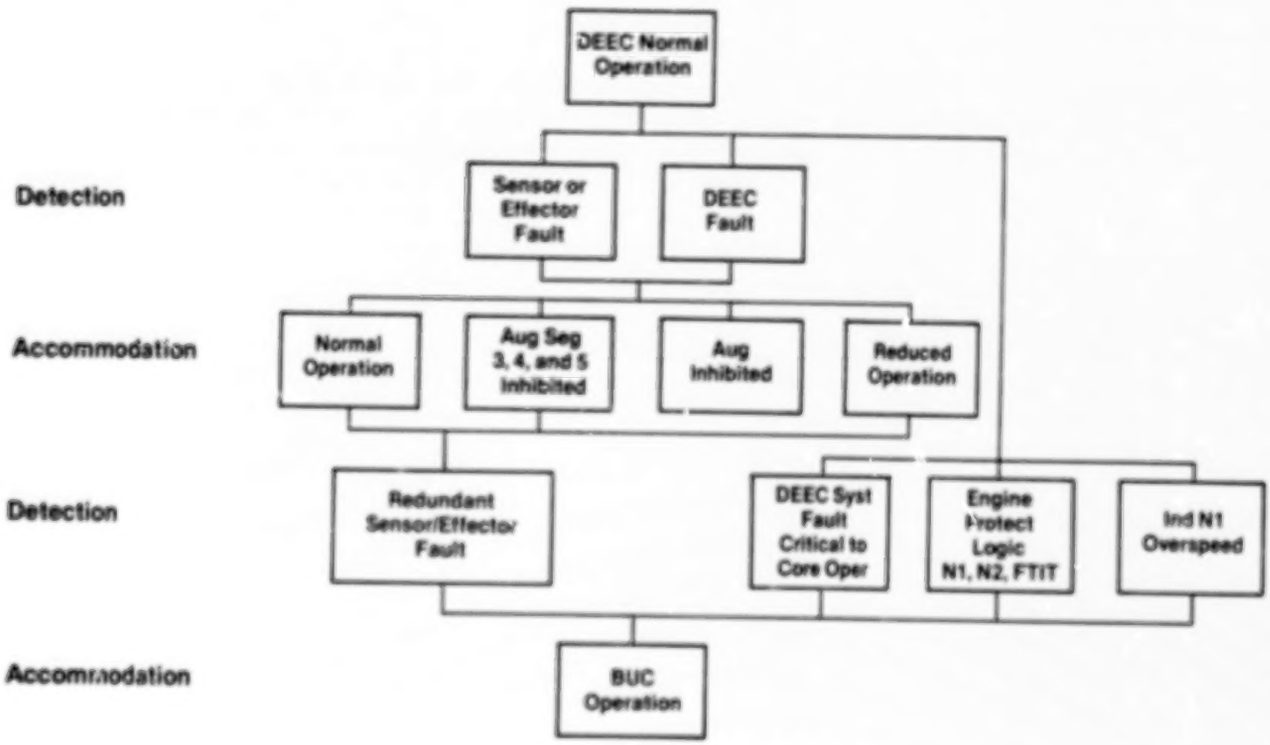

Table 1 FDA logic and actions

	Failure checks	Action
Redundant inputs:		
TT2, N1, N2, RCVV, FTIT, WFGG	Out of range Soft in range	Use in-range/BUC Use safer value
PLA	Out of range Soft in range	Use in-range/BUC Buc transfer
Single inputs:		
WFC, SVP	Out of range Open loop	A/B inhibited
WFD	Out of range Open loop	A/B limited to segment 2
PS2, PT6M	Out of range Soft in range	PS2 = PS2SYN A/B inhibited AJ trim inhibited PB soft fail-bypassed PS2 or PT6M, and PB fail-BUC
PB	Out of range Soft in range	PB = PBSYN A/B inhibited No stall detect logic PS2 or PT6M fail-BUC
TPS2, TPT6M, TPB	Out of range	Sub good temp sensors If all fail, fail pressure
Feedback sensors - single:		
CIVV	Out of range	CIVV full-cambered A/B inhibited
AJ	Out of range	AJ full closed A/B inhibited
Other		
Power (dual)	Out of range	BUC transfer
M.N.	Out of range	Mach = 0.15, limit set
Selftest (hardware)	Loss of interface	BUC transfer (critical loss)
Selftest (software)	Integrity check	BUC transfer

The functions of the PS2 sensor involve a full-time and part-time importance level as it is used in the fan speed request, nozzle request and trimming, and EPR request and feedback logic. A declared hard failure of the parameter causes the DEEC to use a synthesized PS2, based on corrected engine speed, engine inlet temperature, and burner pressure. Augmentor and nozzle trim functions of the engine are inhibited by the DEEC. In addition, the soft failure detection logic for burner pressure is bypassed as part of the FDA.

Burner pressure is classified as a full-time critical parameter since it is used in the scheduling of the core fuel flow and in the stall detection logic. It has a part-time criticality for the acceleration-deceleration limiting and limiting-engine burner pressure during high dynamic pressure (Q) conditions. As with PS2, detected sensor failures (hard or soft) cause a synthesized PB value to be substituted. There is no stall detection logic and augmentation is inhibited with this failure.

PT6M is used primarily at the intermediate and augmentor operation of the engine as part of the EPR feedback logic, blowout detection, and nozzle trimming functions. This parameter is not synthesized; hard failures which are detected result in elimination of augmentor operations and nozzle trim functions and the bypassing of the PB soft-fail logic.

DEEC Non-Redundant Sensors

NASA
DFRF83-490

Function	PS 2 Inlet pressure	PB Burner pressure	PT6M Turbine discharge pressure
Full time—critical		• Core fuel flow scheduling • Stall detection	
Full time—important	• Fan speed req. • Nozzle area req.		
Part time—critical		• PB limiting (high Q) • Accel-decel limiting (full env.)	
Part time—important (intermediate & augmented power)	• EPR req. • EPR feedback • Nozzle trim		• EPR feedback • Blowout detection • Nozzle trim
Synthesis	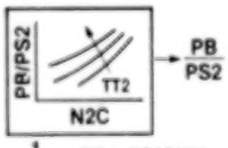 $\frac{1}{\frac{PB}{PS2}} \times PB = PS2SYN$	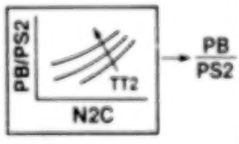 $\frac{PB}{PS2} \times PS2 = PBSYN$	None (Augmentation inhibited) (AJ trim inhibited)

NONREDUNDANT SENSOR LOGIC - PS2, PT6M

The FDA logic of the nonredundant pressure sensors (PS2 and PT6M) involve checks to be performed on the validity of the temperatures and pressures of the transducers, and the substitution of the transducer temperatures in the event of a temperature failure. The chart below shows the procedure for PT6M. A range check is made on the limits of the transducer pressure and temperature, with the sensor being declared failed after a specified number cycles. The detection and accommodation logic of the transducer temperatures consists of a substitution of the alternate transducer temperatures, since all three sensors are located together in the fuel-cooled electronic unit.

A check sum is made of the software locations, prior to this logic, to ensure there are no internal computer anomalies. If the three transducer temperatures or the check sum have failed, the affected pressure is declared failed and the system reverts to the BUC control mode. Following the transducer temperature FDA checks, the parameter is converted into engineering units and a range check, similar to the transducer temperature range check, is made. This particular logic sequence is utilized for the PS2, PB, and PT6M sensors. The PB sensor has an additional in-range logic check which compares the sensor value to the synthesized pressure value.

NASA
DFRF83-489

Non-Redundant Sensors FDA Logic
(PT6M)

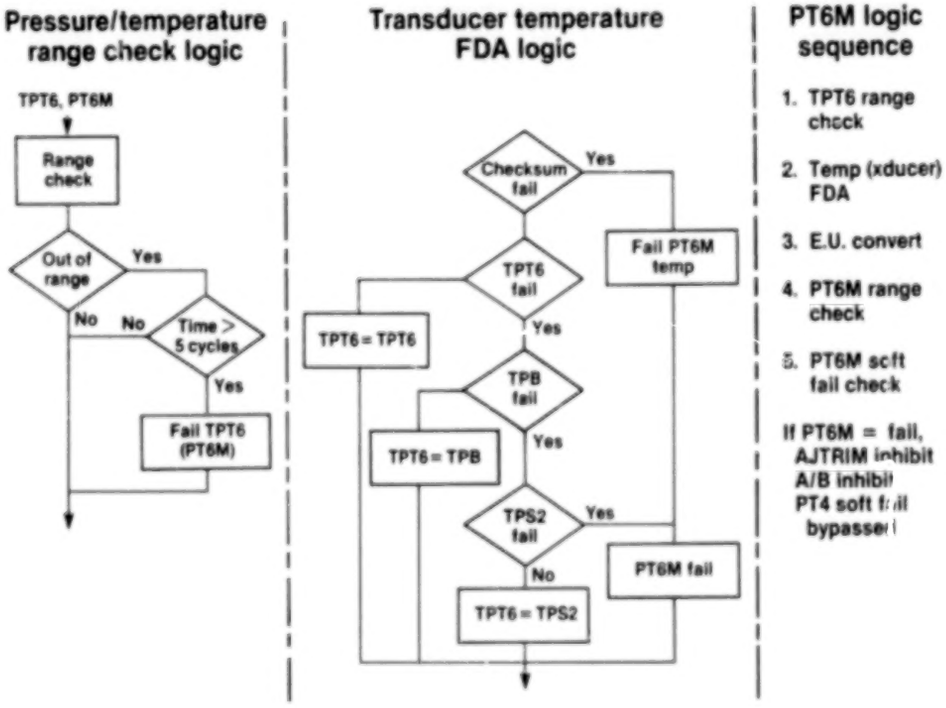

REDUNDANT SENSOR LOGIC - TT2

The fan inlet total temperature (TT2) parameter is one of the redundant sensor inputs used by the DEEC. The FDA logic checks for the redundant sensors are a range check for out of range and a check for agreement between sensors. If both sensors are in range, the sensors are compared. A disagreement between the signals by more than a predescribed tolerance causes the higher, or safer, value to be used. If either signal is out of range, the good value is used. With both signals out of range, an automatic transfer to the hydromechanical backup control is accomplished. Similar logic is used for the other dual sensors.

DEEC FDA Logic - Redundant Inputs

NASA
DFRF83-610

FDA Logic

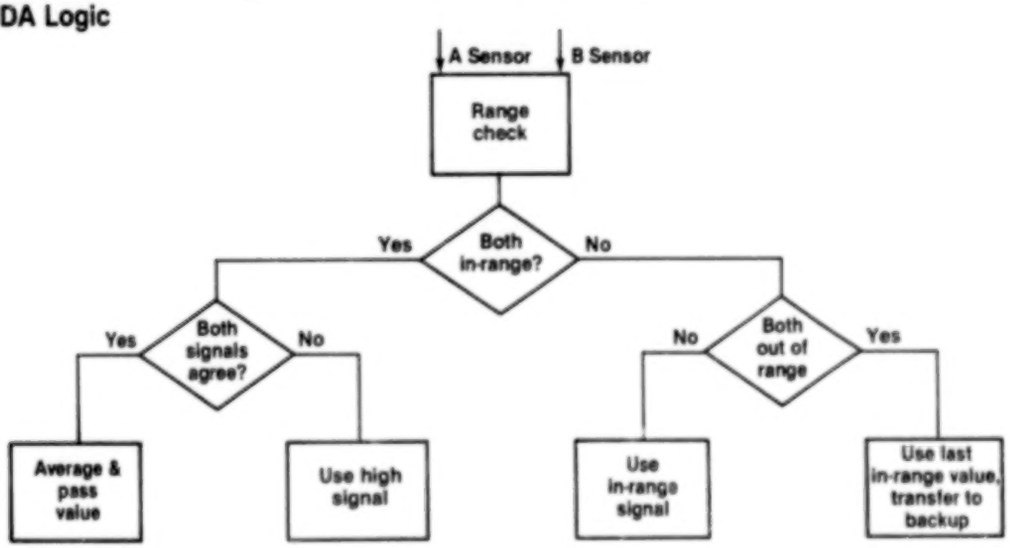

ORIGINAL PAGE IS
OF POOR QUALITY

FDA - FLIGHT RESULTS

Extensive testing has been performed on the fault detection and accommodation (FDA) logic operation and ability to transfer to BUC under selected failure conditions. The closed-loop bench test allowed operation of hydromechanical and electronic components to be run while operating the engine computer simulation. This allowed testing of the FDA by intentionally introducing faults into the system without the risk of damaging an engine. Additional testing included sea level and altitude tests, and simulation testing of selected failures and resulting accommodation process.

The DEEC diagnostic words provide information on the health of the DEEC system. The words are displayed in the control room on the cathode ray tube (CRT) in a matrix format, as shown below. Failures which result in a transfer to the BUC mode are annunciated in the darker shade. Indication of other system faults are displayed on the light background. During the course of the DEEC flight test program, two faults were detected and accommodated. The first was a detected failure of the TT2 sensor which resulted in the use of the redundant sensor and no loss in performance. Post-flight inspection revealed the failure was due to a contaminated connector. The second failure involved the PT6M sensor, causing the nozzle trim feature and augmentor to be inhibited while DEEC engine control was maintained. The failure of the sensor was traced to the contamination of a PROM socket at the vibrating cylinder transducer. To date, there have been no false failures detected by the DEEC and no required transfers to BUC due to control system anomalies.

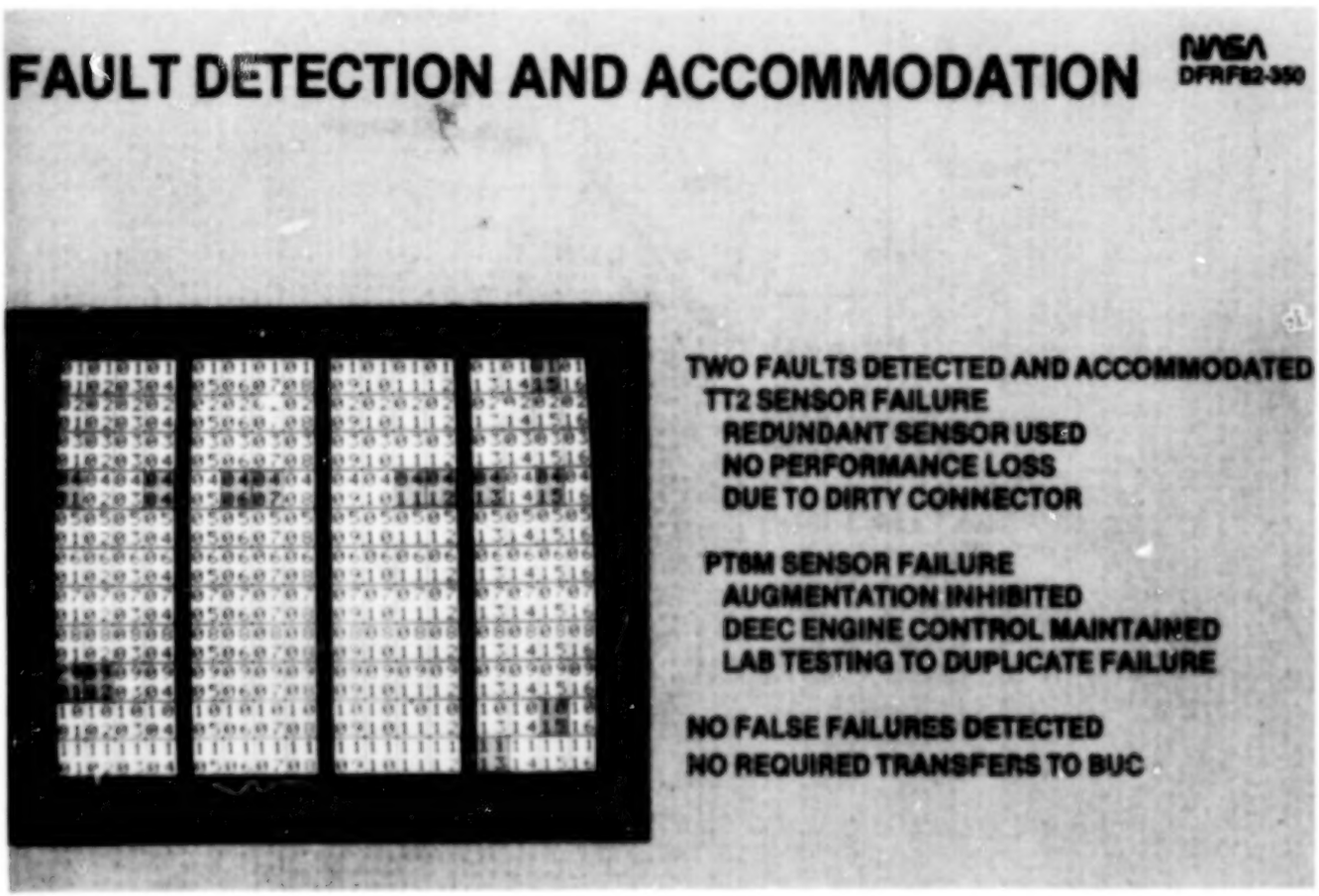

PT6M FAILURE DURING IDLE-TO-MAXIMUM TRANSIENT

The turbine discharge total pressure (PT6M) failure occurred during an idle-to-maximum transient at Mach 0.8 and 30,000 ft. The PT6M signal initially failed to a value of 92 lb/in^2, less than the upper limit of 110 lb/in^2. In response to this, the nozzle was driven open by the high PT6M signal in an attempt to accommodate the nozzle trim logic to hold EPR. The augmentor static pressure (PAB) trace shows the actual pressure change near the turbine discharge during the nozzle transient. When the PT6M sensor exceeded the 110 lb/in^2 maximum limit, the failure was flagged and the nozzle was commanded to the basic schedule value.

NASA
DFRF83-493

PT6M Failure During Idle-Max Transient
M = 0.8, 30,000 ft

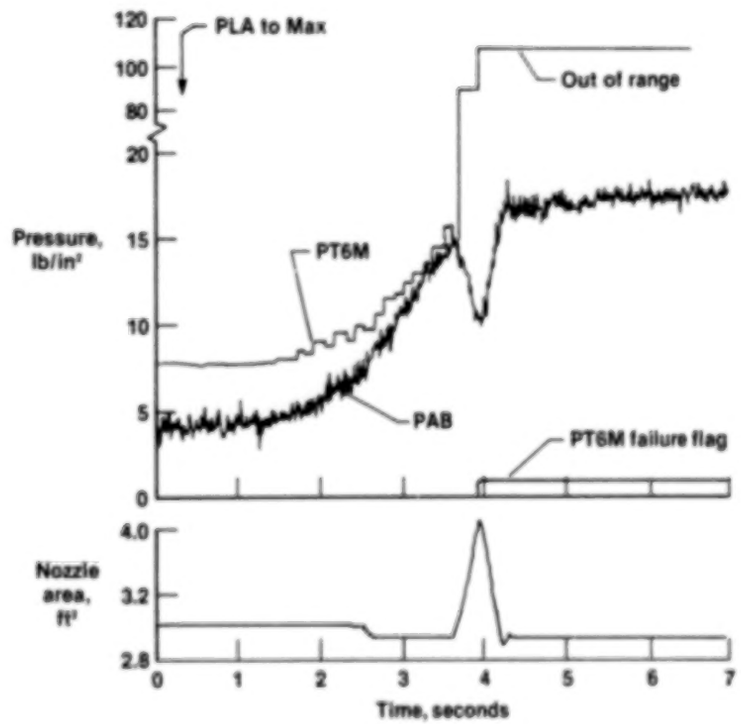

TT2 FAILURE

One of the two fan inlet total temperature (TT2) sensors failed following an acceleration to Mach 1.4 and 30,000 ft. The TT2 "A" sensor had been intermittent just prior to the data shown below, where it became a hard failure. The TT2 fail flag was set when the sensor exceeded the -110^{0} F limit. Since the detected failure was one of the redundant sensors, no performance loss was noted during the time the sensor had failed.

NASA
DFRF83-648

TT2 Failure

M = 1.4, 30,000 ft

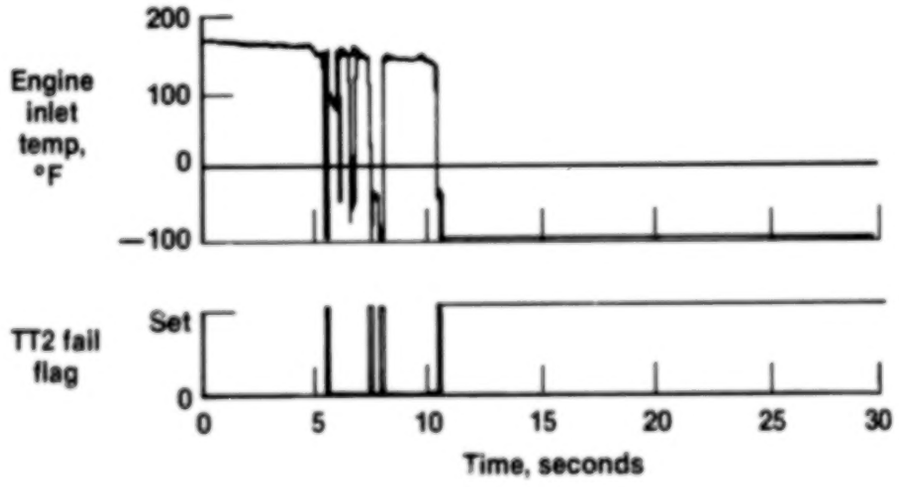

FDA FLIGHT TEST PROGRAM

Early in the flight program, one of the ground rules was to abort the mission and return to base in the event of a failure. As more confidence was gained in the system and there was more interest in evaluating the failures in flight, contingency cards were made which contained selected testing to be accomplished in the event of a particular failure. The opportunity exists to use these procedures by inducing faults into the system and evaluating the outcome.

One of the objectives of the DEEC FDA flight program will be to evaluate the FDA logic for the PS2, PB, CIVV, and FTIT sensors by inducing faults in flight. The manner in which the faults are induced and the test techniques that will be developed will be applicable to other programs. The second objective will be the comparison of the flight results with predictions and facility results. Included in the comparison will be an evaluation on engine performance using synthesized values of PS2 and PB.

ORIGINAL PAGE IS
OF POOR QUALITY

FDA TEST SCHEMATIC

The DEEC engine will be modified to allow switches and valves to be installed on the sensor lines. The sensor lines to be modified, and FDA logic which will be evaluated, are PS2, PB, CIVV, and FTIT. Selection of the failure mode to be induced will be controlled by switches in the cockpit. No changes will be necessary to the DEEC software. The configuration of these switches and valves will be such that the normal and fail-safe modes allow normal DEEC operation.

DEEC FDA Test Schematic

NASA
DFRF-3-491

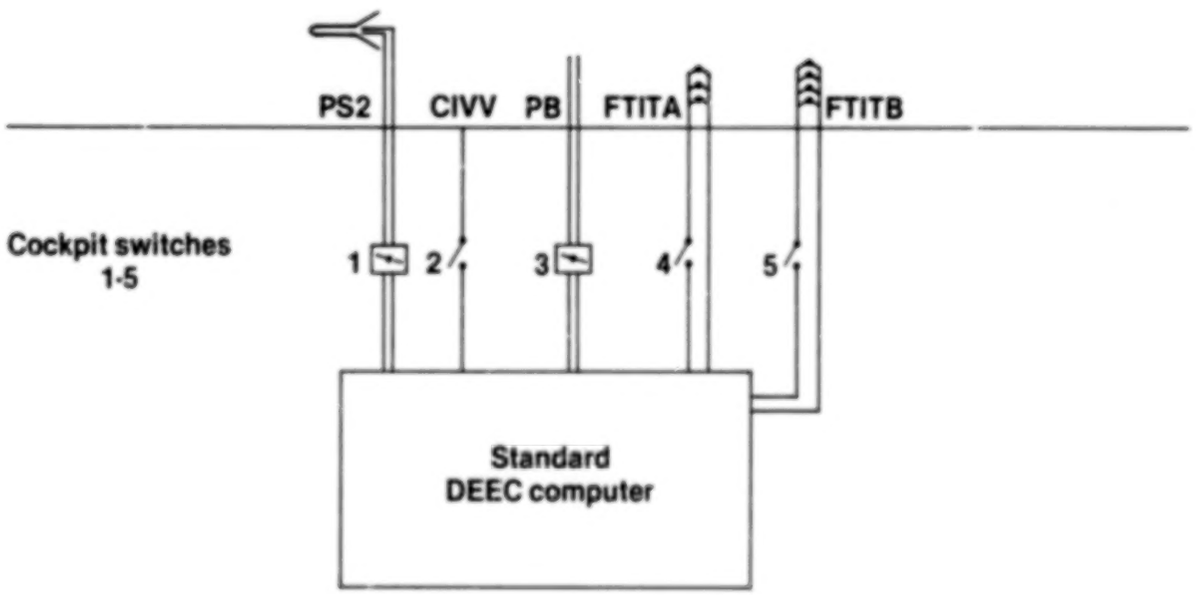

The test matrix shown contains all possible faults that may be induced during the flight program. The flight conditions selected represent the engine envelope and are based on simulation and facility data that are available for comparison. Steady-state tests and engine transients will be performed with the failures being induced before and during the maneuvers. Computer simulation will be used to evaluate each of these test conditions and induce failures prior to the actual flights to ensure there are no predicted adverse effects to the engine. Some of these points combine dual failures which may not be accommodated in the FDA logic and could result in an undesirable engine operating condition.

The FTIT failures will evaluate the redundant sensor logic. Sensor failures of PS2 and PB, both hard and soft, will exercise the nonredundant logic and pressure synthesis accommodation. The CIVV failures will be used to evaluate the open-loop actuator logic.

NASA
DFRF83-612

DEEC FDA Flight Test Matrix

Test Conditions

	Failure Modes	.8M, 30Kft	.8M, 50Kft	1.6M, 30Kft	1.6M, 50Kft	2.0M, 50Kft	Accel, 30K .8-1.6M	Accel, 50K .8-2.0M
FTIT	A - Fail	1-5			1-5			
	B- Fail		1-5					6
	Both - Fail	1-5	1-5		1-5	1-5	6	
PS2 & PB	PS2, Soft	1-5	1-5	1-5		1-5	6	
	PS2, Hard	1-5	1-5	1-5	1-5	1-5	6	
	PB, Soft	1-5	1-5	1-4	1-4	1-5		6
	PB, Hard	1-5	1-4	1-5	1-4	1-4		6
	PS2, Soft PB, Hard	1-5	1-5	1-4	1-5	1-4		
	PS2, Hard PB, Hard	1-5		1-4	1-5	1-4		
	PS2, Soft PB, Soft	1-5	1-5	1-4	1-5	1-4		
	PS2, Hard PB, Soft	1-5	1-5	1-4	1-5	1-4		
CIVV		1-4		1-4			6	

Legend
1 = Idle, steady-state
2 = Idle - I/M snap
3 = I/M, steady-state
4 = I/M - I snap
5 = I - max snap
6 = Fixed throttle

CIVV COMPARISON

Detection of a failure of the compressor inlet variable vane (CIVV) position feedback results in the CIVVs being commanded to the full-cambered position. This position, while it is a fail-safe mode, produces a significantly lower stall margin than the nominal schedule. The figure below illustrates the predicted amount of reduced stall margin at 30,000 ft with the CIVV failed to the full camber position. Because of the reduced fan stall margin, augmentor operation could result in stalls. Therefore, a CIVV failure inhibits augmentation. The flight test results with this failure will include nonaugmented transients and airplane maneuvers.

Effects of Failed CIVV on Fan Stall Margin

NASA DFRF83-488

Results from DEEC Simulation
30,000 ft

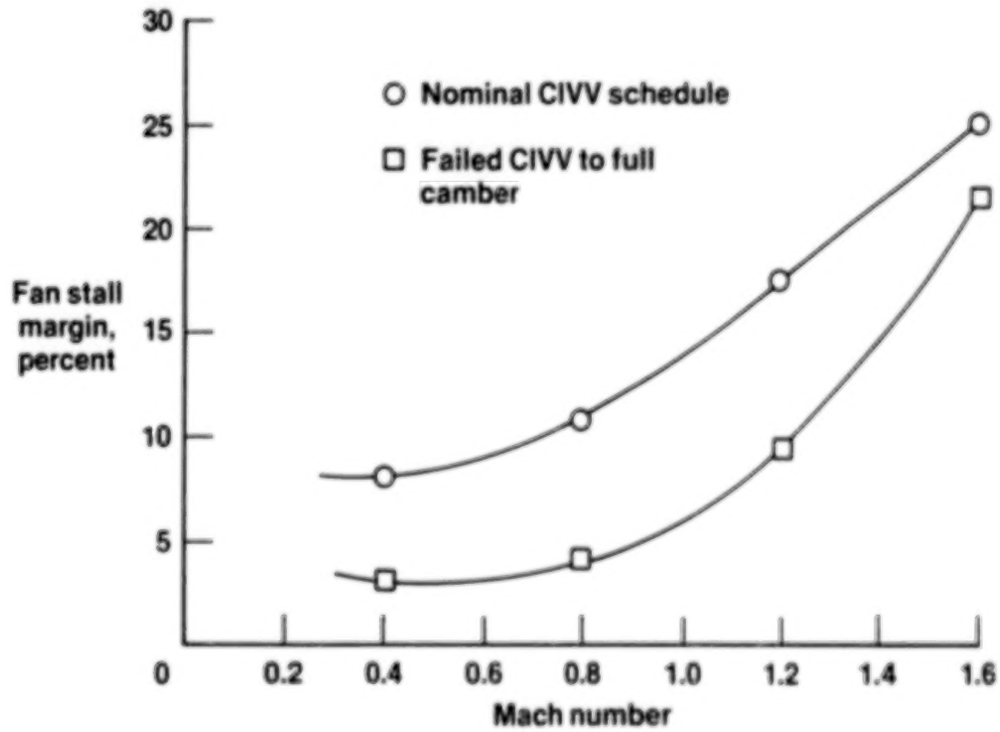

PB COMPARISON

The figure below shows altitude facility data on the effect of a failed burner pressure (PB) sensor on the engine thrust during an idle-to-maximum snap at Mach 0.8 and 30,000 ft. The facility data shows the accommodation of the failure by inhibiting augmentation and scheduling the engine, using a synthesized burner pressure input. The flight results will be compared to facility data such as these, and include an evaluation of engine performance using a synthesized PB. The knowledge gained from the flight-program will be used to expand the existing data base of FDA information and include test techniques and validation processes of simulation and facility information.

Effect of Failed PB Sensor on Thrust

NASA
DFRF83-492

M = 0.8, 30,000 ft
Idle-to-Max Snap

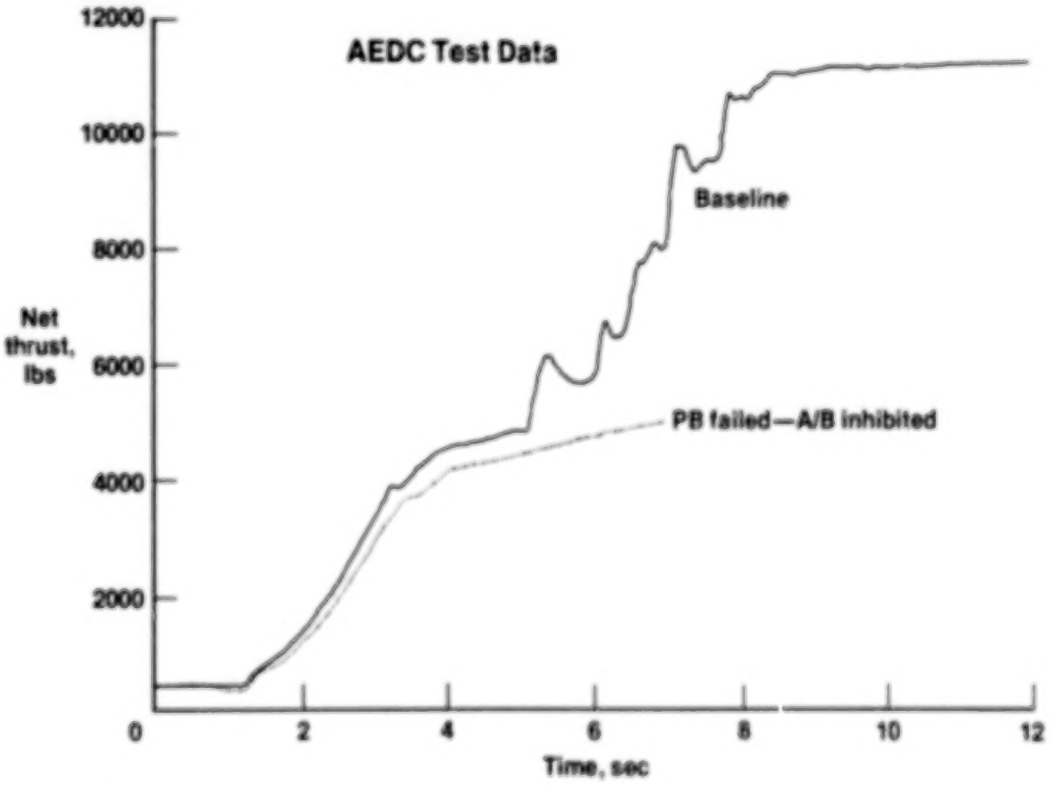

CONCLUDING REMARKS

The FDA methodology used in the DEEC is a fairly simplified parametric comparison process, but represents about 40 percent of the DEEC control program. The extensive testing and development of the FDA have included closed-loop bench tests, sea level and altitude engine tests, and computer simulation. This has resulted in a high level of confidence in the DEEC FDA logic. Successful fault detection and accommodation have been demonstrated with the flight failures of the PT6M and TT2 sensors. To date, there have been no false failures or required transfers to the backup control because of control system anomalies. The high degree of confidence in the DEEC system and the opportunity to expand the FDA data base to include additional flight data has made future flight evaluation of the DEEC FDA a highly desirable and realistic goal.

Summary

NASA
DFRF83-614

- DEEC FDA is a fairly simplified methodology, but represents a significant portion of the control program
- Testing of FDA included closed loop bench tests, sea-level and altitude engine tests, and computer simulation
- Flight failures of PT6 and TT2 demonstrated successful fault detection and accommodation
- There were no false failures or required transfers to BUC due to control system anomolies
- Further flight evaluation of the DEEC FDA is a highly desirable and realistic goal

N86
25350

UNCLAS

N86-25350

AIRSTART PERFORMANCE OF A DIGITAL ELECTRONIC ENGINE CONTROL SYSTEM ON AN F100 ENGINE

Frank W. Burcham, Jr.
NASA Ames Research Center
Dryden Flight Research Facility
Edwards, California

SUMMARY

The ability to achieve reliable and rapid airstarts is an important feature of an engine. Engine shutdowns may occur as a result of nonrecoverable stalls or overtemperatures. The airstart logic in the engine control system meters fuel to the combustor to achieve combustor light off, and then to accelerate the compressor. If the fuel flow is too high, the compressor will stall, resulting in a hot start. If the fuel flow is too low, the compressor will not accelerate, resulting in a hung start. The allowable fuel flow range between the hot start and the hung start may be very small, particularly for turbofan engines. Most engine control systems have an open-loop airstart system in which the fuel flow is preprogrammed as a function of time. Due to the normal variations between engines, the control system tolerances, and differences in fuel characteristics, these airstarts are not always successful.

The NASA Ames Research Center's Dryden Flight Research Facility (DFRF) has recently tested the digital electronic engine control (DEEC) system installed on an F100 engine in an F-15 airplane. The DEEC incorporates a closed-loop airstart feature, in which the fuel flow is modulated to achieve the desired rate of compressor acceleration. With this logic, the DEEC-equipped F100 engine is capable of achieving airstarts over a larger envelope. This paper describes the DEEC airstart logic, the test program conducted on the F-15, and the results.

N86-25830

AIRSTART LOGIC

In the event of an engine shutdown or flameout, the DEEC monitors several parameters to ensure a successful airstart. A simplified block diagram of DEEC airstart logic is given in the following figure. An open-loop fuel scheduling routine is used until the burner "light" (fuel mixture ignition) is indicated by a rise in the fan turbine inlet temperature (FTIT) signal. Once the burner light has been detected by the DEEC, fuel flow (WF) and the compressor bleed control switches to the closed-loop logic shown in the figure. This logic attempts to maintain a desired core rotor speed (N2) rate by varying fuel flow. The desired N2 rate is a function of fan inlet static pressure (PS2), fan inlet total temperature (TT2), and N2. If the fuel flow is too high, the compressor will stall, resulting in a hot start. If the fuel flow is too low, the available energy will not be sufficient to overcome the losses in the engine and the accessory power drain, resulting in a hung start. The DEEC airstart logic maintains the optimal N2 rate subject to a bias if FTIT exceeds a limit of approximately 760^{0} C. The minimum fuel flow set by a stop in the fuel metering valve is approximately 115 kg/hr. The compressor bleeds are held open until 56 percent N2 is attained.

The jet fuel starter (JFS) may also be used to assist in airstarts. The JFS is an auxiliary power unit that may be connected to the N2 rotor via a gearbox. It is normally used for ground starting and may also be used for airstarts below 6100 m. For JFS-assisted airstarts, the DEEC uses a higher scheduled N2 rate and a higher FTIT limit.

DEEC Airstart Logic

NASA
DFRF83-538

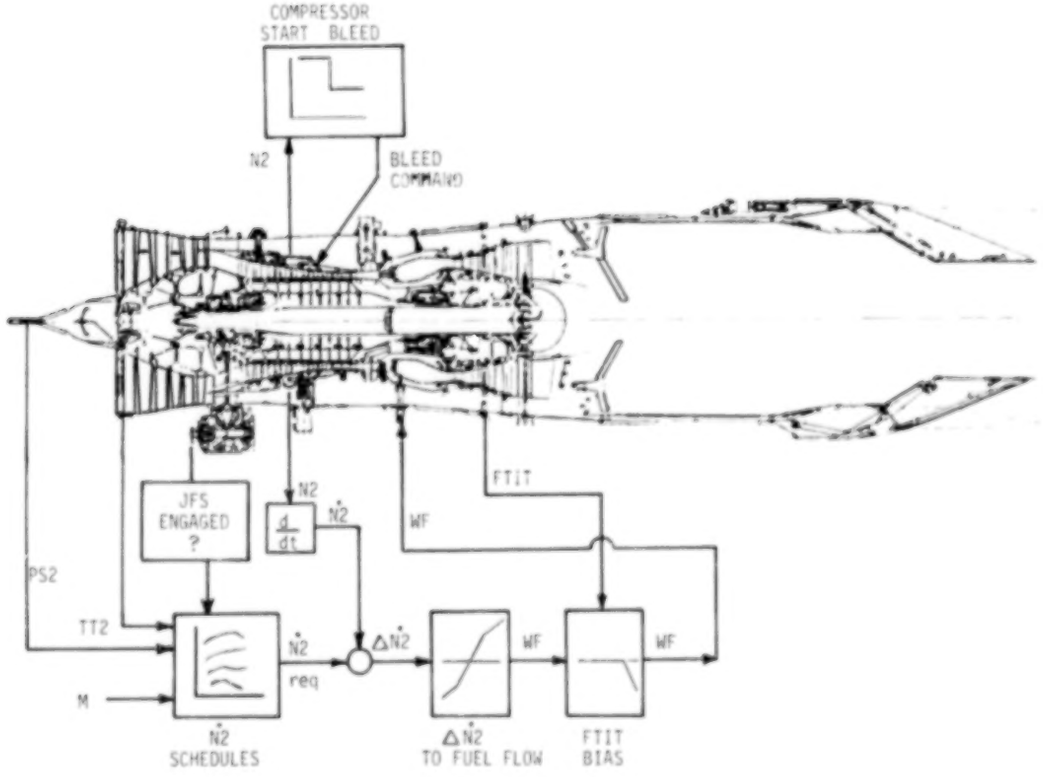

SPOOLDOWN AIRSTART AT 250 KNOTS

The next figure is a time history of a DEEC 40-percent spooldown airstart at an airspeed of 250 knots and an altitude of 9100 m, which also illustrates the use of closed-loop airstart logic. The power lever angle (PLA) was moved to the on/off position to shut down the engine at time (t) = 10 sec. Immediately after shutdown there was a corresponding drop in core speed (N2), fan turbine inlet temperature (FTIT), and fuel flow to the engine. The pilot initiated the ignition sequence by moving the throttle up over the idle detent to the idle power setting at t = 22 sec as the core rpm reached 40 percent. At this point the fuel flow began at the minimum value of 115 kg/hr. At t = 31 sec, the fuel mixture was ignited (light) as noted by the increase in FTIT. The DEEC closed-loop logic modulated the fuel flow to achieve the desired rate of acceleration of the engine core. N2 increased uniformly to t = 45 sec, then increased more rapidly. Idle speed was reached at t = 77 sec. FTIT varied between 450° C and 520° C during the airstart. The time required for the airstart, defined as the difference between idle and pressurization times, was 55 sec.

DEEC Airstart

NASA
DFRF83-532

40 Percent Spooldown
250 Knots

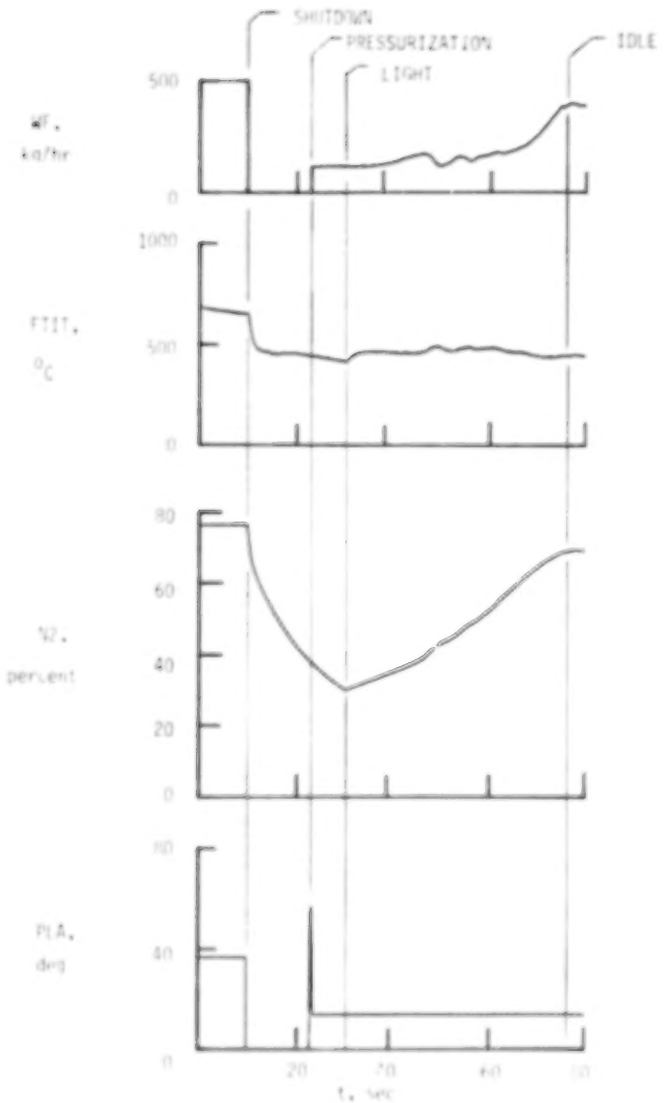

AIRSTART AT 200 KNOTS AT 9250 METERS

Airstarts at lower airspeeds took longer, due to the reduced energy of the inlet flow and lower burner pressures. The figure below shows a 40-percent spool-down airstart at an airspeed of 200 knots and an altitude of 9250 m. Shutdown time was t = 12 sec, pressurization at t = 23 sec, light at t = 32 sec, and idle at t = 108 sec. Airstart time was 86 sec. The FTIT reached 600° C at t = 38 sec, with the fuel flow on the minimum flow stop.

NASA
DFRF83-530

DEEC Airstart

40 Percent Spooldown
200 Knots

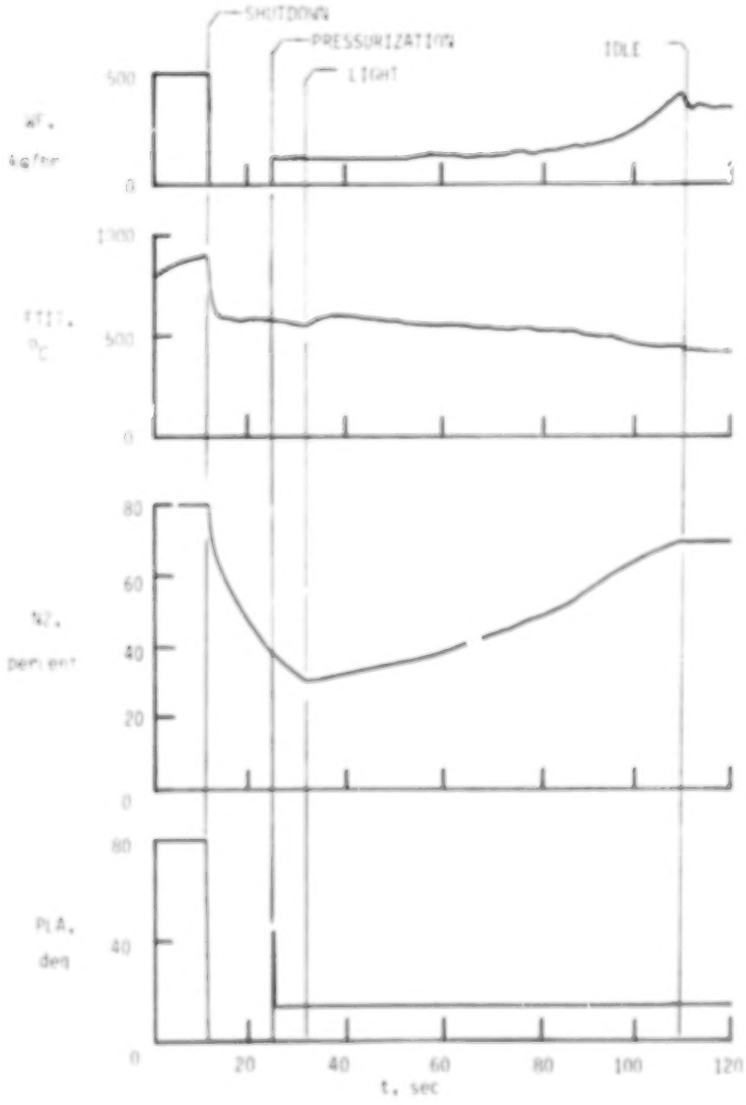

AIRSTART AT 200 KNOTS AT 4600 METERS

A DEEC 40-percent spooldown airstart at 200 knots, at an altitude of 4600 m, is shown below. Shutdown occurred at t = 9 sec, pressurization at t = 15 sec and light at t = 23 sec. Following the light, the N2 continued to decrease for 10 sec as fuel flow was increased. At t = 40 sec, a positive N2 rate was achieved and fuel flow was cut back as FTIT reached 600° C. In the time between t = 50 sec and 70 sec, oscillations in N2, FTIT, and WF occurred indicating that the gains in the closed-loop control logic were slightly high. The airstart continued and idle was reached at t = 104 sec, for an airstart time from pressurization to idle (T) = 89 sec, slightly longer than the 86 sec time from the previous figure at the higher altitude but a similar airspeed.

NASA
DFRF83-531

DEEC Airstart
40 Percent Spooldown
200 Knots

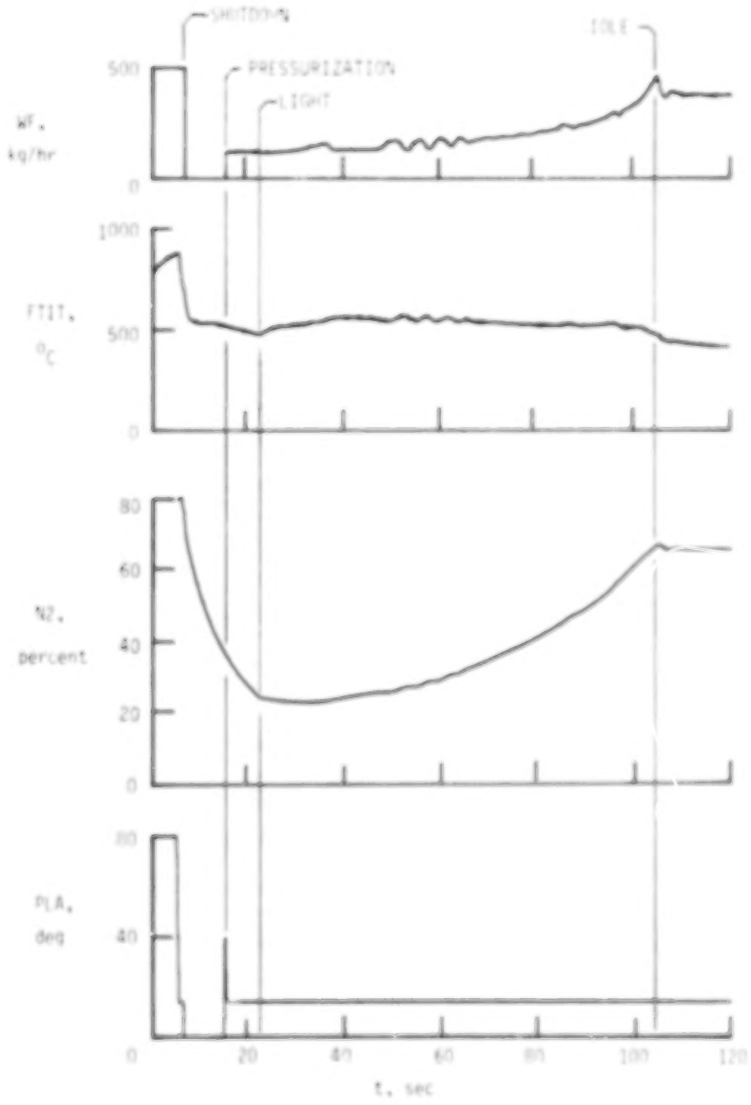

JFS-ASSISTED AIRSTARTS

For more rapid airstarts at altitudes below 6100 m, the jet fuel starter was used for assisted airstarts. The figure below shows a time history of a JFS-assisted airstart at calibrated airspeed (VC) = 255 knots at an altitude of 6100 m. Shutdown occurred at t = 11 sec and the JFS was engaged at t = 33 sec at an N2 of 25 percent. The N2 increased as a result of the JFS assist and stabilized at N2 = 32 percent. The pressurization was delayed for this test until stable JFS motoring speed was observed at t = 68 sec. After the light at t = 79 sec, N2 increased rapidly and idle was achieved at t = 106 sec for an airstart time of 38 sec.

NASA
DFRF83-533

DEEC JFS Airstart
255 Knots

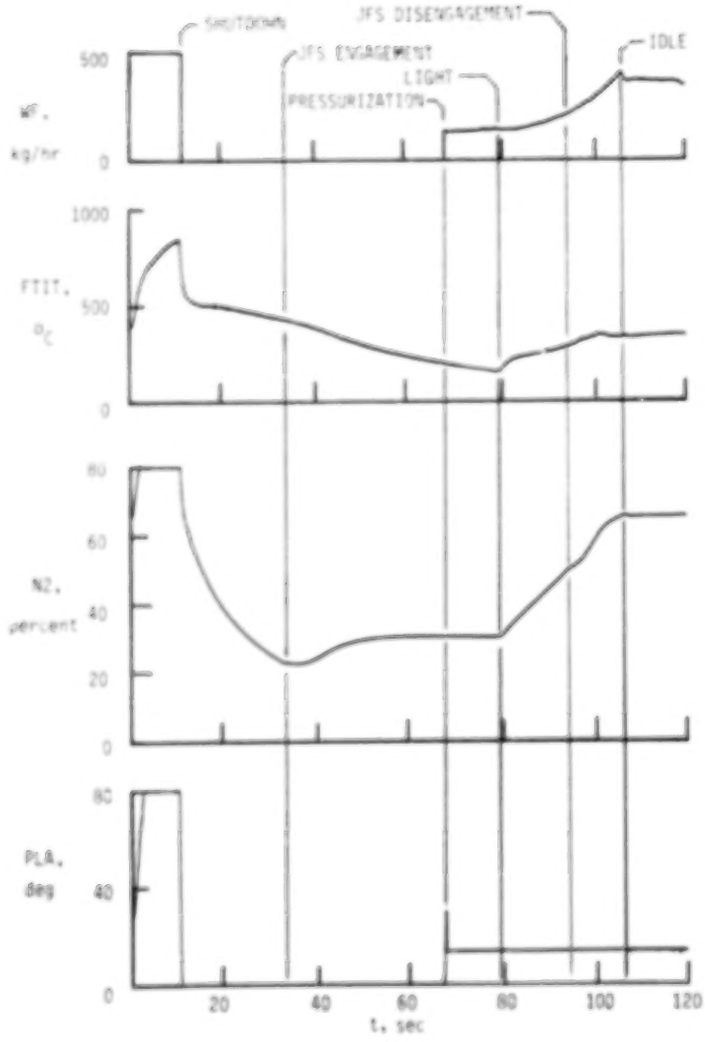

JFS-ASSISTED AIRSTART AT 210 KNOTS

A JFS-assisted airstart at a lower speed of VC = 210 knots and at an altitude of 6100 m is shown below. Shutdown occurred at t = 14 sec, JFS engage at t = 34 sec, pressurization at t = 36 sec, and light at t = 46 sec. The N2 rate was reduced to nearly zero at t = 65 sec prior to JFS disengage. Following the JFS disengage an increase in N2 rate occurred. The airstart was completed at t = 83 sec, for an airstart time of 47 sec.

All JFS-assisted airstarts attempted were successful from VC = 400 knots to 200 knots over a wide range of altitudes.

NASA
DFRF83-534

DEEC JFS Airstart
210 Knots

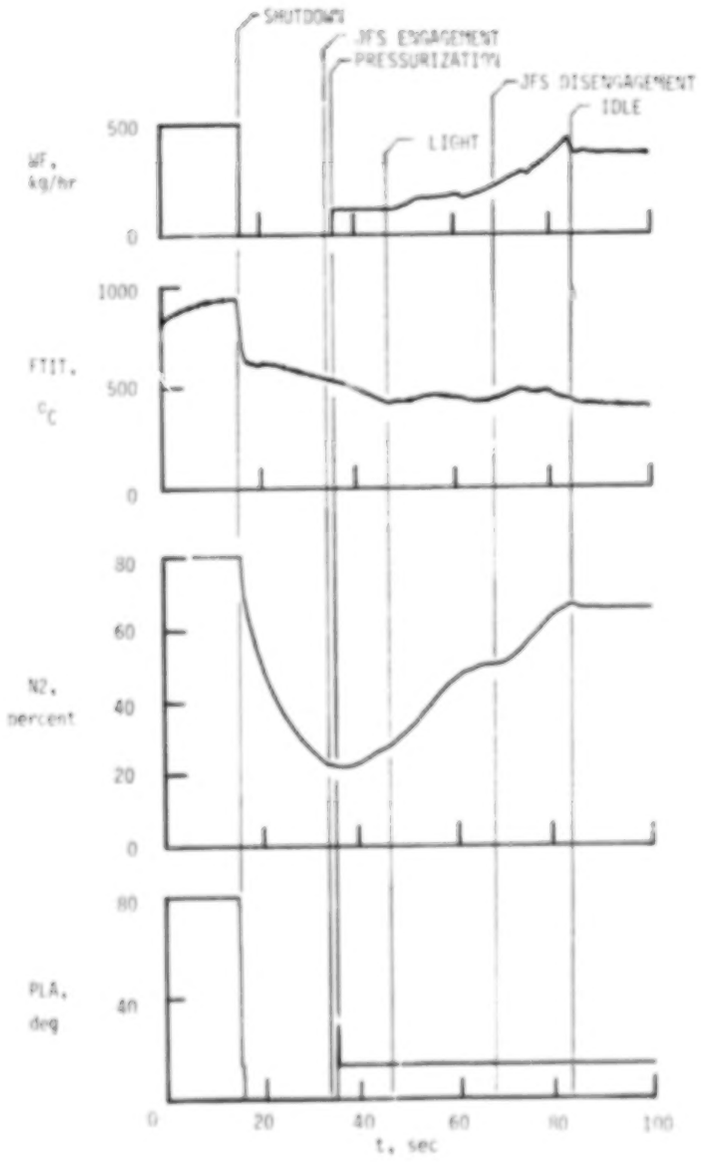

SUMMARY OF AIRSTART TIMES

Airstart times - T - for the DEEC airstarts are shown in the figure below for the 40-percent spooldown airstarts, for the 25-percent spooldown airstarts, and for JFS-assisted airstarts. Airstart times for the 40-percent spooldown airstarts were approximately 50 sec at VC = 250 knots, 85 sec at VC = 200 knots, and up to 192 sec at VC = 175 knots. For the 25-percent spooldown airstarts, times were approximately 65 sec at VC = 250 knots, and from 97 sec to 135 sec at airspeeds of 205 knots to 210 knots. It is clear that airstarts at VC = 200 knots are only marginally successful, due to the long start times.

NASA
DFRF 82-260

EFFECT OF AIRSPEED AND ALTITUDE ON AIRSTART TIMES

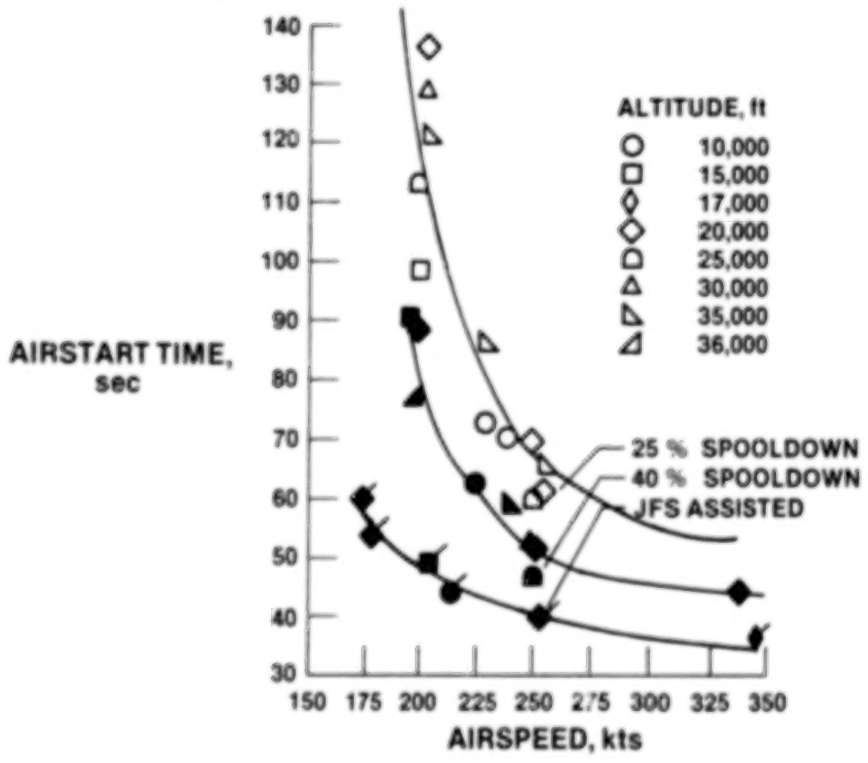

HUNG AIRSTART

At airspeeds below 200 knots, most of the spooldown airstarts were unsuccessful. The unsuccessful airstarts were mostly hung starts in which the N2 either decreased or did not increase. A typical example of a hung start, shown in the figure below, is a 25-percent spooldown airstart attempt at VC = 180 knots at an altitude of 7600 m. Following the light, N2 increased very slowly to 28 percent and then stabilized. The fuel flow remained on the minimum flow stop; FTIT initially exceeded 600° C and then slowly decreased.

NASA
DFRF83-535

DEEC Hung Airstart
25 Percent Spooldown
180 Knots

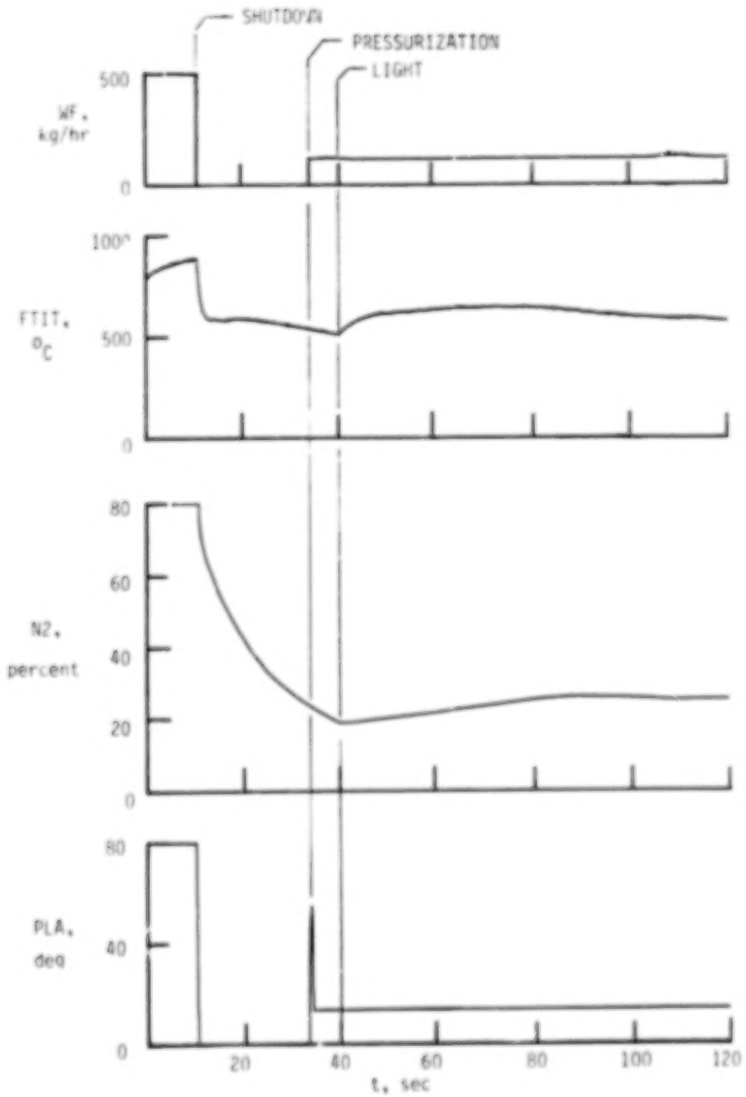

HOT START

Only one hot start occurred in the airstart test; it is shown in the figure below. It was a 40-percent spooldown airstart attempt at VC = 160 knots at 7600 m. Following the burner light at t = 35 sec, N2 continued to decrease, while FTIT increased rapidly, even with the fuel flow at the minimum value, indicating a stalled compressor condition. When the FTIT reached the maximum allowable value of 800° C, the pilot shut down the engine.

NASA
DFRF83-536

DEEC Hot Start
40 Percent Spooldown
160 Knots

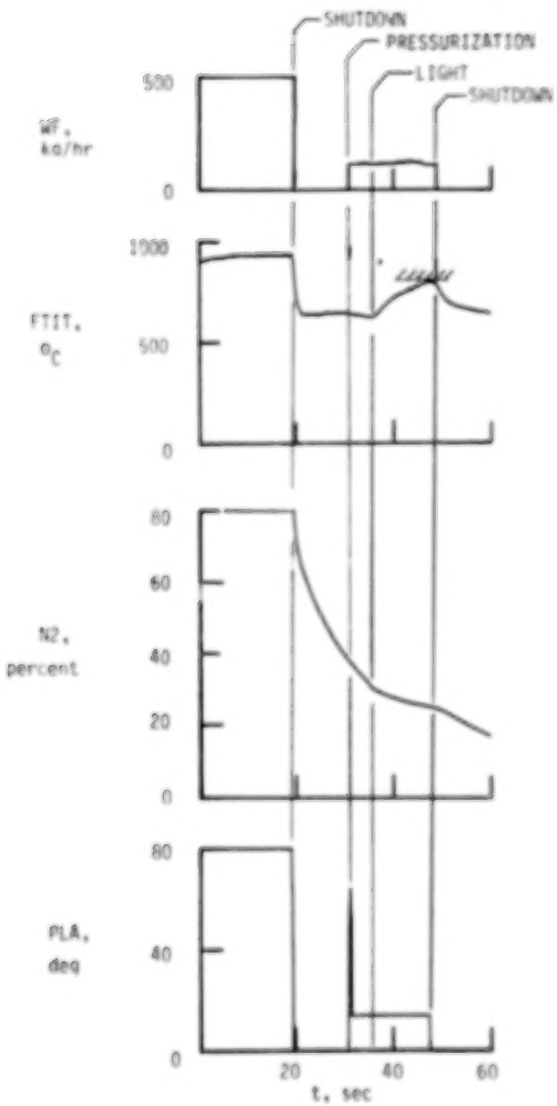

SUMMARY OF AIRSTART SUCCESS

A summary of the DEEC spooldown airstart success is shown in the figure below. All DEEC airstarts at and above 200 knots were successful, both for 25-percent and 40-percent spooldown airstarts. This capability represented a 50-knot to 100-knot improvement over the standard F100 engine handbook limit.

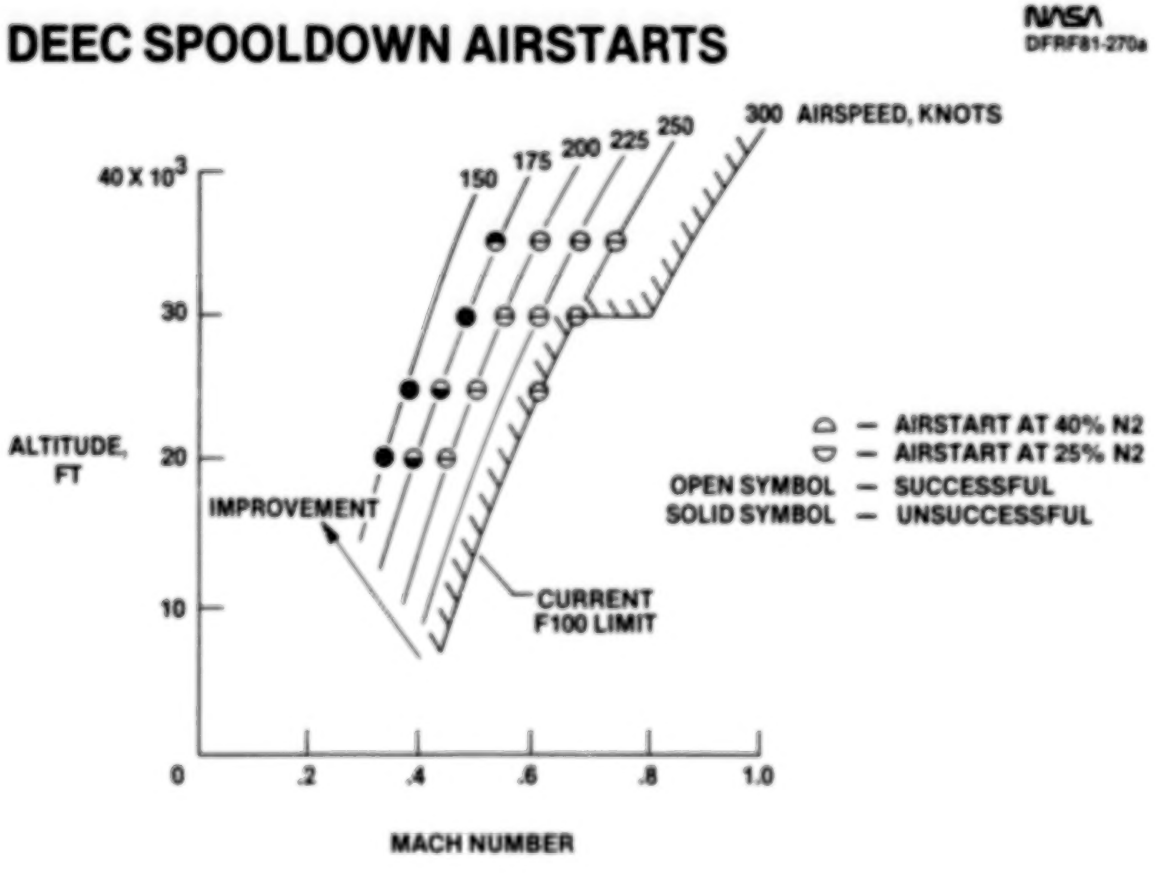

CONCLUDING REMARKS

The summary of the DEEC airstart capability of an F100 engine equipped with a DEEC is shown below. The DEEC airstart capability with the closed-loop control logic was very effective. All airstarts at 200 knots and above were successful, a 50-knot to 100-knot improvement over the standard F100 engine. Airstart times for spooldown airstarts ranged from 50 sec to 70 sec at 250 knots to 80 sec to 130 sec at 200 knots. All JFS-assisted airstarts were successful at airspeeds between 170 knots and 400 knots. At speeds below 200 knots, most of the airstarts were unsuccessful, as expected, due to hung starts.

Summary

NASA
DFRF83-537a

- DEEC closed-loop airstart logic effective
- All airstarts at airspeeds of 200 knots or greater were successful, 50 to 100 knot improvement over standard F100
- Airstart times between 50 to 70 sec at 250 knots and 80 to 130 sec at 200 knots
- All JFS-assisted airstarts were successful
- Unsuccessful starts at airspeeds of 175 knots and below, as expected

N86
25351

UNCLAS

N86-25351

FLIGHT EVALUATION OF A HYDROMECHANICAL BACKUP CONTROL FOR THE DIGITAL ELECTRONIC ENGINE CONTROL SYSTEM IN AN F100 ENGINE

Kevin R. Walsh and Frank W. Burcham
NASA Ames Research Center
Dryden Flight Research Facility
Edwards, California

SUMMARY

The backup control (BUC) for the DEEC system is a simple hydromechanical system provided in the event a major malfunction occurs in the DEEC. The DEEC detects and accommodates engine faults in real time by using digital computation electronics which sustains full authority control over all the engine-controlled variables.

This paper will describe the BUC features, the operation of the BUC system, the BUC control logic, and the BUC flight test results. The flight test results included: transfers to the BUC at military and maximum power settings; a military power acceleration showing comparisons between flight and simulation for BUC and primary modes; steady-state idle power showing idle compressor speeds at different flight conditions; and idle-to-military power BUC transients showing where compressor stalls occurred for different ramp rates and idle speeds. All the BUC transfers which have occurred during the DEEC flight program were initiated by the pilot. There were no automatic transfers to the BUC.

PRECEDING PAGE BLANK NOT FILMED

BUC FEATURES

The hydromechanical BUC for the DEEC is a simple system designed for safety purposes. The main purpose of its operation is returning to base and landing. The DEEC will automatically transfer to the BUC when one of the following occurs:

(1) a fault is detected that could damage the engine;

(2) a DEEC power failure occurs; or

(3) at the pilot's discretion.

Other BUC features include:

(1) operation over the entire F100 operating envelope, which includes the F-15 flight envelope as shown in the next figure. Also shown, for comparison, is the F-16 BUC envelope. The F-16 BUC is less complex and has fewer capabilities than the F-15 BUC;

(2) intermediate thrust at least 70 percent of DEEC intermediate thrust;

(3) automatic airstart capability;

(4) no augmentation;

(5) closed nozzle; and

(6) throttle rate limited.

For the DEEC tests the throttle rate was limited by the pilot. The evaluation of different throttle rates helped Pratt and Whitney Aircraft decide on a rate limiter for a future BUC. This rate limiter is a part of the group III logic and will be 5 sec for an idle-to-military throttle transient.

BUC Envelopes

NASA
DFRF83-519

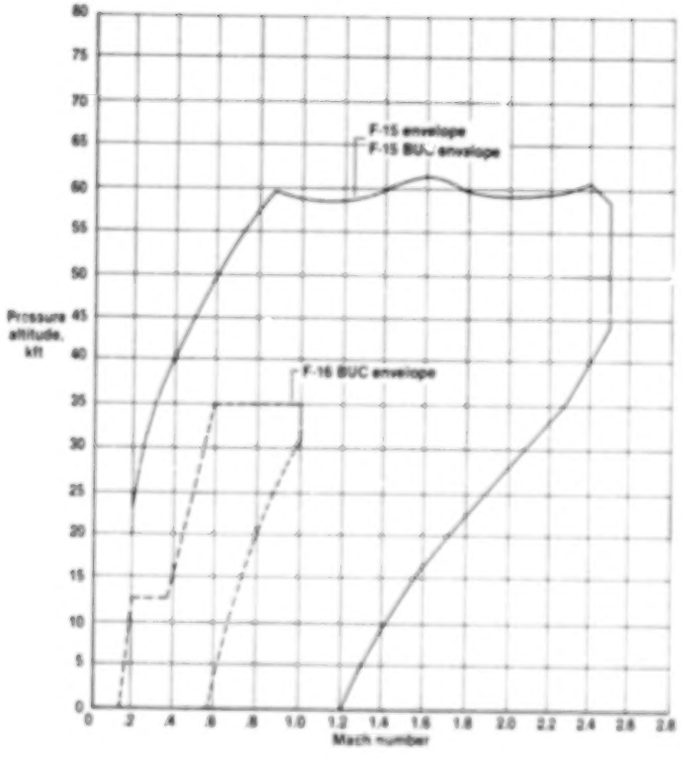

The dashed lines shown in the block diagram of the DEEC system represent the BUC system. The BUC is housed in the same package as the DEEC gas generator fuel-metering valves. A hydraulically operated transfer valve is positioned so the BUC components will control the following:

(1) gas generator fuel flow (WFGG) to the main (core) burner;

(2) the position of the start bleeds; and

(3) the position of the core compressor variable vanes (RCVV).

The BUC operates on the following inputs:

(1) fan inlet static pressure (PS2);

(2) fan inlet total temperature (TT2);

(3) power lever angle (PLA); and

(4) RCVV feedback cable indicating RCVV position.

DEEC Control System Block Diagram

NASA
DFRF83-319

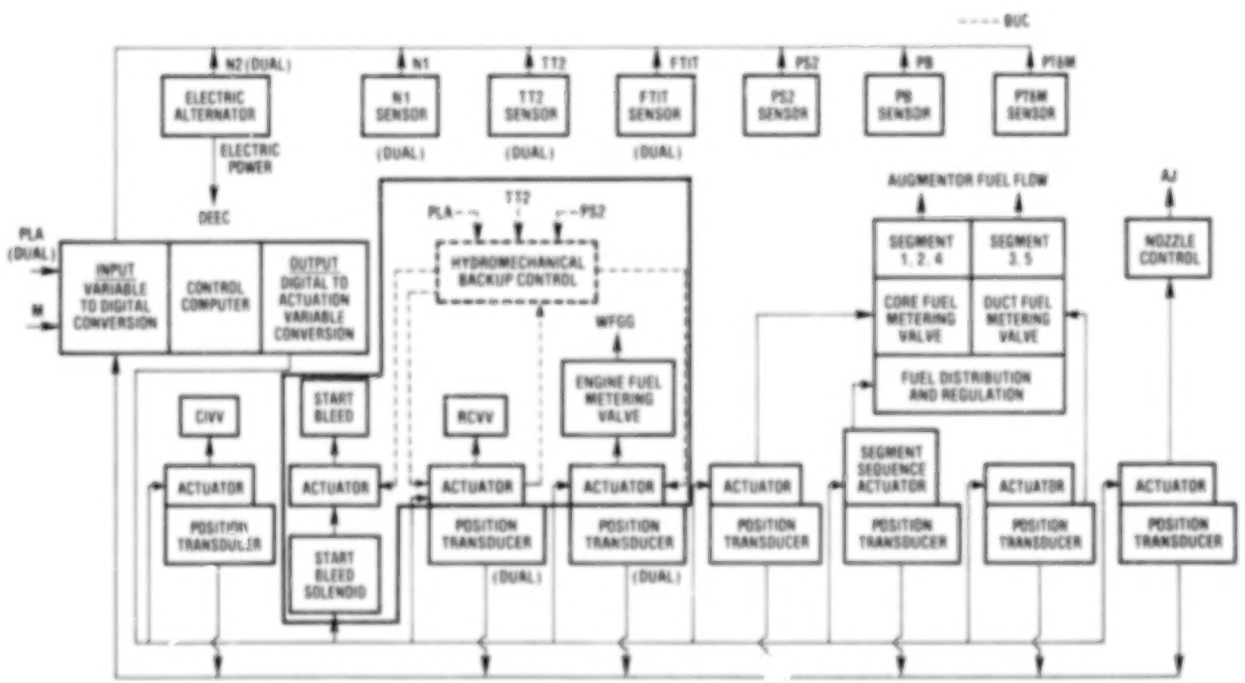

A diagram of how the BUC implements the input variables to obtain metered fuel flow (WFGG) and RCVV position is shown in the figure below. Fuel-air ratio in the form of WF/PS2 is derived from a cam that moves as a function of PLA and TT2. This WF/PS2 value and PS2 is fed to a different cam that outputs a corrected value of PS2 called compensated fan inlet static pressure (PS2C). A multiplier cam then multiplies the PS2C value and the WF/PS2 ratio to obtain the WFGG. The RCVV position is derived from a cam that moves as a function of PLA and TT2.

The gas generator control/BUC also provides the following functions when in BUC:

(1) a fuel pressure mode signal (PFMO), indicating BUC operation is supplied to the augmentor control and the nozzle control to cancel augmentation and to close the engine nozzle;

(2) a null voltage, supplied to the CIVV torque motor, drives the CIVVs to their full cambered position; and

(3) an electrical signal supplied to the cockpit to indicate BUC operation.

In addition, there are no fan rotor speed (N1), core rotor speed (N2), or fan turbine inlet temperature (FTIT) inputs to the BUC.

Backup Control Logic

NASA
DFRF83-425

- Nozzle closed
- CIVV Full cambered
- No afterburner
- No N1, N2 or FTIT inputs

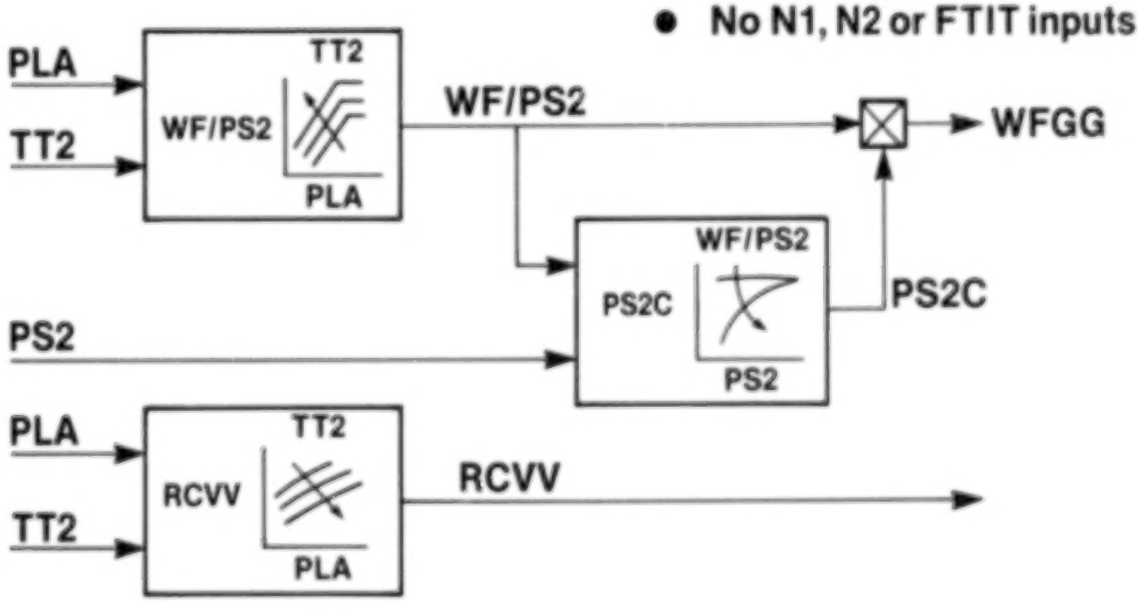

BUC TRANSFERS

The BUC transfer points that were accomplished are shown in the figure below. One hundred twenty-five BUC transfers were successful, including the transfers at maximum power and at ground level.

BUC Transfers

NASA
DFRF83-520

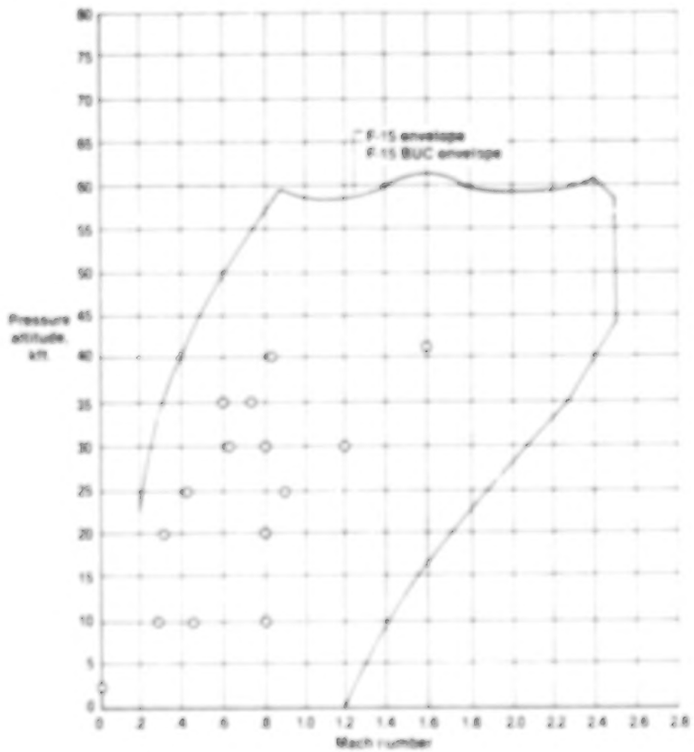

BUC TRANSFER, MILITARY POWER

The next figure is a time history of a BUC transfer at military power, at Mach 0.6 and 30,000 ft. The BUC transfer was initiated by the pilot at t = 4.2 sec, as indicated by the rise in PFMO. At that time, the CIVV torque motor received a null voltage which drove the CIVVs to full cambered position. The jet primary nozzle area (AJ) torque motor received the fuel pressure mode signal (PFMO), which fully closed the nozzle. Because the BUC gas generator fuel flow schedule requested a lower fuel flow than the DEEC, the fuel flow decreased at transfer. The RCVVs were also scheduled to new positions.

After a small delay, burner pressure and fan turbine inlet temperature began to respond to the fuel flow decrease. Also, a time lag occurred for N1 and N2 to register the transfer because of the slow scheduling of the variable vanes and the large angular momentum of the fan and compressor. For this military power BUC transfer, N1 and N2 speeds decreased only slightly.

BUC Transfer

NASA
DFRF83-526

Military Power
30,000 Ft, M = 0.6

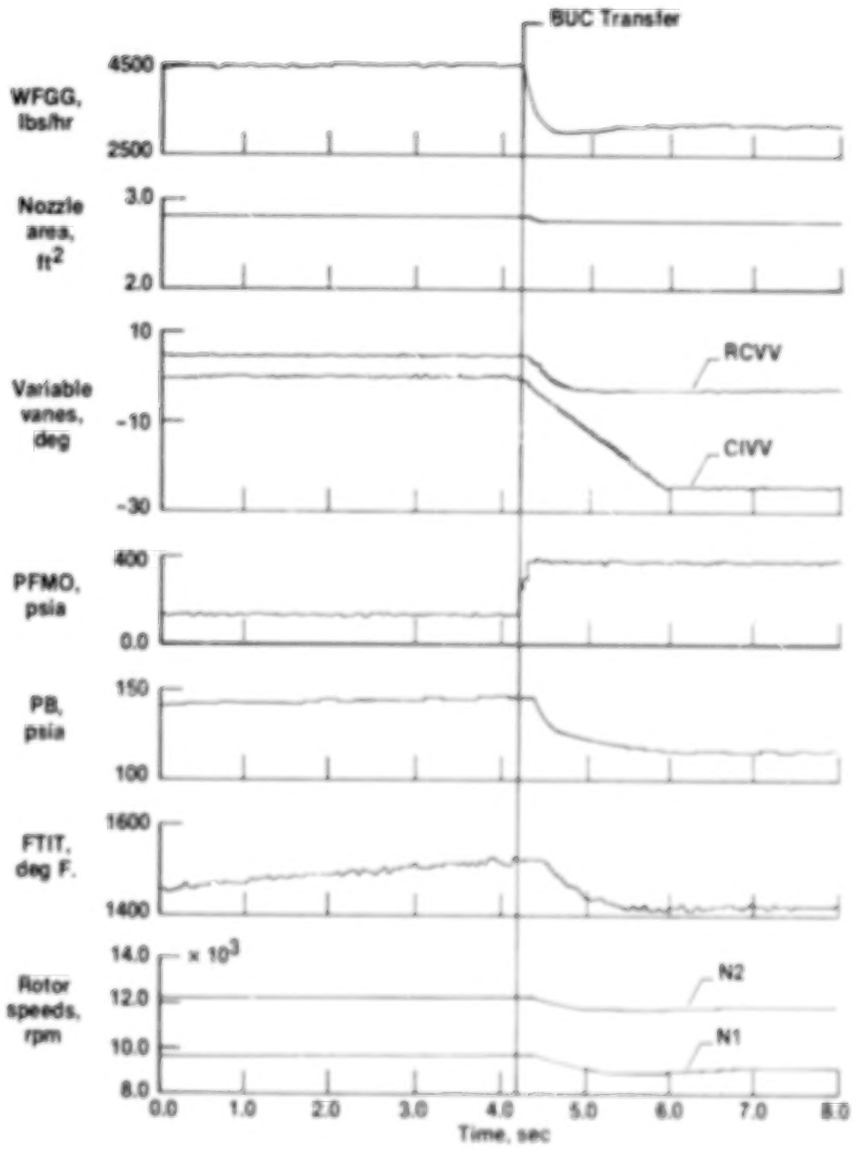

BUC TRANSFER, MAXIMUM POWER

A time history of a BUC transfer at maximum power, and Mach 1.2 at 30,000 ft is presented in the following figure. The same sequence of events occur as for the military power transfer. The BUC transfer occurred at t = 1.5 sec as indicated by the rise in PFMO. The CIVV torque motor received a null voltage, which drove the CIVVs to full cambered position. The AJ torque motor received the PFMO, which fully closed the nozzle. For this condition the nozzle closed at its maximum rate. WFGG decreased to its BUC schedule and the RCVVs changed setting.

At transfer, the augmentor fuel flow was shut off. This rapid decrease of fuel to the augmentor, with the nozzle open, caused a sudden drop in augmentor pressure. This reduced the back pressure on the fan, resulting in the increase in fan speed. The fan speed recovered when the nozzle approached its full closed position.

BUC Transfer

NASA
DFRF83-525

Maximum Power
30,000 Ft, M = 1.2

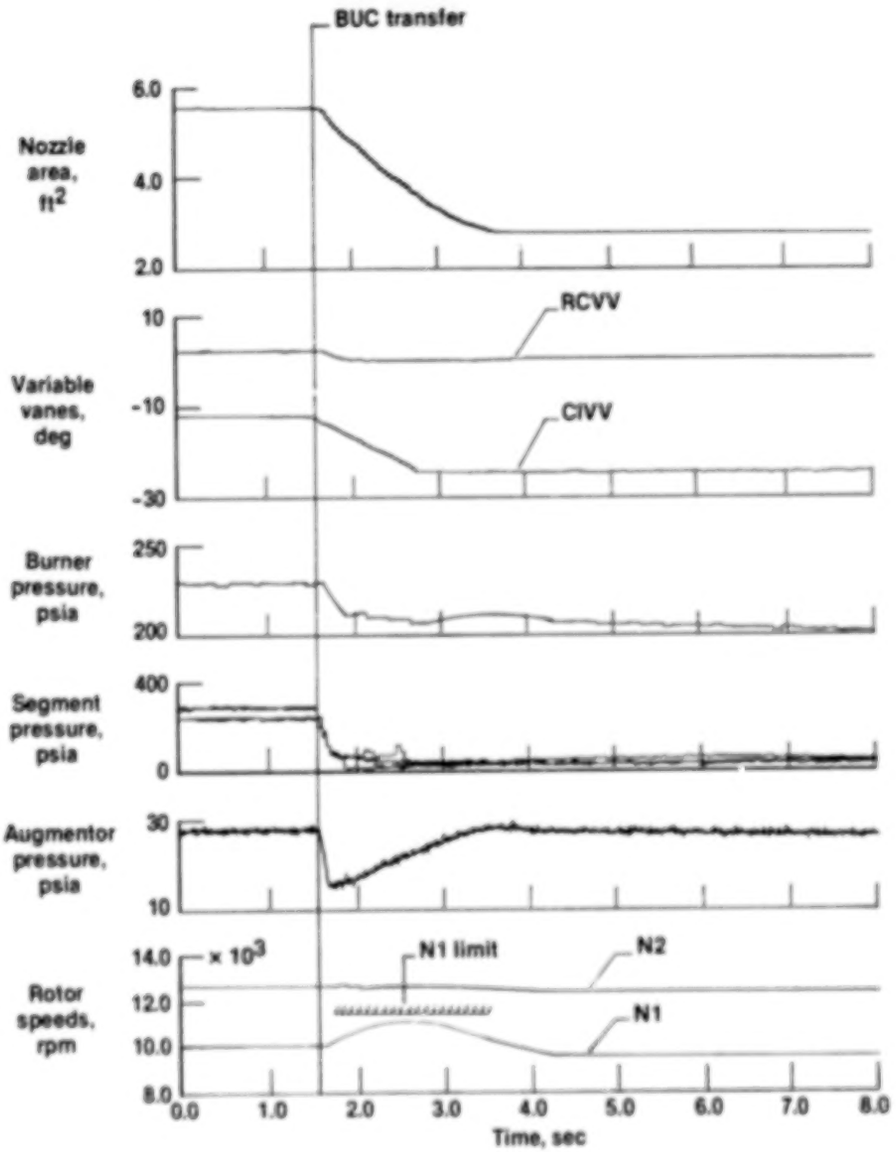

The figure below represents a military power level acceleration accomplished in BUC at an altitude of 30,000 ft and a range of Mach from 0.5 to 0.98. Other military power accelerations were performed, but this one provided the best comparison with a military power acceleration under DEEC (primary) control, which is also shown below. Open symbols are the BUC acceleration and solid symbols are the primary acceleration. In addition, a simulation of a BUC and primary military power acceleration obtained from the F100 engine status deck is shown.

In general, the BUC flight performance was lower than the BUC simulation performance except for the corrected fan speed, which was higher than predicted. The primary flight performance agreed well to the primary simulation except for the corrected fan speed, which was higher than predicted, and the fan turbine inlet temperature, which was lower than predicted. For net thrust (FN), the agreement between flight and simulation was good. The thrust was calculated using the real-time thrust method, which will be discussed in Paper 13. The BUC thrust averaged about 1700 lb less than the primary thrust or 70 percent of primary thrust at Mach 0.8. FTIT averaged approximately 230° less for BUC than primary.

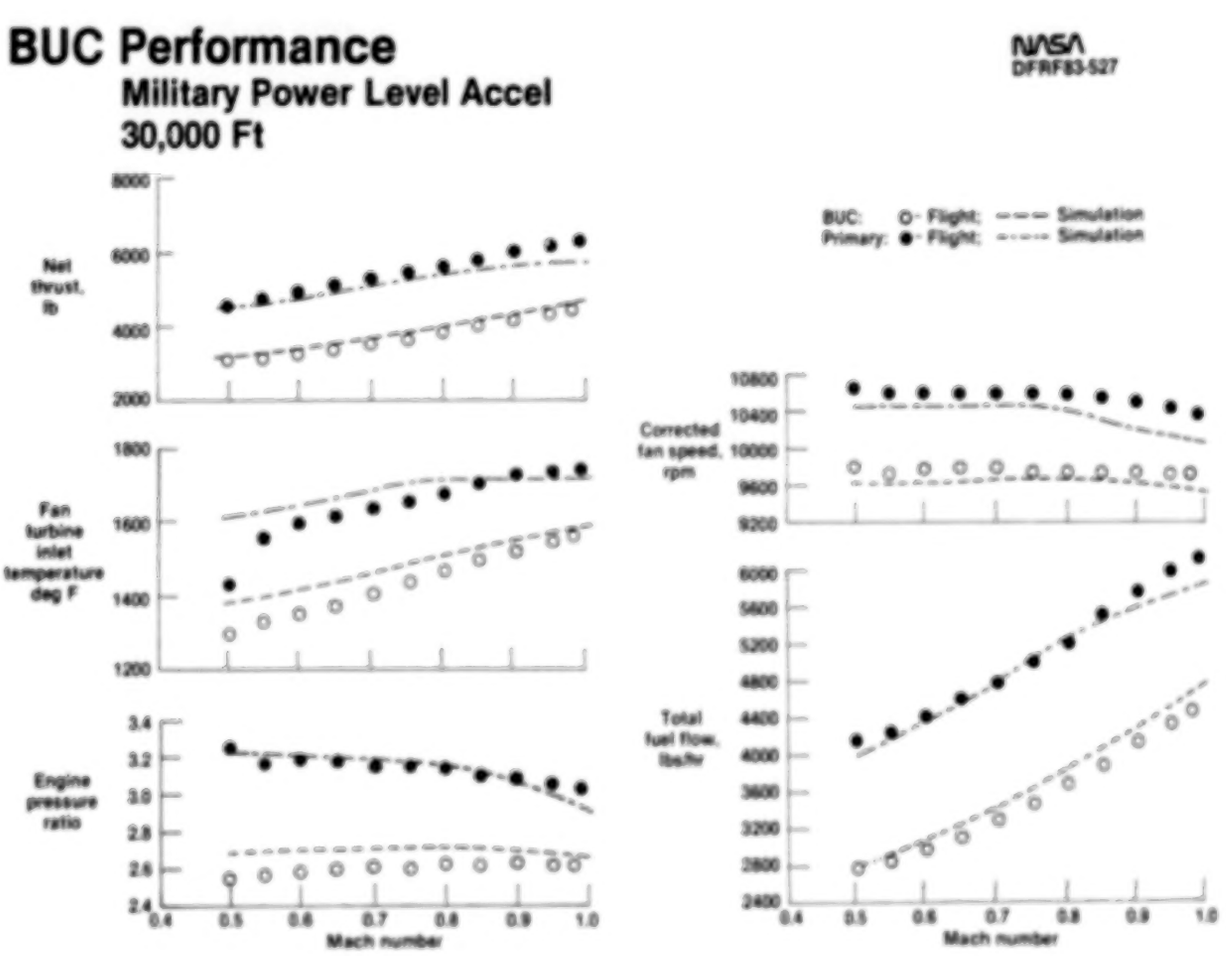

BUC IDLE POWER

At steady-state idle power, the figure below shows trends of percent compressor speeds versus Mach numbers at different altitudes. At 10,000 to 20,000 ft, idle compressor speeds – at all Mach numbers tested – remained at or above 60 percent. At a Mach number of between 0.6 and 0.7 and 35,000 ft, the compressor speed dropped below 60 percent. Idle compressor speeds should be at least 65 percent – below 65 percent is marginal and below 60 percent is undesirable. In this situation the pilot must be aware of the compressor speed to avoid a possible sub-idle compressor stall. Decreasing altitude and gaining airspeed would alleviate this problem. However, this may not be a serious problem because the BUC is not usually operated at high altitude and low airspeed.

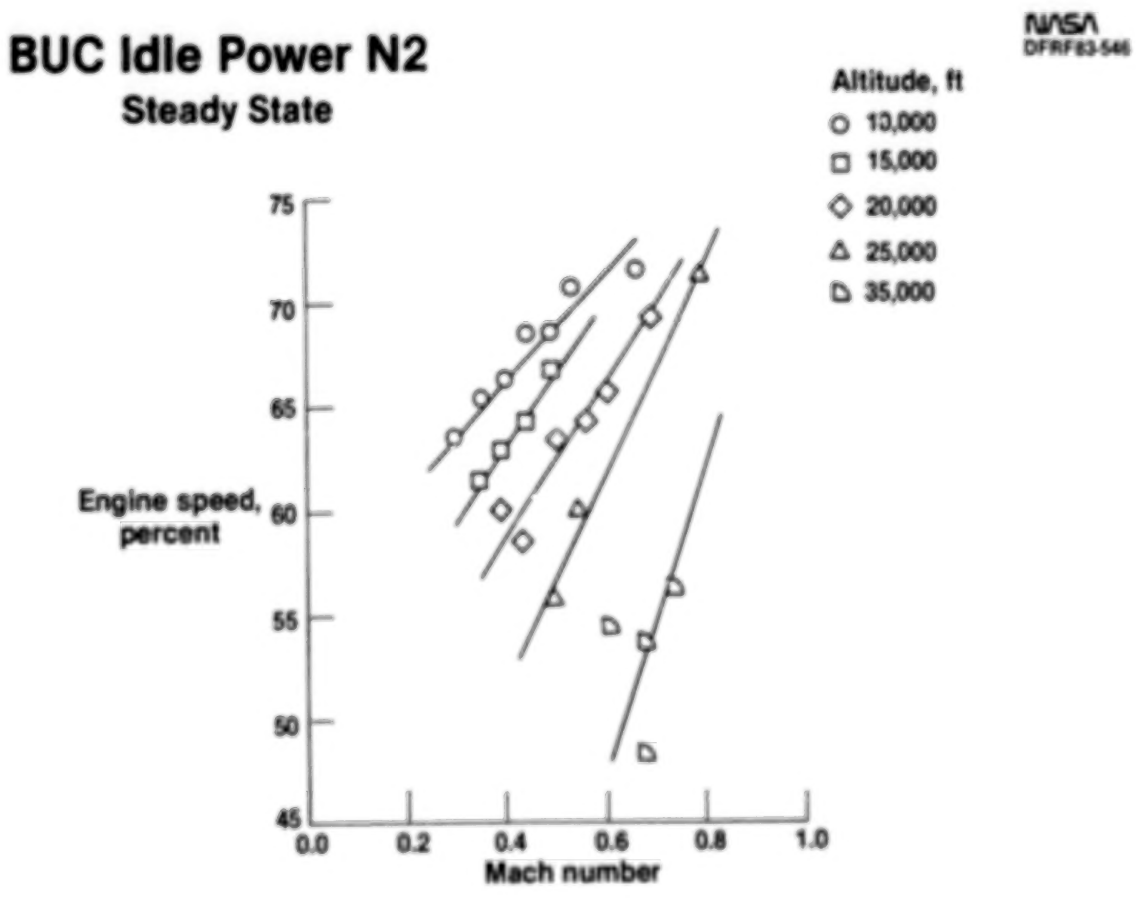

BUC TRANSIENTS

Idle-to-military power BUC transients were performed at various altitudes. The figure below shows the transients that were performed. These transients were snaps and throttle ramps of 3, 5, and 7 sec. The purpose of performing the transients was twofold – to determine the limits where and when compressor stalls occur, and to determine the BUC throttle rate limits for future control designs.

NASA
DFRF83-528

BUC Throttle Ramps
Idle-To-Mil Power

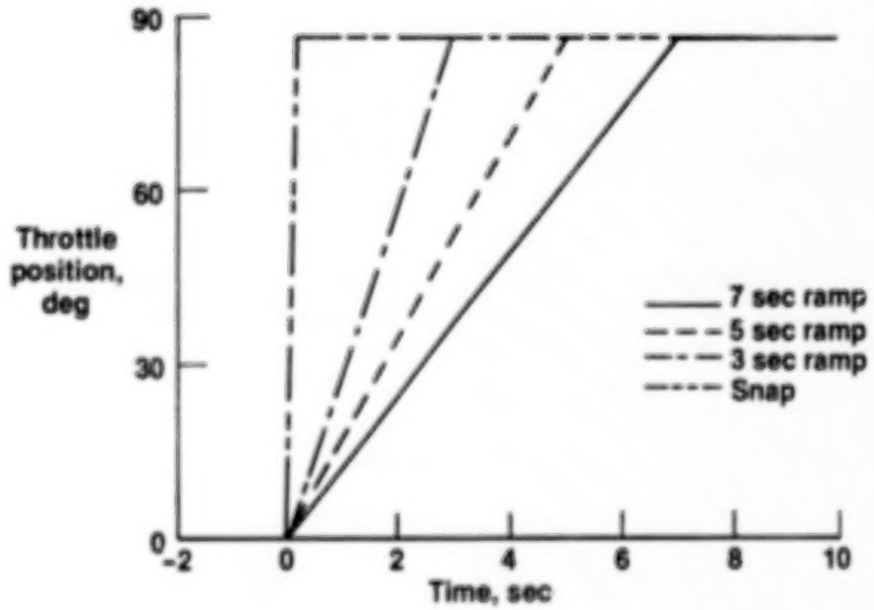

BUC TRANSIENTS RESULTS

Idle-to-military power ramp rates at four altitudes, versus idle speed, are shown in the figure below. It also shows the boundary where compressor stalls occurred for different ramp rates and idle speeds. At idle speeds of above 70 percent N2, all snaps and ramps were successful. Additional transients, not shown in the figure, were successfully completed at compressor speeds greater than 70 percent. At idle speeds of below 60-percent N2, a ramp rate of 7 sec or longer is required to prevent a compressor stall. For a 5-sec ramp N2, idle speed must be maintained above 63 percent.

NASA
DFRF83-547

BUC Throttle Ramp Results
Idle-To-Mil Power

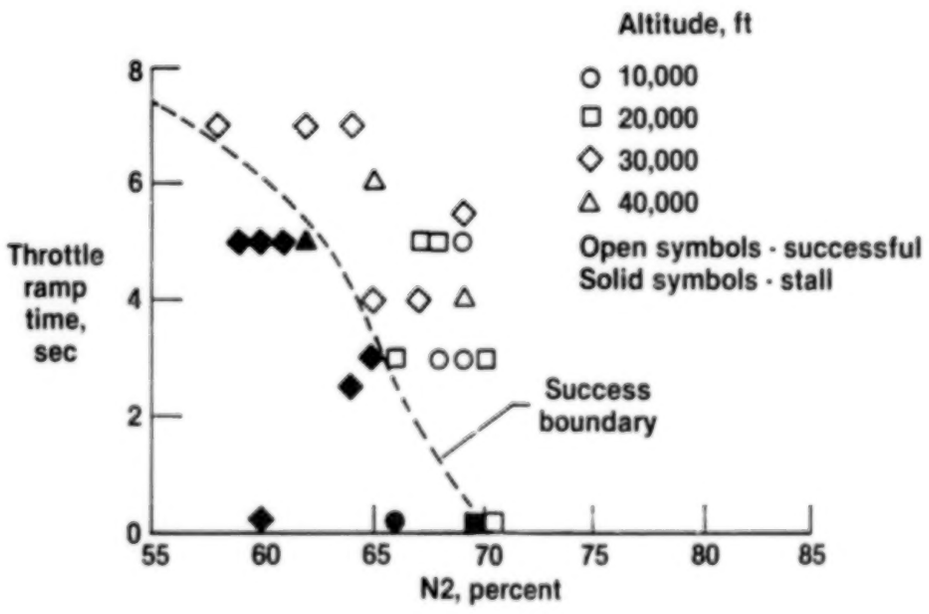

CONCLUDING REMARKS

The performance of the BUC for the DEEC has been evaluated. The following is a summary of this investigation.

(1) All of the attempted transfers to the BUC were successful.

(2) BUC intermediate thrust is 70 percent of DEEC intermediate thrust.

(3) BUC throttle ramp times of 5 sec were successful when N2 was greater than 63 percent.

(4) At high altitudes and low airspeeds, BUC idle speeds were less than 60-percent N2.

(5) Pilots like the BUC system.

N86
25352

UNCLAS

N86-25352

BACKUP CONTROL AIRSTART PERFORMANCE ON A DIGITAL ELECTRONIC ENGINE CONTROL-EQUIPPED F100 ENGINE

J. Blair Johnson
NASA Ames Research Center
Dryden Flight Research Facility
Edwards, California

SUMMARY

The airstart capability of a backup control (BUC) was tested for a digital electronic engine control- (DEEC-) equipped F100 engine, which was installed in an F-15 airplane. Two airstart schedules were tested. The first was referred to as the group I schedule and the second, or revised schedule, was referred to as the group II start schedule.

Using the group I start schedule, based on a 40-sec timer, an airspeed of 300 knots was required to ensure successful 40- and 25-percent BUC mode spooldown airstarts. If core rotor speed (N2) was less than 40 percent, a stall would occur when the start bleeds closed – 40 sec after initiation of the airstart. All jet fuel starter- (JFS-) assisted airstarts were successful with the group I start schedule.

For the group II schedule, the time between pressurization and start bleed closure ranged between 50 sec and 72 sec, depending on altitude. All airstarts were successful above approximately 200 knots giving a 75- to 100-knot reduction in required airspeed for a successful airstart. Forty-percent spooldown airstarts were successful at 200 knots, at altitudes up to 10,650 meters, and were successful at 175 knots at altitudes up to 6100 meters. Idle rpm was lower than the desired 65 percent for airstarts at higher altitudes and lower airspeeds. All JFS-assisted airstarts were successful.

PRECEDING PAGE BLANK NOT FILMED

N86-25352

BACKUP CONTROL LOGIC

The BUC logic is shown below. In the BUC mode, the compressor inlet variable vanes (CIVV) go to the full camber position, the nozzle closes, and augmentation is cancelled. The BUC schedules fuel flow (WF) and the rear compressor variable vane (RCVV) position, based on fan inlet total temperature (TT2), power lever angle (PLA), and fan inlet static pressure (PS2). There are no rpm (fan rotor speed (N1), core rotor speed (N2)) or fan turbine inlet temperature (FTIT) inputs to the BUC. More information on the BUC is presented in reference 1 and Paper 9. Airstarts conducted on the same engine with the digital control system are discussed in reference 2 and Paper 8.

Backup Control Logic

NASA
ADFRF83-449a

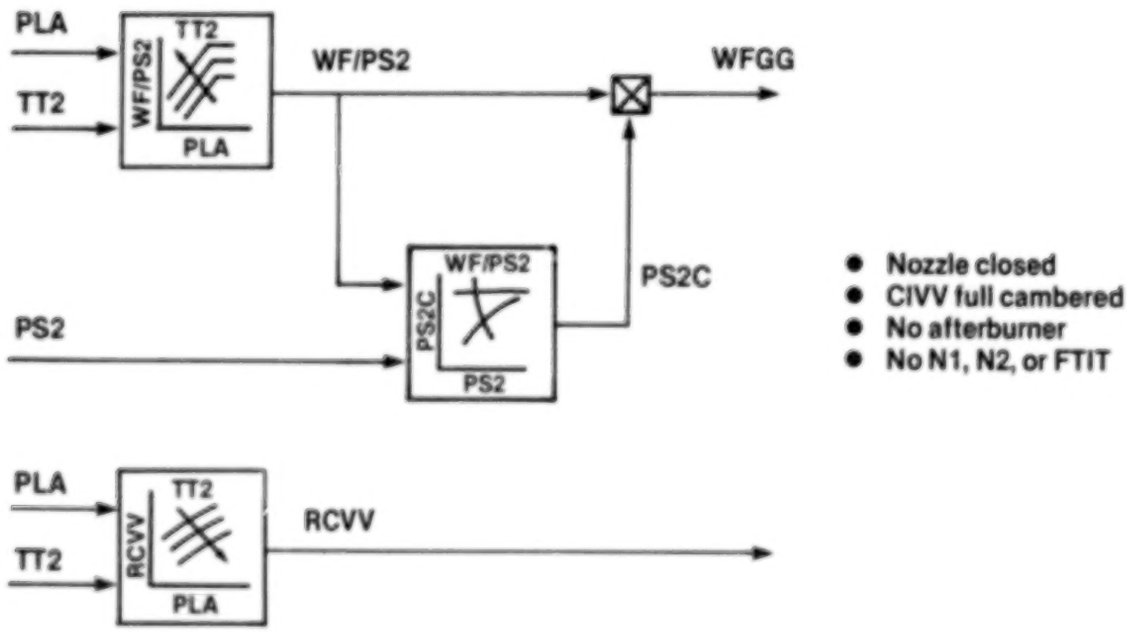

- Nozzle closed
- CIVV full cambered
- No afterburner
- No N1, N2, or FTIT

BUC FUEL FLOW SCHEDULE

The BUC airstart logic is an automatic schedule derived from a cam in the backup control. The start cam schedules a percentage of the idle fuel flow biased by PS2. The RCVV and compressor bleeds are held in the cambered and open positions.

Two start schedules were tested – the group I schedule and a revised schedule called group II. For the revised schedule, the initial fuel flow was slightly higher, and the elapsed time to start bleed closure and RCVV release was dependent on PS2, whereas the group I schedule released the RCVV and closed the start bleeds after approximately 40 sec for all values of PS2.

BUC Airstart Fuel Flow Schedule

NASA DFRF83-460

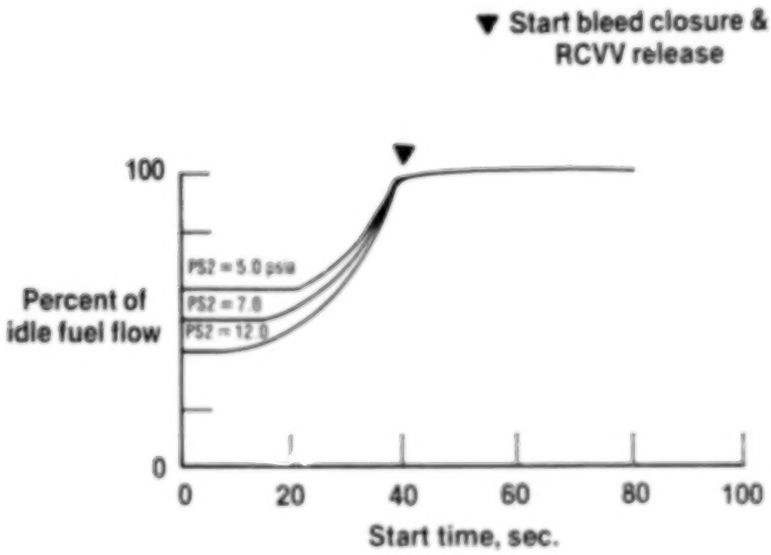

(a) Group I schedule

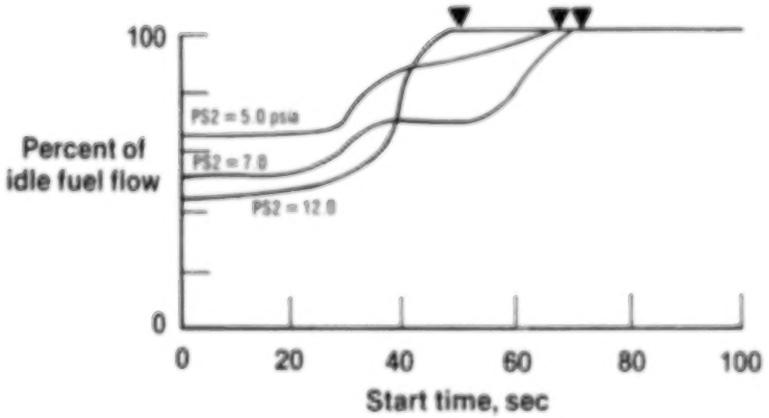

(b) Group II schedule

SUCCESSFUL BUC SPOOLDOWN AIRSTART
GROUP I

This figure presents a time history of a successful, 40-percent spooldown airstart, using the group I start schedule. The start was conducted at an altitude of 4600 meters and an airspeed of 310 knots. Start bleed closure and RCVV release occurred 40 sec after pressurization, as indicated by the drop in FTIT. However, N2 was approximately 43 percent and was still increasing to an idle condition. Although this start was successful, it is apparent the start timer elapsed before the start was complete.

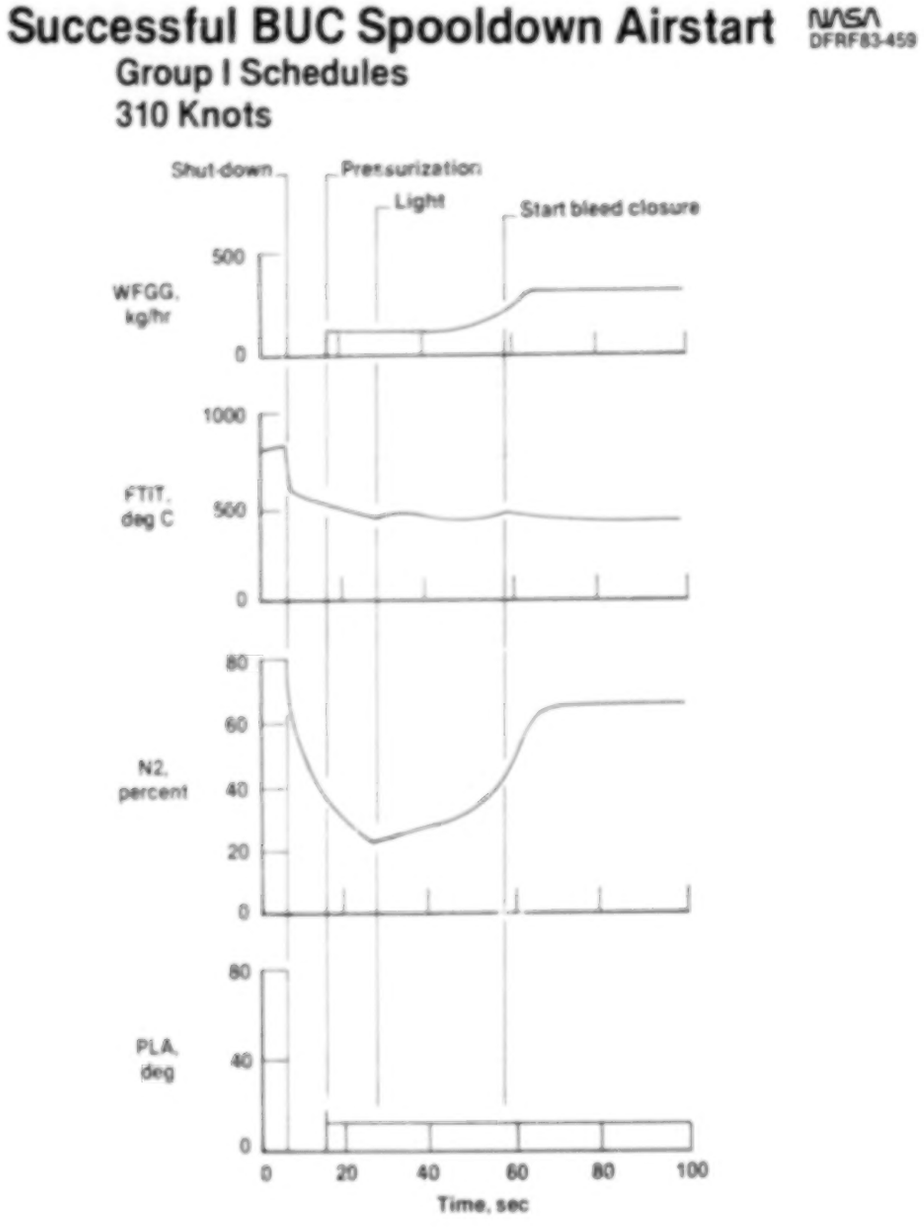

BUC 40-PERCENT SPOOLDOWN AIRSTART TIMES
GROUP I

With the group I start schedule, the time required for successful spooldown airstarts is primarily a function of airspeed, with no significant altitude effects. Airstart times were generally in the 50- to 60-sec range. JFS-assisted airstart times ranged from 40 sec to 65 sec.

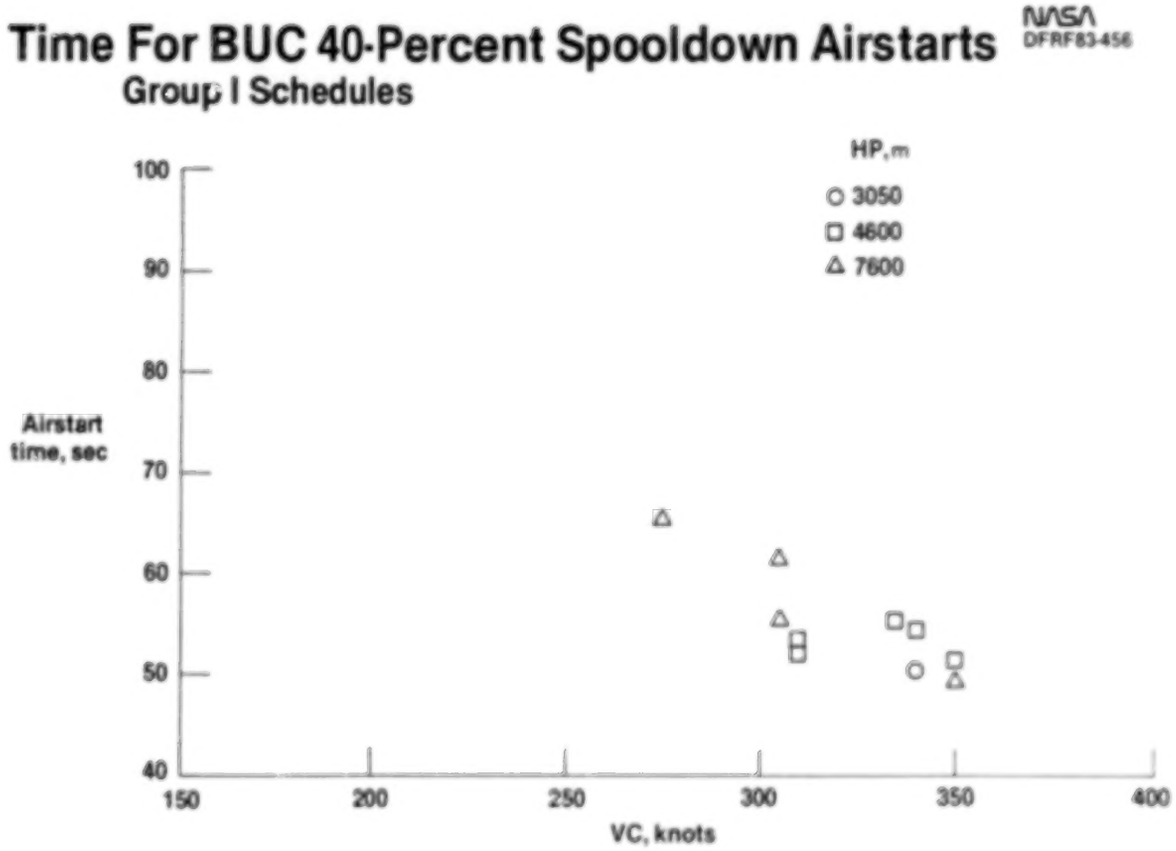

UNSUCCESSFUL BUC SPOOLDOWN AIRSTART

This figure presents a 40-percent spooldown airstart at 4600 meters and an airspeed of 280 knots. This case resulted in a stall rather than a successful airstart. The stall occurred 40 sec after pressurization at a rotor speed of approximately 38 percent, when the start bleeds closed and the RCVV released, effectively lowering the stall margin. This start was unsuccessful because the rotor acceleration was slower, due to the lower inlet pressure and fuel flow (WF).

In general, if N2 was less than 40 percent when the timer elapsed, stalls occurred.

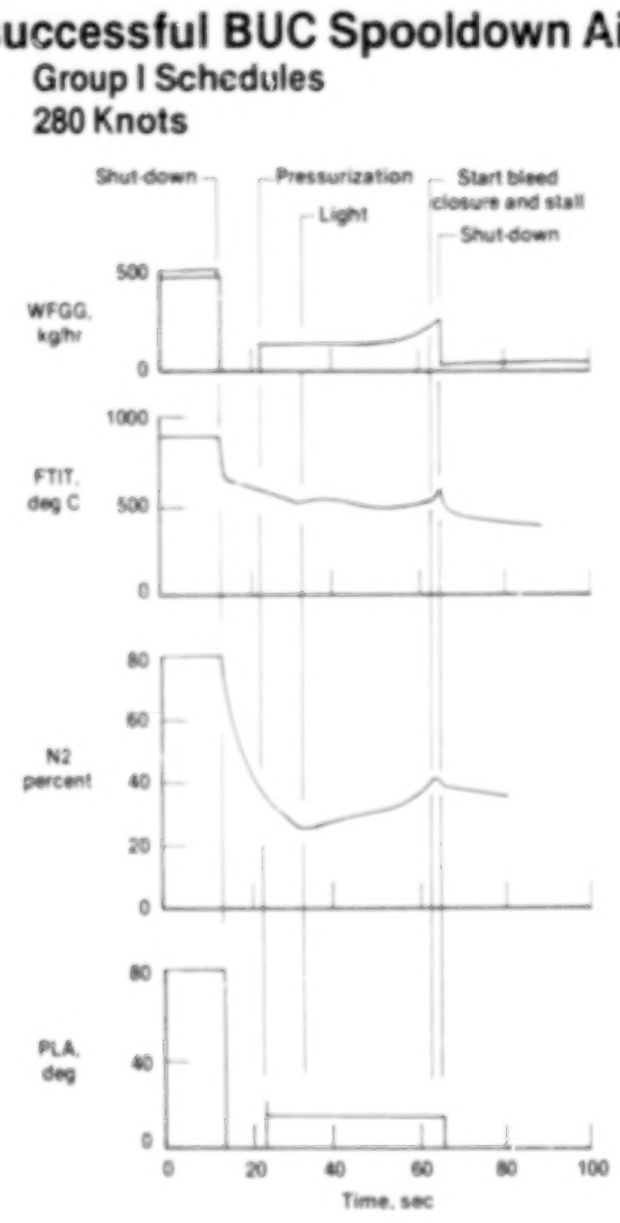

SUMMARY OF GROUP I BUC MODE AIRSTARTS

The group I flight summary chart shows that BUC mode spooldown airstarts below 300 knots, at any flight altitude, were unsuccessful except for a 40-percent spooldown airstart at 275 knots and 7600 meters. Also shown is a success line established during altitude facility testing at the Arnold Engineering Development Center (AEDC) (ref. 3). BUC mode airstarts were successful at airspeeds that were approximately 50 knots lower than in flight. However, there were no horsepower or bleed extractions during the altitude facility testing.

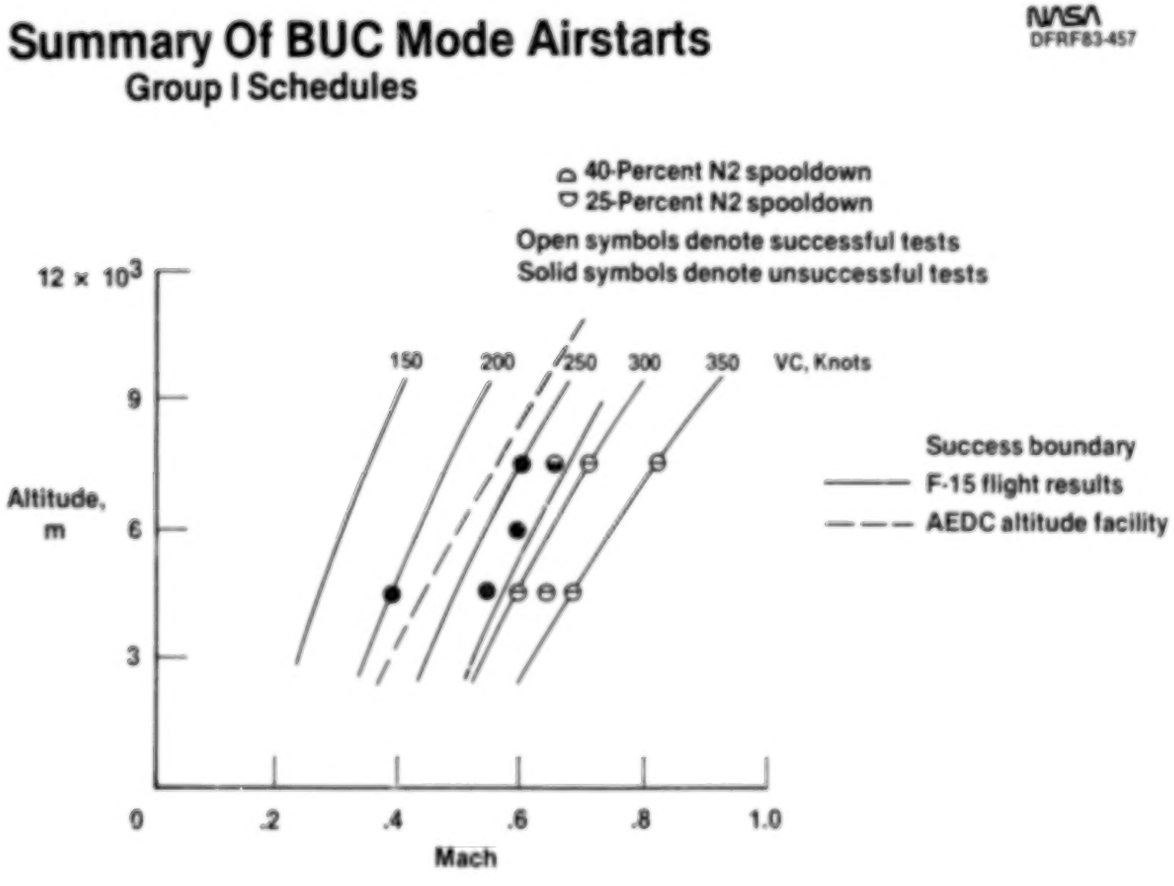

BUC SPOOLDOWN AIRSTART, 300 KNOTS
GROUP II

A spooldown airstart, using the group II schedule, was flown at similar flight conditions to one flown with the group I schedule. Even though the group I schedule provided a successful start at these conditions (300 knots and 6100 m) the group II schedule closed the start bleeds later, taking approximately 63 sec from pressurization to start bleed closure. This allowed N2 to accelerate to values in excess of 63 percent, a near-idle condition.

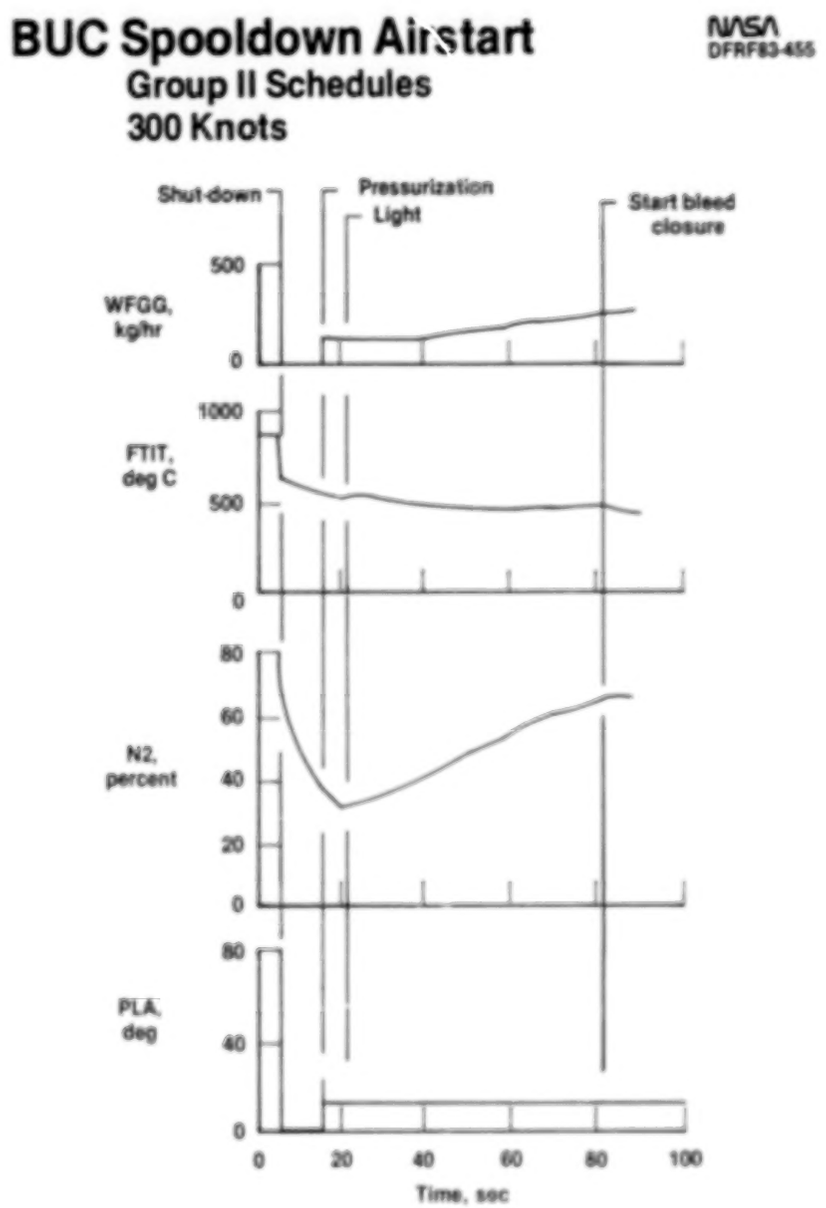

BUC SPOOLDOWN AIRSTART, 200 KNOTS
GROUP II

A spooldown airstart at 200 knots and 4600 meters, using the group II schedule, allowed a successful start where it would have been unsuccessful using the group I schedule. Although this start was termed successful, the idle N2 value was approximately 60 percent, which was lower than the desired idle speed of 65 percent. In this case, the pilot would have to advance the throttle slowly while accelerating the engine from 60 to 65 percent.

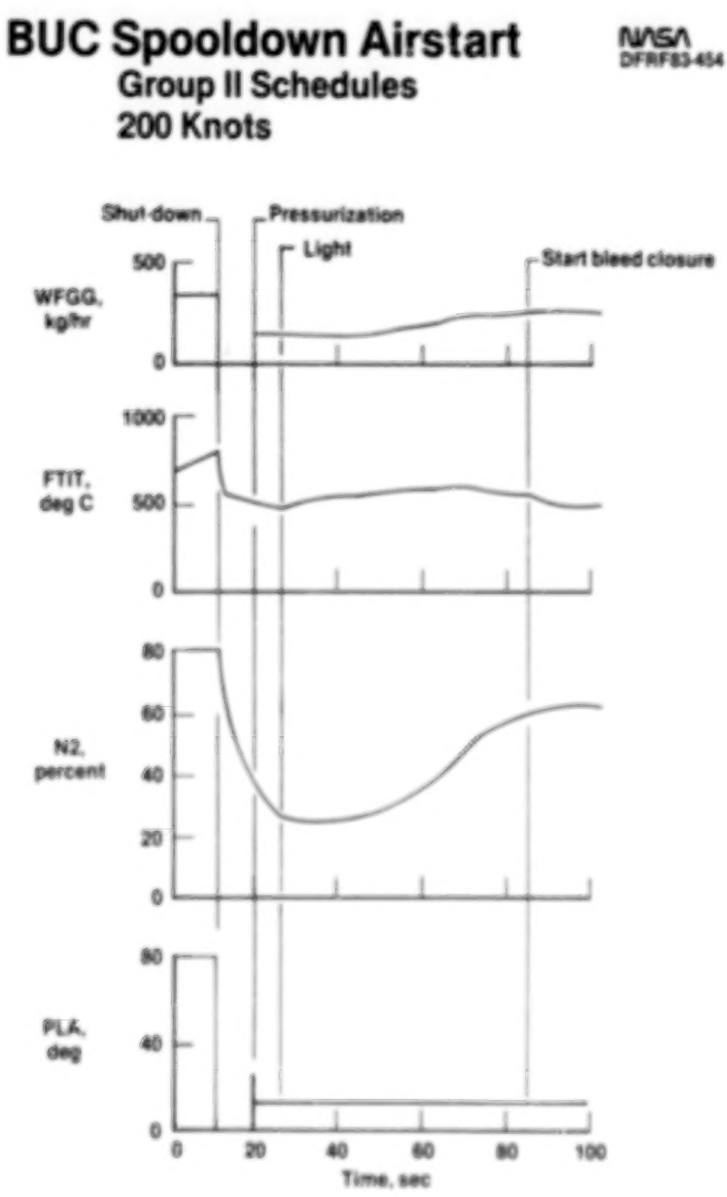

JFS-ASSISTED BUC AIRSTART

This time history of a JFS-assisted airstart shows the relatively rapid increase in N2 even at an airspeed as low as 150 knots. The airstart is termed successful, but the idle speed of 50 percent is much lower than desired.

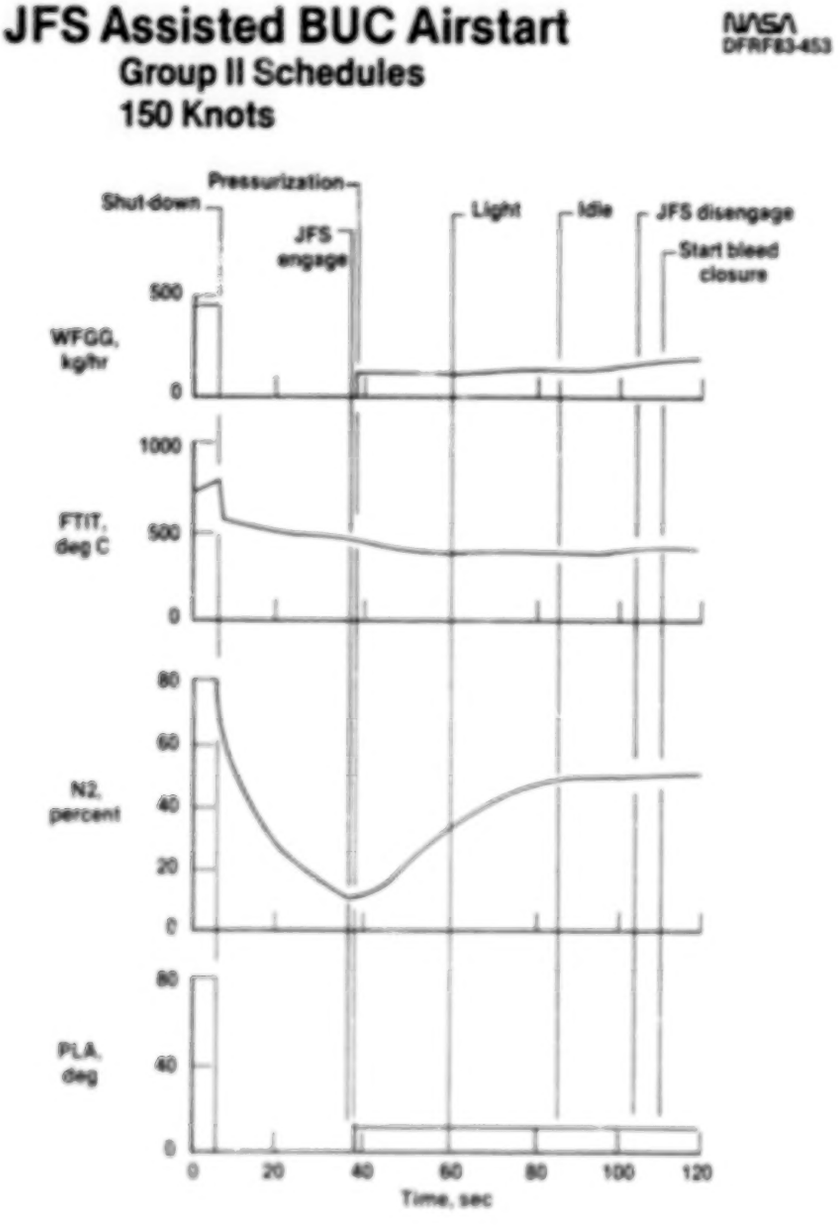

BUC SPOOLDOWN AIRSTART TIMES
GROUP II

For both 40- and 25-percent spooldown airstarts, the revision caused the airstart time to become more altitude-dependent rather than totally airspeed-dependent as evidenced with the group I start schedule. This is a result of biasing the time to start bleed closure by PS2. Also shown are airstarts in which the idle rpm was less than the desired 65 percent.

Time For BUC 40 Percent Spooldown Airstarts

NASA DFRF83-450

Group II Schedules

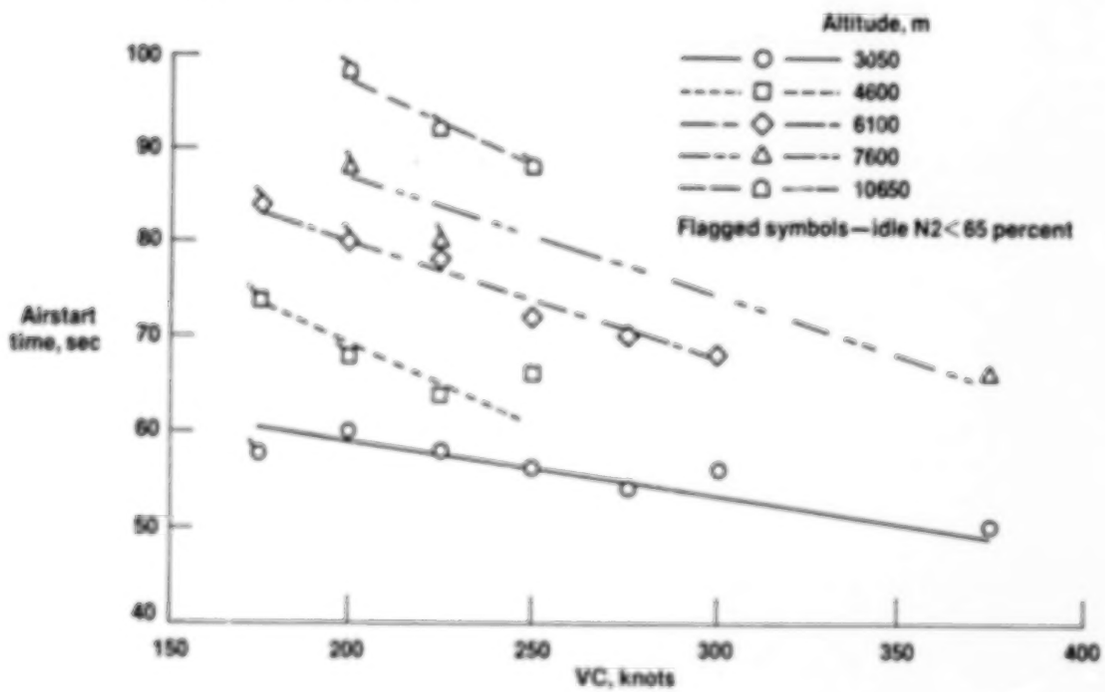

UNSUCCESSFUL BUC AIRSTART
GROUP II

This figure presents a time history of an unsuccessful 40-percent spooldown airstart at 175 knots and 7600 meters. In this case, the scheduled fuel flow was too low to accelerate the core to a sufficient speed before the bleeds closed. The result was a stall and the pilot shut down the engine.

Unsuccessful BUC Spooldown Airstart

NASA DFRF83-451

Group II Schedules
175 Knots

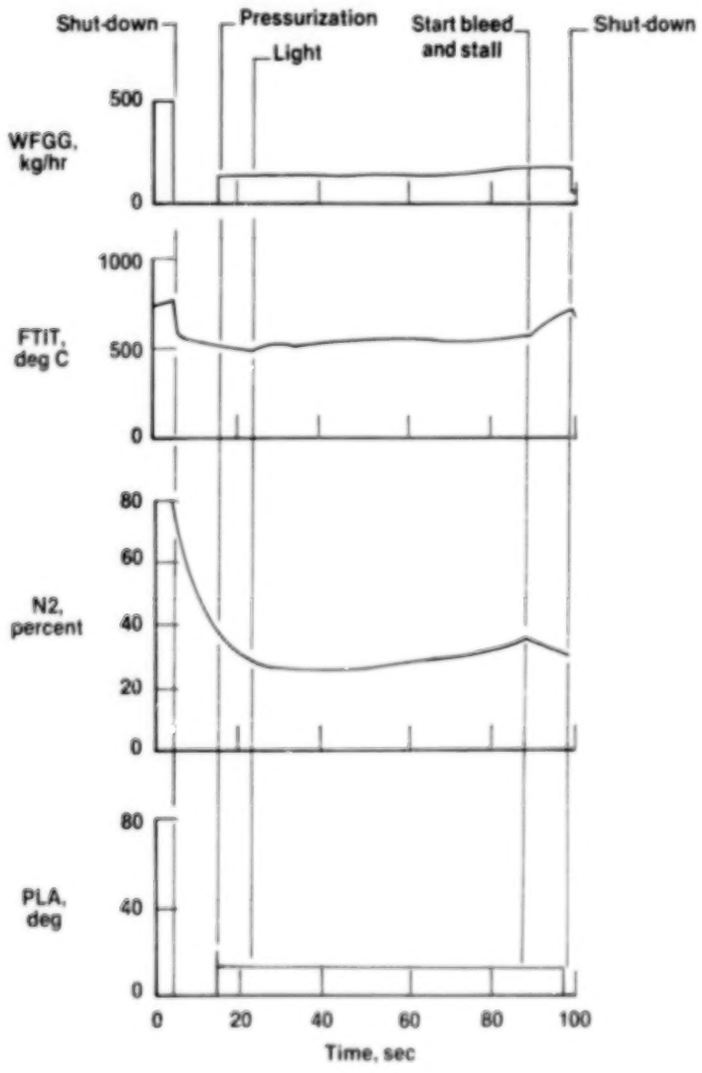

SUMMARY OF GROUP II BUC MODE AIRSTARTS

A summary of successful and unsuccessful 40- and 25-percent spooldown airstarts is shown in order to summarize the effectiveness of the group II start schedule. The solid line establishes a success boundary for these airstarts. All starts attempted above 225 knots were successful. Forty-percent spooldown airstarts were successful above 200 knots at all altitudes tested, and were successful at 175 knots below 6100 meters.

The success boundary established from the group I summary chart is indicated by the broken line and shows the improvement gained by revising the start schedule. Essentially, the revision decreased the airspeed required for a successful BUC mode airstart by approximately 75 knots.

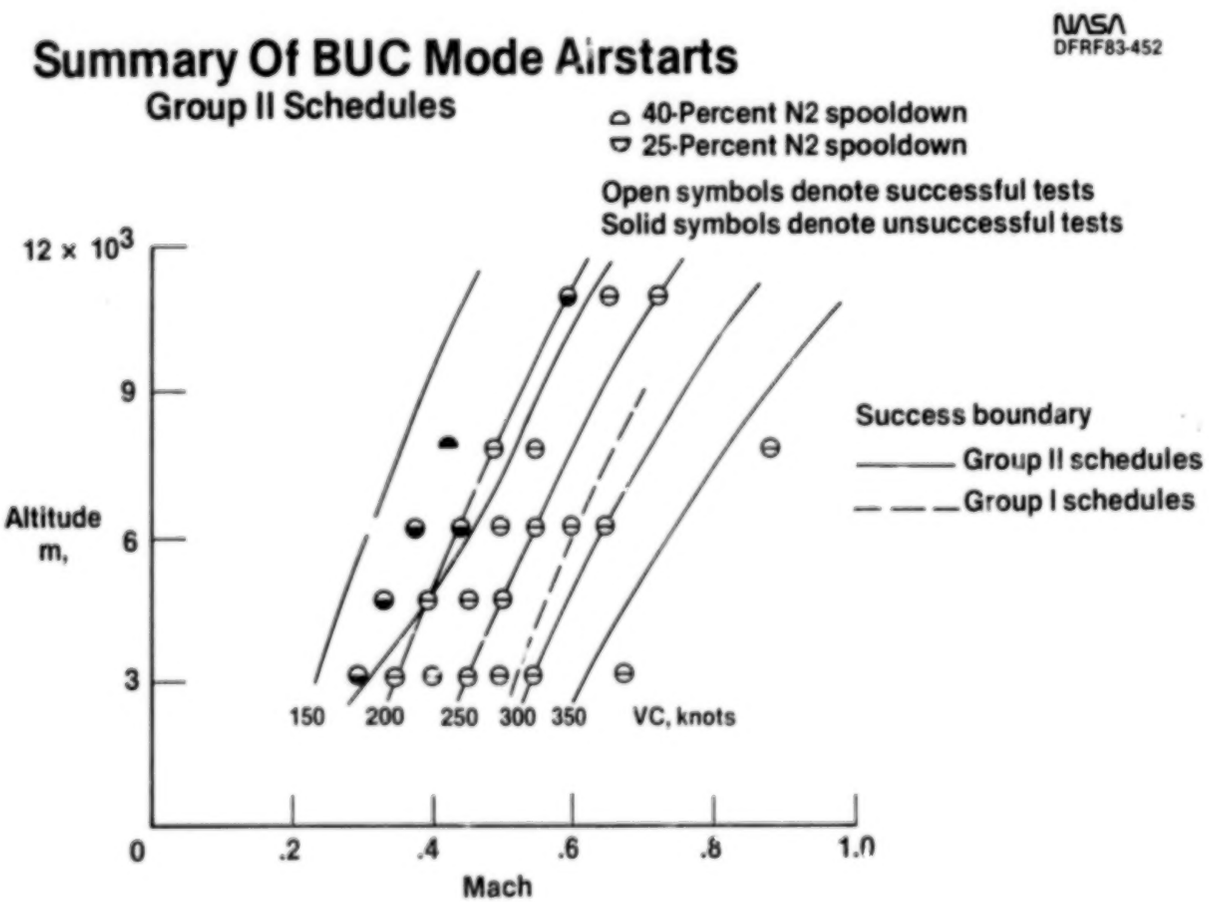

REFERENCES

1. Myers, Larry; Mackall, Karen; and Burcham, F. W., Jr.: Flight Test Result of a Digital Electronic Engine Control System in a F-15 Airplane. AIAA Paper 82-1080, June 1982.

2. Licata, S.; and Burcham, F. W. Jr., The Airstart Performance of a Digital Electronic Engine Control System on a F-15 Airplane. NASA TM-84908, 1983.

3. Ewen, J. S.; and Walter, W. A.: F100 Engine Model Derivative Program/Initial Engine Altitude Test Report. Pratt and Whitney Aircraft Report PWA FR-14785, July 1981.

N86
25353

UNCLAS

N86-25353

AUGMENTOR TRANSIENT CAPABILITY OF AN F100 ENGINE EQUIPPED WITH A DIGITAL ELECTRONIC ENGINE CONTROL

Frank W. Burcham Jr. and G. David Pai
NASA Ames Research Center
Dryden Flight Research Facility
Edwards, California

SUMMARY

An F100 augmented turbofan engine equipped with a digital electronic engine control (DEEC) system has recently completed a flight evaluation at thc NASA Ames Research Center's Dryden Flight Research Facility (DFRF). This engine was equipped with a specially modified augmentor to provide improved steady-state and transient augmentor capability, particularly in the upper left hand corner (ULHC) of the flight envelope where the standard F100 has limited capability. The combination of the DEEC and the modified augmentor was evaluated in sea level and altitude facility tests and then in four different flight phases in an F-15 airplane. This paper describes the augmentor configuration, logic, and test results. An overall description of the DEEC, the test engine, and the test procedures was presented in previous papers.

The augmentor of the F100 engine equipped with a DEEC system is shown below. It consists of a mixed-flow, fully variable, five-segment augmentor, which exhausts through a variable convergent-divergent nozzle. The augmentor incorporates five segments which start sequentially. Segments 1, 2, and 4 are located in the core stream, while segments 3 and 5 are located in the fan duct stream. The ignitor provides a stream of sparks into the segment 1 flameholder for augmentor ignition. The flameholder consists of radial and circumferential gutters to stabilize and propagate the flame.

F100 DEEC Augmentor

NASA
DFRF85-320a

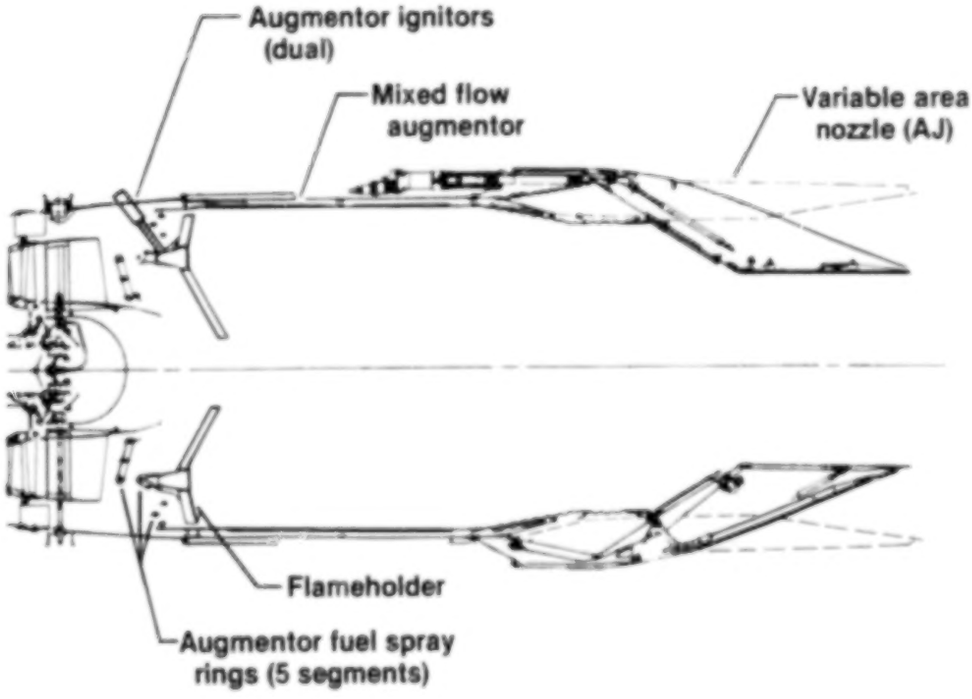

AUGMENTOR CONTROL HARDWARE

The augmentor control hardware is shown in the figure below. The DEEC controls the segment sequence valve, which handles the fuel distribution. Each of the five segments has a hydromechanical "quickfill" feature, in which a high fuel flow is supplied to rapidly fill the fuel manifold and spray ring. A quickfill sensor which determines when each segment is full by the rise in fuel pressure turns off quick-fill to that segment and transfers it to metered fuel flow, scheduled by the DEEC computer. Metered flow to segments 1, 2, and 4 is handled by the core fuel metering valve, while flow to segments 3 and 5 is handled by a separate duct fuel flow metering valve, as shown.

The primary nozzle is modulated ty the DEEC computer to maintain the desired engine pressure ratio.

Positions of the augmentor and nozzle actuators are measured by resolvers which are fed back to the DEEC. The torque motor drivers used in the actuators and the resolvers are not redundant for the augmentor.

DEEC Control System Block Diagram

NASA
DFRF83-319

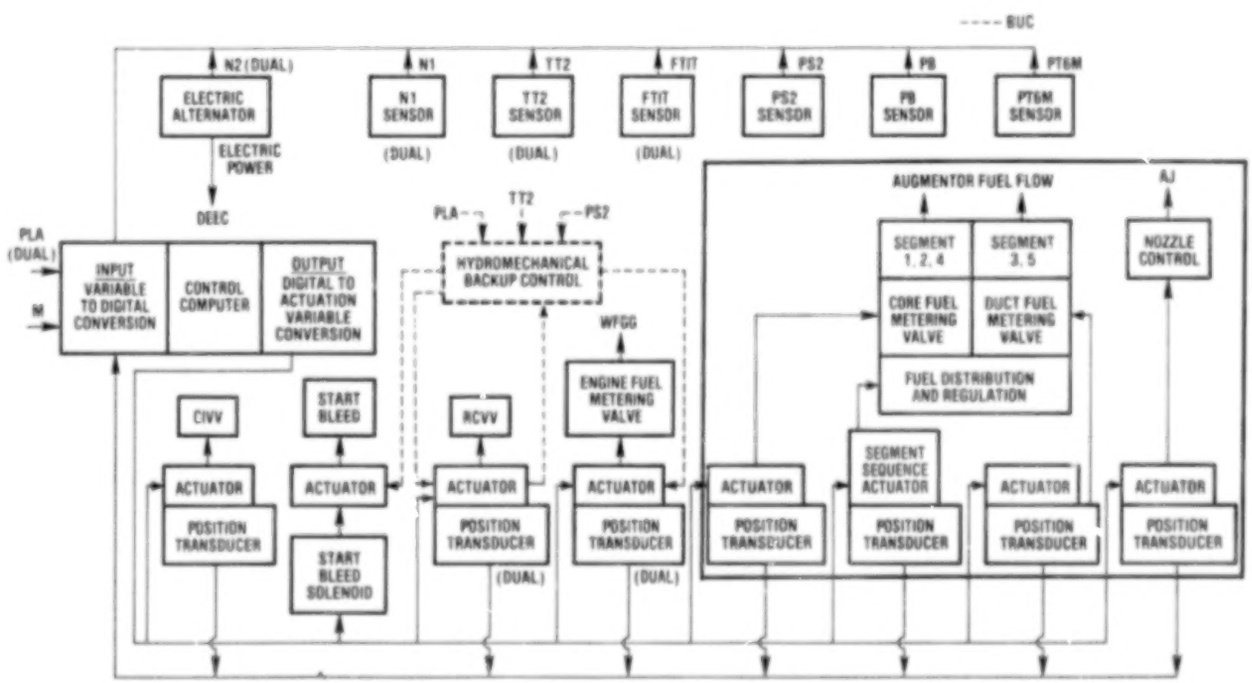

AUGMENTOR LOGIC

The DEEC logic consists of three basic sections - the fuel flow-scheduling logic, the sequencing logic, and the nozzle control logic.

Augmentor Fuel Flow Scheduling Logic

The DEEC control system provides improved logic for augmentor control over the standard F100 engine. Fuel-flow-scheduling logic is shown below. The total and core airflow computations are performed as shown. Core and duct stream fuel-air ratios are scheduled as a function of power level angle (PLA) biased by additional variables. Rumble and durability limits are also observed for the duct stream, while ignition and light-off limits are computed for the core stream. The computed duct and core fuel flow commands are sent to the augmentor control metering valves.

DEEC Fuel Flow Logic

NASA
DFRF83-322a

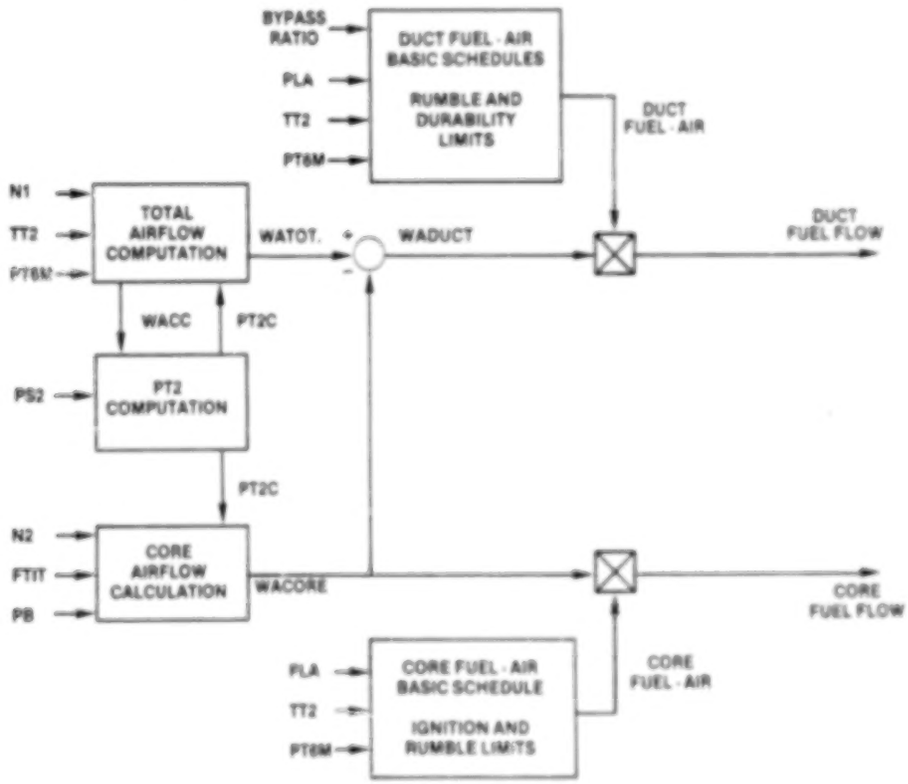

Augmentor Sequencing Logic

Augmentor sequencing logic is shown below. Prior to augmentor initiation, the augmentor permission requirements must be satisfied. Once these limits are met, the sequencing begins with segment 1 quickfill and augmentor ignition on. The augmentor rate limiting logic is used to slow the sequencing at lower values of calculated fan inlet total pressure (PT2C) where the possibility of stalls and blowouts is greater. The sequencing valve logic is a function of time and accepts signals from the fill sensor and light off detector (LOD), if installed. At lower values of PT2C, there are delays between segments 1 and 2 to allow the flame to stabilize.

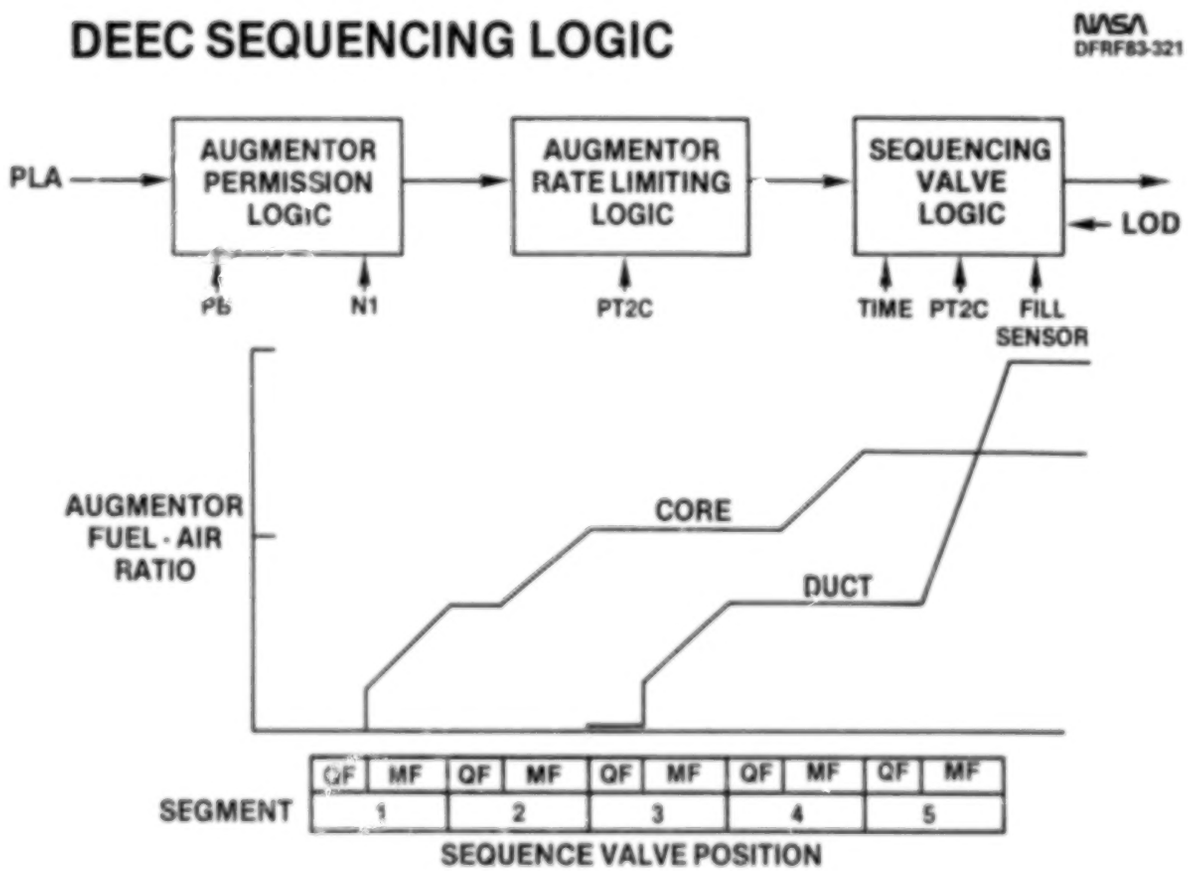

Nozzle Control

The DEEC system modulates the nozzle during augmentation to maintain the desired engine pressure ratio (EPR). A base jet primary nozzle area (AJ) schedule is generated, which is primarily a function of PLA-AB. The measured EPR, based on fan inlet static pressure (PS2) and turbine discharge total pressure (PT6M), is compared to the requested EPR, based on fan rotor speed (N1) and fan inlet total pressure (PT2). The error in EPR is multiplied by proportional and integral gains and the resulting nozzle trim signal is multiplied by the base AJ command to form the AJ request. The convergent exhaust nozzle control (CENC) drives the nozzle to the requested position. The dashed line encloses the parts of the nozzle control system that were modeled in a nozzle simulation, discussed in Paper 12.

DEEC EPR Control Mode

Nozzle Controls EPR

NASA
DFRF83-485

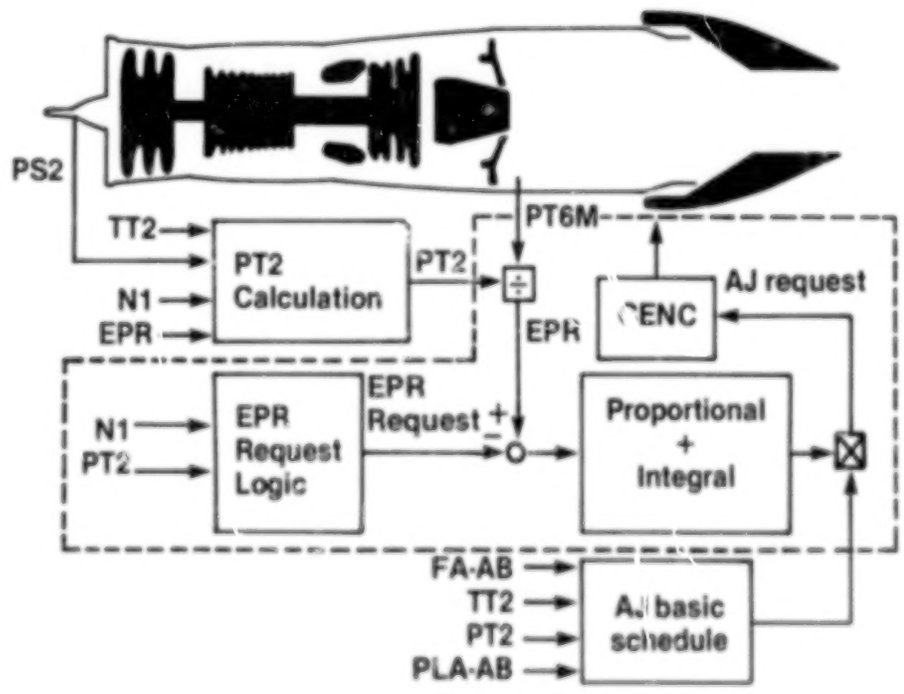

FLIGHT INSTRUMENTATION AND FUEL SYSTEM

The instrumentation that is pertinent to the augmentor is shown below. The pressure in each of the five augmentor fuel segments is measured with a close-coupled pressure transducer. A high-response pressure transducer is also used to measure augmentor static pressure (PAB). The nozzle area, AJ, is also measured. The DEEC data includes the augmentor fuel flow rates, position of the segment-sequence valve, light off detector output, and other data.

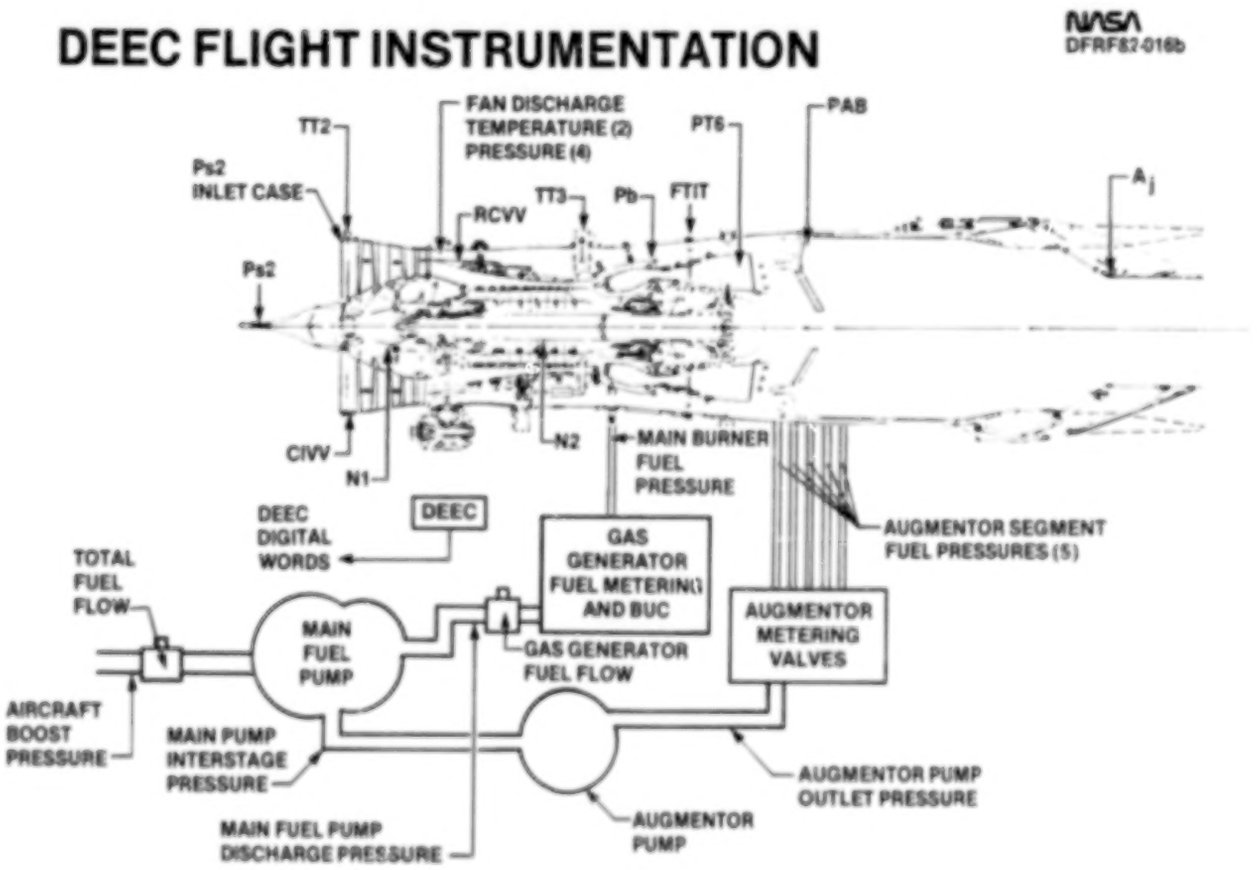

PHASE 2 AND 3 AUGMENTOR CONFIGURATION

Details of the phase 2 and 3 augmentor configuration are shown below. The spray rings had been specially tailored to provide good fuel distribution at the low segment pressures encountered in the upper left hand corner of the flight envelope. Dual ignitiors were installed, one in the normal location, and a second in an area of slightly leaner fuel-air ratios. A ducted core flameholder was used. It scooped a small amount of hot core flow and distributed it into the fan stream gutters to improve the augmentor stability.

In the upper left hand corner of the engine operating envelope, there was a segment 1 limiting feature in the DEEC software. This limited augmentor operation to maximum segment 1 fuel flow even if higher power settings had been requested. There was a switch in the cockpit that permitted the pilot to override the segment 1 limit for special tests. Also shown is the segment 5 redistribution line, above which the segment 5 fuel flow is redistributed into segment 3. This eliminated the very low segment 5 fuel pressures that occur when the segment 5 flows are reduced to prevent rumble in the upper left hand corner.

NASA
DFRF82-950

DEEC P063 AUGMENTOR CONFIGURATION PHASE 2 & 3

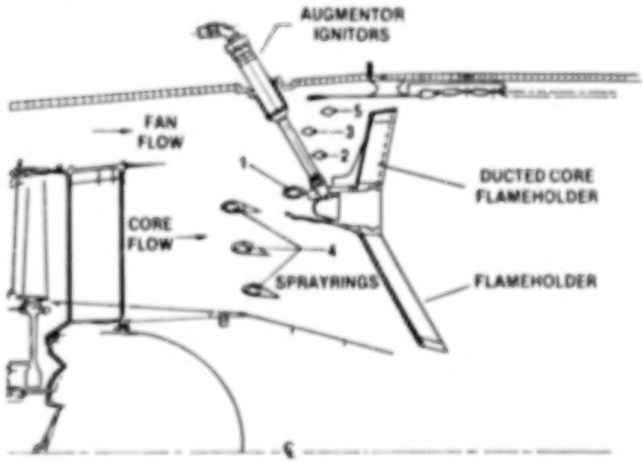

- TAILORED SPRAYRINGS
- DUAL IGNITORS
- DUCTED CORE FLAMEHOLDER
- SEGMENT 1 LIMITING—WITH OVERRIDE
- SEGMENT 5 REDISTRIBUTION

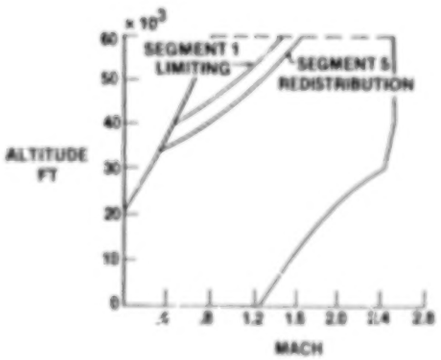

TYPICAL AUGMENTOR MILITARY-TO-MAXIMUM TRANSIENT

An example of a military-to-maximum power throttle transient is shown below. The parameters shown are time histories of AJ, PAB, and the augmentor segment pressures. At t = 3 sec, the throttle is snapped from military-to-maximum. Segment 1 quickfill begins immediately and the nozzle opens in anticipation of the light. The ignitors are also turned on. The quickfill ends and segment 1 metered flow begins at t = 3.4 sec. The light occurs as indicated by the increase in PAB. A short-hold occurs to allow the flame to stabilize prior to turning on segment 2 quickfill. A quickfill spike occurs as indicated by the rapid rise in segment 2 pressure and the effect is seen in PAB. There is a small quickfill spike in segment 3 but no effect is seen in PAB. At this flight condition, all five segments are used at maximum power. The nozzle modulates to maintain the desired EPR during the sequencing operation, and the transient is completed at t = 7 sec.

NASA
DFRF 82-347

MILITARY-MAXIMUM 175 KNOTS

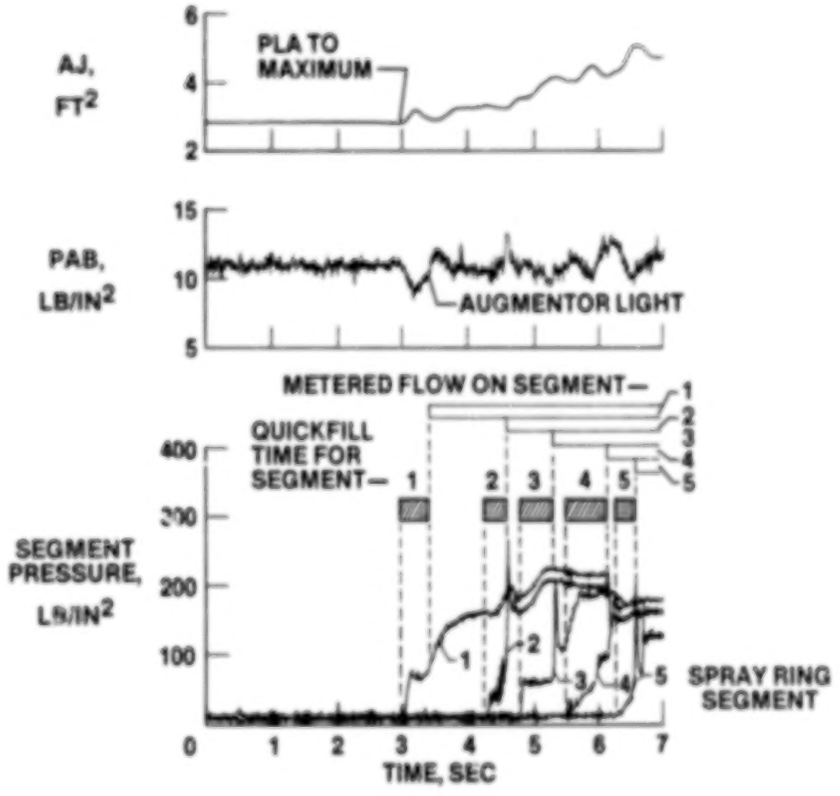

SUMMARY OF SEGMENT 1 LIMITED THROTTLE TRANSIENTS

The DEEC phase 2 military-to-maximum and idle-to-maximum throttle transients, with segment 1 limiting, are summarized below. All transients were successful at altitudes to 50,000 ft and airspeeds as low as 150 knots.

SEGMENT 1 LIMITING SUMMARY

NASA
DFRF82-367

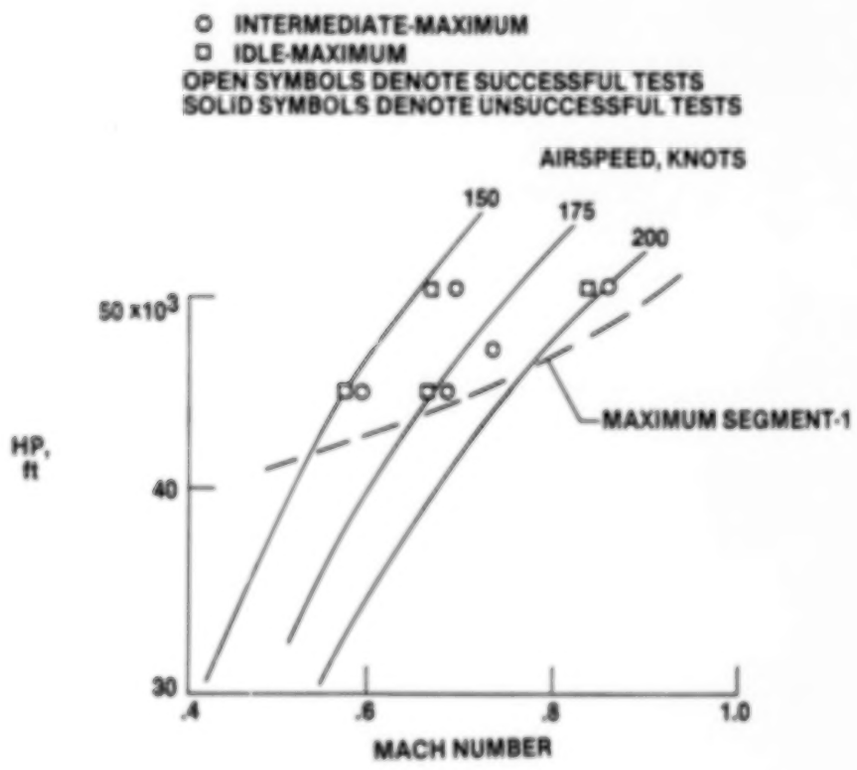

SUMMARY OF PHASE 2 MILITARY-TO-MAXIMUM TRANSIENTS

The phase 2 military-to-maximum throttle transients are summarized below. The segment 1 override switch in the cockpit was used to obtain full augmentor operation above the segment 1 limiting line. Stalls and blowouts occurred at airspeeds of 175 knots or less at altitudes of 40,000 ft and above. The stalls were due to quick-fill spikes and nozzle instabilities, while the blowouts were caused by nozzle instabilities and sequencing problems. Additional information on these problems will be discussed in later sections.

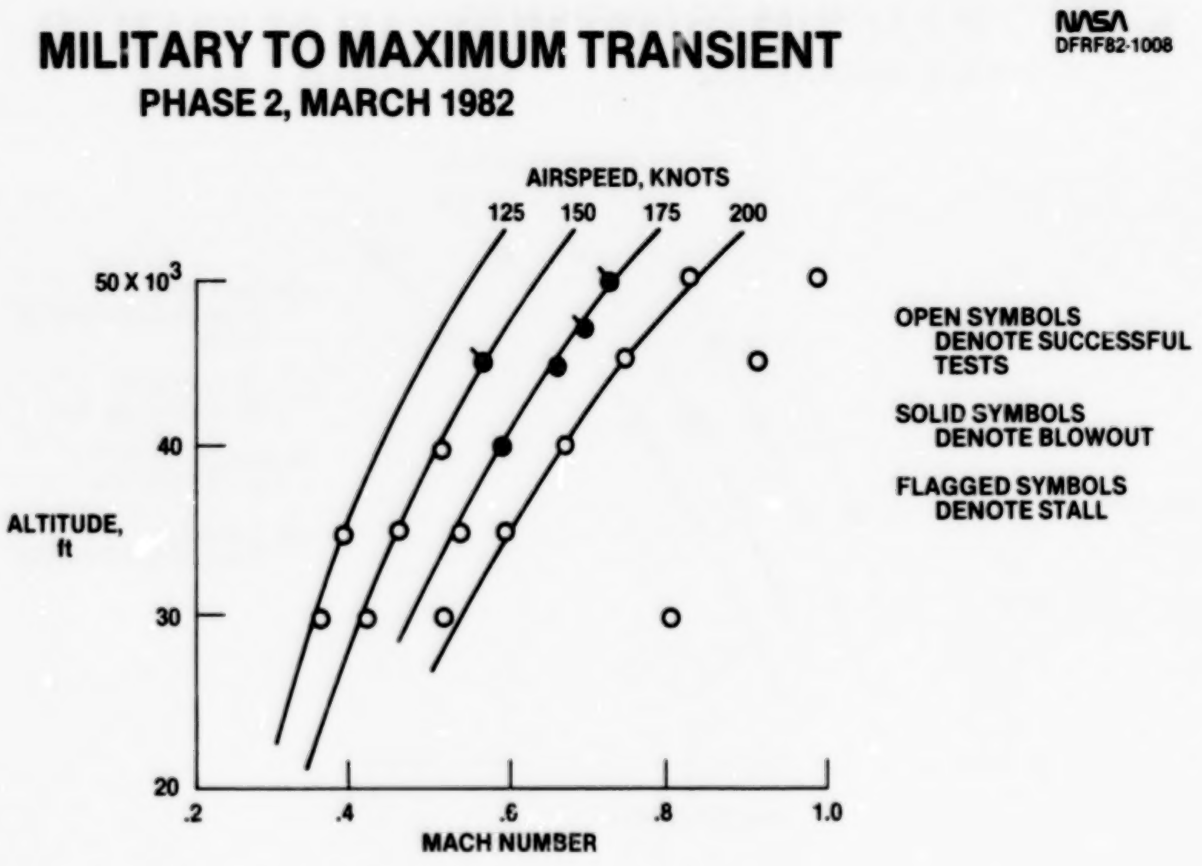

C-3

SUMMARY OF PHASE 2 IDLE-TO-MAXIMUM TRANSIENTS

The phase 2 idle-to-maximum transients are shown below. The segment 1 override switch was used to get full augmentor operation above the segment 1 limiting line. These transients were successful at 30,000 ft and airspeeds above 200 knots. Stalls, blowouts, and two nonrecoverable stalls (stagnations) occurred, as shown. These unsuccessful transients were caused by nozzle instabilities, quickfill spikes, rumble, and sequencing problems.

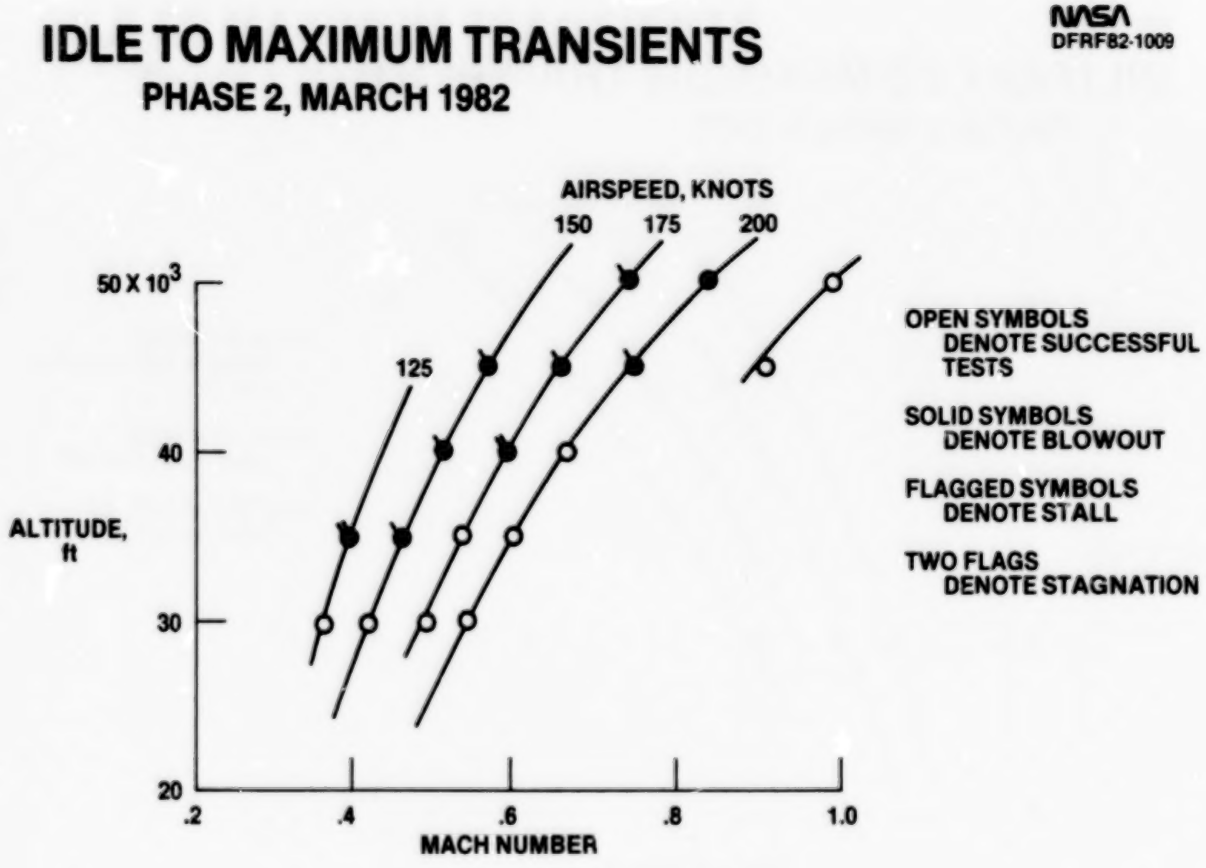

QUICKFILL STALL

An example of a stall caused by a quickfill spike is shown below. The segment 1 light is normal, but during the segment 2 quickfill, the pressure rises to 300 lb/in^2 causing excess fuel to enter the augmentor. When this fuel burns, the pressure pulse propagates upstream to the fan, and increases its pressure ratio above the stall line, resulting in a stall. Quickfill stalls occurred primarily in the upper left hand corner and mostly during segment 2 quickfill, although occasional segment 3 quickfill stalls were noted, and one segment 1 quickfill stall occurred in 994 augmentor lights.

QUICKFILL STALL 150 KNOTS

NASA
DFRF 82-348

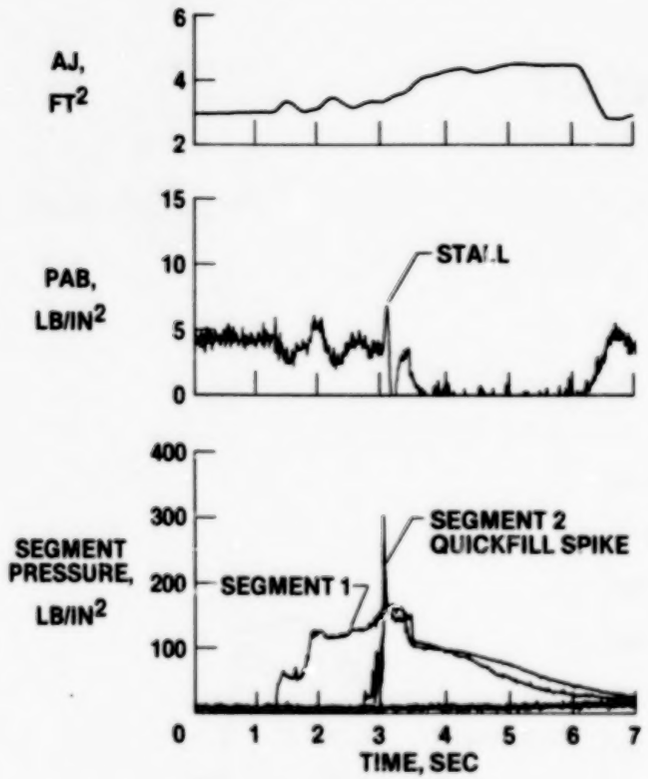

AUGMENTOR RUMBLE

Rumble is a moderate frequency (50 Hz to 60 Hz) oscillation caused by acoustic-combustion coupling phenomena. It generally results when a locally overrich fuel-air ratio occurs somewhere in the augmentor. The DEEC logic incorporates rumble protection features which reduce the fuel-air ratio in the upper left hand corner of the operating envelope. The logic was developed based on previous experience and on altitude tests of DEEC engines at Arnold Engineering Development Center (AEDC).

Shown below is a time history of an idle-to-maximum throttle transient at 175 knots and 45,000 ft. An augmentor blowout occurred at t = 7.2 sec. A detailed examination of the PAB trace at a sampling rate of 200/sec revealed that just prior to the blowout, a discrete 60 Hz oscillation had developed with an amplitude of 2 lb/in^2 peak to peak. This development of rumble coincides with the segment 4 fuel flow reaching its full scheduled flow. Rumble was detected in at least eight idle-to-maximum transients in the upper left hand corner. In each case this occurred just as segment 4 reached full flow. In a few cases, a few cycles of rumble were detected but blowout did not occur and stable operation was established.

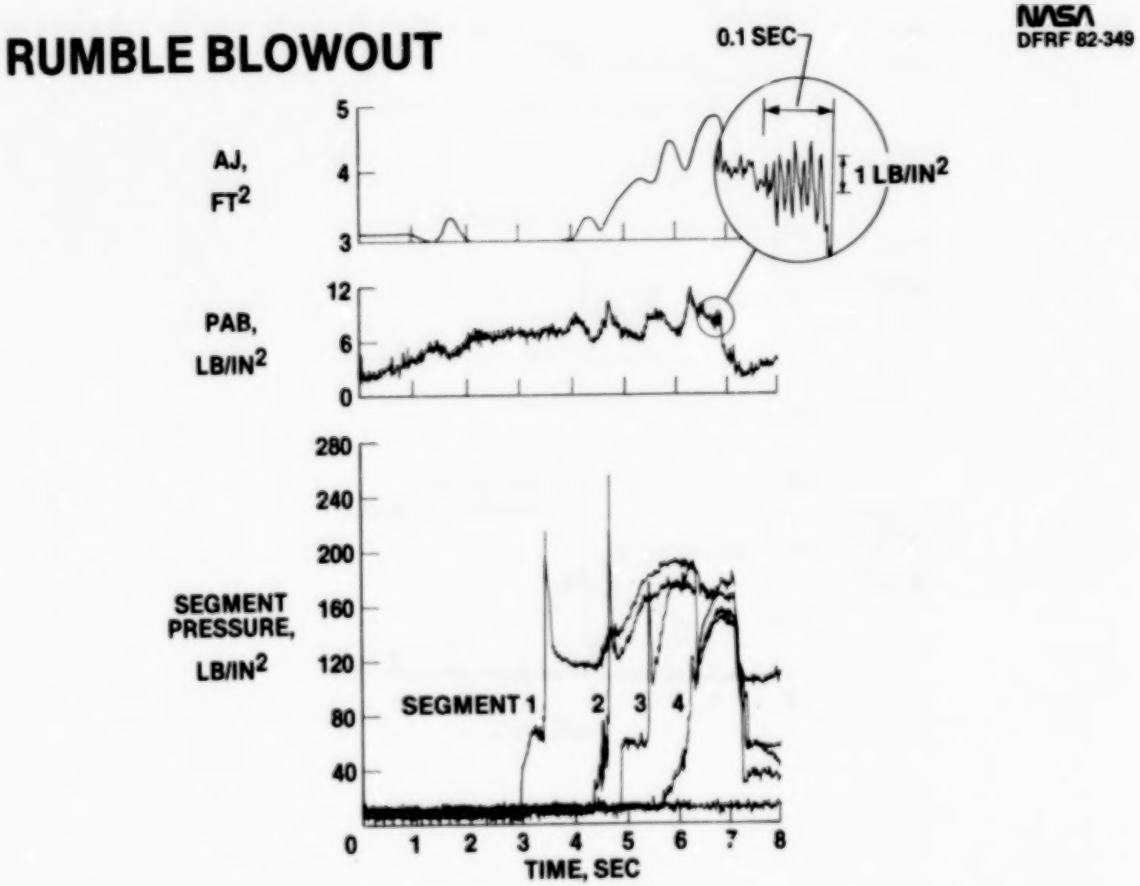

SEGMENT TRANSFER BLOWOUTS

Augmentor blowouts sometimes occurred during transfers from one segment to the next. A military-to-maximum snap at an altitude of 45,000 ft and 150 knots is shown below. At t = 6 sec, segment 4 quickfill has been completed. When segment 4 metered flow begins, the pressure in segments 1 and 2 drops, since these segments are all supplied by the core metering valve. The increase in PAB indicates that the core fuel flow has increased significantly during the transfer. The nozzle opens rapidly to lower the EPR and the rapid drop in pressure causes a blowout. Many of the blowouts in phase 2 occurred during this segment 3 to 4 transfer. Some stalls also occurred when the PAB increase was sufficient to stall the fan.

NASA
DFRF83-395

DEEC Augmentor Blowout - Phase 2

Following Segment 3 To 4 Transfer
45,000 Ft, 150 Knots

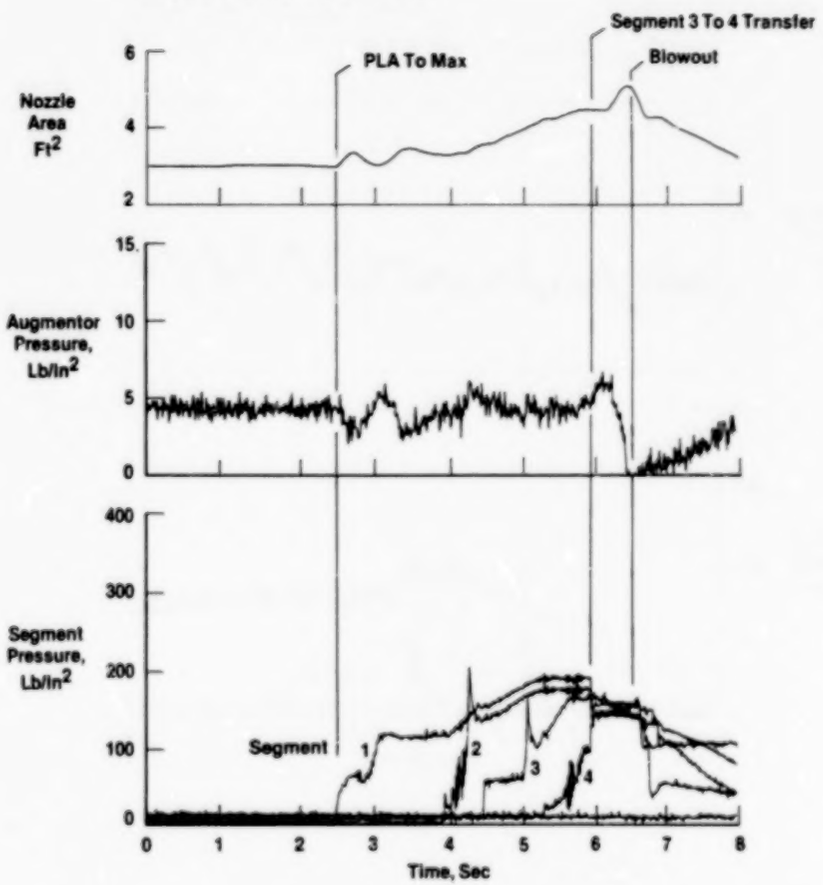

NOZZLE INSTABILITY

In the upper left hand corner of the operating envelope, the nozzle experienced an instability. As shown below, following a military-to-maximum snap, the nozzle began a limit cycle with PAB oscillations. On each cycle, positive peaks indicate when the engine approached a stall condition and negative valleys represent when the engine approached a blowout condition. This instability caused many problems during augmentor operation and is discussed in more detail in Paper 12.

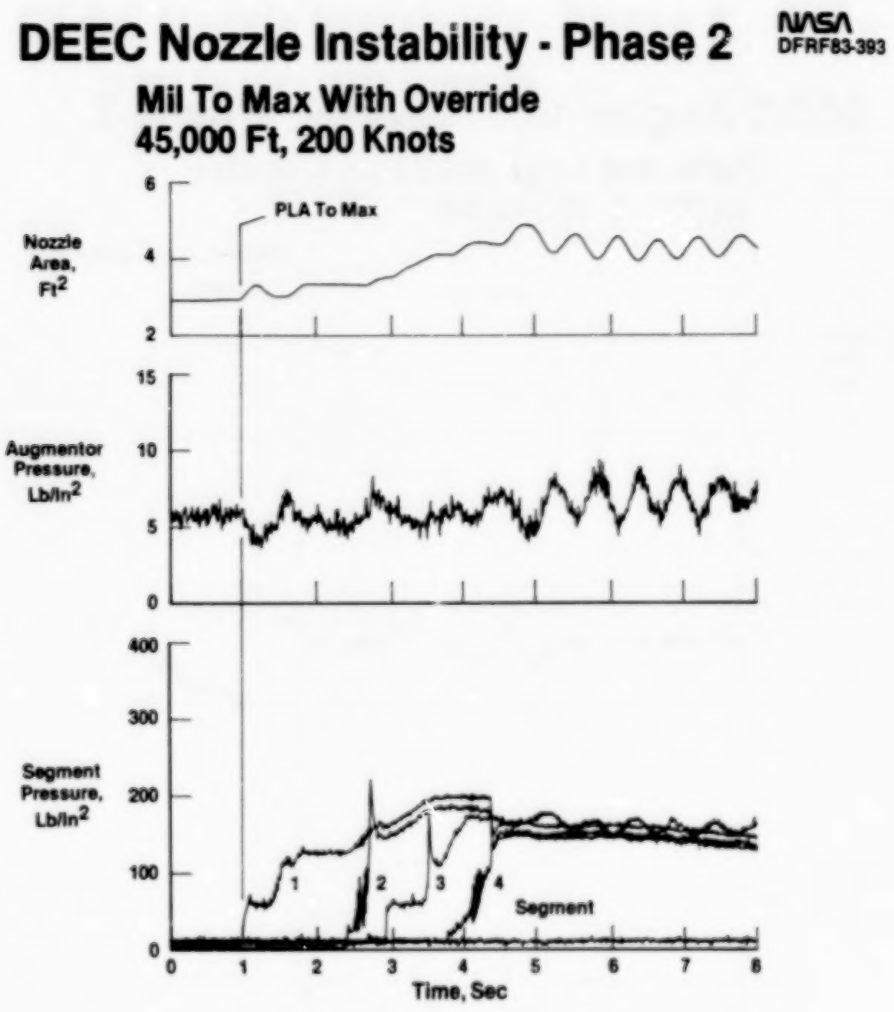

PHASE 2 RESULTS SUMMARY

At the end of phase 2 flight testing, the augmentor performance was strongly influenced by various factors. These were: blowouts due to rumble, stalls due to quickfill spikes, stalls and blowouts due to segment transfers, and stalls and blowouts due to nozzle instability. An additional cause of blowouts was the early augmentor permission that allowed augmentor lighting on idle-to-maximum snaps at fan speeds of 80 percent.

DEEC Status-End of Phase 2

NASA
DFRF83-484

- Blowouts due to rumble
- Stalls due to quickfill spikes
- Stalls and blowouts during segment transfers
- Stalls and blowouts due to nozzle instability
- Blowouts due to early augmentor permission

PHASE 3 OBJECTIVES

For phase 3, there were several changes to the augmentor logic and hardware to try to improve the augmentor performance. Logic changes were incorporated to eliminate rumble and augmentor instability. A quickfill sensor change was made to incorporate a sensor with better damping characteristics, called the damped quickfill sensor. In addition, it was desirable to replace the ducted core flameholder with the F100 production flameholder. In the phase 3 flight evaluation, these changes were made systematically to allow the individual effects to be determined.

DEEC PHASE 3 OBJECTIVES

NASA
DFRF82-946

- EVALUATE EFFECTS OF SOFTWARE AND HARDWARE CHANGES ON AUGMENTOR TRANSIENT PERFORMANCE
- EVALUATE SOFTWARE FIX FOR AUGMENTOR INSTABILITY

PHASE 3 MILITARY-TO-MAXIMUM TRANSIENT RESULTS

The first flights in phase 3 were made with the same hardware as phase 2, but with the new logic to eliminate rumble and nozzle instability. The results are shown below. In phase 3A, the improved logic successful transient line was moved up by as much as 5000 ft. No augmentor instability or rumble was noted. The addition of the damped quickfill sensor in phase 3B had no discernable effect on military-to-maximum transients. In phase 3C, the production flameholder seemed to be slightly better at Mach 0.6 at 45,000 ft. Other than blowouts at 50,000 ft, the augmentor performance was quite good.

NASA
DFRF82-36Sc

Military-To-Maximum Transient
Phase 3, October 1982

Open symbols denote successful tests
Solid symbols denote blowout

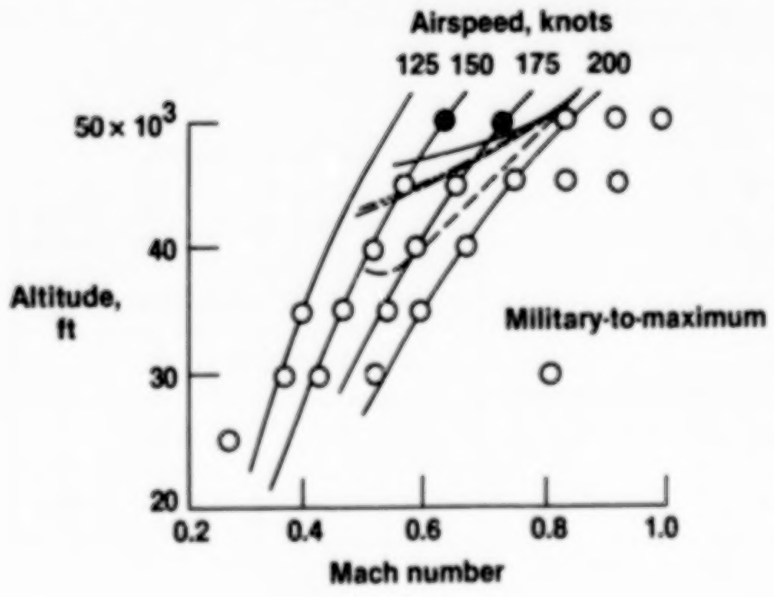

Success boundary

	Phase	Logic	Q/F sensor	Flame-holder
- - -	2	2.3.7A	Undamped	Ducted core
—·—	3a	2.3.7B	↓	↓
—··—	3b	↓	Damped	↓
———	3c	↓	↓	Prod.

PHASE 3 IDLE-TO-MAXIMUM TRANSIENTS RESULTS

The same changes for phase 3 were also evaluated for idle-to-maximum transients. The logic changes of phase 3A produced slight improvement, while the change to the damped quickfill sensor resulted in bigger improvements. The production flameholder had no apparent effect. Again, no rumble or nozzle instability was noted. The total altitude improvement was as much as 5000 ft. Due to the small number (eight) of flights in phase 3 and the statistical nature of augmentor transient success, these individual improvements should be viewed as indicating trends rather than absolute results. One problem that still remained on idle-to-maximum transients was early augmentor permission. The logic was permitting the augmentor to begin sequencing at fan speeds as low as 80 percent. This resulted in the lighting and sequencing taking place at considerably lower pressures and temperatures than on military-to-maximum snaps.

NASA
DFRF82-346c

Idle-To-Maximum Transients
Phase 3, October 1982

Open symbols denote successful tests
Solid symbols denote blowout
Flagged symbols denote stall

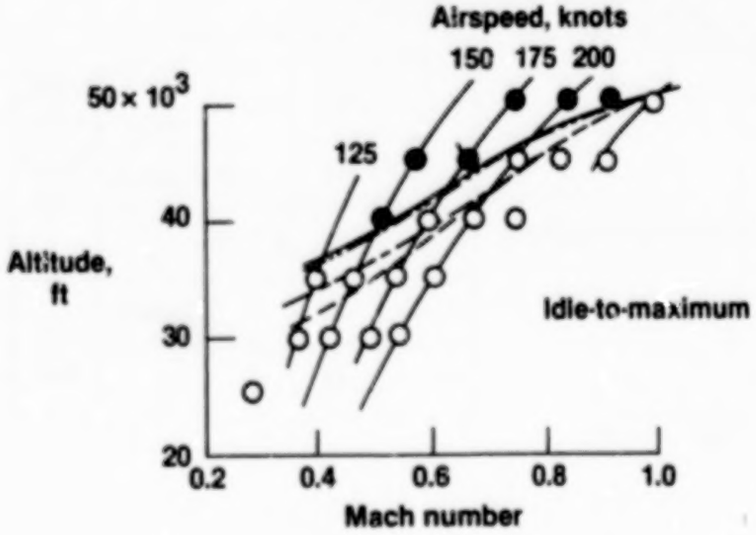

Success boundary

	Phase	Logic	Q/F sensor	Flame-holder
- - -	2	2.3.7A	Undamped	Ducted core
—·—	3a	2.3.7B	↓	↓
—··—	3b	↓	Damped	↓
———	3c	↓	↓	Prod.

PHASE 4 OBJECTIVES AND LOGIC CHANGES

For the phase 4 flight evaluation, the augmentor light off detector (LOD) was available. Logic changes were made to incorporate the LOD and to make further improvements based on previous results. The availability of the LOD made it practical to incorporate a fast acceleration capability in which, on idle-to-maximum throttle snaps, the augmentor lighting sequence took place during the gas generator spoolup. Also, because of the LOD, logic was installed to automatically recycle the DEEC power level angle (PLA) in case of augmentor blowout.

DEEC PHASE 4

NASA
DFRF82-955

- **AUGMENTOR IMPROVEMENTS**
  - **LIGHT OFF DETECTOR**
  - **LOGIC CHANGES**
- **FASTER THROTTLE TRANSIENTS**
  - **REDUCE IDLE TO MAX TIME FROM 7 TO 3.5 SEC**
  - **AUTOMATIC RELIGHT FOR AUGMENTOR BLOWOUTS**
- **BACKUP CONTROL IMPROVEMENTS**

PHASE 4 AUGMENTOR CONFIGURATION

The augmentor configuration for phase 4 is shown below. The LOD, an ultraviolet sensor, was installed so the flame just downstream of the flameholder could be viewed. It provided an output proportional to flame intensity to the DEEC. Also incorporated in phase 4 was the F100 production flameholder and a recalibrated segment 1 spray ring. The segment 1 limiting line and the segment 5 redistribution line were unchanged from phase 3. In the region shown, augmentor permission was available immediately on idle-to-maximum snaps. At lower airspeeds, the augmentor permission required higher fan speeds, and in the upper left hand corner, the fan speed for augmentor permission was raised to 98 percent of the intermediate fan speed request.

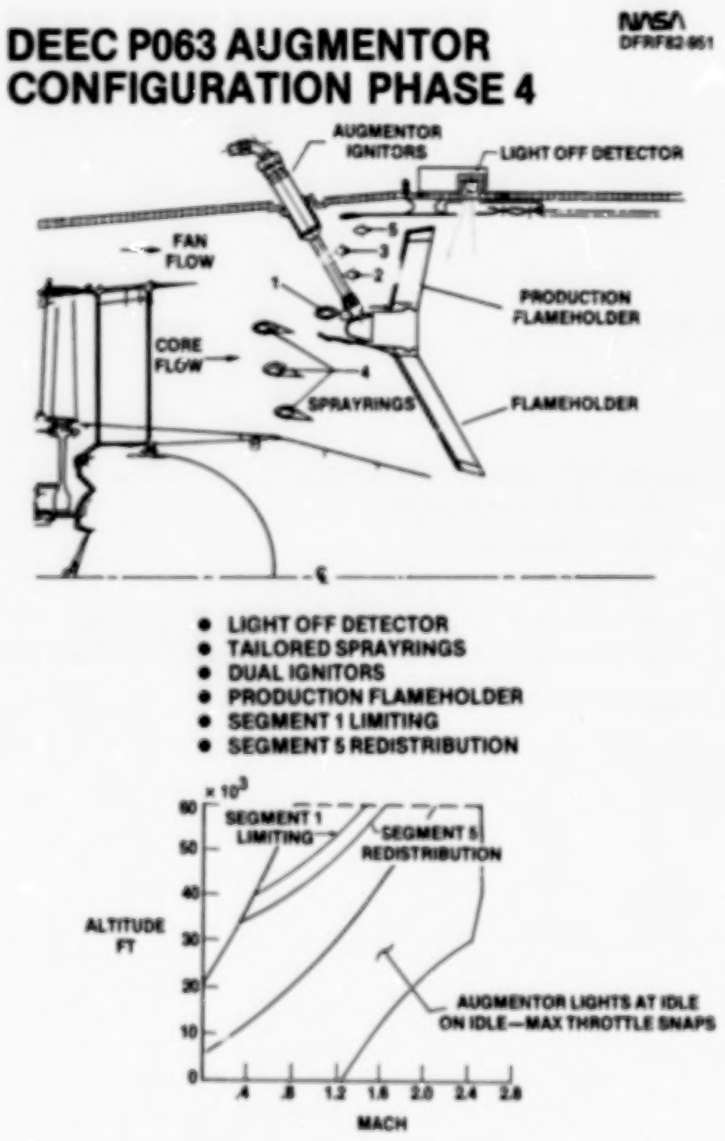

PHASE 4 SUMMARY OF MILITARY-TO-MAXIMUM TRANSIENTS

The DEEC phase 4 military-to-maximum transient summary is shown below. A large improvement over phase 3 is shown with successful transients at all conditions at 50,000 ft and below, even with the override to allow full augmentation. At altitudes above 50,000 ft one stall-stagnation occurred, but successful transients were completed up to 58,000 ft. This provided full augmentation capability almost to the edge of the F-15 flight envelope, as shown. Some PLA recycles were required to complete the transients at 50,000 ft and above.

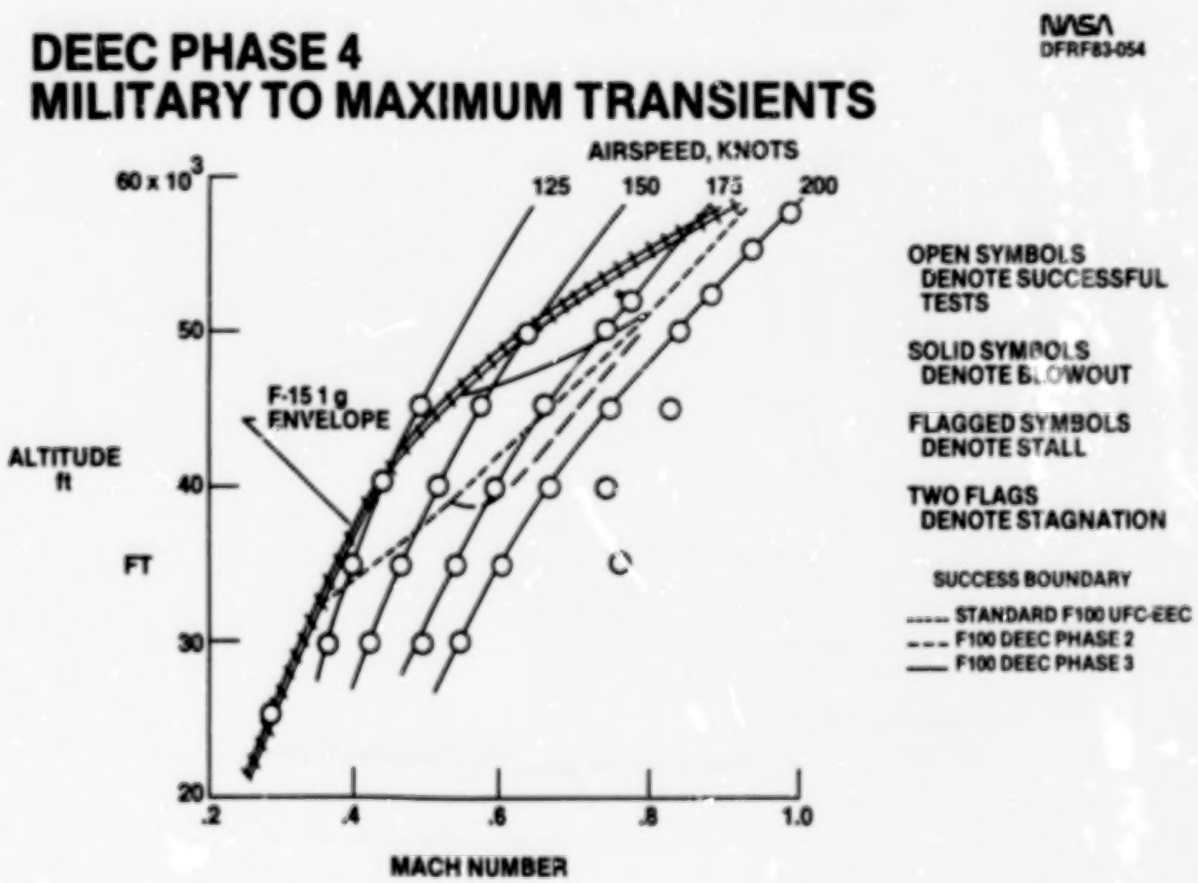

PHASE 4 MILITARY-TO-MAXIMUM TRANSIENT

An example of a military-to-maximum snap at 45,000 ft and 125 knots is shown below to illustrate the performance of the LOD. Following the snap to maximum power segment 1 fuel flow is turned on and the light occurs almost immediately, as indicated by the rise in LOD counts. The light is also seen on PAB. The logic requires a 1.25 sec hold in segment 1 to allow the flame to stabilize, and then allows the sequencing to continue. Once segment 3 is lit, the LOD counts drop off as the flame pattern shifts. At maximum power, a slight nozzle oscillation causes the flame pattern to shift back and forth, as seen in the LOD output.

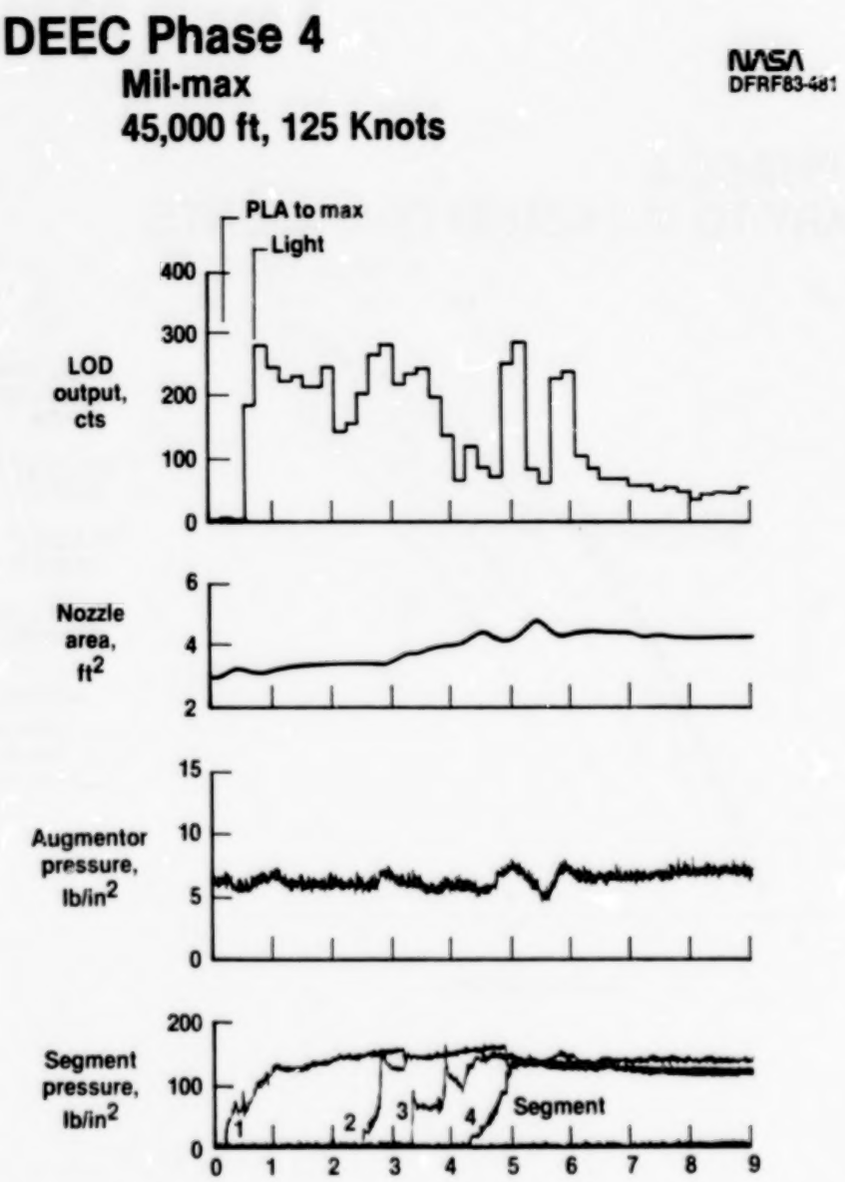

PLA RECYCLE

An example of the LOD performance and logic action following a blowout is shown below at 50,000 ft and 175 knots. Following the snap to maximum, segment 1 quickfill begins and the light is detected. During the segment 1 hold, the LOD counts drop to less than 40, indicating a weak flame. Segment 2 flow increases the LOD output only briefly, and by the segment 4 turn-on, the LOD output falls to 0. Augmentor fuel is shut off and the DEEC PLA is cycled back to intermediate to begin a recycle. The LOD goes through a self-test cycle, as shown, to verify proper operation prior to the attempted relight. Note the much higher LOD counts in segment 1 on the recycle. The rest of the light is normal. Up to three PLA recycles are allowed by the DEEC logic; however, no more than two were ever required in phase 4 testing.

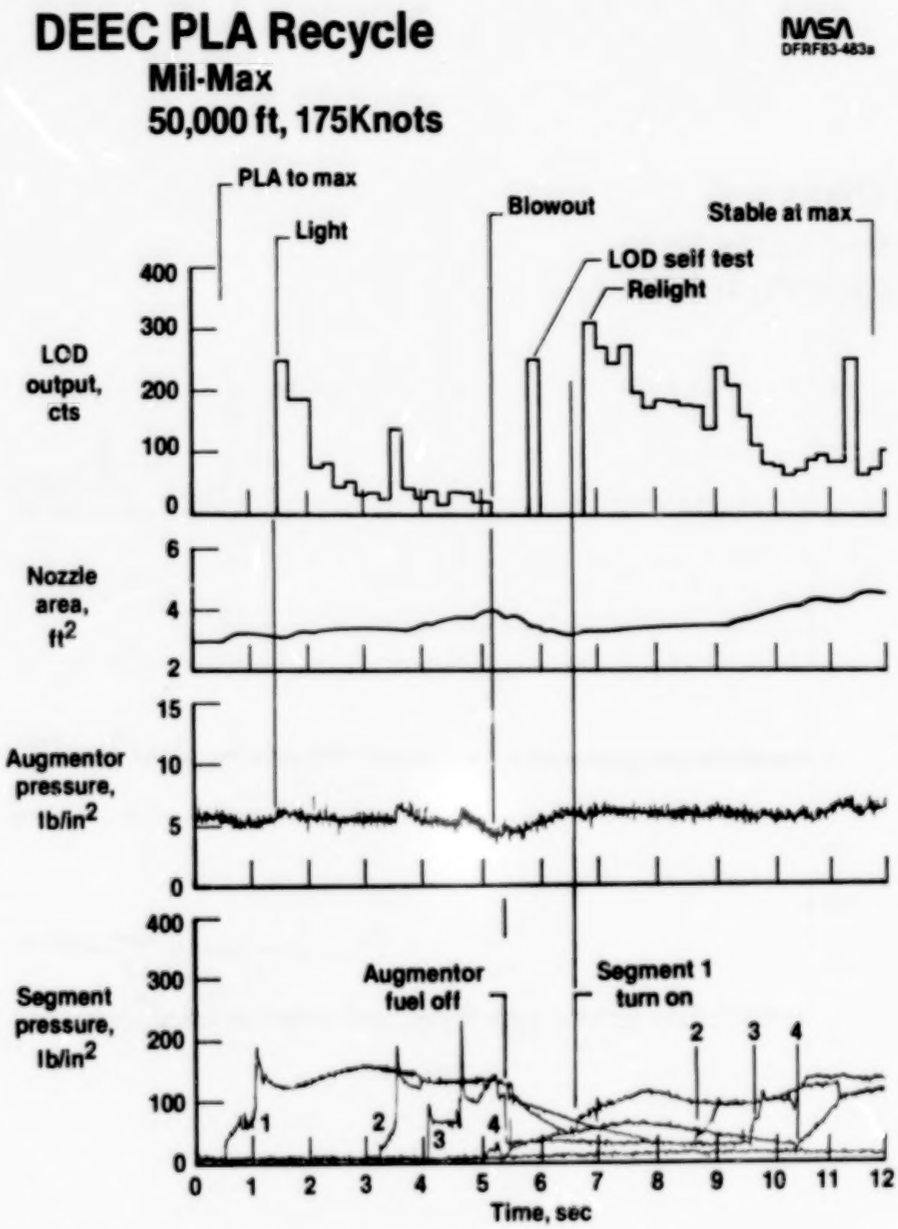

PHASE 4 IDLE-TO-MAXIMUM TRANSIENT

An idle-to-maximum snap transient at 50,000 ft and 150 knots, with the override switch on, is shown below. The PLA was advanced to maximum at t = 1.5 sec. Augmentor permission was delayed at this flight condition until the fan speed reached 98 percent of its request, which, in this case, took 5.5 sec. Augmentor quickfill began at t = 7 sec, and the light was detected at t = 8 sec. After the 1.25 sec segment 1 hold, the logic released the sequencing and maximum power was achieved at t = 12 sec. The segment 3 to 4 transfer caused an overfill that increased PAB, but no stall occurred. There was some nozzle oscillation which damped out quickly. The effect of the delayed augmentor permission is to make the idle-to-maximum transient very similar to a military-to-maximum transient, with hot core flow and higher pressure levels in the augmentor prior to augmentor sequencing.

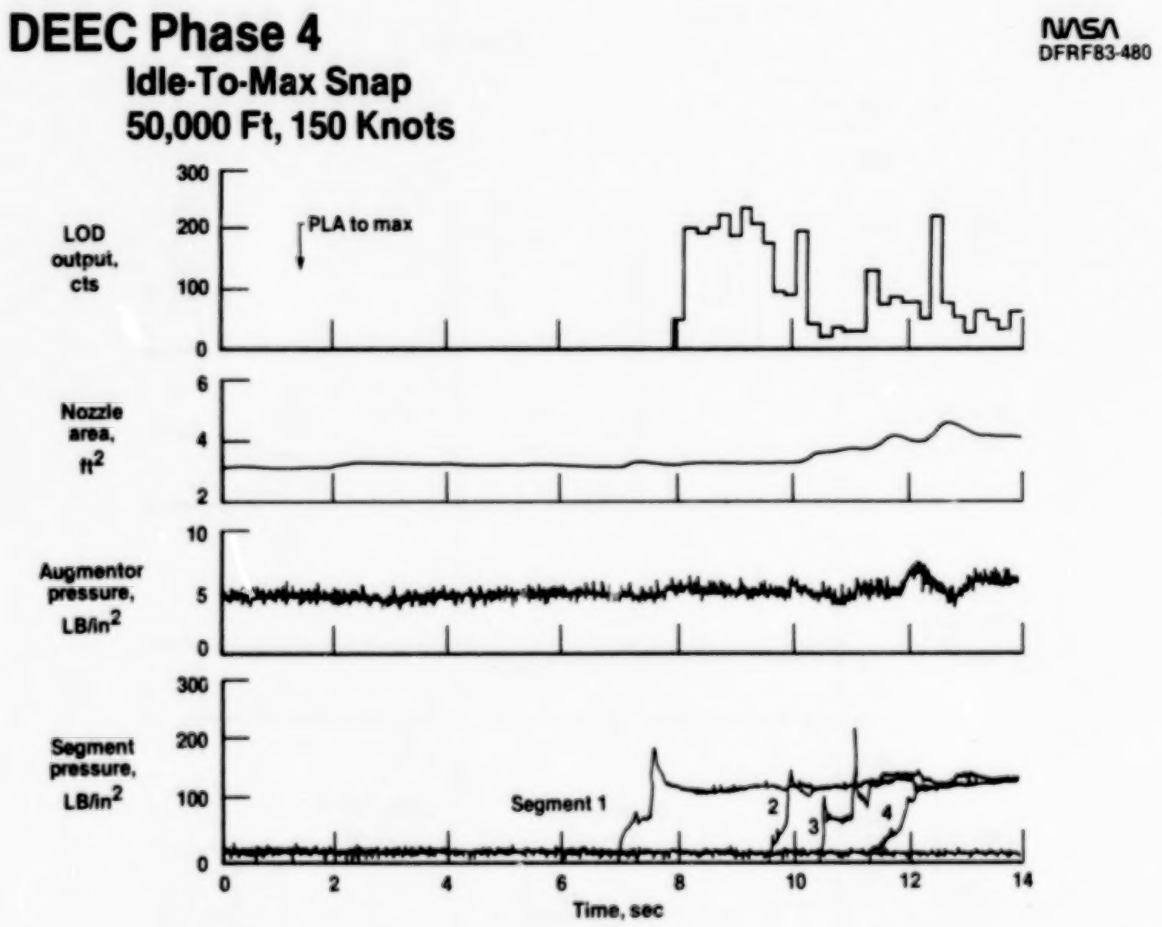

SUMMARY OF PHASE 4 IDLE-TO-MAXIMUM TRANSIENTS

A summary of the DEEC phase 4 idle-to-maximum power transients is shown below. Most of these transient tests were made with the augmentor override switch, since they would otherwise have been limited to segment 1. All transients were successful, including tests at altitudes up to 58,000 ft and airspeeds of 125 knots at 45,000 ft. Some PLA recycles were required at the higher altitudes. As is seen, the test conditions extended to the 1 g flight envelope of the F-15. No stalls occurred, and no more than two PLA recycles were required. Factors contributing to the large improvement in success, compared to previous phases, included the LOD, the segment 1 hold logic, and the revised augmentor permission logic, as will be shown later.

NASA
DFRF83-053

DEEC PHASE 4
IDLE TO MAXIMUM TRANSIENTS

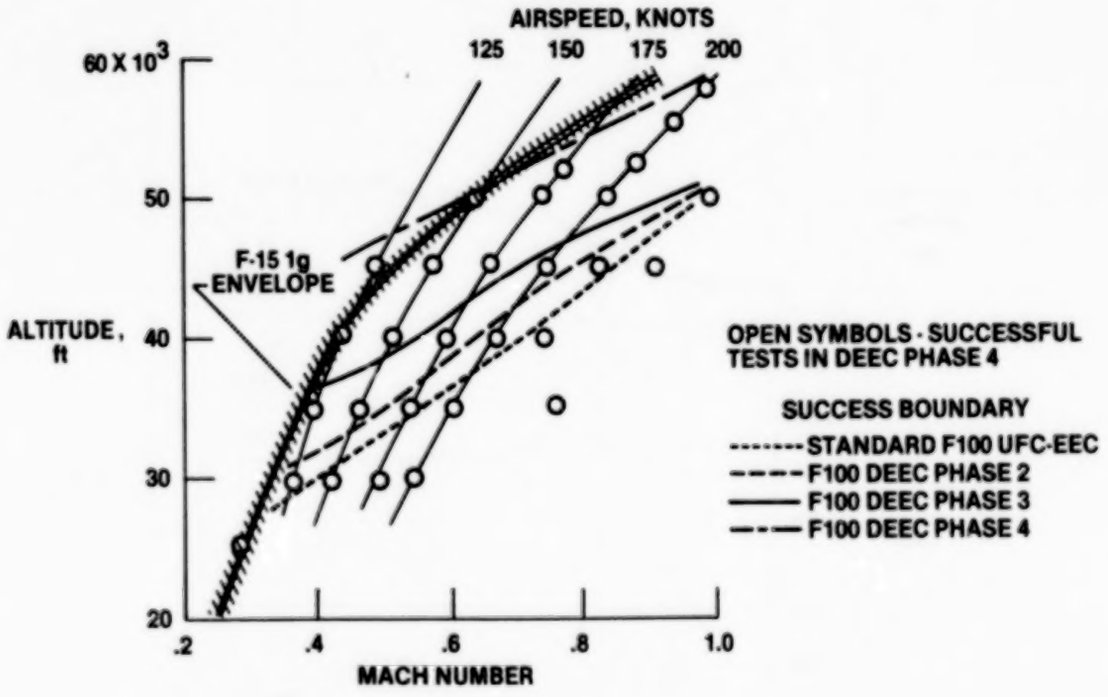

FAST ACCELERATION

The phase 4 DEEC logic had the capability to allow the augmentor sequencing to begin immediately on idle-to-maximum snaps at low altitude-high airspeed conditions. An example is shown below, at 21,000 ft and 400 knots. Following the snap from idle-to-maximum at t = 0 sec, the gas generator spoolup and augmentor sequencing began. Segment 1 quickfill began at t = 0.2 sec. The light occurred at t = 1 sec. The logic held the sequence valve in segment 1 until 80 percent of the requested fan speed was achieved and then allowed the remaining segments to sequence normally. The entire transient was completed within 4.5 sec. Without the fast acceleration logic, this transient would have taken almost 7 seconds. The fast acceleration logic is inhibited following a bodie and is gradually washed out in the region above the line shown in the phase 4 augmentor configuration chart.

DEEC Phase 4 "Fast Accel"

Idle-To-Max Snap
21,000 Ft, 400 Knots

NASA
DFRF83-482

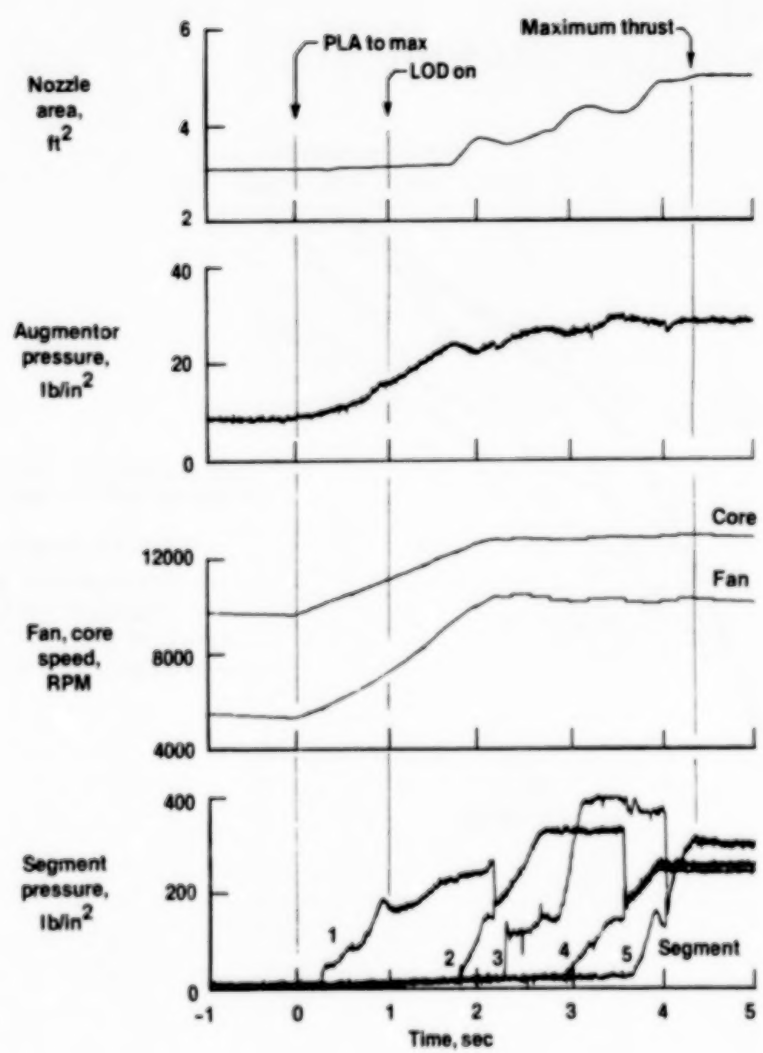

SUMMARY OF AUGMENTOR IMPROVEMENTS

The chart below summarizes the improvement in augmentor performance between the standard F100 engine and the DEEC phase 4 results. With the addition of the DEEC logic, LOD, damped quickfill sensor, automatic PLA recycle, and tailored spray rings, all idle-to-maximum transients were successful, even with the segment 1 limiting override on. This increase in altitude capability was as much as 15,000 ft. Additional tests will be required to verify that this improvement will be realized on all DEEC-equipped engines over a range of test altitudes, airspeeds, and temperatures.

NASA
DFRF83-053a

F-15/DEEC
IDLE TO MAXIMUM TRANSIENTS

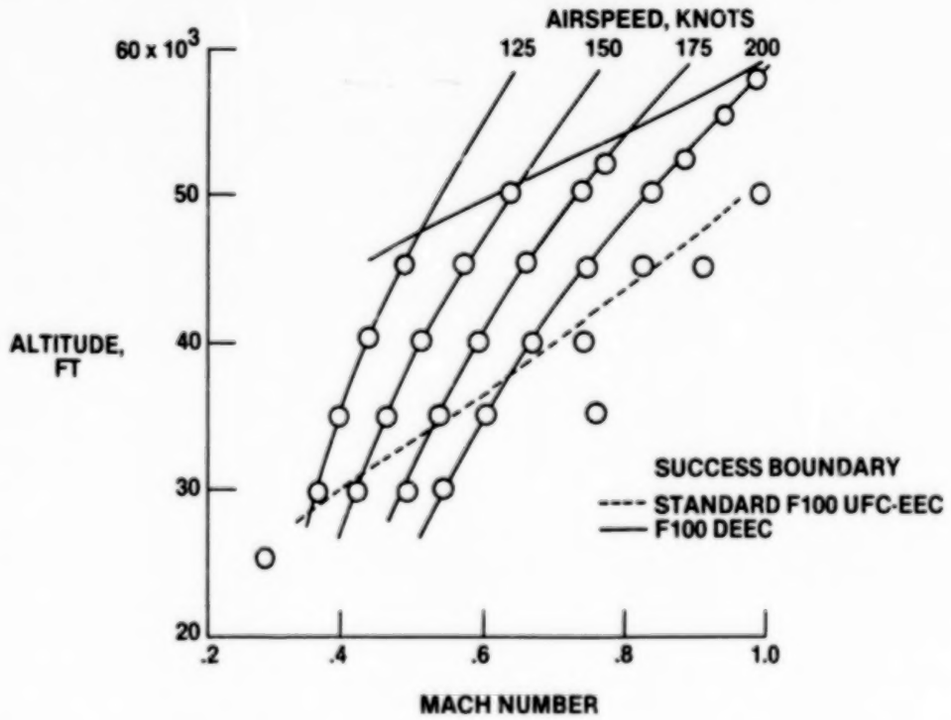

N86
25354

UNCLAS

N86-25354

Paper 12

INVESTIGATION OF A NOZZLE INSTABILITY ON AN F100 ENGINE EQUIPPED WITH A DIGITAL FLECTRONIC ENGINE CONTROL

Frank W. Burcham, Jr.
NASA Ames Research Center
Dryden Flight Research Facility
Edwards, California

and

John R. Zeller
NASA Lewis Research Center
Cleveland, Ohio

SUMMARY

An instability in the nozzle of the F100 engine, equipped with a digital electronic engine control (DEEC), was observed during a flight evaluation on an F-15 airplane. This instability occurred in the upper left hand corner (ULHC) of the flight envelope during augmentation. The instability had not been predicted by stability analyses, closed-loop simulations of the engine, or altitude testing of the engine. The instability caused stalls and augmentor blowouts. This paper will describe the nozzle instability and the altitude testing done to study the problem at the NASA Lewis Research Center (LeRC). The analysis of the test results, both from a linear analysis and a nonlinear digital simulation, will be presented. Results of software modifications on further flight tests will also be discussed.

PRECEDING PAGE BLANK NOT FILMED

N86-25334

NOZZLE INSTABILITY

A nozzle instability was noted during augmented operation in the upper left hand corner of the flight envelope during DEEC/F-15 phase 2 testing. The instability, shown in the figure on the next page, consisted of a 1 Hz to 2 Hz oscillation in the nozzle, with an amplitude up to +0.2 ft^2. This oscillation affected augmentor pressure (PAB) as shown, with each peak driving the fan toward stall, and each valley driving the augmentor toward blowout.

The stability of the engine pressure ratio (EPR) control loop that controls the nozzle had been evaluated with analytical methods during the DEEC software design. Then, the loop stability was evaluated with the engine manufacturer's dynamic simulation. Finally, the loop stability was tested on the flight engine in the altitude facility at Arnold Engineering Development Center (AEDC), but only at intermediate power. During all of these tests, the stability was determined to be adequate. Since the flight data did not show adequate stability, an investigation was conducted to determine the cause of the instability and to develop a fix.

NASA
DFRF82-351a

DEEC NOZZLE INSTABILITY

EPR CONTROL MODE STABILITY AT HIGH ALTITUDE - LOW AIRSPEED
- EVALUATED WITH DYNAMIC ENGINE SIMULATION - OK
- EVALUATED IN AEDC FLIGHT CLEARANCE TESTING - OK
- EVALUATED IN FLIGHT - UNSTABLE

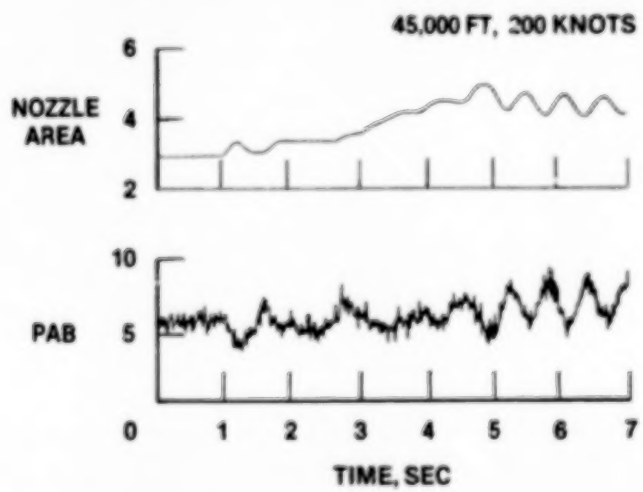

NOZZLE INSTABILITY IN SEGMENT 1

The nozzle instability was not present during nonaugmented operation even though the EPR loop was controlling the nozzle at this condition. In the segment 1 limited part of the envelope, the instability did occur, but was limited in amplitude to ± 0.1 ft^2 and did not cause any stalls or blowouts. As shown below, the oscillation began when the light occurred at t = 2.3 sec and then slowly damped out. The oscillations would sometimes begin, damp out, and then reoccur. Sometimes no oscillations would occur, indicating a marginal stability condition.

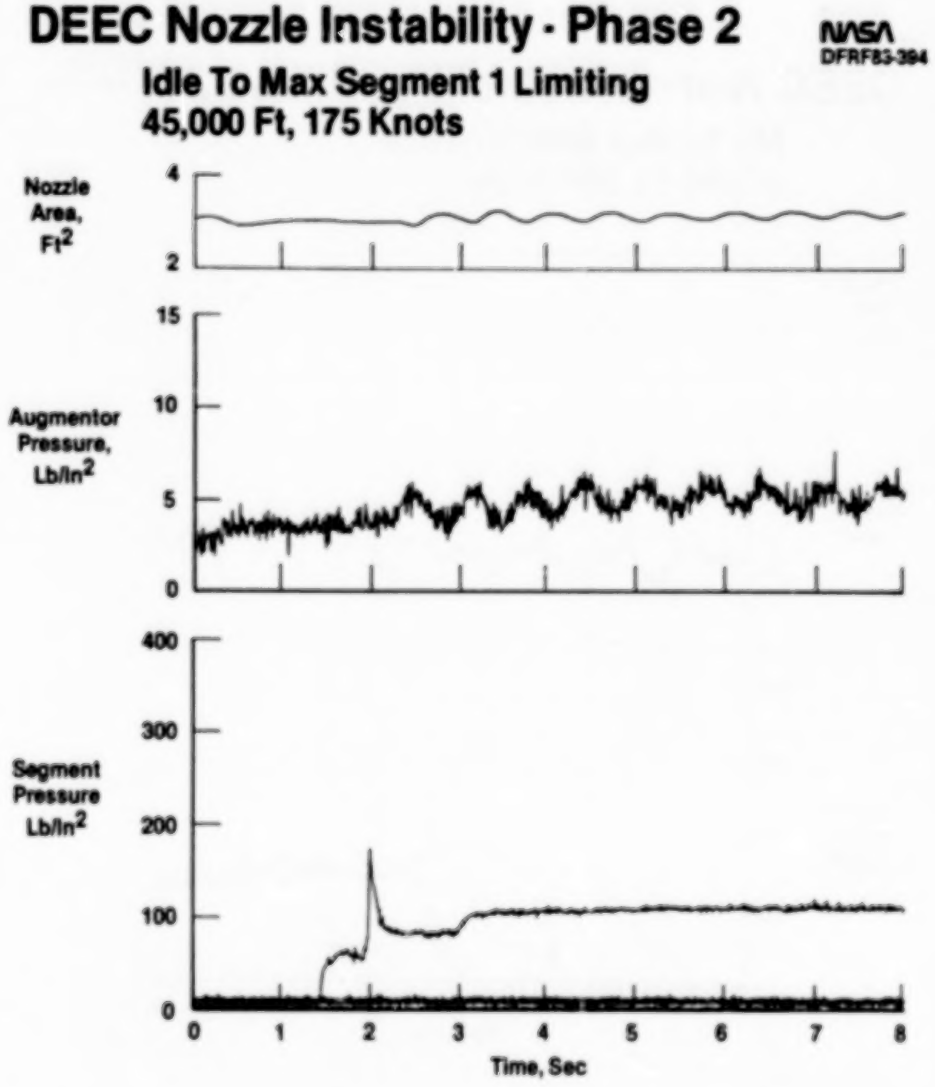

NOZZLE INSTABILITY AT MAXIMUM POWER

During maximum power operation, the nozzle oscillations were larger, as shown below. Following a military-to-maximum transient, the nozzle oscillated at a frequency of approximately 1.4 Hz with an amplitude of ± 0.2 ft^2. Large oscillations in PAB were seen, up to ± 2.5 lb/in^2; fan speed oscillations also occurred. The segment 3 augmentor pressure was also observed to oscillate in response to the changing fan duct airflow.

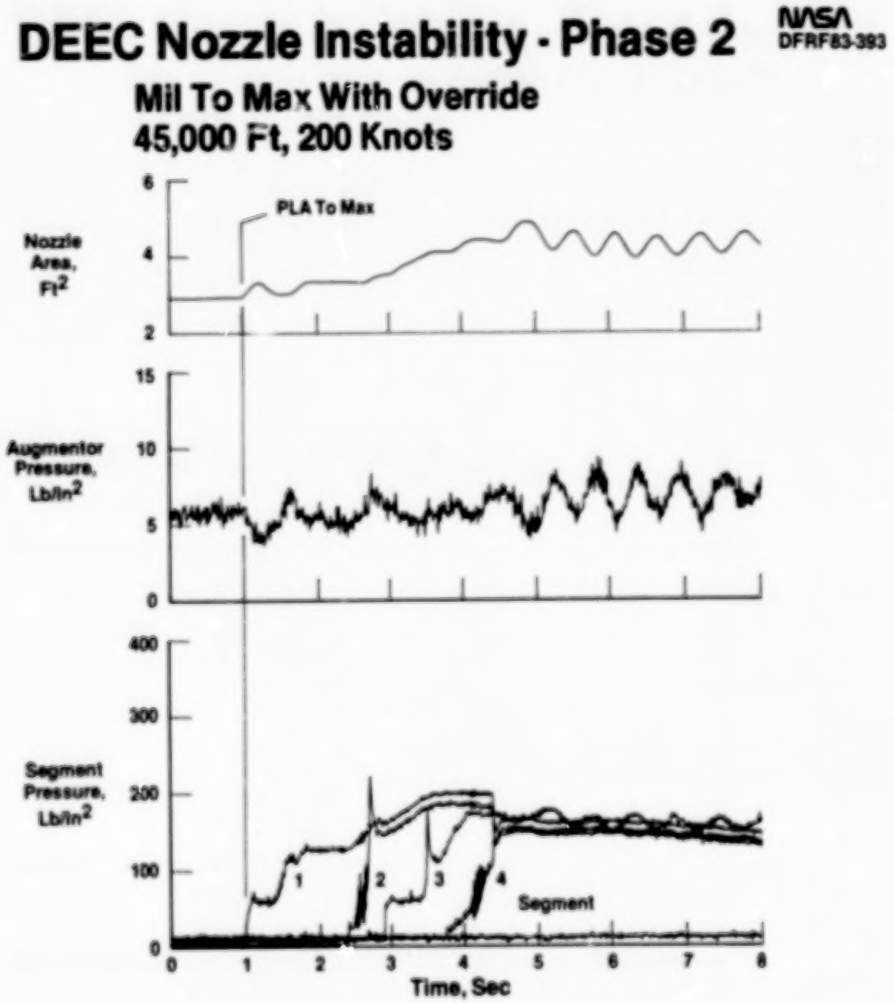

When the nozzle oscillations became large enough, the fan stalled due to the high back pressure, as shown below. Following a military-to-maximum transient at 45,000 ft and 175 knots, a divergent oscillation occurred, resulting in a stall. Stalls also occurred during sequencing when segment transfers or quickfill spikes happened to coincide with a cycle of the oscillation that raised PAB.

NOZZLE INSTABILITY CAUSES STALL

NASA
DFRF82-336b

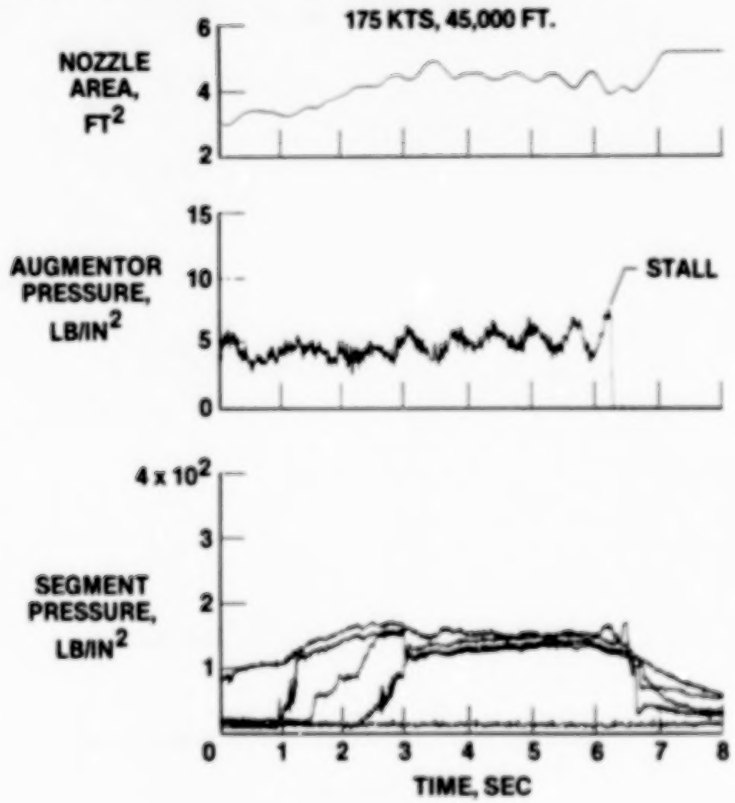

NOZZLE INSTABILITY CAUSES BLOWOUT

Numerous augmentor blowouts were caused by the nozzle oscillation. An example is shown below, at an altitude of 50,000 ft at 200 knots. The low pressure in the augmentor, when the nozzle opened farther than normal, caused the blowout. Blowouts also occurred during augmentor sequencing. Fortunately, the DEEC logic successfully detected the blowouts and turned off the augmentor fuel quickly, thus avoiding any relight stalls.

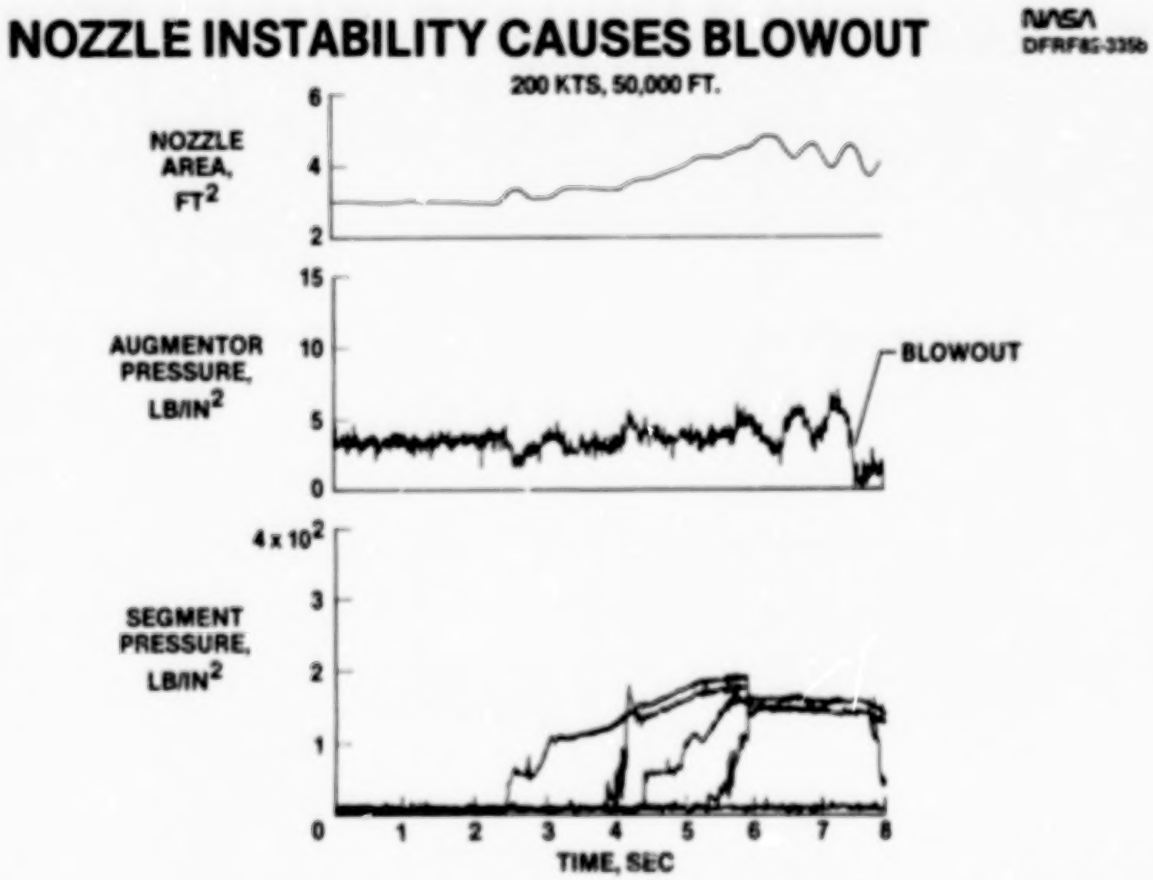

OBSERVATIONS OF NOZZLE INSTABILITY

At the conclusion of the DEEC phase 2 flight evaluation, there were some observations made concerning the nozzle instability. First, the instability had never been observed at intermediate power, even though the EPR loop was controlling the nozzle. At segment 1 limited conditions, the oscillation occurred; it was limited in amplitude to the point where it was a nuisance, but not a threat to operability. At maximum power, the amplitude of the oscillation was large enough to cause numerous stalls and blowouts. At all times, the occurrence of the oscillation was very sensitive to conditions, often beginning at steady conditions and then damping out later at the same conditions.

DEEC NOZZLE INSTABILITY

NASA
DFRF83-323

OBSERVATIONS

- **NO INSTABILITY AT INTERMEDIATE POWER**
- **LOW AMPLITUDE LIMIT CYCLE AT SEG 1**
- **HIGH AMPLITUDE LIMIT CYCLE AT MAX POWER**
- **SENSITIVE TO CONDITIONS**

ORIGINAL PAGE IS
OF POOR QUALITY

NASA LEWIS NOZZLE INSTABILITY TESTING

Because the DEEC/F100 dynamic simulation did not indicate the nozzle instability, it was necessary to perform some actual engine tests to determine the cause of the instability. It was not practical to get the flight engine into an altitude facility because of the long lead time required. However, a test engine, XD11, was running at the NASA Lewis Research Center (LeRC) in the Propulsion System Laboratory (PSL) altitude facility. The XD11 engine had been modified to the F100 Engine Model Derivative (EMD) configuration but was thought to be close enough to the flight engine configuration to provide useful data.

The XD11 engine was controlled by a breadboard DEEC that could be reprogrammed easily. LeRC agreed to provide time to conduct nozzle stability tests and assist in the testing and analysis. The flight software was loaded and augmentor transients were performed at Mach 0.6 and 45,000 ft. No instability was noted. Gains in the EPR loop were increased until nozzle oscillations were observed.

As shown in the figure below, when the integral gain was increased by a factor of 2.5, nozzle oscillations occurred. No sustained limit cycle oscillations occurred, but the frequency was similar to that seen in flight. In order to gain additional insight into the EPR loop stability, further tests were performed to acquire dynamic characteristics of the engine and control system. Forced sine and step functions were introduced into the nozzle through the DEEC breadboard control, and the resulting data were used to generate transfer functions. These transfer functions were then used to update the engine simulation.

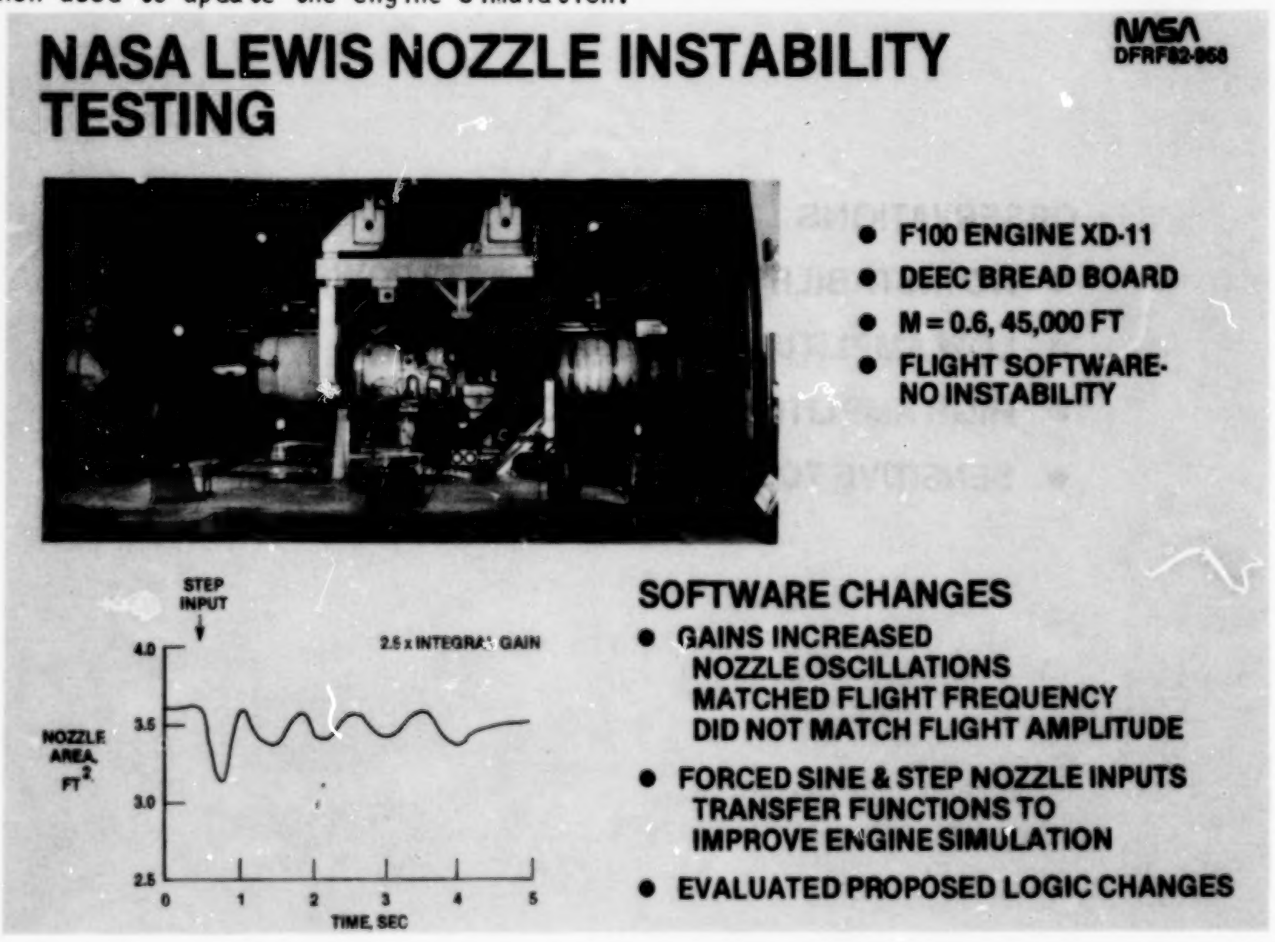

ERP LOOP LINEAR ANALYSIS

The engine manufacturer, Pratt and Whitney Aircraft, took the transfer function data from the LeRC tests and conducted a linear analysis of the EPR loop. A block diagram of the system is shown on the next page. It models the part of the EPR control mode that was enclosed in the dashed lines of the nozzle control figure of Paper 11. The EPR request was multiplied by integral and proportional gains and by the nozzle base gain to generate the nozzle request. The nozzle request was passed to the nozzle dynamics block - which models the servo loop dynamics - the air motor that drives the actuators, and the actuators themselves. The nozzle output was used to generate the appropriate EPR dynamics, the jet primary nozzle area (AJ)/EPR transfer function having been determined from the LeRC tests. The resulting EPR was fed back to the DEEC pressure sensors, the DEEC filter, and the DEEC computational cycle to generate the EPR feedback. Another feedback loop was also modeled. As the nozzle area and EPR changed, the fan speed also changed, as modeled in the AJ/fan rotor speed (N1) dynamics block, determined from the LeRC test data. The N1 to EPR constant was the slope of the N1 to EPR request table in the DEEC logic. That was then fed back to the EPR request to complete the generation of the EPR error.

This linear simulation of the EPR control loop was reduced to a single transfer function and a stability analysis was conducted. At the upper left hand corner flight condition, the gain and phase margins were very small, indicating a marginal stability condition. The stability analysis was also conducted at two other flight conditions - sea level static, and Mach 0.9 at 30,000 ft - where the engine dynamics were well documented, and the results were consistent with test data. Based on these results, the engine manufacturer recommended reducing the gain in the upper left hand corner by a factor of 2. In addition, a deadband between the EPR error and the proportional and integral gains that had been very small (0.001), was to be increased by a factor of 30 to 0.03. These proposed logic changes were then evaluated on the test engine at LeRC and were found to stabilize the EPR loop.

In comparing the engine dynamics derived from the LeRC test and the dynamics that had been used in the engine manufacturer's nonlinear simulation, no major differences were seen. Rather, there appeared to be a number of relatively small effects, which, when combined, caused a significant difference in dynamic characteristics to occur.

PWA EPR/NOZZLE LOOP LINEAR ANALYSIS

NASA
DFRF82-1006a

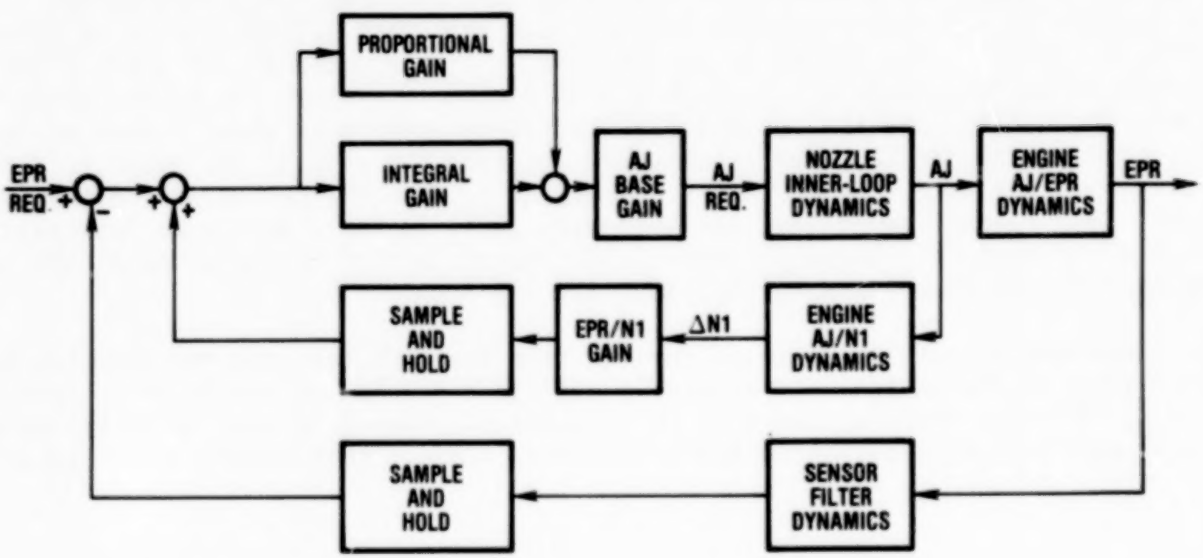

DRYDEN NONLINEAR EPR LOOP SIMULATION

In order to study the nozzle instability further, NASA Ames Research Center's Dryden Flight Research Facility (DFRF) developed a nonlinear digital simulation of the EPR loop. The basic block diagram of the linear analysis was modified by the addition of the deadband, nonlinearities in the nozzle, and more accurate modeling of the DEEC cycle times. The simulation was mechanized in the time domain using Z transform techniques. The digital computer program used an integration interval of 0.005 sec and modeled the DEEC computational minor cycle time of 0.02 sec. A step input in EPR request was used to evaluate the EPR loop stability. Variations in proportional and integral gains, deadband, and nozzle hysteresis were investigated.

DEEC EPR/NOZZLE LOOP SIMULATION

NASA
DFRF82-1006

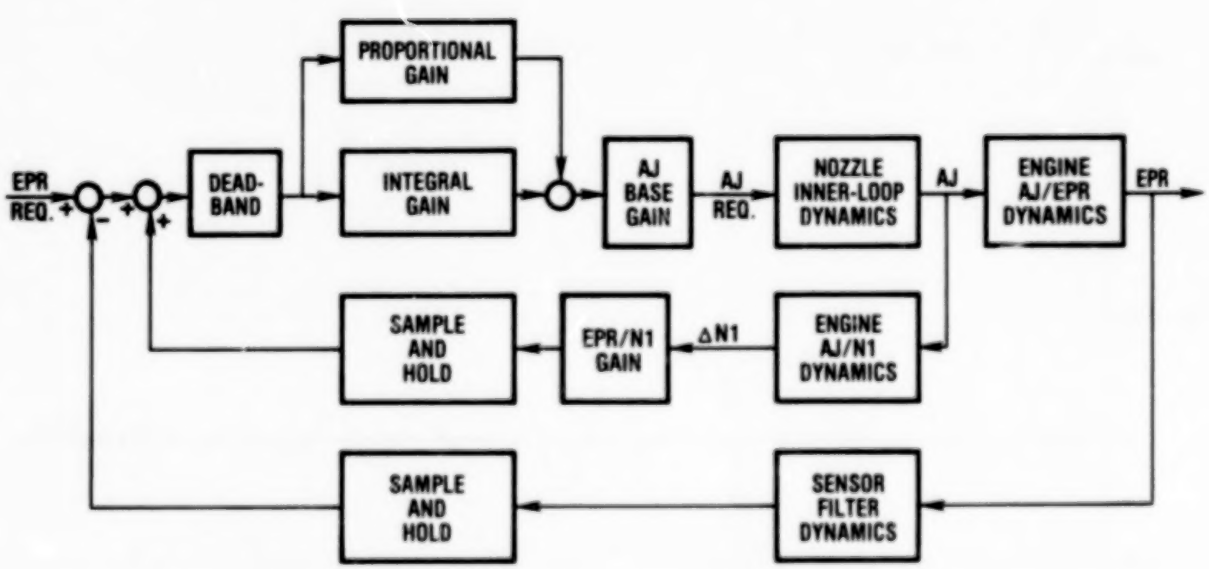

RESULTS OF NONLINEAR EPR LOOP SIMULATION

Results of the DFRF nonlinear simulation of the EPR loop at Mach 0.6 and 45,000 ft are shown below. The deadband, proportional, and integral gains from the DEEC phase 2 logic are incorporated. As shown, the step input in EPR request initiates a very lightly damped limit cycle oscillation with a frequency and amplitude similar to that observed in flight. This nonlinear simulation, which incorporated LeRC test results, essentially duplicated the flight results - whereas the engine manufacturer's full nonlinear simulation did not predict the oscillation. This points out the importance of having very high quality engine modeling data.

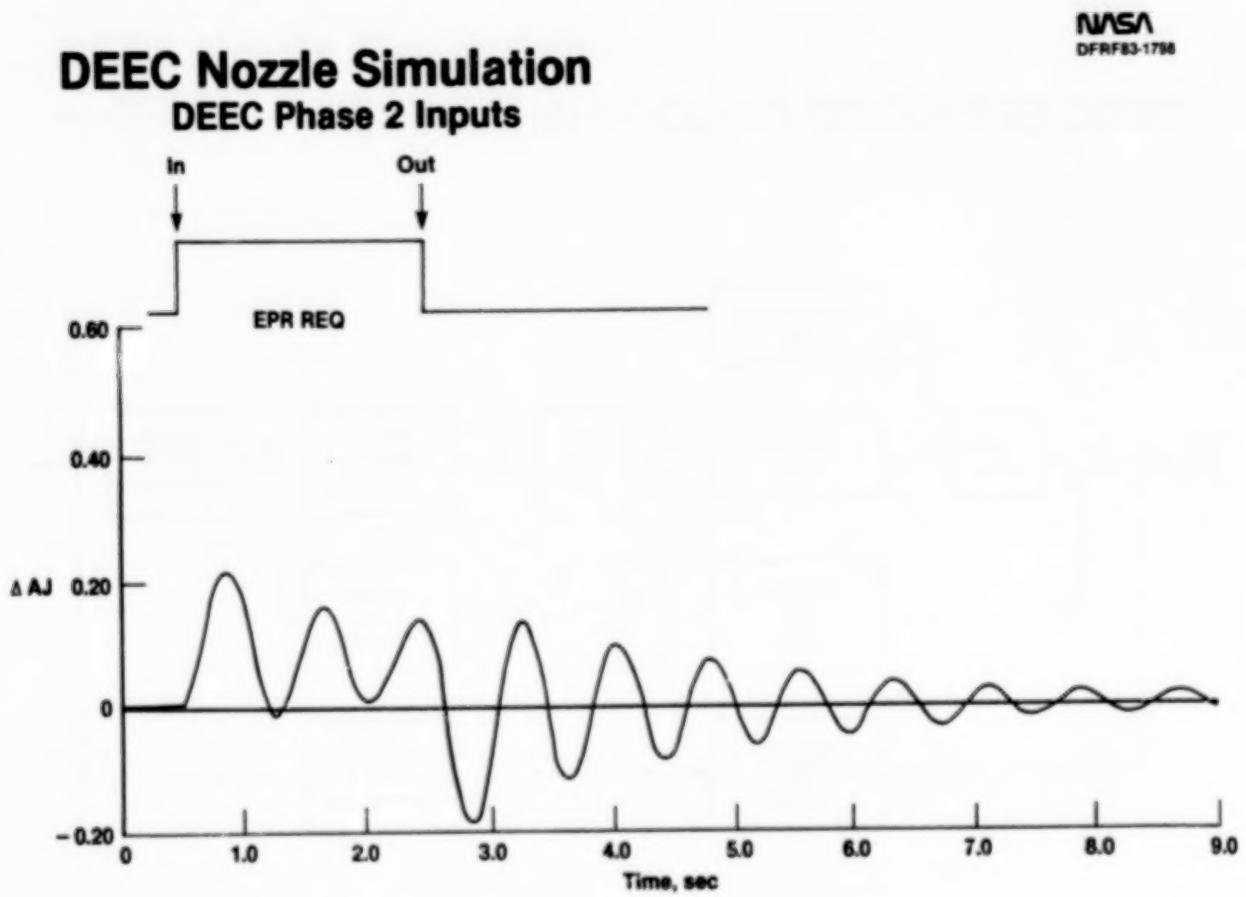

NONLINEAR SIMULATION OF PROPOSED SOFTWARE CHANGES

The proposed logic changes for the phase 3 software were evaluated on the DFRF simulation and were again verified. As shown below, when the deadband was increased and the integral gain was cut in half, the response to the same step input in EPR request produced only a small overshoot that rapidly damped. This response was judged to be acceptable. The phase 3 flight results showed that the nozzle instability had been effectively eliminated. During phase 4 testing at very high altitudes and low airspeeds, some tendency for nozzle overshoots was observed, but this did not cause any stalls or blowouts.

NASA
DFRF83-1797

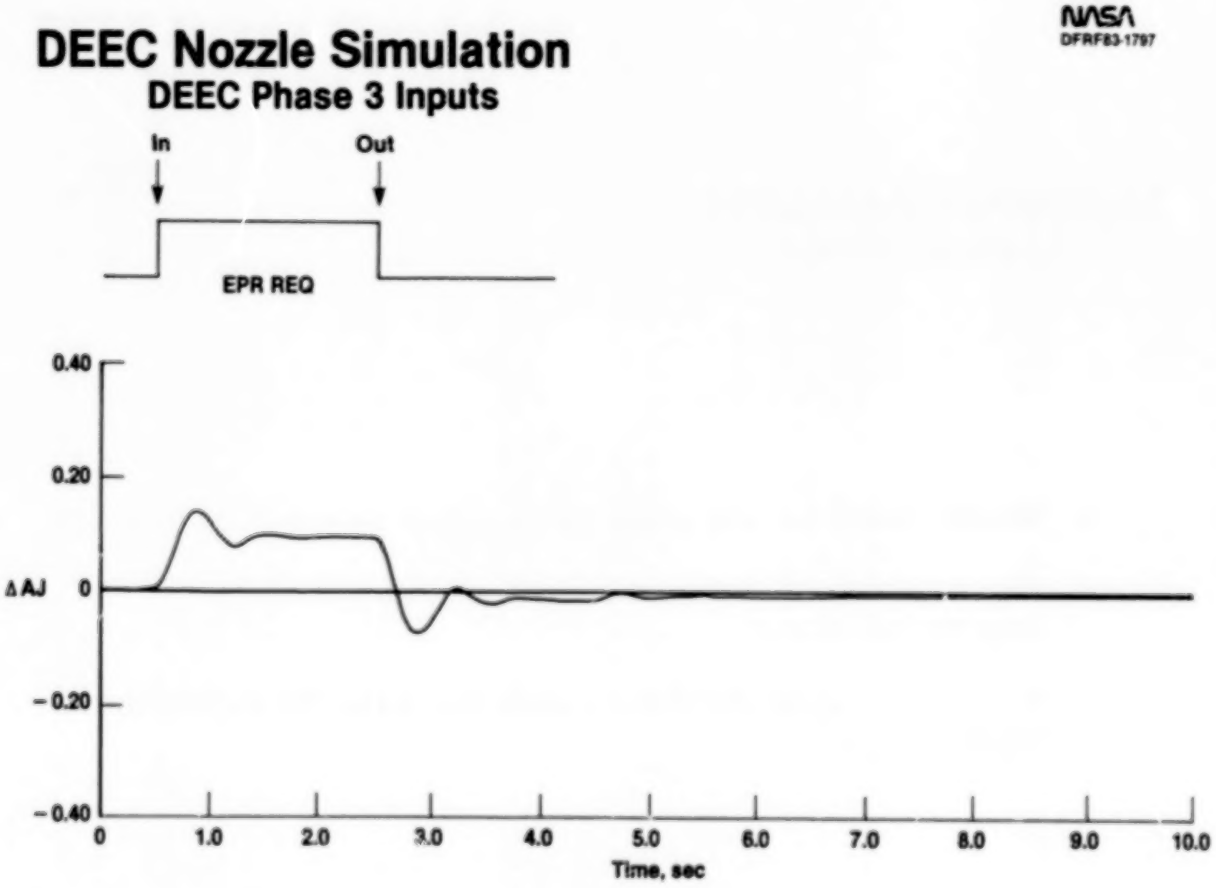

LESSONS LEARNED ON AUGMENTOR INSTABILITY

The augmentor instability investigation on the DEEC-equipped F100 engine has provided several lessons for future engine developments. First, it was shown that engine dynamic models must be very accurate to reveal instabilities, particularly for operation in the upper left hand corner of the flight envelope. It was also found that loop stability testing should be performed at augmented power if possible, since the DEEC flight clearance testing at intermediate power did not reveal the instability. It was also found that a nonlinear simulation could essentially duplicate the observed engine behavior in flight if accurate engine test data were included.

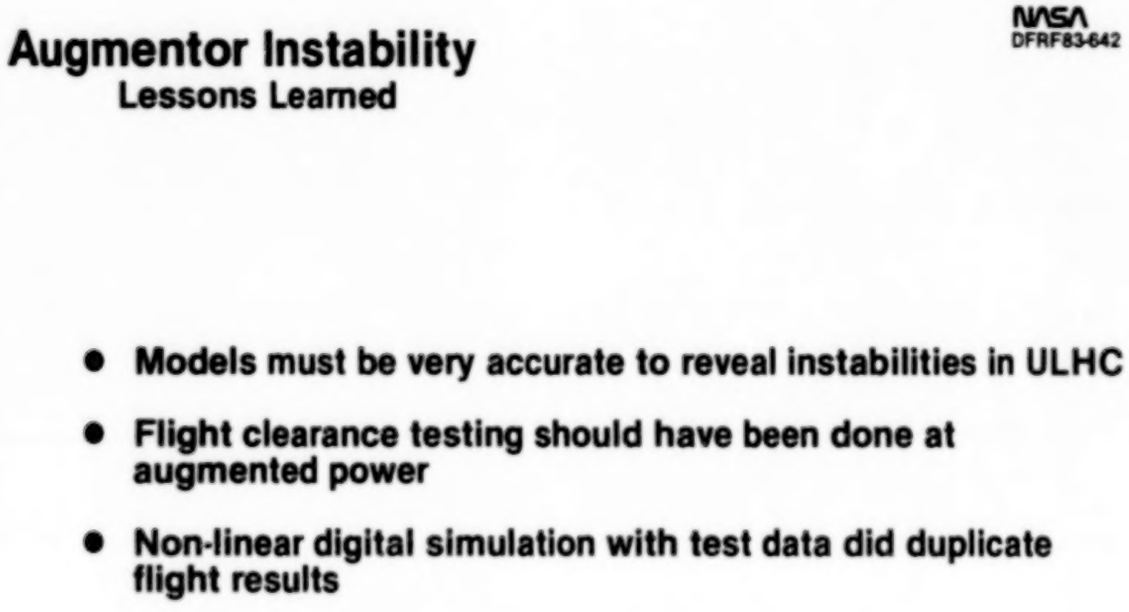
NASA
DFRF83-642
Augmentor Instability
Lessons Learned
• Models must be very accurate to reveal instabilities in ULHC
• Flight clearance testing should have been done at augmented power
• Non-linear digital simulation with test data did duplicate flight results

N86
25355

UNCLAS

N86-25355

Paper 13

REAL-TIME IN-FLIGHT THRUST CALCULATION ON A DIGITAL ELECTRONIC ENGINE CONTROL-EQUIPPED F100 ENGINE IN AN F-15 AIRPLANE

Ronald J. Ray
California Polytechnic State University
San Luis Obispo, California

and

Lawrence P. Myers
NASA Ames Research Center
Dryden Flight Research Facility
Edwards, California

SUMMARY

One of the important objectives in many flight programs is the measurement of performance. This is particularly true for programs like the digital electronic engine control (DEEC) and the Engine Model Derivative (EMD). With the DEEC, there is interest in measuring engine thrust and the effect of software changes. In the EMD program there is interest in determining increases in engine performance, due to hardware advancements and modifications. Normally, performance is calculated post flight, often weeks or months after the flight.

Recently, NASA began to implement a series of computer algorithms that will calculate in-flight engine and aircraft performance real-time. The necessary first step in this goal has been completed with the implementation of a real-time thrust calculation program on a DEEC-equipped F100 engine in an F-15 airplane. This paper will present the in-flight thrust modifications that permitted calculations to be performed in real-time, which enabled results to be compared to predictions.

N86-25355

OBJECTIVES

The main objective of this program was to accurately determine the thrust developed during a test flight and have it displayed in real-time. This data, displayed in the control room, would assist in determining the performance of the DEEC/EMD F100 engines. It would also provide a base for more advanced real-time performance programs to be used in future projects.

Objectives

NASA
DFRF83-550

- **To determine the internal thrust developed during powered flight and have it displayed real time**
- **Aid in the performance analysis of the DEEC F100 Engine**
- **Set a base for more advanced real time performance programs to be used in future projects**

ADVANTAGES OF DEEC

There are some important advantages of having the DEEC available to supply engine data for the calculation of thrust. All of the required parameters to calculate thrust are available from the DEEC real time and are measured with accurate, state-of-the-art instrumentation. In addition, the DEEC computer supplies calculated airflow and fan inlet total pressure (PT2), reducing the computational requirement on the ground.

Advantage of DEEC

NASA
DFRF83-551

- DEEC instrumentation is state of the art, accurate and available real time - NO ADDITIONAL INSTRUMENTATION NEEDED
- Calculated airflow is available from DEEC
- Post flight computer program already written and tested by Pratt and Whitney

F100 ENGINE STATIONS

The F100 engine is a twin-spool, low-bypass ratio, afterburning turbofan of the 25,000 lb thrust class. The three-stage fan is driven by a low pressure, two-stage turbine and the 10-stage high pressure compressor is driven by a two-stage high pressure turbine. To increase fan efficiency and achieve high performance over a wide range of operating conditions the engine incorporates compressor inlet variable vanes (CIVV) and rear compressor variable vanes (RCVV). Continuously variable thrust augmentation is provided by a mixed-flow afterburner. The augmentor incorporates five spray ring segments, which are ignited sequentially, allowing variable afterburner thrust. The high energy gas is exhausted through a variable-area, convergent-divergent nozzle of the balance beam design that enables simultaneous optimization of nozzle area, expansion ratio, and boattail drag.

This figure shows the designated engine stations. In the calculation of thrust, the primary concern is to determine the conditions at the engine inlet (station 2) and the exhaust nozzle throat (station 7).

F100 Engine Stations

NASA
DFRF83-552

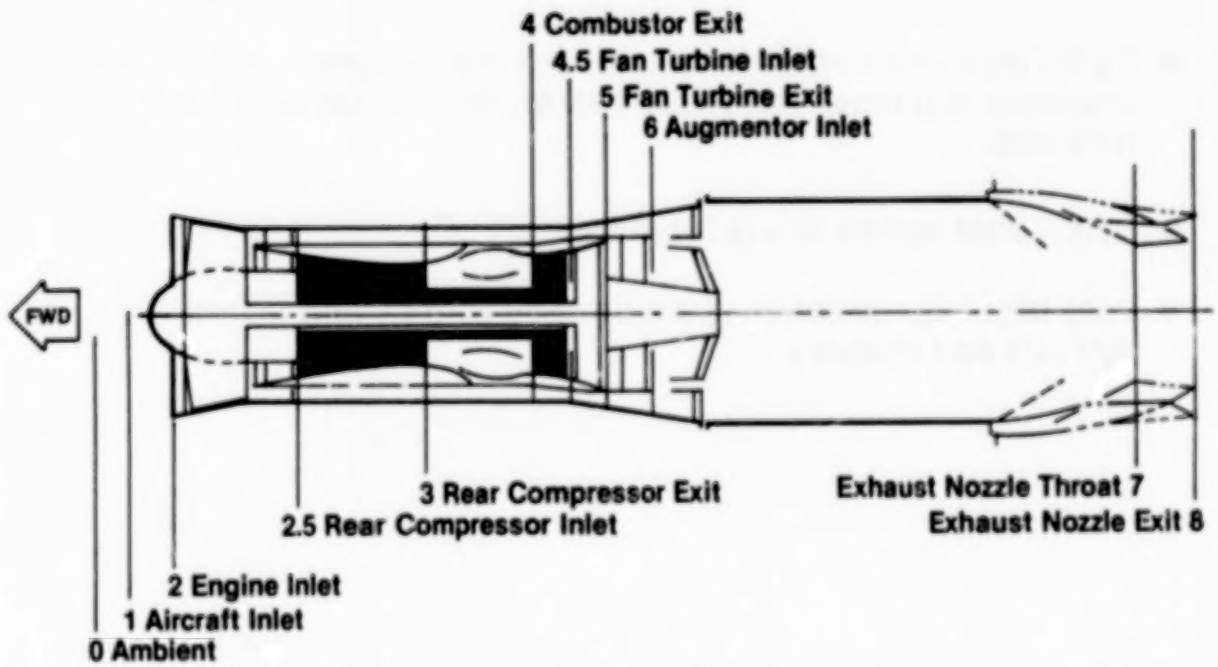

THRUST MEASUREMENT INSTRUMENTATION

The figure below shows the location of engine instrumentation used in the calculation of in-flight thrust. All of these measurements are part of the DEEC control system and are available from the DEEC output in real time. The DEEC computer also calculated PT2 from fan inlet static pressure (PS2) as described in the PS2 Correlation Paper 5. Corrected engine airflow (WAC) is also calculated from PT2, fan inlet total temperature, (TT2), fan rotor speed (N1), and CIVV position. Because of this, no special instrumentation was required. In addition, free stream static pressure, temperature, Mach number, and altitude were available from the aircraft data system.

NASA
DFRF83-553

Thrust Measurement Instrumentation On DEEC Engine

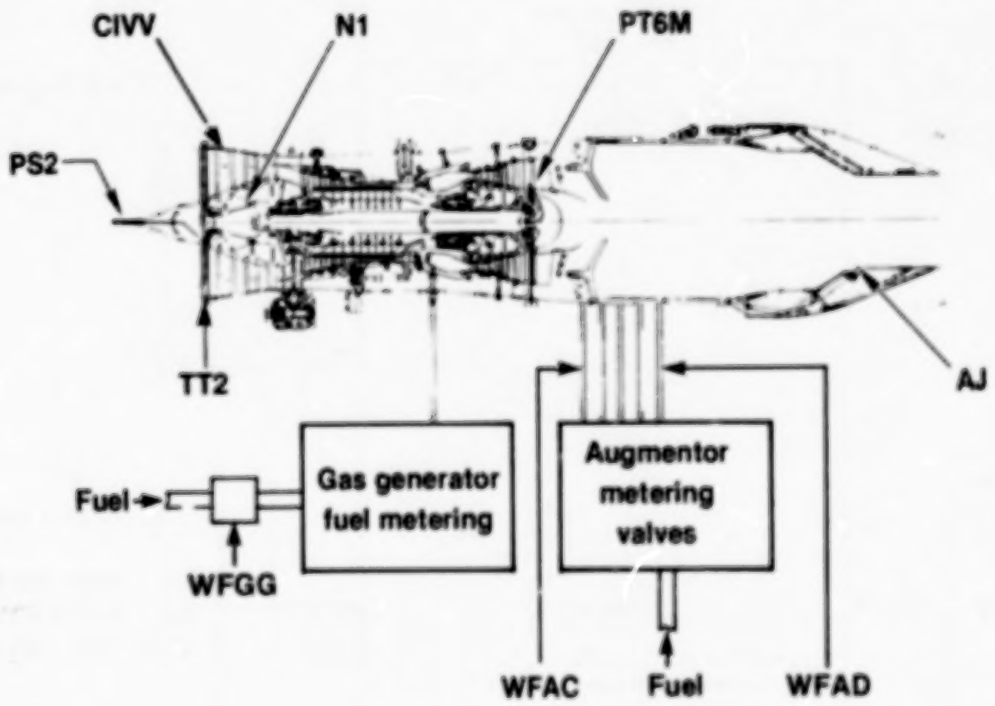

REAL-TIME THRUST CALCULATION

The software used to calculate in-flight thrust real time is a modified version of the engine manufacturers' Fortran IV data reduction routine for determining in-flight performance, and was intended for off-line analysis. The in-flight thrust deck uses gas generator methods in which a combination of measured parameters and math models of engine characteristics are used to calculate gross thrust. Empirical data comes from sea level static tests and altitude facility tests. Two gas generator models are used; one based on pressure and nozzle throat area, the other on temperature and the gas flow rate.

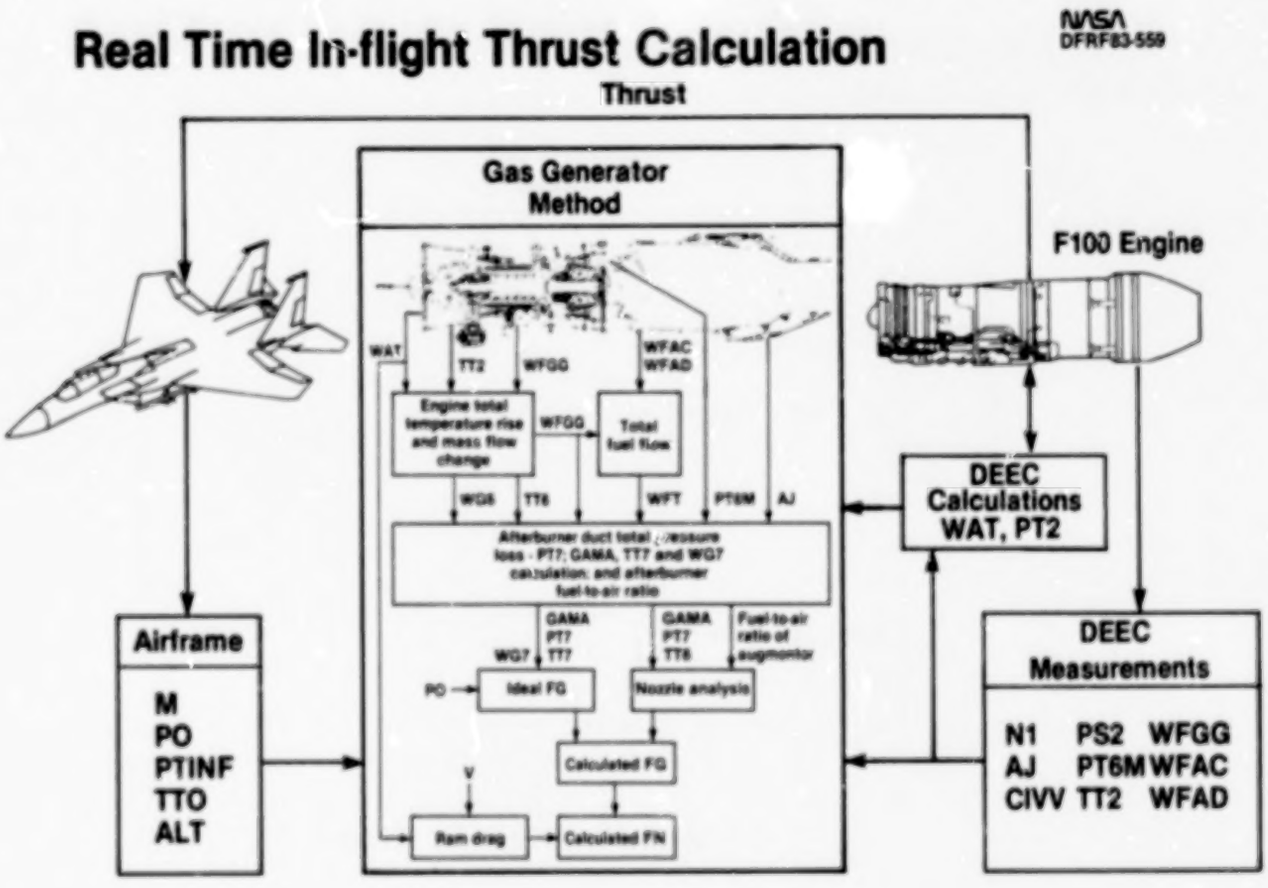

MODIFICATIONS MADE TO RUN REAL TIME

To increase the efficiency of the program and to meet real-time compatibility requirements, the modifications shown below were made to the original program. These changes were made primarily to increase the speed of data reduction; no changes were made to the method of calculation. Input and output was accomplished by use of a common block statement which allowed instantaneous updating of all parameters.

Modifications Made to Run Real Time

NASA
DFRF83-556

Total airflow calculation logic including 5 subroutines were removed because of its availability from the DEEC

Uncertainty logic was changed to allow the user control over the rate the uncertainty analysis is made

The original output format was deleted and the number of output parameters was reduced to 10

Input data from the airframe and engine/DEEC was accessed instantaneously from the main ground computer program.

THRUST EQUATIONS

The primary equations used to calculate thrust are given below. The pressure-area thrust calculation method (PTA) relies on four variables to calculate thrust, with total pressure (station 7) and nozzle area being the most sensitive parameters. The temperature-mass flow method of thrust (TTW) relies on five variables to calculate thrust, with the gas flow rate being the most sensitive parameter. Both methods use empirical data to correct from ideal to actual gross thrust.

Equations

NASA
DFRF83-555

Gross Thrust

$$FG(PTA) = PT7 \cdot AJ \cdot \gamma \sqrt{\frac{2}{(\gamma-1)} \left(\frac{2}{\gamma+1}\right)^{\left(\frac{\gamma+1}{\gamma-1}\right)}} \sqrt{1-\left(\frac{PT7}{PO}\right)^{\left(\frac{1-\gamma}{\gamma}\right)}} CG$$

$$FG(TTW) = \frac{WG7}{g} \sqrt{TT7 \ \frac{2\,Rg}{\gamma-1}} \sqrt{1-\left(\frac{PT7}{PO}\right)^{\left(\frac{1-\gamma}{\gamma}\right)}} CV$$

Ram Drag

$$FR = \frac{WAT}{g} \cdot V$$

Net Thrust

$$FN = FG - FR$$

RESULTS OF MODIFICATIONS

The results of the modification made to run real-time, in comparison to the original postflight program, are tabulated below. The most significant result is that thrust can be calculated real-time with no loss in accuracy from the original postflight program. This is a major improvement in flight test productivity and allows decisions concerning thrust output to be made in the control room.

NASA
DFRF83-557

Results of Modifications

Item	Original	Modified
Method of Data Reduction	Postflight	Real-time
Time between test maneuver and data reduction	2-5 days	40 millisecs 1-2 hrs. hard copy
Program length	21 subroutines	12 subroutines
Accuracy (estimated)	2 to 5 percent	-- same --
Uncertainty calculation	Available	Not available
Output form	Lengthy hard copy with plotting available	Tabulated hard copy with plotting available, strip-charts

GAS GENERATOR METHOD CALCULATION FLOW

The gas generator calculation flow chart shown below is a schematic representation of the flow of data and mathematical model calculations. The blocks within the schematic illustrate calculations. The engine core and afterburner are modeled separately. The thrust model uses a combination of theoretical values, component test data, and full-scale engine data to generate the relationships necessary for the analysis. Ideal gross thrust is calculated and then corrected by a thrust coefficient, determined from the nozzle analysis, to get the actual gross thrust. Ram drag is calculated, using airflow and aircraft velocity data, and then subtracted from gross thrust to obtain the actual net thrust.

NASA
DFRF83-560

Gas Generator Method

Calculation Flow

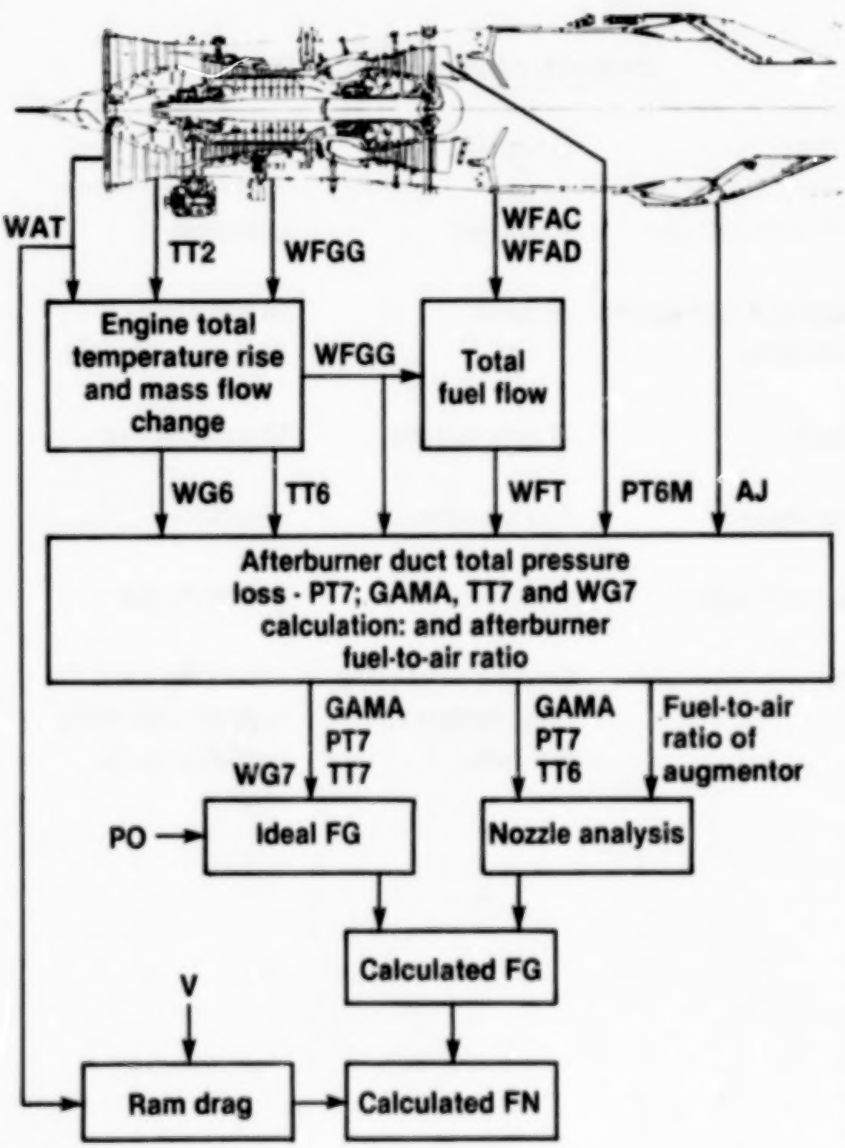

REAL-TIME DATA SYSTEM

The real-time data system, used during DEEC testing, is shown below. Data from the engine and airframe instrumentation is captured and then telemetered to the ground station, where the raw data is stored on digital tape. This raw data is also supplied to the real-time computer for engineering unit conversions and calculations. The computer then supplies the output to the appropriate device. Thrust, ram drag, and specific fuel consumption are displayed on the cathode ray tube (CRT).

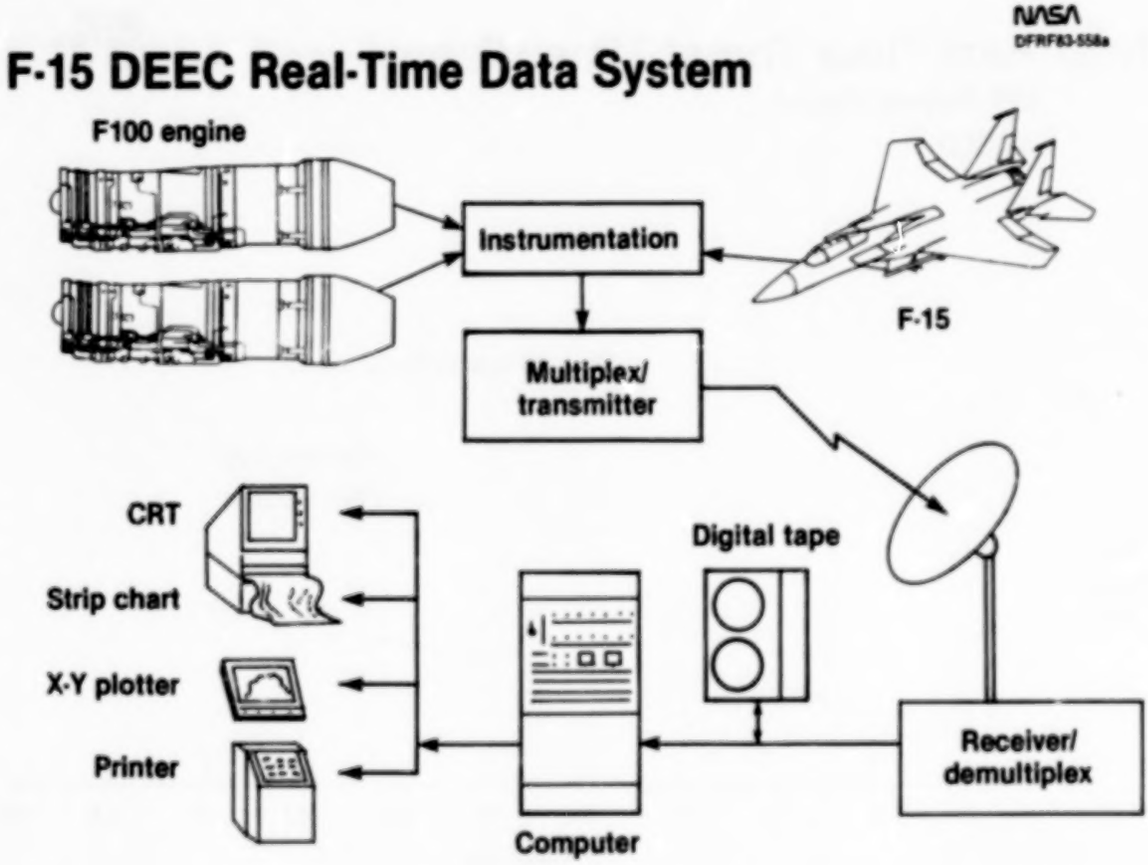

NEAR REAL-TIME THRUST TIME HISTORY

To aid in the performance analysis during a test flight, hard copy plots such as the one below are available shortly after any maneuvers. Excellent agreement between the two calculated thrust parameters is shown for the last half of the test. The discrepancy between the calculated thrust values for the first part of the test could have been due to nonstabilized engine conditions. This is an example in which the real-time thrust computation data could be used in the flight control room to repeat the first part of the acceleration run, in an attempt to obtain improved agreement between the two methods.

Near Real-Time Thrust Time History

NASA
DFRF83-562

Mil Power Accel
30,000 ft

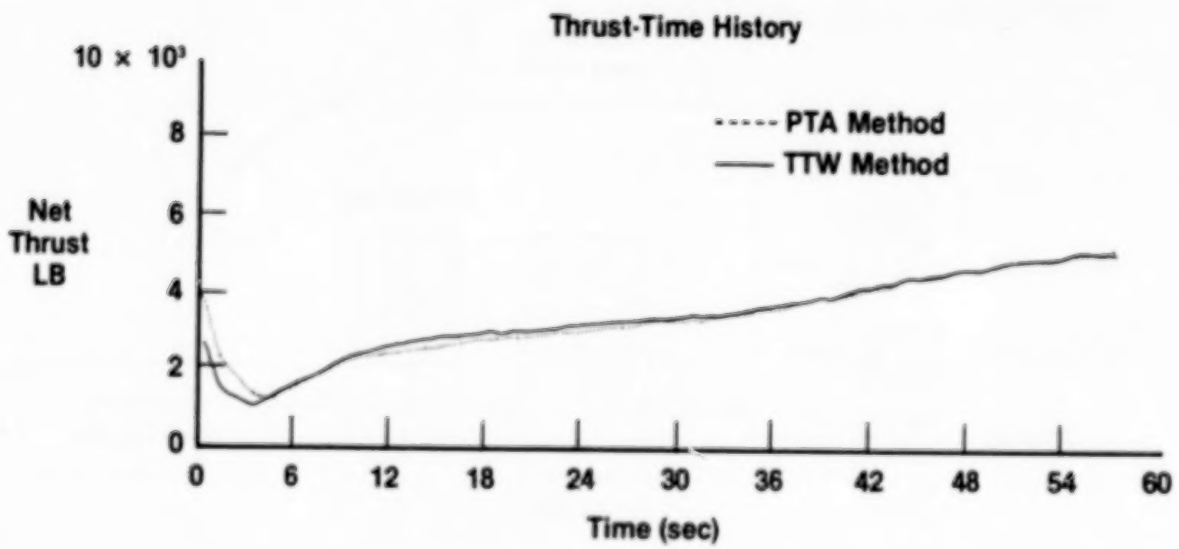

DIFFERENCE BETWEEN PTA AND TTW CALCULATED THRUST AND PREDICTED UNCERTAINTY

To compare the two gas generator methods, the following plot was made for a 30,000 ft maximum power acceleration run. The predicted uncertainty is based on a root sum square calculation, using the uncertainty of each method. The large difference between the two methods, at the beginning of the run, may be due to the transient time required for the engine to stabilize at a steady-state condition, or the very rapid airplane acceleration that occurred in this test. At supersonic speeds, the two methods agree better than the uncertainty analysis would predict.

NASA
DFRF83-563a

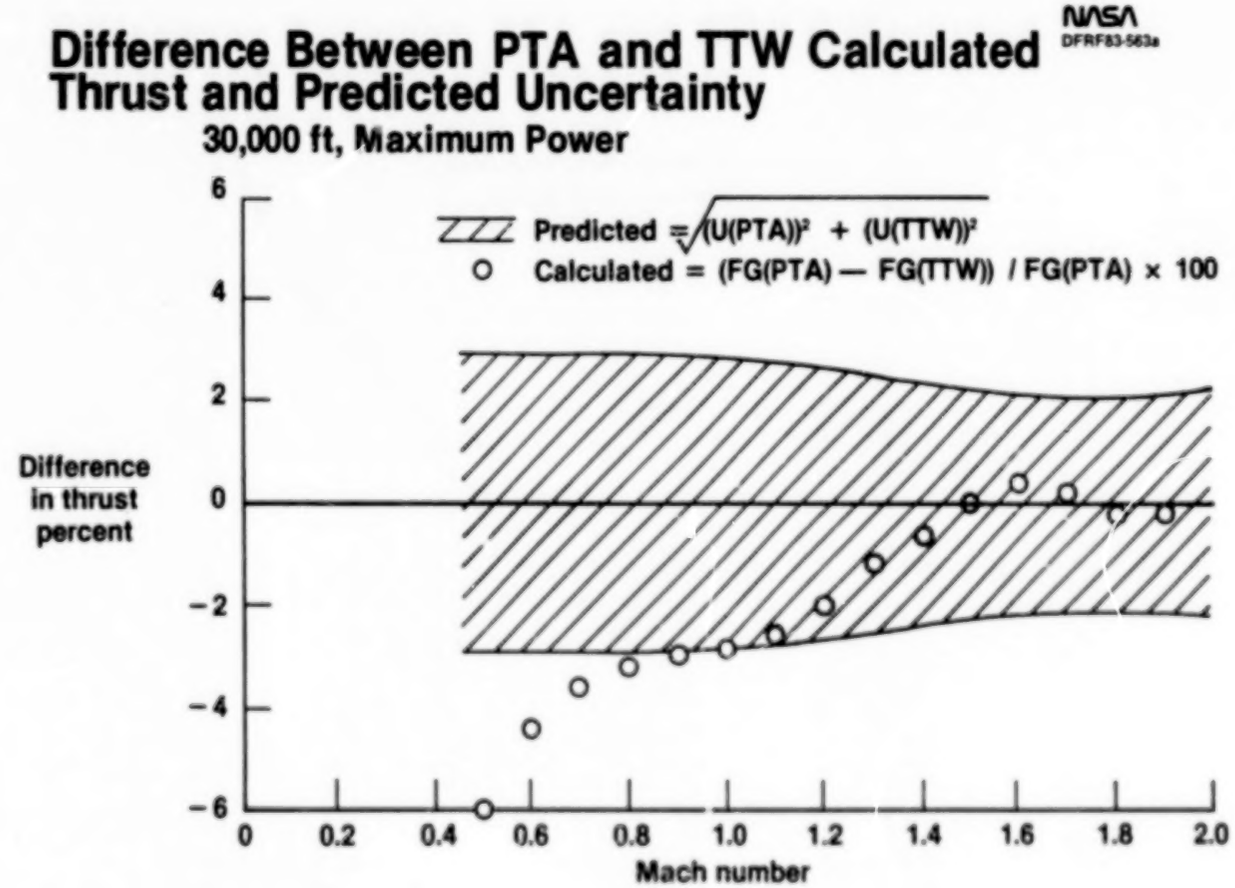

PREDICTED VERSUS CALCULATED NET THRUST

The plot below is a comparison of the predicted net thrust and the two real-time values of calculated net thrust for a maximum power, 40,000 ft level aircraft acceleration. Predicted thrust is calculated with the engine simulation deck using input data for test day conditions and ram air recovery factors. Agreement between the predicted and actual calculated values is good with a 2 to 5 percent difference.

NASA
DFRF83-561

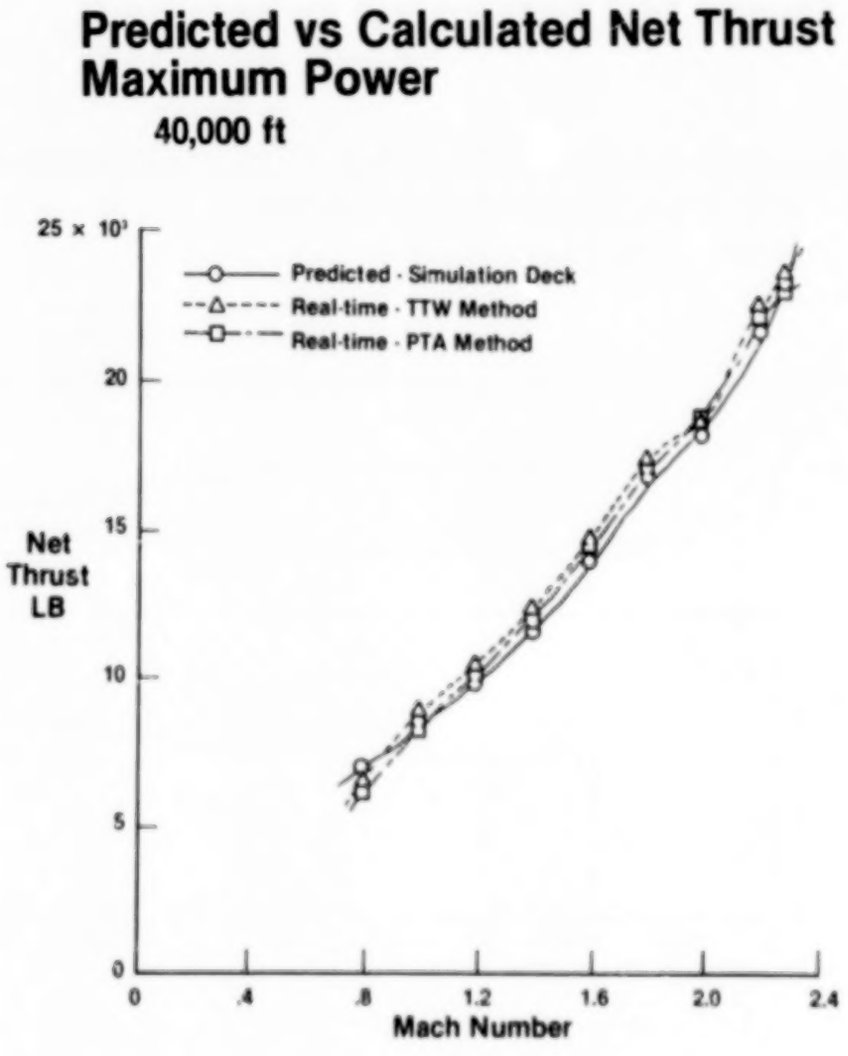

AIRPLANE PERFORMANCE TIME LINE

The figure below shows the overall goal of the real-time performance analysis and the essential steps required to meet this goal. Ultimately, there is a need to accurately calculate standard day performance, including lift and drag real time, and compare to wind tunnel and theoretical values. Real-time thrust is an important step in this direction.

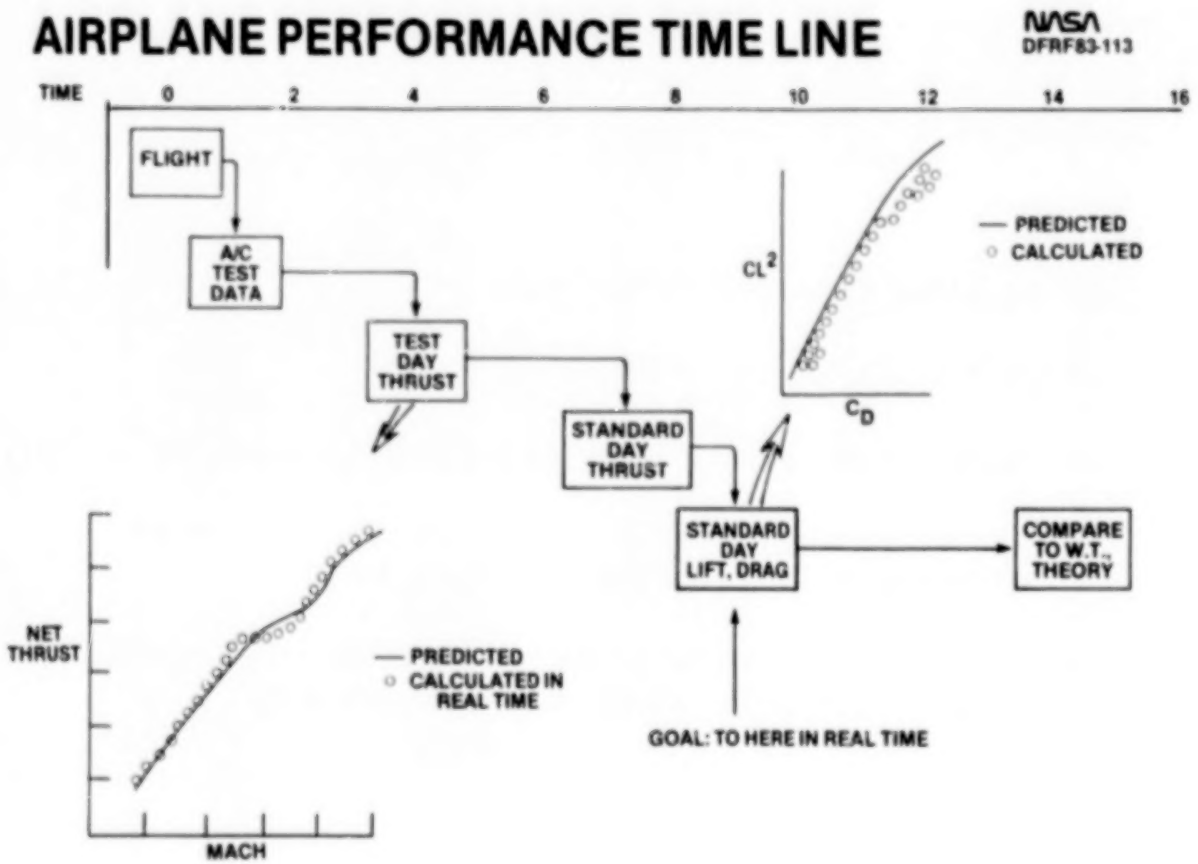

CONCLUDING REMARKS

The summary shown below indicates that implementing the real-time in-flight thrust calculation on the DEEC program has proved to be practical. The availability of the DEEC contributed greatly to the success of calculating real-time thrust, with no loss in accuracy from previous postflight methods. Real-time thrust was also a major advancement in flight test productivity and efficiency, and has helped significantly in the performance analysis of the DEEC F100 engine.

NASA
DFRF83-564

Summary

- Real-time thrust calculation practical
- Little or no loss in calculated accuracy
- Permits major improvements in flight test productivity
- The availability of DEEC parameters was a major factor in the success of calculating real-time thrust
- Obtaining real-time thrust was an important step towards calculating real-time, standard day lift and drag

N86
25356

UNCLAS

N86-25356

CONTROL TECHNOLOGY FOR FUTURE AIRCRAFT PROPULSION SYSTEMS

John R. Zeller, John R. Szuch,
Walter C. Merrill, Bruce Lehtinen, and James F. Soeder
NASA Lewis Research Center
Cleveland, Ohio

SUMMARY

The thrust toward improved aircraft powerplants for both military and civilian applications has created a need for significantly more sophisticated engine control systems. The improvements in better thrust-to-weight ratios have usually demanded the manipulation of more control inputs. The computational and schedular needs associated with these additional tasks severely tax the capabilities of the well-proven analog hydromechanical fuel controllers. As a result, new technological solutions to the engine control problem are being put into pratice. Electronic controllers, especially digital computer-based, are being applied to the need. The digital electronic engine control (DEEC) system is one very sophisticated step in the evolution to digital electronic engine control.

This paper is intended to:

(1) enumerate the technology issues being addressed to ensure a growth in confidence in sophisticated electronic controls for aircraft turbine engines; and

(2) establish the needs of a control system architecture which will permit propulsion controls to be functionally integrated with other aircraft systems, such as flight controls.

This paper will include areas of technology being studied by the NASA Lewis Research Center (LeRC), either alone or in conjunction with the Air Force Aeropropulsion Laboratory. The work encompasses the areas of: (1) control design methodology; (2) improved modeling and simulation methods; and (3) implementation technologies. Objectives, results and future thrusts will be summarized.

The emerging new technologies of electronic hardware and software being planned for future engine controls raise some new issues. One is the prediction of the reliability and integrity of these technologies as they take on the new task of aircraft turbine engine control. Another is the validation of these systems which are based on software as well as hardware, and incorporation of computational innovations for which the industry has little operational experience. An example of the second item is the desire to accommodate faults by diagnosing them and reconfiguring the control on-line. Validation methods for fault-tolerant hardware/software systems require new and innovative approaches to address these issues.

N86-25356

Coupled with improved propulsion system performance is the evolution in the military aircraft arena toward highly maneuverable weapons systems, featuring such items as relaxed stability, forward swept wing technology, vectored nozzles, and more. For total system performance goals to be achieved, there will need to be a certain amount of dynamic coupling of the aircraft's powerplant with the flight control. This will lead to functional integration of various aircraft control subsystems, including engine and inlet control subsystems. The technology needed to design, implement and validate such an integrated system is being pursued but much remains to be done. The major issues concerning integrated control, and some recommendations based on the results of some recent Langley Research Center (LaRC)/LeRC contracted studies, will conclude this paper.

ORIGINAL PAGE IS
OF POOR QUALITY

ENGINE CONTROLS EVOLUTION

Over the years the control complexity of aircraft turbine engines has increased significantly. This complexity is required to extract more thrust for less weight from the turbomachinery. The figure below shows this increased complexity in terms of the number of controlled variables. Initially the system only had to control a single variable-engine fuel flow. Today an engine such as the joint technology demonstrator engine (JTDE) can have as many as 9 to 10 controlled variables. To accommodate this increased complexity, the proven hydromechanical control, which has been the implementation device for many years, is giving way to electronic controls and, in most cases, digital electronic controls. The electronic approach offers a great deal more computational capability than is possible with a hydromechanical computing device.

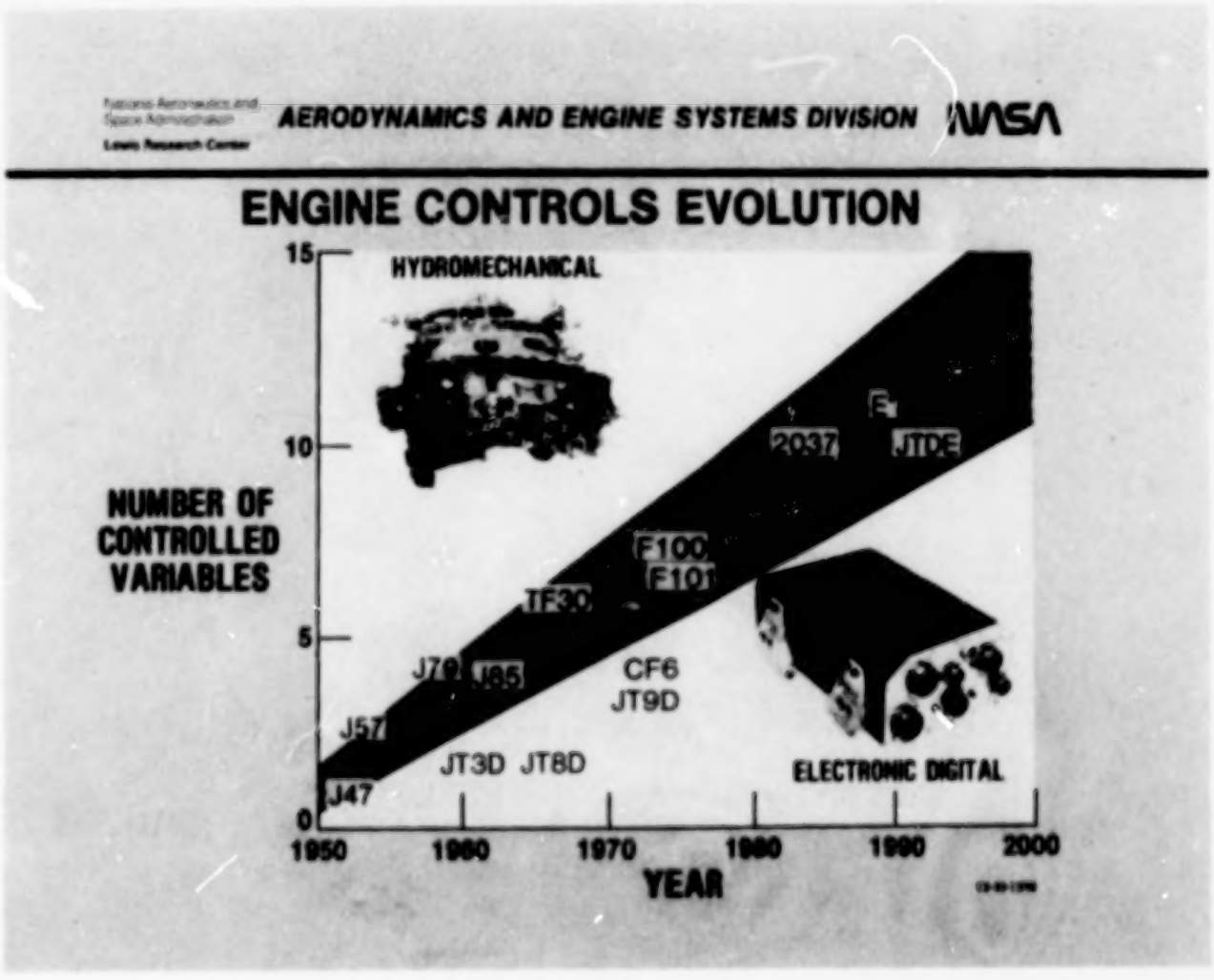

PROPULSION CONTROL HARDWARE

This figure shows the many different components that make up an electronic propulsion control system. Since we are entering a new application environment, these components (sensors, actuators, computers, and others) will not have the maturity that exists with elements of hydromechanical control. Thus LeRC is working on technology which will provide components that stress simplicity, reliability, and low cost for the future electronic propulsion controllers. The areas most actively being pursued are the sensors and actuators. To minimize problems of signal transmission, optical sensing devices are being developed. The next figure will summarize the important LeRC thrusts in these areas.

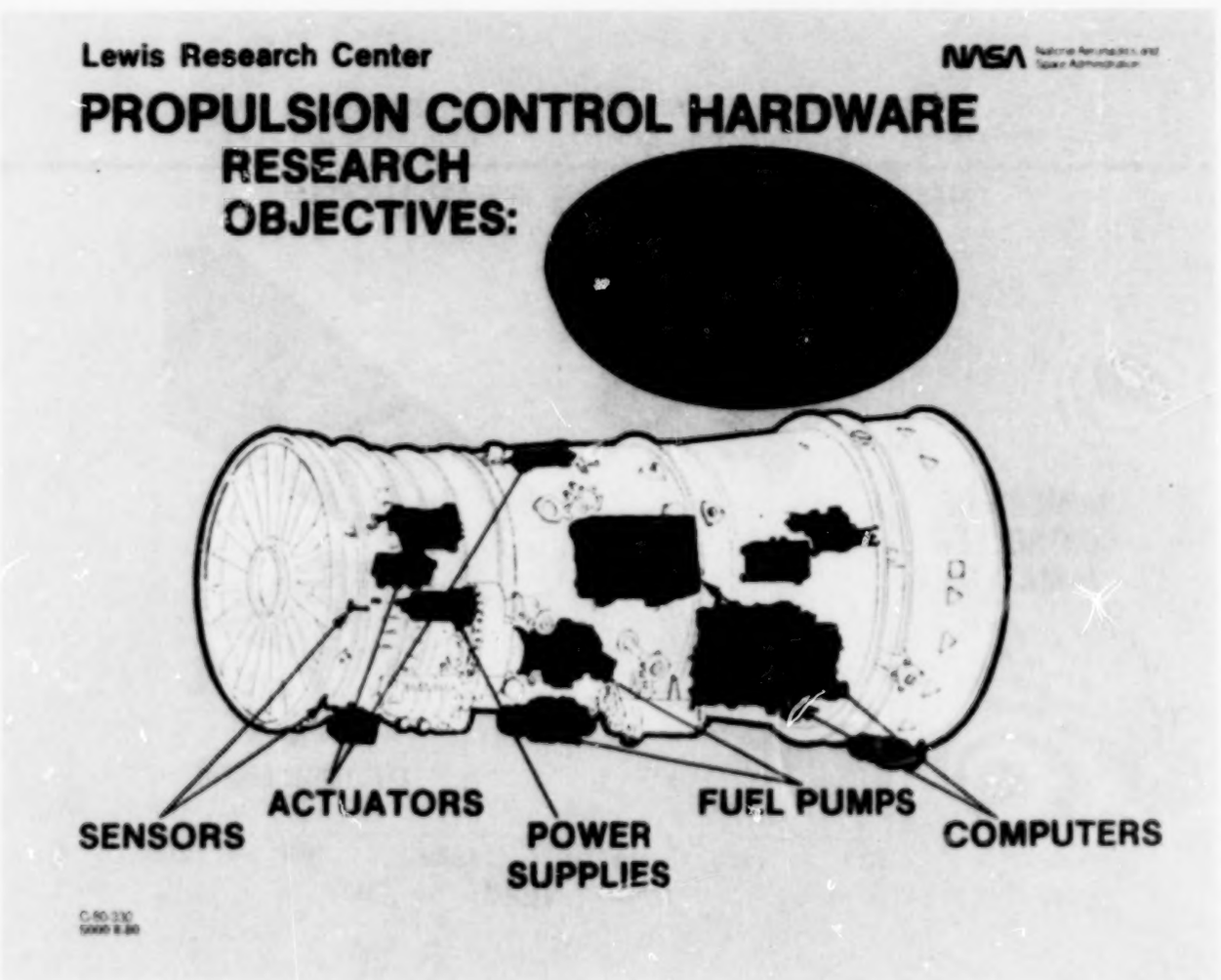

OPTICAL SENSOR/ACTUATOR ACTIVITY

The optical tachometer and position encoders were the first remote sensors developed for aircraft systems. Remote sensing is when no electrical energy is directed to the sensor. A fiberoptic wave guide connected the sensors with the source and detector. The rotary encoder is a nine-bit 360° encoder and the tachometer is a nine-pulse/revolution encoder. The sensors were installed on an F100 engine tested in an altitude chamber. These sensors worked during more than 100 hours of engine testing. The sensors were built under contract, by Spectronics, a division of Honeywell.

The optical gas temperature sensor was developed under contract by United Technologies Research Center (UTRC). Operation of this sensor is based on the temperature-dependent absorptive characteristics of a rare-earth- (europium-) doped optical fiber. Rare-earth materials like europium have energy states close to the ground state. These states are optically connected to higher excited states with energy differences that correspond to wavelengths in the visible region. The strength of absorption is a function of the number of electrons in the state from which the transition originates. The number of electrons in each state is a unique function of temperature. Optical energy directed through the rare-earth is absorbed. The strength of the absorption is dependent on temperature of the rare-earth material. A rare-earth sensor was delivered to LeRC and will be installed in the inter-turbine region of a turboshaft engine. Temperatures in this region are expected to approach 840° C. The sensor tests on the engine will occur in the near future.

Actuators that are powered or controlled by light may be part of future aircraft systems. In these schemes the actuator in driven by an electrohydraulic servovalve. Hydraulic power is supplied to the servovalve. In one scheme optical energy is converted to electrical energy (solar cell). This electrical energy is used to drive the torque motor directly. In another scheme optical power is used to control the flow of electrical energy to the torque motor. In the second configuration, electrical energy is generated at the point of use. Optical control signals generated at the control computer are sent to a phototransistor. The phototransistor drives a power transistor that controls power to the actuator. UTRC, under contract to LeRC, is developing high-temperature components for this type of application. These devices must operate at temperatures to 260° C. Gallium arsenide is being used for devices because of the high temperatures. The validity of design has been verified by operating a gallium arsenide - a junction field effect transistor switch — with a gallium arsenide phototransistor at 260° C. A current of 50 mA was switched into a resistive load with 235 μW of optical power incident on the phototransistor. A follow-on program with Pratt and Whitney Aircraft and UTRC to design and build a high temperature photoswitch that will control power to a direct drive servovalve is planned. This servovalve will drive a two-dimensional exhaust nozzle actuator on a JTDE engine in the 1986 to 1987 time frame.

LeRC OPTICAL SENSOR/ACTUATOR ACTIVITY

- OPTICAL TACHOMETER & POSITION ENCODER
  TESTED ON F 100 ENGINE (ALTITUDE CHAMBER)
- OPTICAL GAS TEMPERATURE SENSOR
  FOR TURBINE REGION (T 700 ENGINE)
- OPTICAL CONTROL OF DIRECT DRIVE
  ACTUATOR (P&W JTDE ENGINE)

F100 CONTROL INPUTS

The figure below shows the complexity of a modern aircraft turbine engine in terms of its controlled variables. This Pratt and Whitney F100 engine shows six manipulable input variables. This number of inputs, many of which will effect a number of engine parameters, can benefit from some organized method for designing the control law. Modern multivarible design techniques such as linear quadratic regulator (LQR) and the frequency domain approach of the multivariable Nyquist array (MNA) offer potential methods for organized design. LeRC and industry have evaluated this technology for the turbine engine control problem.

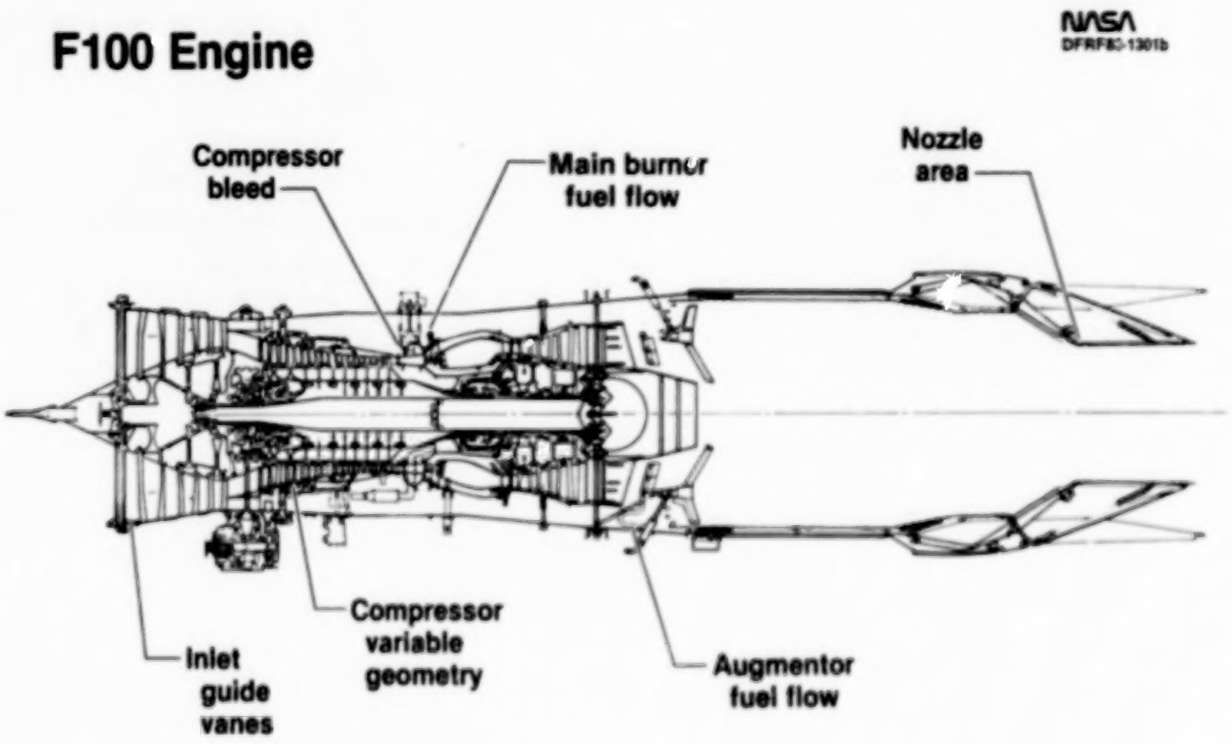

F100 MULTIVARIABLE CONTROL SYNTHESIS

The figure below shows the interrelationships of the participants in a government-sponsored program to evaluate control design methodology. The multivariable control synthesis (MVCS) program was jointly sponsored by the Air Force Aeropropulsion Laboratory (AFAPL) and the LeRC. Pratt and Whitney, Government Products Division, was cortracted to provide engine models and control design criteria for the F100 engine. Systems Control Technology (SCT), formerly Systems Control Incorporated, designed a multivariable control based upon LQR. The control algorithm was put into software by LeRC personnel. It was evaluated and debugged using a real-time engine simulation and then evaluated in a real engine in a LeRC altitude facility. The program was quite successful and demonstrated that the design methodology, although restricted to linear systems, could be extended to a highly nonlinear process, such as turbine engine control, by creative engineering judgment.

NASA
CS-79-2747

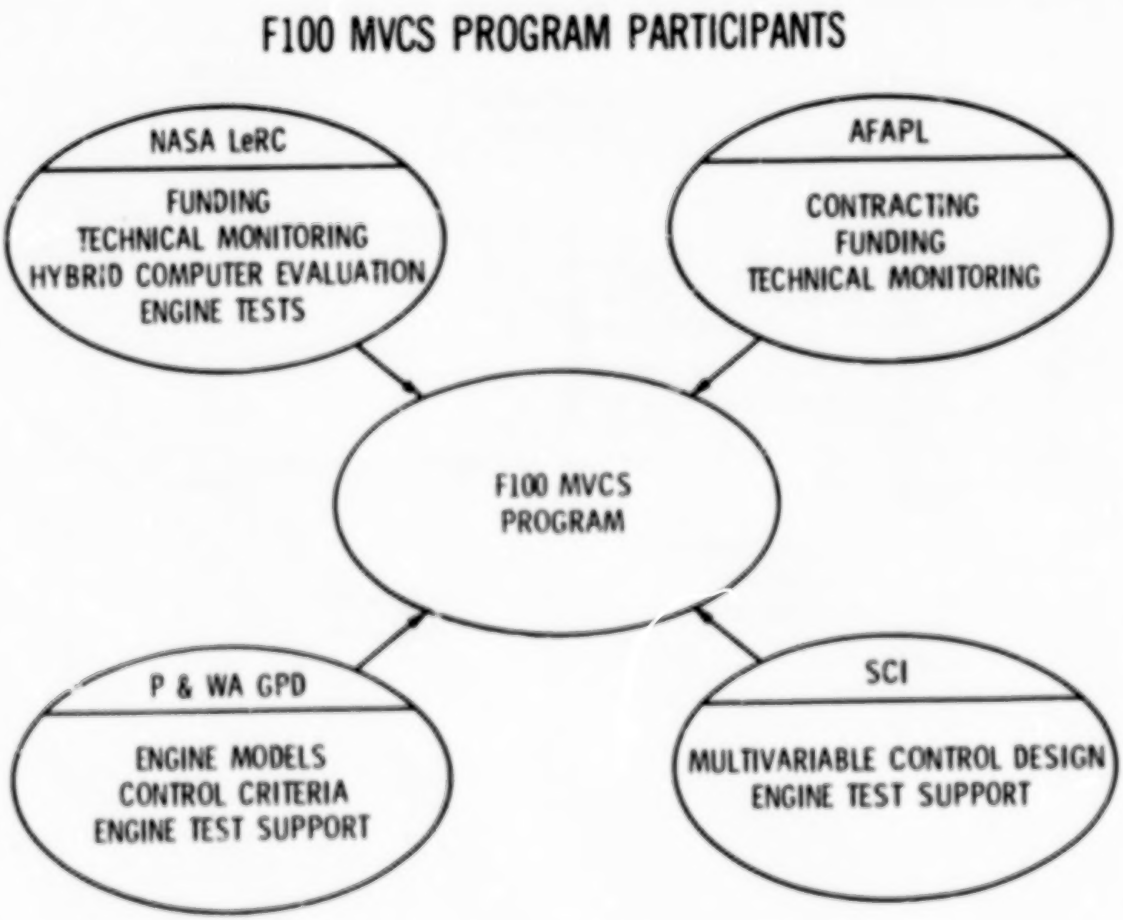

F100 MULTIVARIABLE CONTROL STRUCTURE

A simplified block diagram of the resultant multivariable control (MVC) is shown below. The main elements are a simplified dynamic engine model and a proportional-plus-integral (PI) controller. The engine model, contained in software within the digital electronic computer control, is the mechanism by which a family of linear operating-point PI controllers can be tied together to provide a control which works smoothly over the entire operating envelope. The model accepts the pilot input as well as measurements of the environmental conditions, and provides nominal values of the control inputs. It also provides the engine conditions (pressure, temperatures, and speeds) which are desired for those input conditions. The multivariable PI control block then compares the actual engine conditions against those desired and trims out the errors by modifying the control inputs. The gains of the PI control are functions of the operating conditions since they have been selected by linear design methods. Providing the functional relationships is a task readily accomplished by a digital computer.

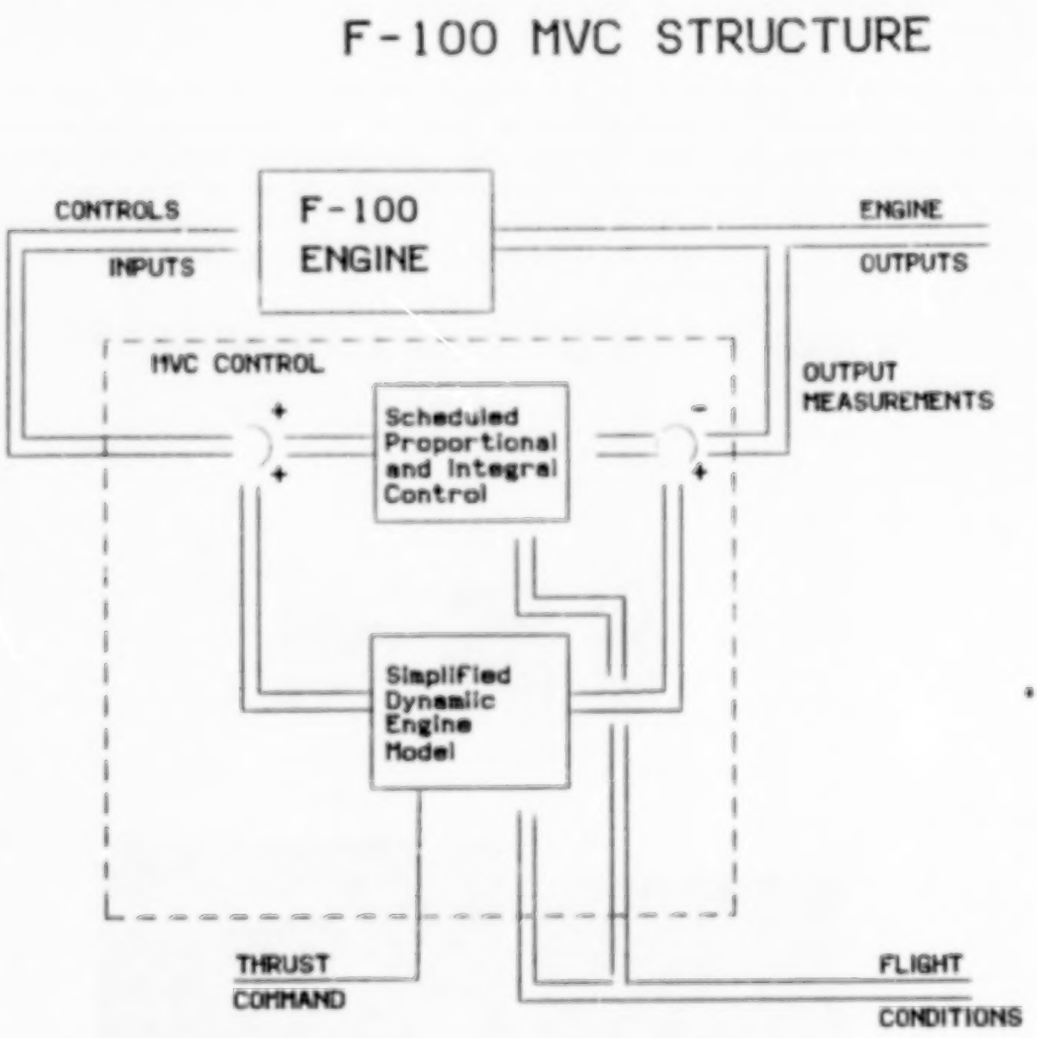

SENSOR FAILURE DETECTION AND ACCOMMODATION

As mentioned earlier, reliability of the components making up an electronic engine control is a real concern. The sensors used will be ones which produce an output compatible with an electronic device. For many of these sensors the engine control application will be new. Hardware redundancy will help overcome the reliability deficiencies; however, this is a costly solution.

Fortunately, the theory of multivariable systems provides some valuable methods for implementing techniques called analytical redundancy. This figure shows how analytical redundancy can detect, isolate, and accommodate sensor failures. The principle behind advanced sensor failure detection/isolation/accommodation (DIA) is the replacement of hardware redundancy with analytical redundancy. In the hardware redundant case multiple, similar sensors (for example, three T4 sensors) could be used to detect failures in a single sensor through a fairly straightforward majority voting procedure. Once a failure is detected, the faulty sensor information is excluded from use in the control system. Multiple sensors would also be required for other measured engine variables (for example, P4 and N). The advantage of this approach is the conceptual simplicity of the decision process. The disadvantages are the cost and weight of the additional sensors.

In an analytically redundant case a single sensor would be used for each measured engine variable. Sensor failures would be detected by comparing the measurement (here T4) with the estimate (EST) of T4. The analytically redundant information in dissimilar sensors such as P4 and N, and a reference model of the engine, are used to generate T4, EST. A fault is detected when a large error between measurement and estimate exists. Once a failure is detected, T4, EST is substituted for the faulty measurement in the control system.

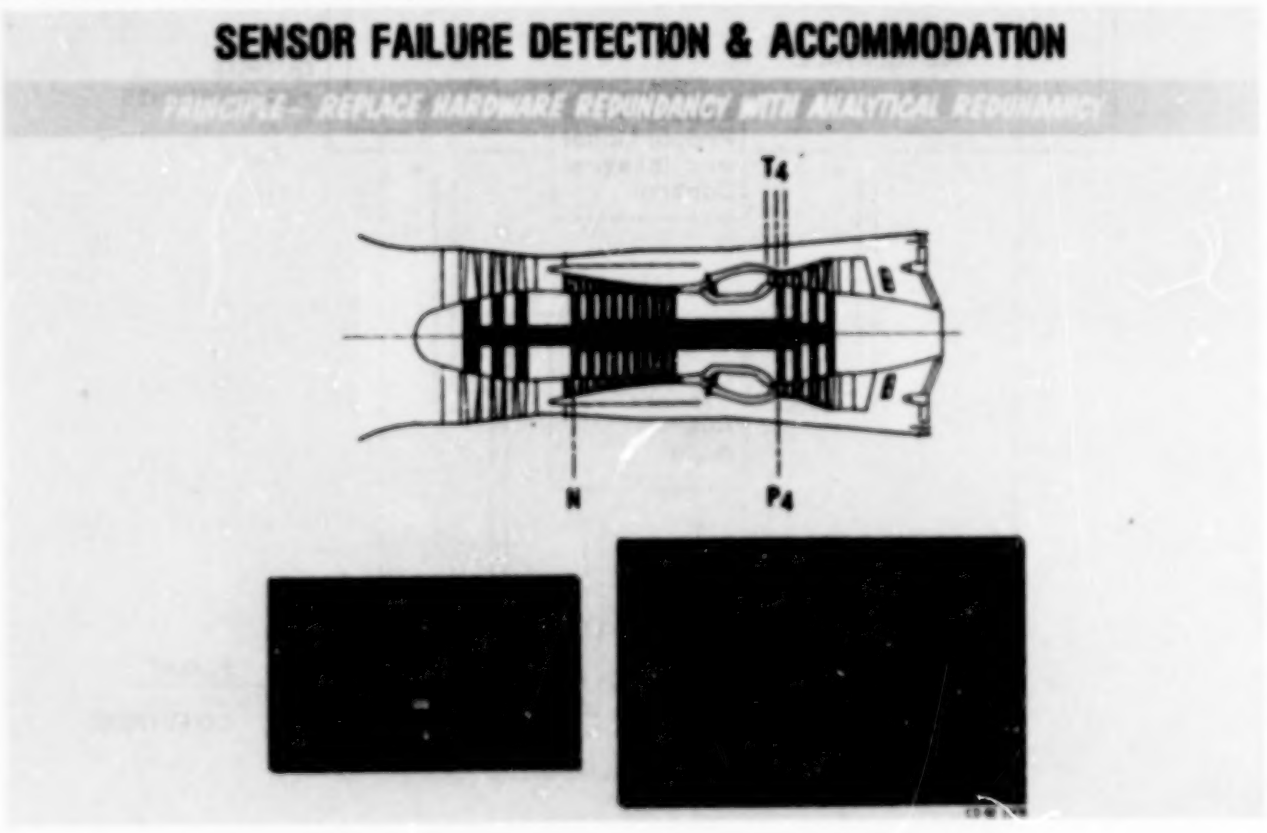

COMPUTATIONAL FLOW OF AUGMENTED TURBOFAN ENGINE SIMULATION

The electronic control technology work done thus far has benefited significantly from the use of accurate engine simulations. Real-time simulations have been invaluable in checking digital control software. Accomplishing a real-time simulation of a complete aircraft turbine engine is not always easily done. The figure below is an example that shows the complexity involved in the modeling of an engine. Compressor and turbine maps, mixing volumes, rotor inertias and other engine characteristics create computational nightmares. Not only are the model's steady-state relationships difficult to compute, but the numerous differential equation terms further complicate the real-time computation objective.

COMPUTATIONAL FLOW DIAGRAM OF AUGMENTED TURBOFAN ENGINE SIMULATION

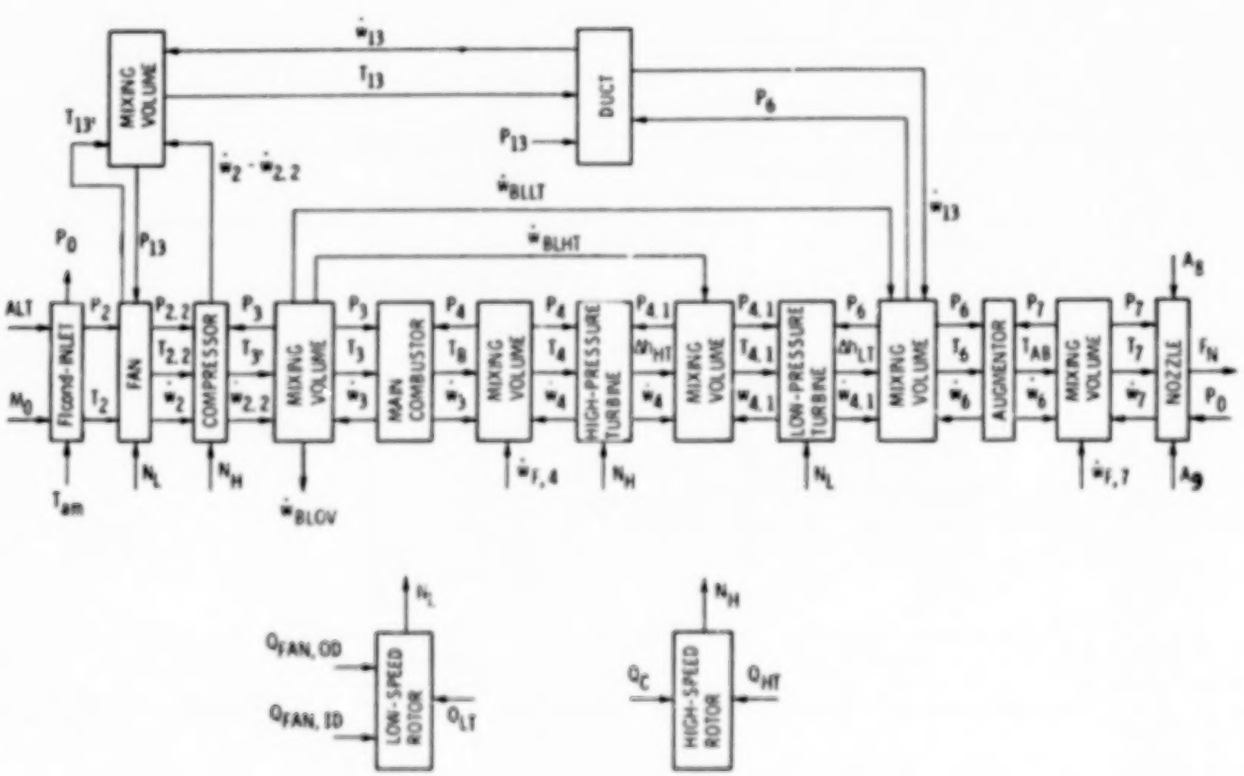

REAL-TIME ENGINE SIMULATION USING A HYBRID COMPUTER

LeRC has used a hybrid computer facility to porvide a real-time high fidelity model for engines such as the F100. This diagram shows how the real-time capability is achieved. The digital portion of the hybrid is used to provide function generation for the compressor, combustor, and turbine maps. The dynamic terms are integrated, using the hybrid's analog components. A digital controller can then exercise the real-time engine through analog inputs and outputs.

NASA
CS-74623

REAL–TIME ENGINE SIMULATION USING A HYBRID COMPUTER

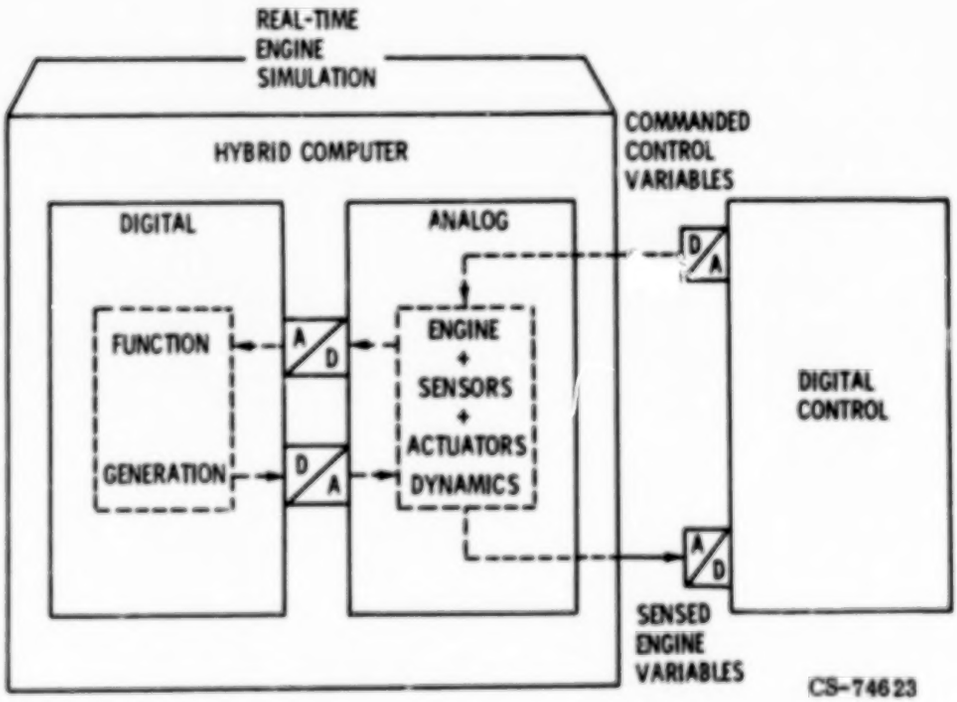

ORIGINAL PAGE IS
OF POOR QUALITY

USING MICROPROCESSORS FOR REAL-TIME SIMULATION

The use of real-time engine simulations is not limited to control law validations. They are also needed in piloted simulators to provide realistic engine models for total vehicle evaluation. To make real-time simulators more readily available at a lower cost and in a compact form, there is an LeRC program to use parallel microprocessors to accomplish real-time engine simulation. Below is a photograph of a forerunner to the parallel processor real-time engine simulator (RTES). The particular unit shown is a single microprocessor simulator of a rather simple helicopter engine. This unit will serve as a RTES in a vertical motion simulator at the Ames Research Center (ARC) during helicopter control studies.

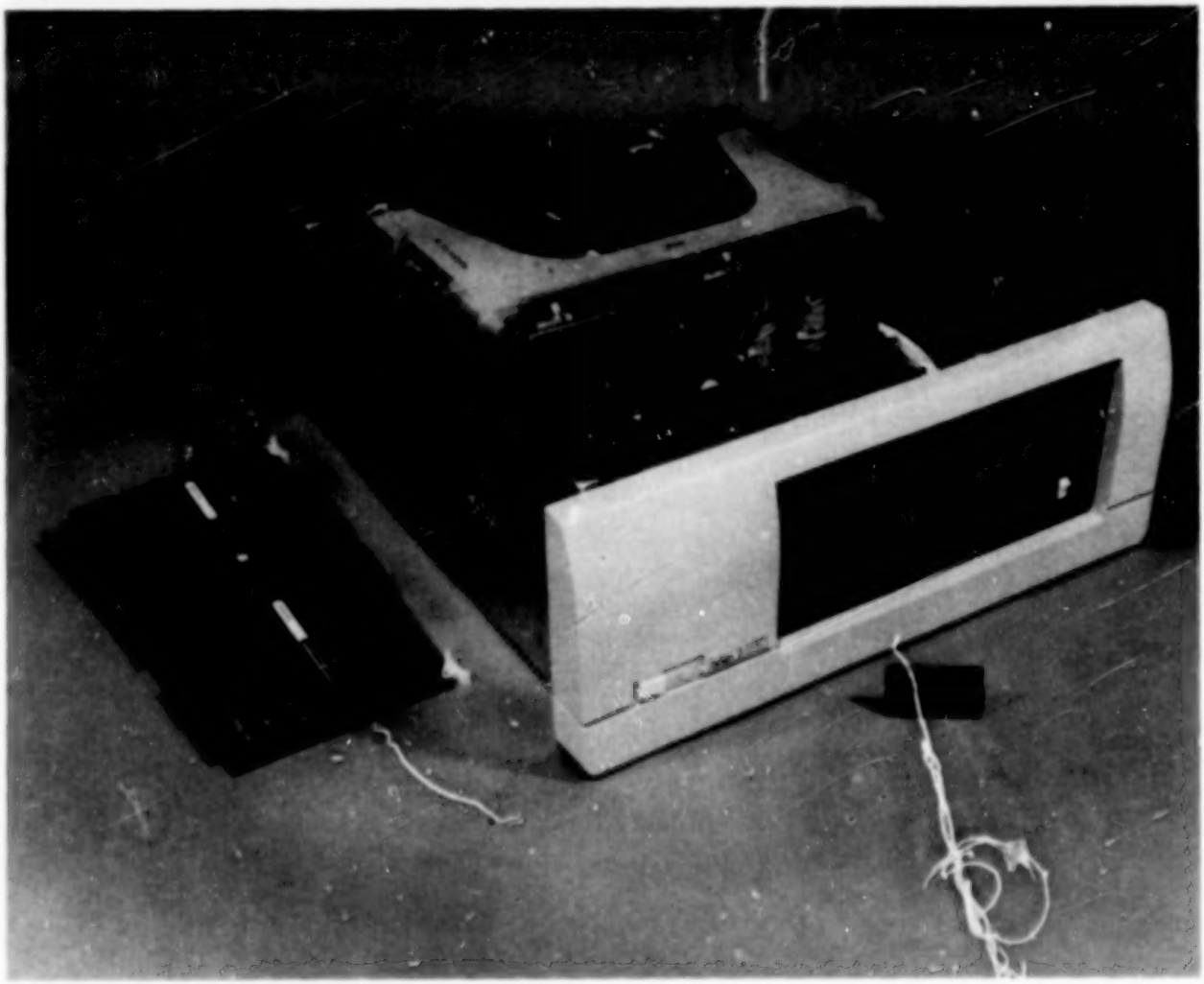

PROGRESS TOWARD INTEGRATED CONTROL

Many programs have been accomplished to provide the technology needed for electronic propulsion controllers. The bubble on the top left of the next figure contains the acronyms for some of these programs. The aircraft is also evolving to electronic control systems for fire control, flight control and other functions. Programs have been undertaken to integrate portions of the aircraft controls. A small sampling is indicated in the bubble on the lower left. However, studies have shown that more maneuverability and other performance improvements can be accomplished by integrating the propulsion system with the other aircraft control systems. The benefits of integrating the supersonic inlet and engine, for example, was demonstrated in the integrated propulsion control system (IPCS) program. The design methods for integrated control systems (DMICS) program is looking at the design tools needed to come up with an integrated aircraft/propulsion control law. The IAPSA program is evaluating the architecture needed to support a control law for a vehicle with strong propulsion/aircraft coupling. These programs are only the beginning. Many issues are yet to be resolved before an aircraft with a highly integrated (propulsion/aircraft) control system will become an operational entity.

PROGRESS TOWARD INTEGRATED CONTROL

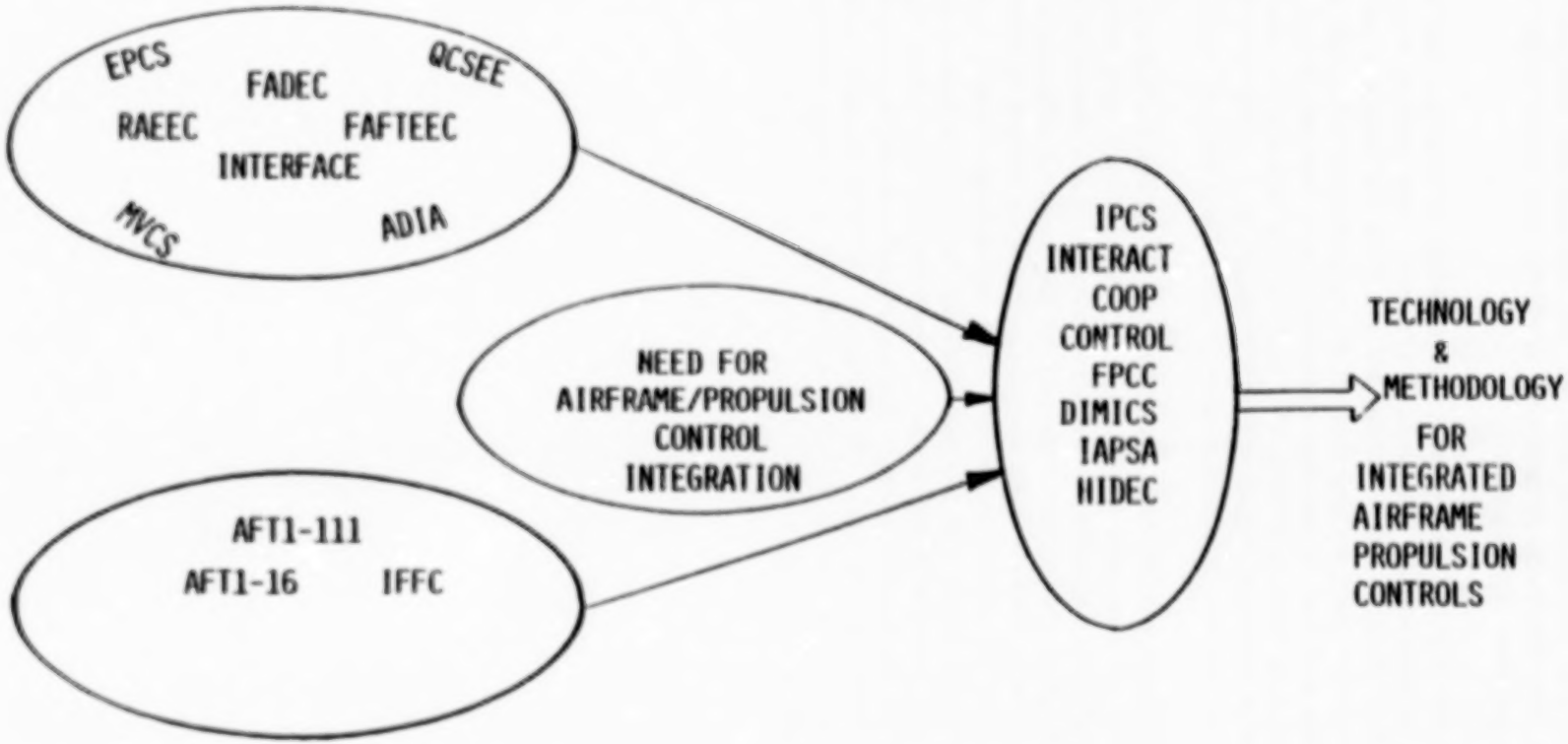

UNRESOLVED ISSUES

This last figure illustrates some of the unresolved issues pertaining to electronic controls for aircraft propulsion systems and control systems which integrate aircraft and propulsion functions.

With regard to digital electronic propulsion controls, realiability is an area requiring a large portion of the design effort. The severe environment of engine-mounted computers, sensors, and actuators results in designs using redundancy for fault-tolerance. How best to achieve high reliability through a combination of hardware and software and how to manage redundancy are issues still being resolved. Also, once a design is complete, methods for validating the final design under all conditions and possible failure modes are still evolving. Both the redundancy and the complexity of the control algorithm itself make validation difficult.

Functionally integrating the aircraft and propulsion system requires the development and maturing of some new technology. Design tools are needed for handling control design of an integrated system where hierarchical considerations may be important. Present multivariable design methods may or may not be adequate. Also, the architecture of the resultant control may require extensive cross communication between distributed elements. In addition to the new technology, there needs to be improved reliability analysis tools and better methods for performance validation. Since an integrated control crosses boundaries of responsibility, some method of bridging the potential gap must be agreed upon. The issue of standard languages, processor and data bus become involved in this resolution. At the present time there seems to be a lack of agreement on the adequacy of the present military standards being mandated. These issues must be resolved.

UNRESOLVED ISSUES

ELECTRONIC PROPULSION CONTROL

- RELIABILITY OF HARDWARE/SOFTWARE
- VALIDATION PROCEDURES

ADVANCED CONTROL ALGORITHMS
REDUNDANCY MANAGEMENT CONCEPTS

INTEGRATED AIRFRAME/PROPULSION CONTROL

- TECHNOLOGY NEEDS
  - DESIGN TOOLS
  - ARCHITECTURAL CONSIDERATIONS
- RELIABILITY ANALYSIS TOOLS
- VALIDATION METHODS
- ISSUE OF STANDARDS
  - DATA BUS
  - LANGUAGE
  - PROCESSOR

1. Report No.	2. Government Accession No.	3. Recipient's Catalog No.
NASA CP-2298		

4. Title and Subtitle	5. Report Date
DIGITAL ELECTRONIC ENGINE CONTROL (DEEC) FLIGHT EVALUATION IN AN F-15 AIRPLANE	March 1984
	6. Performing Organization Code
7. Author(s)	8. Performing Organization Report No. H-1201
	10. Work Unit No.
9. Performing Organization Name and Address NASA Ames Research Center Dryden Flight Research Facility P.O. Box 273 Edwards, CA 93523	11. Contract or Grant No.
	13. Type of Report and Period Covered Conference Publication
12. Sponsoring Agency Name and Address National Aeronautics and Space Administration Washington, D.C. 20546	14. Sponsoring Agency Code RTOP 533-02-21

15. Supplementary Notes

NASA Technical Chairman: Frank W. Burcham, Jr., Ames Research Center, Dryden Flight Research Facility, Edwards, CA 93523

16. Abstract

A flight evaluation of a digital electronic engine control (DEEC) has been conducted on an F100 engine in an F-15 airplane. Following an extensive development program, ground tests, and altitude facility tests, a 30-flight evaluation was flown at the NASA Ames Research Center's Dryden Flight Research Facility. The DEEC is a single-channel, full authority digital control with selective input-output redundancy and a simple hydromechanical backup control. It incorporates closed-loop control logic that eliminates the need for engine trimming, provides automatic airstarts, and greatly improves the augmentor transient capability. The DEEC also incorporates significant fault detection and accommodation logic, and is capable of maintaining digital control of the engine for any single input-output failure.

Results of the DEEC flight evaluation were presented at a minisymposium held at Ames Dryden on May 25 and 26, 1983. This publication contains the papers that were presented.

17. Key Words (Suggested by Author(s))	18. Distribution Statement
Digital control Engine control Flight tests F-15 airplane F100 engine	[redacted]

19. Security Classif. (of this report)	20. Security Classif. (of this page)	21. No. of Pages	22. Price
Unclassified	Unclassified	255	

[redacted]

NASA-Langley, 1984

END

DATE

FILMED

JUL 31 1986